BIOTECHNOLOGY FOR DETECTING OXIDATIVE MODIFICATIONS TO FIBRINOGEN

STUART P. MEREDITH
DOCTOR OF PHILOSOPHY

ASTON UNIVERSITY
SEPTEMBER 2016

Aston University

TRANSLATABLE BIOTECHNOLOGY FOR DETECTING OXIDATIVE AMINO ACID MODIFICATIONS AND UNDERSTANDING OF THE ROLE OF RADICALS IN INFLAMMATION

Stuart Meredith
Doctor of Philosophy
2016

THESIS SUMMARY

Systemic inflammation has been recognized as a risk factor for a number of diseases, including type 2 diabetes. There is a growing awareness that inflammatory diseases have an oxidative pathology, which can result in specific oxidation of amino acids within proteins. Patients with inflammatory disease have higher levels of plasma protein 3-nitrotyrosine than healthy controls. Fibrinogen is an abundant plasma protein, and has been shown to be highly susceptible to such oxidative modifications, and is therefore a potential marker. Oxidative damage and modifications to fibrinogen offer potential as biomarkers of disease, and for diagnosis and a greater understanding of the pathology. The aim of this study was to map the *in-vitro* locations of oxidatively-modified fibrinogen, and test the possibility of producing antibodies that show increased binding to protein-specific modification sites. Fibrinogen was nitrated using the peroxynitrite generator SIN-1, and analyzed by liquid chromatography tandem mass spectrometry. Several modified peptides that consistently occurred were identified with the Mascot© search engine and manually validated. Based on literature or mass spectrometry results, peptides with the core amino acid sequence STSYGTGC or DYEDDQQKQLC, either unmodified, or containing 3-chlorotyrosine or 3-nitrotyrosine were synthesized and subsequently antibodies were produced. Each subsequently produced sheep anti-serum was tested against various native and modified peptides containing a variety of different amino acid sequences. Anti-STSY-(NO_2)-GTGC serum showed modification site specificity, whereas anti-DY-(Cl)-EDDQQKQLC serum showed sequence specificity but was unable to distinguish between 3-chlorotyrosine and 3-nitrotyrosine. This cross-reactivity between chlorinated and nitrated modification sites might allow broader detection of modified fibrinogen in inflammation. The anti-STSY-(NO_2)-GTGC serum was also tested against plasma from healthy control volunteers and type 2 diabetic patients, but showed limited binding and ability to discriminate the disease state. In conclusion, it has been shown that antibodies can be produced to differentiate between native and modified proteins; however, further work is required to understand sequence-specificity better and monoclonal antibodies might be better suited to achieving sequence-specificity.

Key words: Mass Spectrometry (MS), Oxidative Post-Translational Modifications (OxPTMs), Inflammation, Antibodies, Proteins

ACKNOWLEDGMENTS

My journey to date has been an unconventional one, I started university with no relevant academic qualifications, and faced my fair share of naysayers and adversity along the way. I hope my success encourages others to stay true to their dreams regardless.

“Nothing in this world can take the place of persistence. Talent will not: nothing is more common than unsuccessful men with talent.

Genius will not; unrewarded genius is almost a proverb. Education will not: the world is full of educated derelicts.

Persistence and determination alone are omnipotent.” - Calvin Coolidge.

I would like to start by thanking my supervisors at Aston University, Professor Corinne Spickett and Professor Helen Griffiths for providing me with the opportunity to do a Ph.D., welcoming me into their research groups, and moulding me into a research scientist.

With particular thanks to Professor Corinne Spickett. The guidance, skills and mindset that she has provided me with are invaluable.

The Oxidative Stress team at Aston, Dr Karina Tveen-Jensen, Dr Sabah Pasha and Dr Ivan Verrastro have been supportive colleagues, great friends, and from who I have learnt a lot about the field of analytical biochemistry. The first-class mass spectrometry training I received from Professor Andy Pitt is unrivalled, thank you.

I would like to take this opportunity to acknowledge research placement student Aneesa Ali for the hard work and dedication she showed in performing many ELISA assays throughout her placement year, never deterred by the challenging workload I provided her with.

I acknowledge Arian Mustafa for his help testing the reproducibility of anti-sera, in a parallel study used to produce an averaged data set (figures 4.16, 4.18 and 4.20).

Thank you to Professor Paul Davis and the friendly professional staff at Mologic who welcomed me into their team, helped to train me in various scientific techniques, and have always been generally very supportive throughout my research project, thank you.

Finally, I would like to thank Jasmine Foley and my father Jeffrey Meredith for being staunch supporters, spending multiple hours proof-reading my thesis in the stressful final stages. Thank you all.

List of Abbreviations

AD	Alzheimer's disease
ALS	Amyotrophic lateral sclerosis
AP	Affinity purification
ARD	Acute respiratory disease
BCA	Bicinchoninic acid
BSA	Bovine serum albumin
CID	Collision induced dissociation
COPD	Chronic obstructive pulmonary disease
CRP	C-reactive protein
CV	Coefficient of variance
CVD	Cardiovascular disease
DCM	Dichloromethane
DMF	Dimethylformamide
DNP	Dinitrophenylhydrazone
DNPH	2,4-Dinitrophenylhydrazine
ELISA	Enzyme-linked immunosorbent assay
ESI	Electrospray ionisation
ETC	Electron transport chain
ETD	Electron transfer dissociation
Exp.	Experiment
GSH	Glutathione
GSSG	Glutathione disulphide
HCD	Higher-energy collisional dissociation
HOBT	Hydroxybenzotriazole
HPLC	High performance liquid chromatography
HRP	Horseradish peroxidase
HSA	Human serum albumin
ICC	Immunocytochemistry
IHC	Immunohistochemistry
KLH	Keyhole limpet haemocyanin
MALDI	Matrix-assisted laser desorption ionisation
MDA	Malondialdehyde
MRM	Multiple reaction monitoring

List of Abbreviations (Cont.)

MS	Mass spectrometry
MS^2	Tandem mass spectrometry
MSR	Methionine sulfoxide reductase
PB	Phosphate buffer
pNPP	para-Nitrophenylphosphate
PRR	Pattern recognition receptor
PVDF	Polyvinylidene fluoride
RCS	Reactive chlorine species
RNS	Reactive nitrogen species
ROS	Reactive oxygen species
SIN-1	3-morpholinosydnonimine
SRM	Single reaction monitoring
SULFO-SMCC	sulfosuccinimidyl 4-N-maleimidomethyl)cyclohexane-1-carboxylate
TBST	Tris-buffered saline tween
TCA	Trichloroacetic acid
TEMED	Tetramethylethylenediamine
TFA	Trifluoroacetic acid
TIPS	triisopropylsilane
TNF- α	Tumour necrosis factor alpha
WB	Western blot
XIC	Extracted ion chromatogram

Table of Contents

Chapter 1

General Introduction

1.1 Research Overview

Systemic inflammation has been recognized as a risk factor for a number of diseases, including type 2 diabetes, atherosclerosis and chronic obstructive pulmonary disease (COPD) (Gan *et al.,* 2004). Diseases that involve systemic inflammation, such as COPD, have been shown to cost the national health service £1 billion a year in indirect costs, illustrating the importance of techniques to detect inflammation (Gani *et al.,* 2010). There is a growing awareness that inflammatory diseases have an oxidative pathology, which can result in specific oxidation of amino acids within proteins. Patients with inflammatory disease have higher levels of plasma protein 3-nitrotyrosine than healthy controls. Fibrinogen is an abundant plasma protein, and has been shown to be highly susceptible to such oxidative modifications, and therefore a potential marker (Weigandt *et al*., 2012, and Shacter *et al.,* 1994). Oxidative damage and modifications to fibrinogen offer potential as biomarkers of disease, providing potential for diagnosis and a greater understanding of the pathology. Identification of these susceptible peptides will allow design of sequence-specific biomarkers of oxidative, chlorinative and nitrative damage to plasma protein in inflammatory conditions. The aim of this project was to develop diagnostic tools for detecting oxidative markers of inflammatory disease. Antibody-based techniques for detecting oxidative post-translational modifications (oxPTMs) are often used to measure protein oxidation. There are many commercially available antibodies but some uncertainty regarding the cross reactivity they exhibit; moreover little information regarding the specific target epitopes is available. The specific objectives were to map tyrosine nitration and chlorination in fibrinogen under oxidative conditions to identify susceptible residues, and to investigate the potential of antibodies to distinguish between specific peptides with and without oxPTMs.

1.2 Inflammation in the Pathology of Disease

The fundamental principles of inflammation are well established. Inflammation is traditionally defined by heat, pain, redness and swelling, of which the latter three are explained by the dilation and increased permeability of blood vessels, which causes greater local blood and fluid flow. The pain present during inflammation is explained by the migration and action of cells into the tissue (Murphy, Travers and Walport, 2008). The skin, mucosal and epithelia lining of the gut and lungs make up the first point of defence of the immune system. Pathogens that breach this initial line of defence are met by molecules and cells of the innate immune system. Macrophages are abundant phagocytes in the tissue, and are the next line of defence, recognising pathogens by cell surface proteins known as pattern recognition receptors (PRR) such as toll like receptor (Beutler *et al.,* 2006). Once the macrophage's receptors are triggered by invading pathogens, it then becomes activated, and the invading species is phagocytosed. The macrophages also secrete chemokines and cytokines. Tumour necrosis factor α (TNF-α), affects the behaviour of nearby cells with TNF-α receptors, more specifically, TNF-α is a potent chemoattractant for neutrophils and stimulant for macrophage phagocytosis. Chemokines, such as CCL2, CCL3 and CCL5, CXCL1, CXCL2 and CXCL8, also attract cells that have chemokine receptors; for example, CXCL8 attracts neutrophils and monocytes into infected tissue (Graham *et al.,* 2013). These released macrophage, chemokines and cytokines initiate the process of inflammation. During inflammation, cells of the innate immune system are recruited into the area of infection. Macrophages and neutrophils are considered the primary responders. Neutrophils, much like macrophages, have surface receptors that recognise pathogens and as such are recruited in large numbers during inflammation, in fact neutrophils are the most abundant, and principal, phagocytising cells of the immune system (Ermert *et al.,* 2013). In the next stages, at a slower rate, eosinophils migrate to the site of

inflammation and destroy pathogens. In addition to destroying the invading pathogens the inflammatory immune response also increases the flow of antigen-presenting cells to nearby lymphoid tissues, where they activate lymphocytes, initiating the adaptive immune response (Murphy, Travers and Walport, 2008). Many diseases are defined as inflammatory disorders; there are also many more diseases whereby Inflammation is part of the pathology. Diseases such as type 2 diabetes (Kadiiska, *et al*., 2012), COPD, atherosclerosis (Gan *et al.,* 2004) and rheumatoid arthritis (Tetik, *et al*., 2010) are all defined as inflammatory. The mechanisms between diseases however, are different. Inflammation in type 2 diabetes involves hyperglycaemic dependant b-cell dysfunction and the subsequent induction of pro-inflammatory mediators and oxidative stress (Akash *et al*., 2013). In patients with COPD the inflammation is similar to that seen in healthy patients, but amplified, whereby inhaled irritants activate surface macrophages of the respiratory tract, and subsequently a cascade of pro-inflammatory chemokines and oxidative insult follow. This inflammation persists after the initial response, suggesting a self-perpetuating mechanism, which is yet to be elucidated (Barnes, 2016). The inflammation in Atherosclerosis is caused by atherosclerotic plaques, and alteration of the phenotypes of vascular cells, more specifically, arterial endothelial cells express vascular cell adhesion molecule-1 (VCAM-1) which binds to leukocytes, and promote inflammation (Galkina and Ley, 2009, and Libby, 2002). The mechanisms of RA pathogenesis are not fully understood; however, it is thought to involve synovial inflammation, hyperplasia and autoantibody production (McInnes and Schett, 2011).

A study performed by Ichinose (2009) showed high levels of 3-nitrotyrosine in COPD patients, supporting the involvement of the modification in the pathogenesis of the disease (Ichinose, 2009). More specifically, throughout the inflammatory response macrophages and neutrophils respond to chemo-attractants, and subsequently produce superoxide and nitric oxide, shown to form peroxynitrite (Wall *et al*., 2012 and Pacher *et al*., 2007). Peroxynitrite is highly reactive, and has been shown to oxidatively modify tyrosine residues to form 3-nitrotyrosine. A number of biological oxidants can be produced during an inflammatory response, these include hypochlorous acid (HOCl), hydrogen peroxide (H_2O_2), hydroxyl radical and peroxynitrite ($ONOO^-$) (Dalle-Donne *et al*., 2003).

1.3 Sources of Biological Oxidants

1.3 .1 Reactive Oxygen Species

There are many types of biological oxidants involved in maintaining cellular homeostasis, such as those seen during inflammation. Amongst these biological oxidants and reactive species are the radicals, superoxide ($O_2^{\bullet-}$), hydroxyl ($OH^{\bullet}$), peroxyl ($RO_2^{\bullet}$), alkoxyl ($RO^{\bullet}$), hydroperoxyl ($HO_2^{\bullet}$); and non-radical species such as hydrogen peroxide (H_2O_2), hypochlorous acid (HOCl), singlet oxygen (O_2), and peroxynitrite ($ONOO^-$) (Dalle-Donne *et al*., 2003).

The radicals derived from oxygen represent the most important class of radical species generated in living systems (Valko *et al*., 2007). Molecular oxygen (dioxygen) is ubiquitous, and is itself a radical forming species, the addition of one electron to which forms the reactive species superoxide ($O_2^{\bullet-}$). Superoxide is produced in a number of ways physiologically, and is considered a primary ROS. One example of which is the production of adenosine triphosphate (ATP) via the mitochondrial electron transport chain. During the electron transport chain, a small number of electrons leak to oxygen prematurely, forming superoxide (Valko et al., 2007). In eukaryotic organisms, it was calculated that more than 90% of the ROS produced were by the mitochondrial electron transport chain (Lushchak, 2014). The inflammatory phagocytic cells of the immune system, such as neutrophils, also utilise superoxide and hydrogen peroxide to destroy pathogens. This reaction is catalysed by the membrane bound enzyme nicotinamide adenine dinucleotide phosphate (NADPH) oxidase, assembling on the membrane and generating superoxide by donating electrons from NADPH in the cell across the membrane to molecular oxygen (Clark, 1999). The overall process is termed respiratory or oxidative burst (Guzik, 2003, Inoguchi, 2003 and Shacter, 2000). The enzymatic antioxidant superoxide dismutase keeps superoxide within safe levels, by converting

it to the less reactive molecular oxygen (O_2) AND hydrogen peroxide (H_2O_2) (Hayyan *et al*., 2016).

The hydroxyl radical ($OH^{\bullet}$) is one of the most reactive ROS; it has a half-life of 10^{-9} seconds in vivo, and hence when produced it reacts at its site of formation (Fiser *et al*., 2013 and Valko *et al*., 2007). Under normal physiological conditions hydroxyl radicals are produced via transition metal catalysed cleavage of hydrogen peroxide (H_2O_2), known as the Fenton reaction (Stadtman, 1998). Under conditions of oxidative stress, such as those during respiratory burst, superoxide excess promotes the release of free iron from iron containing proteins, such as iron-sulphur proteins (4Fe-4S). The released divalent iron (Fe^{2+}) can participate in the metal catalysed, Fenton reaction, producing highly reactive radicals ($Fe^{2+} + H_2O_2 \rightarrow Fe^{3+} + {}^{\bullet}OH + OH^-$) (Valko *et al*., 2007 and Stadtman, 1998).

1.3.2 Reactive Nitrogen Species

The production of nitric oxide ($NO^{\bullet}$) is catalysed by nitric oxide synthases; it is used to regulate vasodilation, modulate mitochondrial respiration, and for immunity based defence (Wall *et al.*, 2012). Nitric oxide is not particularly problematic *in-vivo*, as there are sufficient means of preventing its accumulation. Nitric oxide is less reactive than molecular oxygen and diffuses from the cell via the cell membrane into the red blood cells. Once in the red blood cells it becomes nitrate via a reaction with oxyhaemoglobin, this limits its half-life to half a second (Pacher *et al.*, 2007 and Butler *et al.*, 1998). Nitric oxide in μM concentrations inhibits catalase cytochrome P-450, involved in oxidative metabolism and cytochrome P-450, which is involved in oxidative metabolism. Similarly, it can also inhibit cytochrome c oxidase, which transiently increases the leakage of superoxide from the electron transport chain (ETC) of the mitochondria. Superoxide exists as an anion, which is more likely to donate an electron than accept one from another molecule.

When both superoxide ($O_2^{\bullet-}$) and nitric oxide ($NO^{\bullet}$) are synthesised in close proximity, peroxynitrite ($ONOO^-$) is formed. Nitric oxide reacts with superoxide so quickly that it out-competes dismutation catalysed by superoxide dismutase (Pacher *et al.*, 2007). A 10-fold increase of both superoxide and nitric oxide can result in an overall increase in peroxynitrite formation by 100-fold. Under inflammatory conditions there is often an increased level of both superoxide and nitric oxide in the region of 1,000-fold, this results in a 1,000,000-fold increase in the formation of peroxynitrite (Wall *et al.*, 2012 and Pacher *et al.*, 2007).

There is an inverse relationship between reactivity and specificity, in that highly reactive species are less specific to what they will react with (Wall *et al*., 2012). For example, hydroxyl radicals are shown to be so reactive that they are only able to diffuse approximately the diameter of a protein away from their production site. In contrast, peroxynitrite reacts more slowly than hydroxyl radicals so that its dispersion area is greater and more selective with regard to what it will react with (Pacher *et al*., 2007). Consequently, peroxynitrite can influence biological processes. Peroxynitrite has been shown to be more efficient at producing hydroxyl ions than the Fenton reaction. The hydroxyl radical reacts with aromatic amino acids such as tyrosine, abstracting the hydrogen, and the remaining nitrogen dioxide ($NO_2^{\bullet}$) of peroxynitrite then reacts with the aromatic ring to produce 3-nitrotyrosine via the intermediate tyrosyl radical (Figure 1.1) (Radi, 2013, Pacher *et al*., 2007 and Hipkiss, 2006).

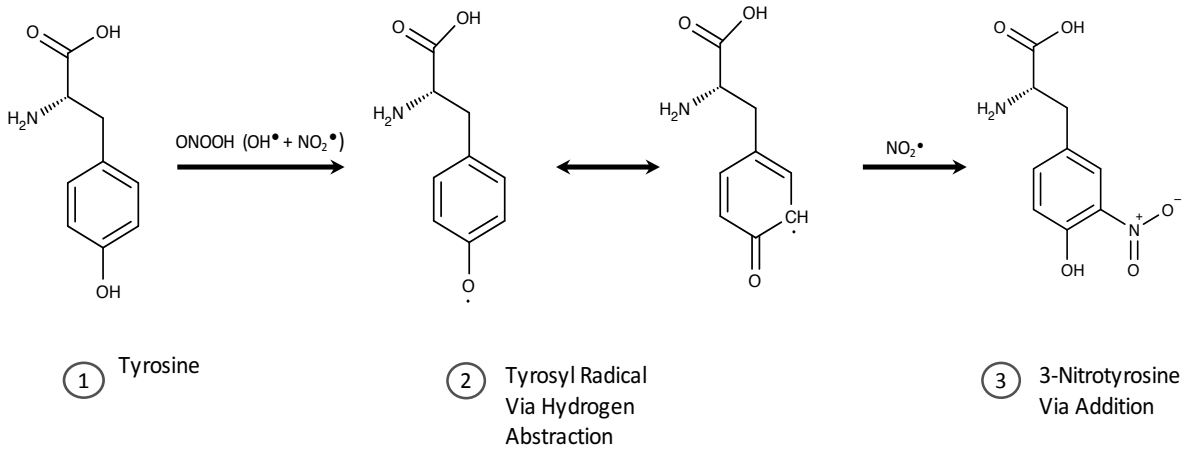

Figure 1.1: Reaction Mechanism of Tyrosine Forming 3-Nitrotyrosine After Peroxynitrite Treatment. Reaction pathway of peroxynitrite-treated tyrosine, showing the formation of the intermediate tyrosyl radical before forming the 3-nitrotyrosine product.

1.3.3 Reactive Chlorine Species

Neutrophils contain the haem enzyme myeloperoxidase (MPO), which converts hydrogen peroxide (H_2O_2) and the chloride anion (Cl^-) into hypochlorous acid (HOCl) (Figure 1.2).

Figure 1.2: Reaction Mechanism of Hypochlorous Acid Formation Catalyzed by the Enzyme Myeloperoxidase.

Hypochlorous acid is a strong oxidant produced by neutrophils (Winterbourn, 2002). In addition to oxidizing biomolecules, hypochlorous acid also reacts with the superoxide radical, to generate the hydroxyl radical. The hydroxyl radical is known to react with a number of aromatic and aliphatic side chains (Valko *et al*., 2007, Stadtman and Levine, 2003 and Gutteridge, 1984). A study performed by Kettle *et al.* (1996) reported the presence of chlorinated amino acids in proteins exposed to myeloperoxidase directly, and also indirectly via stimulated neutrophils. The same study also showed that 3-chlorotyrosine and 3, 5-dichlorotyrosine were formed when peptides and proteins containing tyrosine residues were exposed to hypochlorous acid. These 3-chlorotyrosine and 3, 5-dichlorotyrosine modifications were shown to be minor products of hypochlorous acid reactions, and for this reason sensitive procedures are required to detect tyrosine chlorination (Kettle *et al*., 1996).

In addition to the chlorination reactions, MPO catalyses the oxidation of tyrosine, producing a tyrosyl radical, in a similar way that during 3-nitrotyrosine formation there is an intermediate tyrosyl radical step during formation. HOCl reacts preferentially with sulfur-containing residues, followed by amines (Winterbourn, 2002 and Prütz *et al.*, 1996). The main reaction products of hypochlorous acid with proteins are protein carbonyl groups, formed via breakdown of chloramines to aldehydes (Winterbourn, 2002). The amino acids that can form carbonyl groups include proline, arginine, lysine and threonine (Owen and Butterfield, 2010). At a cellular level, high concentrations of hypochlorous acid have been shown to be cytotoxic, whereas low concentrations have been shown to induce apoptotic pathways (Winterbourn, 2002)

1.4 Overview of Oxidative Stress

The production of biological oxidants is required to maintain cellular homeostasis, and has been shown to be crucial to physiological processes. More specifically, reactive species superoxide ($O_2^{\bullet-}$) and nitric oxide ($NO^{\bullet}$) are products of normal cellular function, and are used in a number of physiological processes. This includes, cell signalling, mitochondrial respiration, vasodilation and cellular defence during phagocytosis by immune cells such as neutrophils (Wall *et al.*, 2012, Karve and Cheema *et al.,* 2011, Valko *et al.*, 2007 and Pacher *et al.*, 2007).

An antioxidant is defined as any substance that delays or inhibits oxidation of a substrate (Sies, 1993). Enzymatic and non-enzymatic anti-oxidants act cooperatively; for example, the reduction of vitamin C, a non-enzymatic antioxidant, by the tri-peptide antioxidant glutathione is supported by glutathione reductase, the enzyme that regenerates reduced glutathione (GSH) using NADPH as a reductant. Another good example of how antioxidants act cooperatively is the antioxidant α-tocopherol (Vitamin E), a non-enzymatic antioxidant, α-tocopherol was shown to be one of the most efficient antioxidants in neutralising lipids by reduction. The resulting tocopheroxyl radical produced is then reduced back to its original form by the aqueous soluble anion ascorbate (Vitamin C). These non-enzymatic antioxidants require enzymatic reduction to return to their former state. In most cells the three most abundant enzymatic antioxidants are superoxide dismutase, catalase and glutathione peroxidase (Sies, 1997 and Sies, 1993).

When reactive species occur in excess, and are not balanced by antioxidant capacity, oxidative stress and associated adverse effects can follow. Oxidative stress has been defined as an imbalance between the homeostatic levels of biological oxidants and their corresponding antioxidants, in favour of the oxidant (Sies, 1997). Some reactive oxygen species (ROS) are free radicals, with one or more unpaired electrons, which are very reactive, and often have short half-lives due to this reactive nature (Toshinori and Heinemann, 2001). The harmful effects of biological oxidants occur when there is an overproduction, and or, a deficiency of enzymatic and non-enzymatic antioxidants used to maintain the balance. In times of oxidative stress these biological oxidants can react with the lipids, proteins and or DNA, altering their normal function, which have various implications in disease (Karve and Cheema, 2011 and Valko *et al.,* 2007).

The regulation of oxidative balance is termed 'redox regulation', meaning the protection of an organism by maintaining redox homeostasis (Valko *et al*., 2007). Under normal healthy biological conditions >90% of glutathione is in its reduced form, GSH, and <10% in the oxidised form, GSSG. When the ratio of oxidised to reduced glutathione increases beyond this, the system may enter oxidative stress, and harmful effects of radicals may ensue (Owen and Butterfield, 2010). The extent and consequences of oxidative stress are dependent on both the intensity and duration of the condition (Karve and Cheema, 2011). Redox balance may fluctuate over a healthy range under normal biological conditions; beyond this the system enters acute or chronic oxidative stress, and may even stabilise at a new, more oxidative level. This is illustrated in Figure 1.3, taken from a review by Lushchak (2014).

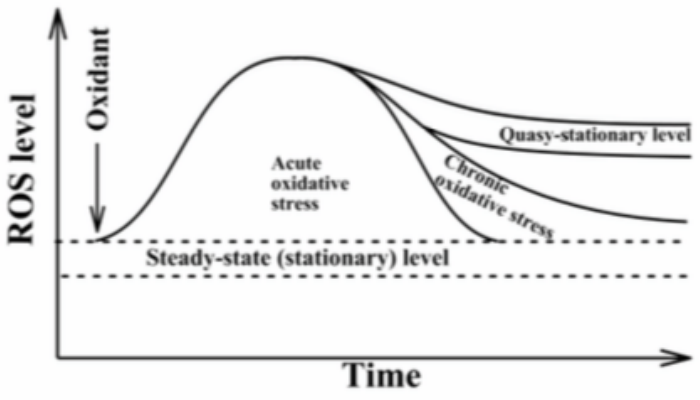

Figure 1.3: How the Dynamic Levels of Biological Oxidants Effect the Degree of Oxidative Stress Over Time. The basic steady-state (stationary) level of biological oxidants fluctuates over a certain range under normal conditions. However, under stress biological oxidants levels may increase beyond the normal range resulting in acute or chronic oxidative stress. Under some conditions, biological oxidants levels may not return to their initial range, and instead stabilize at a new quasi- stationary level (Lushchak, 2014).

1.5 Oxidative Post-Translational Modifications to Proteins

Biological oxidants such as reactive oxygen, nitrogen and chlorine species can modify the biomolecules including DNA, lipids and protein. The main reasons for an increased level of oxidatively modified proteins can be broken down into four main factors: an increase in the rate of production of an oxidising species, a decrease in the scavenging of oxidants by antioxidants, increased susceptibility of proteins (for example, due to altered structure) and finally, a decrease in the rate of removal of modified proteins by proteases including proteasomes (Raynes *et al.*, 2016 and Levine, 2002).

Proteins can become oxidised in a number of different ways, all of which are considered post-translational modifications. These modifications can occur in a multitude of ways, mostly distinguishable by mass spectrometry. The first type of modification involves the oxidative cleavage of either the protein backbone or amino acid side chain. The residues that are most susceptible to these backbone oxidative cleavage type modifications are proline, arginine, lysine, threonine, glutamic acid and aspartic acid (Levine, 2002). The mechanism involves the radical abstraction of the α-hydrogen atom, causing the cleavage of the backbone at the peptide bond; this leaves a carbon-centred radical, which reacts with molecular oxygen (O_2) to form an alkylperoxyl radical intermediate, followed by alkyl peroxide, and finally, an alkoxyl radical. With regard to the alkoxyl radical formed during oxidative peptide fragmentation, in the absence of oxygen the carbon radical may also form a carbon-carbon cross linkage to another protein (Levine, 2002 and Berlett and Stadtman, 1997).

Another type of oxidative modification that can occur is to amino acid side chains, which differ in how easily they can be oxidatively modified (Hoshi and Heinemann, 2001). These modifications can have different effects, some of which alter

physiological cellular homeostasis, and others are a consequence of oxidative stress. For example, phosphorylation is involved in cell signalling pathways, methylation and acetylation in the regulation of gene transcription and protein function, and hydroxylation in the excretion pathways of drug metabolism (Karve and Cheema *et al*., 2011).

Some of these modifications are a chemical consequence of oxidative stress; for example, carbonyl formation on the amino acids lysine, proline, threonine and arginine are well-established hallmarks and measures of general oxidative damage.

The sulphur side chain containing amino acids, cysteine and methionine, are particularly noteworthy as they are amongst the most sensitive residues to oxidation by almost all forms of biological oxidants. Oxidative modifications to cysteine side chains include mono, di and tri oxidation, respectively called sulfenic, sulfinic and sulfonic acids (Poole and Nelson, 2008). Under even mild conditions of oxidative stress, cysteine residues can be modified to disulphides and, methionine, to methionine sulphoxide (MeSOX) (Berlett and Stadtman, 1997). Oxidative modifications of these amino acids are reversible, and could be considered the only truly reversible modifications to amino acid residues. Physiologically, disulphide formation is the most common consequence of cysteine oxidation, and is reversible by reduction back to the thiol state, by thioredoxin system. Methionine also has a side chain containing sulphur, which can be oxidised by a range of biological oxidants. The oxidised form of methionine, methionine sulphoxide (MetO), much like cysteine, can be reduced back to its original state. This reduction is catalysed enzymatically by methionine sulphoxide reductases (MSRs), and consequently MSR is considered an antioxidant and protein repair enzyme (Kim and Gladyshev, 2007; Hoshi and Heinemann, 2001). The oxidation of methionine residues usually has little biological effect, and the cyclic reduction of methionine sulphoxide acts as an innate scavenger of biological oxidants to protect proteins from extensive irreversible

oxidative modifications (Berlett and Stadtman, 1997). Histidine has also been reported to be one of the more susceptible amino acids to oxidation type reactions. A common modification of histidine is 2-oxo-histidine, occurring after exposure to hydrogen peroxide (Uchida, 2003). Another residue susceptible to oxPTMs is tryptophan, which can be modified to N-formylkynureine; kynureine, 5-hydroxytryptophan and 7-hydroxytryptophan. As previously described, modifications to tyrosine residues after exposure to nitrating and chlorinating species can form 3-nitrotyrosine and 3-chlorotyrosine, which are considered potential markers of inflammation (Mann and Jensen 2011, Dalle-Donne *et al*., 2003, and Karve and Cheema *et al*., Levine, 2002). The final type of modification to proteins is the indirect addition of bimolecular oxidative products, for example the addition of lipid peroxidation product malondialehyde (Levine, 2002). Because proteins have many different unique functions, such oxidative modifications can have diverse functional consequences. For example, oxidative structural modifications to enzymes can inhibit their normal activity. Enzymes with metal near their active site are particularly susceptible to metal catalysed oxidation, and a subsequent inhibition of function. These types of modifications can have mild or severe effects on the cellular system, depending on the percentage, and location of the oxidative modification (Shacter, 2000). The cellular function of biological organisms relies on the functionality of proteins, which provide multiple levels of structure, allow intra and extra cellular movement, carry out enzymatic reactions, and conduct cell signalling to manage biological pathways (Raynes *et al*., 2016). The modifications described can therefore have various implications for biological systems and in the pathology of various diseases. Table 1.1 provides an overview of the most common types of side chain oxidative modifications that can occur.

Table 1.1: The Commonly Occurring OxPTMs to Amino Acids by Biological Oxidants.

Amino Acid	Reaction	Modification
Arginine	Oxidation	Glutamic semialdehyde
Lysine	Oxidation	α-aminoadipic semialdehyde
Proline	Oxidation	Glutamic semialdehyde and 5-oxoProline
Threonine	Oxidation	2-amino-3-butyric acid
Histidine	Oxidation	2-oxohistidine
Cysteine	Oxidation	Cysteine sulfenic acid, Cysteine sulfonic acid, Cysteine sulfinic acid and Cystine (disulfide bonds)
Tyrosine	Oxidation	Dityrosine and 3-hydroxytyrosine
Tryptophan	Oxidation	5-hydroxy-tryptophan
Phenylalanine	Oxidation	2,3-dihydroxyphenylalanine, 2-, 3-, and 4-hydroxyphenylalanine
Methionine	Oxidation	Methionine sulfoxide and methionine sulfone
Tyrosine	Nitration	3-nitrotyrosine
Cysteine	S-nitrosylation	S-nitrosocysteine
Tyrosine	Chlorination	3-chlorotyrosine

1.6 Oxidative Modifications to Proteins in Disease

As previously discussed, proteins have a diverse range of cellular functions, and post-translational modifications of these proteins can impair their normal function. And for these reasons, OxPTMs to proteins play a role in the pathology of many diseases (Karve and Cheema, 2011). Carbonyl formation is considered a well-established hallmark of oxidative stress and is currently the commonly used indicator of oxidative stress (Karve and Cheema, 2011). Protein carbonyls have been identified in Alzheimer's disease (Carney *et al*., 1994), amyotrophic lateral sclerosis (Bowling *et al*., 1994), cataractogenesis (Garland *et al*., 1988), systemic amyloidosis (Ando *et al*., 1997), muscular dystrophy (Murphy and Kehrer, 1989), Parkinson's disease (Yoritaka *et al*., 1996), progeria, Werner's syndrome (Oliver *et al*., 1987), rheumatoid arthritis (Tetik *et al*., 2010), and respiratory distress syndrome (Gladstone and Levine, 1994). The measurement of increased oxidative stress by carbonyl formation in these diseases, further confirms the oxidative inflammatory aspect of their pathology.

More specific modifications include, amongst others, oxidation of tryptophan, histidine and cysteine residues. Cysteine modifications, including sulfenic, sulfinic and sulfonic acids, have been observed in diseases with an oxidative pathology. And serve as both markers of cell signalling, and diseases with an oxidative pathology, such as cancer and cardiovascular disease (Pan and Carroll, 2013). Oxidative modifications of tryptophan include, N-formylkynureine; kynureine, 5-hydroxytryptophan and 7-hydroxytryptophan (Dalle-Donne et al., 2003). These modifications have been reported to have implications in infectious and autoimmune diseases, neurological diseases such as Alzheimer's disease (AD), Huntington's disease (HD) and Amyotrophic Lateral Sclerosis (ALS) (Chen and Guillemin, 2009).

The 2-oxo-histidine modification can be produced after exposure to hydrogen peroxide, and has been observed in the enzyme superoxide dismutase, inactivating its active site. This 2-oxo-histidine modification of superoxide dismutase has been linked to the pathology of familial Amyotrophic Lateral Sclerosis disease, and, β-amyloid, a peptide implicated in Alzheimer's disease (Lee and Helmann, 2006 and Uchida, 2003).

The aging process is another good example that illustrates how modifications to proteins can have observable biological effects. One of the first, and most well-established theories of aging was proposed originally by Denham Harman in 1956, where he proposed aging and the associated degenerative diseases to be attributed to excessive production of radicals and the consequent damage to biomolecules (Harman, 1956). This theory was later updated by the rate of living theory, which stated that an increased rate of mitochondrial respiration would lead to an increased production of oxygen radicals and therefore speed up ageing as a consequence (Beckman and Ames, 1998). Several studies have shown specific enzymes to be oxidatively modified during aging e.g. glutamine synthetase. Carbonyl group formation is considered a hallmark of oxidative stress, based on Harman's theory of aging, modifications to biomolecules such as the enyzme glutamine synthetase are indicative of aging. More specifically, a significant increase in the general number of protein carbonyl groups was seen after glutamine synthetase was modified (Hipkiss, 2006 and Shacter, 2000).

1. 7 Susceptibility of the Fibrinogen Protein to Modification

William Hewson was the first to describe the clot formation protein fibrinogen in 1770. Before this the clot formation process was thought to be determined by the activity of red blood cells. Subsequently, this work paved the way for the future work that provided a better understanding of thrombin, prothrombin and the coagulation cascade (Doyle, 2006).

Fibrinogen is a 340 kDa glycoprotein, made up of two pairs of three non-identical chains (hexamer). It is synthesized in the hepatocytes and is one of the most abundant plasma proteins, constituting 4% of the total plasma protein. It is a positive acute phase protein, which means that during inflammation its plasma concentration increases. Epidemiological studies have indicated that increased levels of circulating fibrinogen is a predictor of coronary heart disease (Vadseth *et al*., 2003). Fibrinogen is used biologically in the blood to allow clot formation, essentially, plugging blood vessels and wounds to prevent fatal loss of blood. The mechanisms of this reaction involve the addition of thrombin, which acts as a serine protease, to cleave fibrinopeptides A (FpA) and B (FpB) to expose knob A and knob B. These knobs then go on to associate with each other, and form fibrin type fibers used in the clot formation process (Martinez *et al.,* 2013, Anderson and Anderson, 2002, Castell *et al.,* 1989, and Laki, 1953).

A study performed by Shacter *et al*., 1994 showed fibrinogen as the most susceptible plasma protein to oxidation with Western blotting for carbonyl formation with anti-DNP antibodies. The study showed albumin, being the most abundant plasma protein, as having the greatest absolute oxidation levels. However, as a ratio of protein to oxidation, fibrinogen showed 20 times more oxidation than albumin. The respective study concluded fibrinogen to be the most susceptible plasma protein to oxidation (Shacter *et al*., 1994). The levels of 3-nitrotyrosine were shown to be higher in patients with coronary artery disease when compared to healthy

controls, respectively, 9.1 μmol/mol tyrosine and 5.2 μmol/mol tyrosine. (Shishehbor *et al*., 2003). A study by Vadseth *et al*., in 2003 showed more specific protein nitration with 3-nitrotyosine formation in fibrinogen, and, functional alterations in fibrinogen/fibrins physical properties that could lead to a pro-thrombotic state. The data indicates that tyrosine nitration selectively alters fibrinogens function and physical properties, promoting clot acceleration, which may account for the association between nitration of fibrinogen and coronary artery disease (Vadseth *et al*., in 2003).

1.8 Overview of Methods for Detecting Modifications to Proteins

Measuring carbonyl group formation is a well-established method for quantifying general oxidation. One of the most common methods of detecting carbonyl group formation involves the derivatisation of carbonyl groups with 2,4-dinitrophenylhyrdrazine (DNPH) to 2,4-dinitrophenylhyrdrazone (DNP), followed by either spectrophotometric measurement, or immunodetection with DNP specific antibodies, either in gels or in ELISA type immunoassays (Shacter, 2000). However, such assays lack specificity, and are unable to identify the precise residues modified. The use of MS allows a more precise analysis of carbonylation, identifying and quantifying specific amino acids and their locations within a given protein. Even though these types of techniques are considered the standard methods of detecting protein carbonyls, they are not without limitations. The focus of the limitations resides with the use of DNPH. Where DNPH was shown to rapidly degrade, form further carbonyl groups, react with oxidized thiols, and spectrophotometric measurements in the presence of any other chromophores with an absorbance of 370 nm can provide false positives (Rogowska-Wrzesinska *et al.*, 2014).

There are a number of chromatographic methods for detecting 3-nitrotyrosine, each of which displaying disadvantages as a result of sample preparation intended to overcome either selectivity or sensitivity limitations. Gas chromatography (GC) provides the best sensitivity but requires pre-analysis derivitisation, whereas HPLC does not, but is also less accurate. Coupling HPLC to MS can overcome such limitations, allowing robust unambiguous identification of modifications without producing artefacts during the chromatography derivitisation steps, and for this reason MS is considered the gold standard technique for identifying modifications to proteins (Teixeira *et al.*, 2016, and Pitt and Spickett, 2008). The process involved in MS analysis is, however, both time consuming and complex. Immunological assays

are a quick and cheap means of identifying such modifications. Many antibodies and ELISA type techniques exist for identifying and quantifying 3-nitrotyrosine (Tsuneki *et al*., 2015, Ashraf *et al*., 2014, Satoh *et al*., 2008, Zhang *et al*., 2014, Nagai *et al*., 2002). A study performed by Safinowski *et al*., 2009 compared different immunoassays for 3-nitrotyrosine. The study concluded inconsistencies in the reliability of the results. The observed discrepancies were thought to relate to the low abundance of 3-nitrotyrosine (Safinowski *et al*., 2009). There are a few critical limitations with the ELISA, including: (i) antibodies may display some non-specific binding, and (ii) 3-nitrotyrosine may not be accessible to the antibody in some protein sites due to tertiary and quaternary structure (Teixeira *et al*., 2016). Similarly to 3-nitrotyrosine, chromatographic and MS techniques to detect and quantify 3-chlorotyrosine exist, along with their limitations (Hazen and Heinecke, 1997). With regard to antibody-based techniques, detecting 3-chlorotyrosine is limited by the availability of specific antibodies. Several cited studies that have successfully utilized the polyclonal anti-chlorotyrosine antibody from Hycult Biotech (Zhou *et al*., 2015, Nishikawa *et al*., 2012, Robaszkiewicz *et al*., 2011, Rudolph *et al*., 2010, Siwak et al., 2013). A study by Lu *et al*., 2015 successfully used the anti-3-chlorotyrosine antibody (Hycult, Biotech) in Western blotting and immuno-precipitation experiments (Lu *et al*., 2015). The reliability of immunoassay techniques is largely dependent on the specificity and avidity of the antibodies used; currently available commercial antibodies are known to show variance in avidity (Khan *et al*., 1998).

1.9 Fundamentals of Mass Spectrometry for Analysing Proteins

1.9.1 Introduction to Mass Spectrometry

Mass Spectrometry (MS) characterises molecular ions based on their mass-to-charge ratio, and using their response to electrical or magnetic fields (Fenn *et al.*, 1989). It can also be used to characterise and confirm oxidative modifications to amino acid residues, as these alter the mass of the molecular ion. The resulting data output, or spectrum is presented as intensity, y-axis, versus m/z on the x-axis. The mass to charge ratio is the relationship of the ions molecular mass and the number of charges that the ion carries, and intensity is the relative abundance of the molecular ion (Verrastro *et al.*, 2015). Mass spectrometers contain an ionisation source, at least one mass analyser (depending on whether it is single or tandem) and a mass detector. The technique relies on the generation of gas phase ions of the analyte in the ionisation source, followed by separation according to the mass-to-charge ratio of the produced ionised fragments. This involves the use of one of many multiple types of mass analysers, and detection by a micro-channel plate detector. There are a number of different types of MS ionisation sources, mass analysers and detectors, some of which will be discussed further throughout.

1.9.2 High Performance Liquid Chromatography for MS

Samples are first separated before injection into the MS. In order to achieve this the MS is connected to a chromatography system known as high performance liquid chromatography (HPLC). Chromatography relies on different mobile and stationary phases to separate molecules by their affinities. This chromatography system operates at high pressure to achieve good separation resolution. Most HPLC configurations for proteomics utilise reverse phase HPLC, whereby analytes elute into the ionisation source based on their retention time, in reversed HPLC, to a

hydrophobic non-polar stationary phase and an aqueous polar mobile phase. Protein or peptide analytes are eluted off the column using a gradient of non-polar organic solvent introduction. The respective eluents are separated as mentioned by their retention time to a non-polar stationary phase, such as an 18-carbon chain (C-18) silica column. Reverse-phase columns are well suited to MS analysis, as they offer varied analysis, compatibility with ionization systems, and most importantly high reproducibility and separation efficiency (Regalado *et al.,* 2013).

1.9.3 Electrospray Ionisation

Solvent is passed into the source through a fine capillary needle, held at high potential (2-4kV) (figure 1.4), resulting in a fine spray of droplets. These gas phase ions are produced as a result of four main processes: the formation of highly charged spray droplets due to the potential provided by the capillary needle, evaporation of the carrier solvent is enhanced by heating the ion source and the introduction of a flow of warm nitrogen gas known as drying gas, which causes the droplet size to decrease and the charge density to increase. During the final stage the droplet reaches its Raleigh limit, and undergoes coulomb fission, whereby the droplet explodes into smaller more stable droplets. This process continues until gas phase ions of individual molecules are formed. Any remaining solvent vapour, or uncharged material, is swept away by nitrogen gas, known as the curtain gas. Electrospray can produce both positive and negatively charged ions by the addition of volatile acids or bases to the solvents, either providing or removing protons. As a soft ionization technique, producing ionized intact proteins, electrospray is well suited to analysis of biomolecules such as proteins (Pitt, 1998 and Fenn *et al*., 1989). Other soft ionization techniques suited to biomolecules such as proteins also exist, of which the best known is matrix-assisted laser desorption ionisation (MALDI) (Mitchell Wells and McLuckey, 2005).

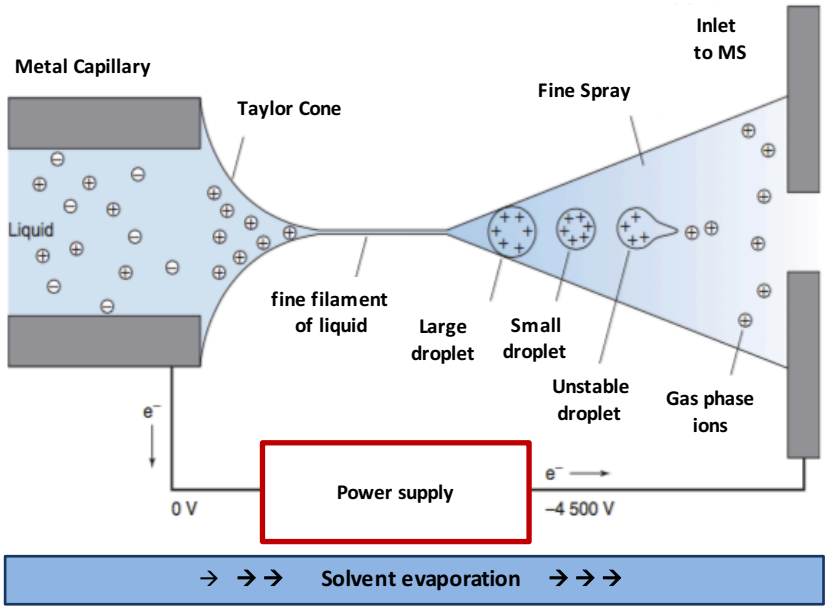

Figure 1.4: Electrospray Ionization Technique Diagram. The electrospray ionization technique is a soft ionization method that is well suited to analysis of biomolecules, due to its ability to produce ions without fragmentation.

1.9.4 Collision Induced Disassociation and Peptide Fragmentation Patterns

Soft ionisation techniques allow the molecular ions, such as peptides, to be analysed without fragmentation. However, structural elucidation of biomolecules requires subsequent fragmentation of the precursor or parent ion. A few different techniques are available for fragmentation of proteins or peptides for further analysis with MS^2; the most common are electron transfer dissociation (ETD), collision induced dissociation (CID) and high-energy collisional dissociation (HCD). The non-targeted mass spectrometry approaches in this study utilised quadrupole-TOF with collision-induced disassociation (CID) fragmentation (figure 1.5). The peptide or protein molecules enter the collision cell (Q2) and collide with inert gas, such as nitrogen or argon, the produced kinetic energy is converted into internal energy, which results in the bonds vibrating and breaking, and the fragmentation of the molecular ion into smaller fragment ions (Mitchell Wells and McLuckey, 2005). There are a number of fragment ions that can be produced from peptides: a, b and c ions correspond to peptide fragments whereby the charge resides on the N-terminus, whereas, x, y and z ions, the charge resides on the C-terminus (Figure 1.5A). Typically, CID generates predominately b and y series fragment ions, whereby the peptides break around the peptide bond, and b and y ions are produced (Ross *et al*., 2004) (Figure 1.5B and 1.5C).

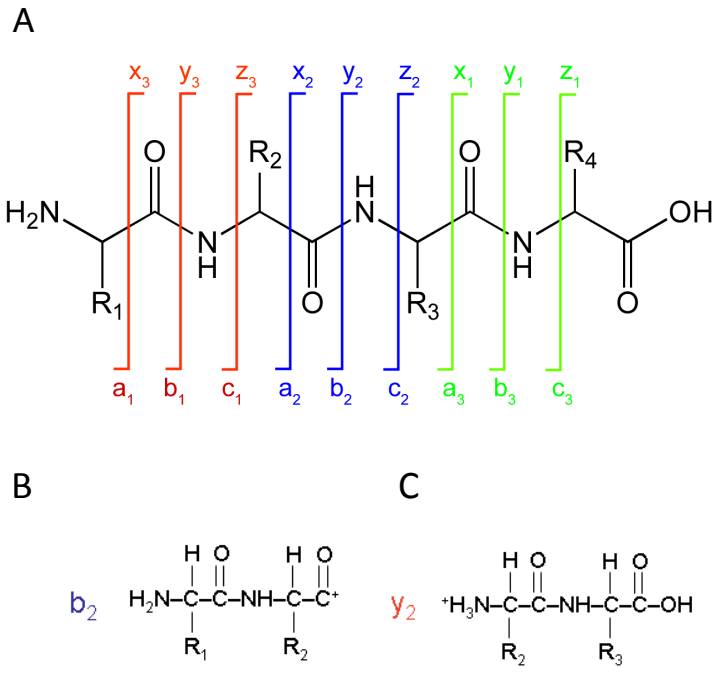

Figure 1.5: Peptide Fragmentation Pattern. (A) Peptide fragment ion nomenclature, a_1, b_1 and c_1 ions represent fragment ions of the first amino acid with the charge residing on the N-terminus, and x_1, y_1 and z_1, fragment ions of the first amino acid with the charge residing on the C-terminus (B) and (C) shows an example of a b and y ion fragment, with the charges residing on the N and C-terminus respectively.

1.9.5 Quadrupole and Time-of-Flight MS Mass Analysers in MS

A quadrupole mass analyser uses four parallel rod electrodes in a square formation around a central axis (figure 1.6). A negative direct current (DC) is applied to all four rods, and a superimposed alternating (AC) radio frequency (RF) positive current is applied to two of the rods at any given time, moving around the rods from x to y-axis in a clockwise direction. The combination of alternating RF and fixed DC are varied in magnitude, and allows the quadrupole to operate as an ion filter. When ions are injected along the central z-axis, if the ratio of the destabilising RF potential applied is not too great or little for the corresponding ions, they will spiral with a clear trajectory through the quadrupole to the detector. The balance of applied potential allows precise mass selectivity, and ions with masses that are not stable with the applied potential will disperse away from the space and not be detected. Thus, the sample ions are separated by the stability of their trajectories in the oscillating electrical field (Hoffmann and Stroobant, 2007). This balance of applied potential can be alternated, and used in a scanning mode, allowing all possible masses in a given range to be selected for detection (Misek, 1993).

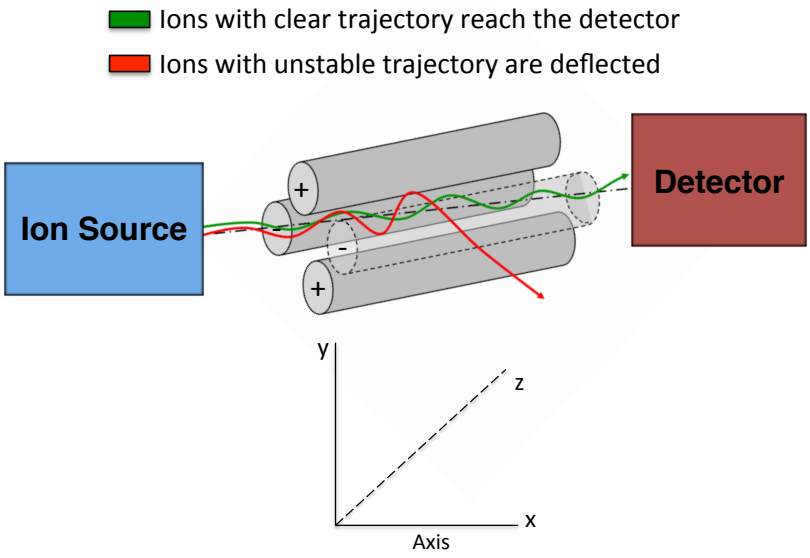

Figure 1.6: Quadrupole Mass Analyser. The electrospray ionization technique is a soft ionization method that is well suited to analysis of biomolecules, due to its ability to produce ions without fragmentation. Ions travel from the ion source through the quadrupole across the z-axis towards the detector. The trajectory of ions to the detector is dependent on the amount of DC and RF potential applied to the rods, acting as an ion filter. Ions move along the z axis. More specifically, the red line illustrates ions moving along the z-axis, which do not have the correct corresponding mass for the applied field, and as such are deflected away from the quadrupole. Whereas, the green line illustrates the ions that have a stable trajectory based on the applied field, and therefore travel through the centre of the quadrupole to the detector.

1.9.6 Quadrupole Multiple and Single Reaction Monitoring Programmes

Multiple (MRM), and single (SRM) reaction monitoring modes are similar MS modes of analysis, whereby MRM analyses multiple precursor and product ions, and SRM just one. In order to understand the procedure, the MRM mode is described. It utilises three quadrupoles, of which 2 are mass analysers and the other is a collision cell. The first quadrupole (Q1) selects the desired precursor ion by mass; the second quadrupole (Q2) generates the fragment ions of this precursor ion via collisional induced disassociation. Finally, the third quadrupole (Q3) is configured to specific fragment ion masses, of the precursor ion. This method provides increased sensitivity. This is because only the ions of interest pass through the first and third quadrupoles and reach the detector (Anderson and Hunter, 2006). In these modes triple quadrupole systems have some advantages over quadrupole-time-of-flight systems. The normal use of the quadrupole system is limited by its scanning nature, scanning through the mass range limits the acquisition rate and as such the sensitivity. However, in MRM and SRM modes this problem is overcome, and triple quadrupoles are more sensitive than quadrupole-time-of-flight systems, relating to the dead time required by the respective system to calculate the TOF. For these reasons triple quadrupole systems are well suited to quantifying known mass ions to high sensitivity. Triple quadrupole mass analysers are however limited by mass resolution and to mass ranges of 1 – 4000 m/z, when compared to a quadrupole–time–of– flight system, with a working mass analysis range of 20 – 20,000 m/z (Harris, 2010 and, Domon and Aebersold, 2006).

The time-of-flight mass analyser works by applying a high voltage of 5,000 V to the back plate, accelerating ions, expelling them from the ion source and into a drift region. Here there is no electrical or magnetic field and as such, no further acceleration. If all ions have the same kinetic energy, but differ in mass, the lighter ions will travel to the detector faster than the ions with a larger mass. The sample ions are separated by the time it takes them to reach the detector, relative to velocity, which is relative to their mass (Hoffmann and Stroobant, 2007). Unfortunately, not all ions leave the ion source and begin the path to the detector with the same kinetic energy. In order to equalise the kinetic energy of the ions, they enter the reflectron. Which is made up of hollow, increasing gradient, of positively charged rings used to stop and redirect the ions. The reflectron is terminated by the grid at the point whereby the potential becomes greater than the original accelerating potential. The more kinetic energy the ion has, the further into the reflectron it will travel, and as such the more it will slow down. This process equalises the kinetic energy of the ions before they begin their measured time-of-flight journey to the detector, meaning all ions of the same mass reach the detector at the same time, improving resolution (Harris, 2010). Time-flight-systems as mentioned show less sensitivity than triple quadrupole based systems in MRM or SRM modes, however, when identifying unknown analytes, the TOF system is better suited. A non-scanning instrument such as a TOF system offers many advantages including fast acquisition rates, spectral continuity, and exceptional dynamic range. But most importantly, under normal conditions, greater mass resolution than triple quadrupole based systems, making it well suited to identifying modifications to amino acids (Domon and Aebersold, 2006).

1.9.7 Mass Spectrometry as a Technique for Analysing Modified Proteins

Tandem mass spectrometry (ESI-MS^2) can be used in protein analysis to confirm peptide sequences that contain oxidative amino acid modifications (Pitt and Spickett, 2008). MS measures the mass-to-charge ratio (m/z) of ionized analytes, and subsequently, oxidative modifications to proteins change the m/z ratio of the intact protein, and of the residues where the oxidative modification occurred, allowing identification of the site of oxidative post-translational modification (oxPTM). The current accepted method of identifying oxidative modifications involves isolating the modified amino acid within the protein sequence (Abello *et al*., 2009). Two main approaches exist for identifying modifications to proteins, top-down and bottom-up. The former involves analysis of intact proteins and their fragmentation products in the MS, while the latter involves proteolyic digestion of proteins into peptides by proteases such as trypsin before analysis. The latter is the most common approach for proteomics and for identifying modifications to proteins in biology. In order to facilitate data analysis, a number of statistical search engines are available, such as Mascot©, PEAKS©, Sequest©, ProteinPilot©, Tandem©, Ommsa© and Phenyx©, each of which has advantages and disadvantages. In most cases, peptide sequences are searched against a protein database (*in-silico* data), and any sequence in the database that partially matches the experimental sequence was investigated for a fit to the data. The search engines are susceptible to false positive identifications due to the error tolerant nature of the search engines, and for this reason, manual validation by *de-novo* sequencing was critical for confidence in the assignments. A study performed by Stevens *et al*. (2008) illustrates the importance of high mass resolving accuracy when identifying nitrated tyrosine residues using tandem mass spectrometry (MS^2), and the need to manually validate data by *de novo* sequencing modification sites, in order to avoid problems with isobaric molecules (peptides of the same mass, constituted of different amino acids). The same study suggested

manually validating all MS^2 spectra peaks with a relative abundance of ~20% and higher (Stevens *et al*., 2008). A study performed by Peterson *et al*. (2001) highlights that precursor ion scanning with a quadrupole mass analyser can be used for selective detection of nitrated peptides, based on a tryptic digest of nitrated blood serum albumin (BSA) (Peterson *et al*., 2001).

There are several specific data analysis techniques and MS modes that can be utilised to identity and quantify modifications to proteins. These include neutral loss, precursor ion scanning and targeted SRM and MRM methods, as mentioned earlier. In precursor ion scanning the second mass analyser (Q3) is fixed to detect a specific fragment ion mass and scans for precursor ions that generate this product ion upon fragmentation in the collision cell. Commonly, immonium ions of oxidised amino acids are detected and quantified as product ions. In neutral loss scanning, the reporter fragment is uncharged and is monitored by scanning with both mass analysers (Q1 and Q3) with a mass offset corresponding to the mass removed. Searching, or mining, of high-resolution data sets of untargeted experiments can also be achieved by narrow-window extracted ion chromatograms. Narrow window extracted ion chromatograms (XIC) utilise high mass resolution to allow the data to be searched for reporter ions, with a very narrow mass window, providing a significant reduction in false positive isobaric molecules (Verrastro *et al*., 2015).

1.10 Fundamentals of Immunoassays

While mass spectrometry approaches are capable of providing very detailed information on oxidized proteins, they are complex and time-consuming to perform, and for these reasons antibody-based approaches to measure protein oxidation is far more popular. The enzyme-linked immunosorbent assay (ELISA) is a well-established type of immunoassay that has many applications, including the detection of oxidised proteins. The assay relies on antibodies conjugated to an enzyme binding electrostatically by Coulomb forces to an antigen, and the quantification of the respective enzyme-substrate reaction is often achieved spectrophotometrically. The addition of the substrate causes a measurable reaction, the extent of which is proportional to the amount of plate bound antigen (Janeway, 2001, Hennion and Barcelo, 1998 Voller *et al*., 1978 and Wisdom, 1976), as shown in figure 1.7.

A number of variations of the ELISA type immunoassays exist (Figure 1.7). The simplest ELISA, 'Antigen capture', requires only one antibody. In contrast, in the direct ELISA antigens such as proteins and peptides adsorb onto the plate wells electrostatically, and are then quantified by enzyme-conjugated antibodies (MacBeath, 2002). The Sandwich ELISA is a slightly modified ELISA, in that a capture antibody is bound to the plate, the sample containing the analyte is added and binds the capture antibody, and finally the primary antibody is added and binds the epitope of the antigen, more specifically via the antibody paratope amino acids hydrogen bonds and Van Der Waals forces to those of the antigen epitope. The competitive inhibition assay is considered relatively quantitative. One example of a competition based ELISA is as follows: biotinylated antigen is added and binds to the plate via the antibody, the sample of unknown concentration is added and competes with the biotinylated antigen for binding to the capture antibody. Enzyme-

bound streptavidin is then added, binding specifically to the biotinylated antigen. The substrate of the enzyme is then added, and after colour development the reaction measured. The level of inhibition is relative to the amount of the non-biotinylated unknown antigen (Owen 2012, Janeway 2001, Voller *et al.*, 1978, and Wisdom, 1976).

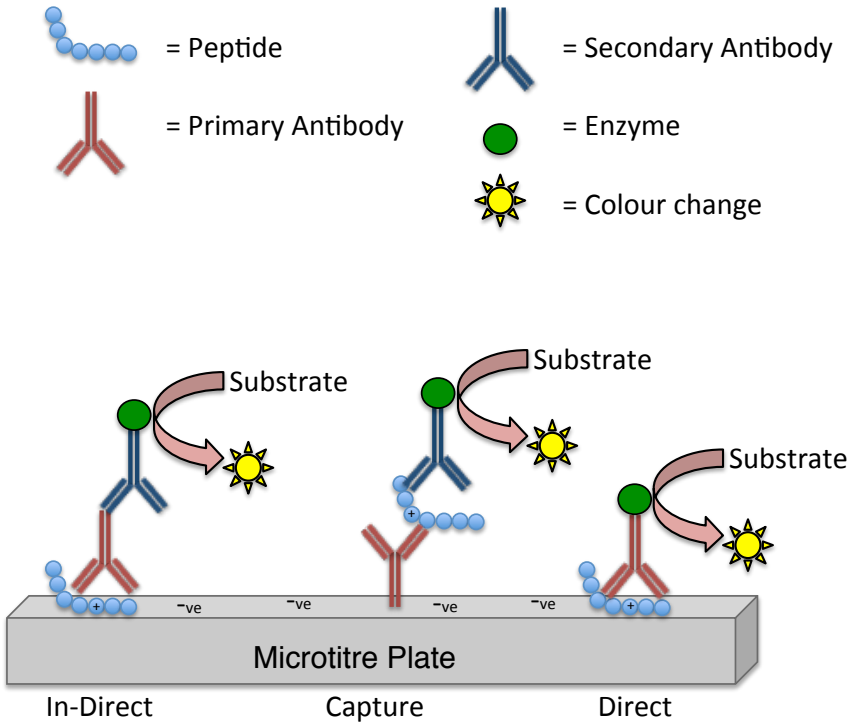

Figure 1.7: A diagram showing the fundamental components of an ELISA type immuno-assay. An in-direct ELISA is comprised of the antigen (peptide) electrostatically bound to the microtitre plate; the complementary antibody, which is bound with an enzyme, is added. Upon binding the substrate is added and the reactions measured. The capture ELISA involves binding the primary antibody to the plate, adding the antigen, followed by the secondary antibody-conjugated to an enzyme, and finally adding the substrate and measuring the reaction. In the direct ELISA, the primary antibody is conjugated with an enzyme; the substrate is added after binding and the reaction measured.

In addition to ELISA type immunoassays, various other antibody techniques exist, such as Western blotting whereby protein binding can be visualised on a membrane. Following gel electrophoresis separation of protein solution, a sandwich including the produced gel and a polyvinylidene fluoride (PVDF) membrane are constructed, as can be seen in chapter 2 (figure 2.1). The proteins are then electrophoretically transferred onto the membrane. The membrane is then used for treatments, similar to other immunoassay techniques. More specifically, the membrane is blocked with a non-reactive protein solution, such as BSA, a specific primary antibody is then added, followed by a secondary enzyme conjugated antibody, such as horseradish peroxidase (HRP). This is often detected by chemiluminescence reagents, and the subsequent signal produced is captured under dark room conditions (Brunette, 1980).

1.10.2 Considerations of Immunoassays for Analysing Modified Proteins

Immunoassays, like all assays, have some advantages and disadvantages, most of which are dependent on the specificity of the antibodies used. Antibodies to a variety of modification-containing residues are available. A few examples include anti-DNP, anti-3-nitrotyrosine and anti-3-chlorotyrosine. Antibodies are known for their cross-reactivity with compounds that are structurally similar to their target analyte /molecule. As the size of the target analyte/molecule decreases, the probability of cross reactivity increases. This is relevant when considering small peptides and modified amino acid residues, as they are considered small molecules. Molecules of low molecular weight (<1000 kDa), such as peptides and modified amino acids, are unable to evoke an immune response by themselves. They therefore require modification by binding them to larger carriers such as whole proteins. A common carrier is keyhole limpet hemocyanin (KLH), which is phylogenetically distant from mammalian proteins, and as such can be conjugated to a molecule of low molecular weight to increase its mass and immunogenicity (Harris and Markl, 1999, and Hennion and Barcelo, 1998). A study performed by Franze *et al*. (2004) produced 6 antibodies with strong affinity for 3-nitrotyrosine, all of which utilised a carrier protein to enhance immunogenicity, and were tested for their ability to detect nitrated proteins in immunoassays such as the ELISA (Franze *et al*., 2004). The 1A6 monoclonal antibody complementary to 3-nitrotyrosine is well characterised, and commercially available. However, it is not clear whether this antibody recognises all proteins containing nitrated tyrosine residues. The study by Franze *et al.* (2004) highlighted the effect of competitive adsorption of the native protein in direct immunoassays, where the proportion of native protein is usually greater than the modified, and the limited plate binding capacity means binding may become saturated before all protein is bound. Hence it is difficult to obtain a true

representation of the proportion of 3-nitrotyrosine in a sample. One way to avoid this problem is to utilise the sandwich assay, which avoids this effect, and is thought to be able to detect trace amounts of nitrated protein in samples, in the presence of a high excess of native protein. The nature of the sandwich ELISA means the nitrated protein is exclusively captured from the sample onto the plate, before adding the detecting antibody. It appeared that the affinities of the antibodies for nitrated proteins are not only governed by the number of 3-nitrotyrosine residues per protein molecule, but also by their position in the structure, with more and less favourable binding sites (Franze *et al*, 2004).

Another major consideration that highlights the cross-reactive nature of many commercially available antibodies is how immunoassay type techniques show variability between laboratory samples. This is true of both antibody specificity and variations in antibody affinity (Onorato et al., 1998). Multiple other factors must also be considered when comparing results between laboratories; for example, the affinity between the antibody and the microtiter plate must also be considered, as significant variations between plate types exist (Matyas, Rao and Alving, 2002). When considering mixtures of proteins, the ELISA is at best semi-quantitative. This relates to protein conformation and the ability of a given antibody to access and bind the epitope of interest, which can be affected by the molecular environment, such as pH. (Khan *et al*, 1998). Both the study performed by Khan *et al*. (1998) and that by Duncan (2002) stated that poor antibody-antigen specificity results in poor data, and that antibodies complementary to 3-nitrotyrosine show variance in their specificity, depending on the amino acids adjacent to the 3-nitrotyrosine residue (Khan *et al*., 1998). Importantly for this work, the study suggested that this sequence-specific discriminatory power might be useful in producing more specific antibodies (Khan *et al*., 1998).

1.11 Focus, Aims and Hypothesis of this Thesis

Protein oxidation occurs in a variety of diseases with an inflammatory pathology, owing to immune cell activation and the release of reactive oxidants, offering potential for diagnostic or prognostic markers of disease. The most commonly used, simple and readily translatable methods are those involving antibody-based assays, such as ELISA and Western blotting, but they are often hampered by the availability of antibodies with suitable specificity, especially if oxidative modifications to a specific protein are of interest.

Fibrinogen is one of the most abundant plasma proteins, and has been implicated in the pathology of various inflammatory diseases. Therefore, the overall aim of the research project was to develop new biomaterials for detecting inflammatory protein oxidative damage to fibrinogen. More specifically, in order to achieve this, the initial goal was to identify stable modifications to fibrinogen as good potential markers of oxidative damage by various oxidizing species, and to produce anti-sera that bind the modified peptides with sequence and modification site specificity. The hypothesis was that antibodies could be produced for human fibrinogen peptides with both sequence and modification site specificity, to a number of oxidative modifications, similar to those that might be expected during inflammation.

Chapter 2

Materials and Methods

2.1 Reagents

All reagents were obtained from Sigma-Aldrich or Fisher Scientific, UK, unless otherwise specified. Human fibrinogen with 70% purity was obtained, and used throughout. Instant blue Coomassie stain was acquired from Expedeon, Cambridge, UK. Skimmed milk powder was purchased from Tesco, UK. Protein marker (10 – 250 kDa) was obtained from Thermo-Fisher (Part of Fisher Scientific). MS grade trypsin was sourced from Promega, Southampton, UK. Polyvinylidene fluoride (PVDF) membrane was obtained from Millipore, Watford, UK. Tween 20 was purchased from Fisher Scientific, Loughborough, UK. SuperSignal West Pico Chemiluminescent substrate (ECL reagent) was purchased from Thermo Scientific (Part of Fisher Scientific). The KLH (77600), maleimide (77164) and sulfosuccinimidyl-4 -[N-maleimidomethyl] cyclohexane-1-carboxylate (sulfo-SMCC) (22322) were also purchased from Thermo-Scientific. High binding Nunc immuno maxi sorp plates (M9410-1CS) were obtained from Thermo Fisher. All solvents were of LC-MS grade and all solution preparations were made using ultra-pure Milli-Q water, and all solutions where a solvent is not specified were prepared in Milli-Q water.

2.2 Synthesis of Novel Peptides with Solid Phase Synthesis

A 70-mL fritted filtration column (Fisher Scientific, UK) was used. The resin used was 0.11 mM FMOC-Cys (Trt) (Novabiochem, UK) in 20% piperidine dimethylformamide (DMF), at a final volume of 20 mL. The 20% piperidine solution de-protected the resin by removing the FMOC group. The solution was vacuum dried. The sample was first washed with dichloromethane (DCM), followed by ethanol. This was repeated to ensure all of the piperidine solution was removed. Each amino acid was added in molar equivalence, based on a 20 mL final volume, to the resin (0.11 mM), followed by 0.55 mM benzotriazol-1-yl-oxytripyrrolidinophosphonium hexafluorophosphate (PyBOP) (CEM) (5:1), 0.55 mM hydroxybenzotriazole (HOBT) (5:1), DMF was added followed by 1.1 mM *N,N*-diisopropylethylamine (Dipea) (10:1). The solution was left in the column for at least 30 minutes. The column was then drained on a vacuum manifold, and washed with DCM and ethanol as before. This process was repeated sequentially according to the peptide sequence. Several different peptides were synthesised throughout, shown in Table 2.1.

Table 2.1: Synthesized Peptides List. The peptide DYEDQQKQLC was selected from a study performed by Bergt *et al.,* 2004, and is further described in chapter 4. The peptides identified in this study by MS are further described in chapter 3. The peptide with the sequence YICENQDSISSKC were identified in Tveen-Jensen *et al.* (2013) as chlorinated, and as such synthesized (Further described in chapter 4) All other peptide variants were synthesised to allow binding specificity to be tested.

Sequence	Protein	Source
DYEDQQKQLC	Fibrinogen	Identified in the literature
DY-(Cl)-EDQQKQLC	Fibrinogen	Identified in the literature (Added chlorination)
DY-(NO_2)-EDQQKQLC	Fibrinogen	Identified in the literature (Added nitration)
STSY-(NO_2)-GTGC	Fibrinogen	Identified with MS
STSY-(Cl)-GTGC	Fibrinogen	Identified with MS (Added chlorination)
STSYGTGC	Fibrinogen	Identified with MS
Y-(Cl)-ICENQDSISSKC	Human Serum Albumin	Identified in the literature
Y-(NO_2)-ICENQDSISSKC	Human Serum Albumin	Identified in the literature (Added nitration)
YICENQDSISSKC	Human Serum Albumin	Identified in the literature
SY-(Cl)-ASY-(Cl)-ASY-(Cl)-C	Non-Specific	Designed
SY-(NO_2)-ASY-(NO_2)-ASY-(NO_2)-C	Non-Specific	Designed
SYASYASYC	Non-Specific	Designed

2.3 Standardisation of Hypochlorous Acid Concentration

Because hypochlorous acid (HOCl) degrades during storage, the concentration was checked before making up molar dilutions for each use. HOCl was made up into dilutions of 1:100, 1:200, 1:1000 and 1:2000 in 0.1 mM sodium chloride. The absorbance was measured using 1 mL of dilutions in quartz cuvettes spectrophotometrically at 292 nm. Based on the absorbance values, the concentration of each was calculated using the Beer Lambert law, with a molar extinction coefficient (ε) of 350 and a path length of 1 cm.

2.4 Protein Oxidative Treatments

Several plasma proteins were oxidatively treated in preparation for immunoassay testing of developed antibodies, and both Western blot, and MS analysis to identify modifications. Proteins treated include the plasma proteins, bovine serum albumin (BSA), fibrinogen, human serum albumin (HSA), transferrin and haemoglobin. Nitrated proteins were individually produced by producing to final concentrations of either 1mg/mL fibrinogen, HSA, transferrin or haemoglobin in PBS at pH 7.2, with final oxidant concentrations ranging from 0.10 mM -100 mM, but predominantly 0.25 mM, 0.5 mM, 0.75 mM, 1 mM or 10 mM 3-morpholinosydnonimine (SIN-1), the peroxynitrite ($ONOO^-$) generator was used. Samples were then incubated for 1 hour at 37°C to allow the reaction to proceed. Similarly, chlorinated proteins were individually produced by treating final concentrations of 1mg/mL fibrinogen, HSA, transferrin or haemoglobin in phosphate buffer (PB) at pH 6.6, with final oxidant concentrations ranging from 0.10 mM -100, but predominantly treated to 0.25 mM, 0.5 mM, 0.75 mM, 1 mM or 10 mM with hypochlorous acid (HOCl), and incubated for 1 hour at 37°C.

2.5 Sodium Dodecyl Sulphate Polyacrylamide Gel Electrophoresis

Proteins were resolved with sodium dodecyl sulphate polyacrylamide gel electrophoresis (SDS-PAGE) in order to prepare for Western blot or MS analysis. The gels were made with acrylamide and bis-acrylamide (10%) according to the Laemmli method (Laemmli, 1970). Proteins were made into a 1:1 ratio of Laemmli buffer and incubated at 90°C for 5 minutes. The loaded protein concentration for each sample was 10 µg/ well. The samples were then cooled to room temperature and electrophoresed at a constant 130 V, in parallel with a protein marker (10- 250 kDa) (Product code: 26619). The gel was stained overnight in 45% methanol, 10% acetic acid, and 0.1% Coomassie blue. It was then de-stained in the same solution without Coomassie blue. Alternatively, the gel was stained with Expedeon Instant blue stain, and washed with multiple exchanges of distilled water (dH_2O). Gels were captured using a Syngene G-box (Syngene, Cambridge, UK) by selecting automatic imaging and choosing the Coomassie stained protein gel option in the GeneSys software (Syngene, Cambridge, UK).

2.6 Bicinchoninic Acid Assay to Measure Protein Concentration

In order to determine protein concentration for various assays described throughout, the bicinchoninic acid assay (BCA) was utilized. Briefly, a solution of bicinchoninic acid (BCA) and copper (II) sulphate was made. Standards were produced to allow the protein concentration of unknown samples to be calculated. Protein standards were made in triplicate (0 µL, 2 µL, 4 µL, 6 µL, 8 µL and 10 µL) corresponding to 0.2, 0.4, 0.6, 0.8 and 1 mg / mL. The samples volumes were standardized to 10 µL with PBS. The unknown samples were made into dilutions of PBS, as for standards, based on their approximate concentration. The BCA and copper sulphate solution was then added to each well of the 96-well-plate that the samples were made up into. The plate was then incubated at 37°C for 20 minutes. The absorbance of each sample was then read at 570 nm using spectrophotometry (ELx800 plate reader, Bio-Tek, USA).

2.7 Spectrophotometric Carbonyl Assay for Quantifying Oxidation

The protein carbonyl group formation was determined according to Carty *et al.* (2000), in order to determine any changes in the level of general oxidation to proteins after treatments. The samples were derivatised with 10 mM 2, 4-dinitrophenylhydrazine (DNPH) in 2 M HCl or 2M HCl as a blank. The samples were then incubated at room temperature for 1 hour with vortexing every 15 minutes. To precipitate the proteins 10 % trichloroacetic acid (TCA) (w/v) was added. Each sample was vortexed and centrifuged to ensure precipitation, and the supernatant discarded. The pellets were washed three times with 1:1 Ethanol: Ethyl Acetate (v/v). The pellets were re-dissolved in 6 M guanidine HCl in 20 mM potassium phosphate; pH adjusted to 2.3 with trifluoroacetic acid (TFA). Each of the samples were vortexed and incubated for 30 minutes at 37 $^{\circ}C$ to allow the pellets to re-dissolve before centrifugation at 13g for 2 minutes to remove any insoluble material. The supernatants absorbance was measured at 360 nm. The carbonyl content was calculated based on the formation of dinitrophenylhydrazone (DNP) adducts and using the molar absorption coefficient of 22,000 for aliphatic hydrazones. The protein content was measured using the Bicinchoninic acid assay (BCA) and the carbonyl content recorded as nano moles of carbonyl groups / milligram of protein.

2.8 Oxidised Protein Standards for Determining Oxidation Level

Oxidised protein standards were produced according to Carty *et al.* (2000). Bovine serum albumin (BSA) was made to 6 mg/mL in PBS and left to solubilise overnight. The negative control was made up of reduced BSA, produced using sodium borohydride in a 2:1 ratio with BSA by adding 240 mg of sodium borohydride to 20 mL of 6 mg/mL BSA in PBS. The reduced BSA control sample was neutralised prior to dialysis with 1 M HCl. All of the buffers used throughout this assay were de-oxygenated by passing nitrogen gas through the solutions for 45 minutes under the fume hood. In order to remove any unreacted sodium borohydride, dialysis was carried out at 4 ^{o}C for 2, 5 and 12-hour equilibration periods, in 2 litre volume exchanges of PBS. A range of ferrous sulphate treated (oxidised samples) were then produced, using the mentioned reduced BSA. The samples were oxidised with superoxide, by way of a solution of 100 mM ferrous sulphate in 100 mM sodium citrate (BDH, USA). The BSA protein samples oxidised to varying degrees by making them to final concentrations of 0.75 mM, 2.5 mM, 5 mM and 10 mM of ferrous sulphate. To remove excess unreacted iron, samples were chelated with a final concentration of 5 mM deferoxamine mesylate and again dialysed as previously described. The protein concentrations were measured using BCA assay.

2.9 Western Blot For DNP-derivatised Carbonyl groups (Oxyblot)

This procedure is similar to Western blotting, with added DNPH derivitization steps. In order to confirm and compare the levels of general oxidation between treated proteins, carbonyl group formation was measured. Proteins were firstly resolved by SDS-PAGE, the loaded protein concentration for each sample was 15 µg/ well. The gel was then made into a Western sandwich (figure 2.1) and transferred onto a PVDF membrane (0.45 µm) (Immobilon -P, Millipore Ltd, Feltham UK) in 25 mM Tris, 192 mM glycine, 10% methanol pH 8.3 (Western transfer buffer) by applying 30V overnight at 4°C.

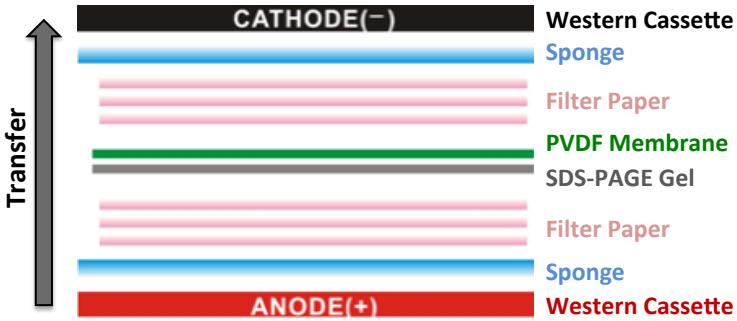

Figure 2.1: Western Blot Membrane Transfer Sandwich. The Western blot cassette is colour coded with black and red to represent sides of the cathode and anode. Each of the components shown in figure 2.1 were soaked in transfer buffer, and layered in the following order: Western blot sponge, two pieces of filter paper, SDS-PAGE gel, PVDF membrane, an additional two filter papers, and finally, another Western blot sponge. The sandwich is carefully put together with tweezers, minimizing contact, and removing any air bubbles with careful placement and a roller. The cassette was then locked and placed into the transfer tank. The protein transfer proceeded, with the addition of current, from the gel onto the membrane.

The membrane was then washed for 5 minutes in Tris buffered saline Tween (TBST) (20 mM Tris, 137 mM NaCl 0.05% Tween-20 pH 7.6), followed by 2 M HCl, and finally an incubation step with 10 mM DNPH for 5 minutes at room temperature.

The membrane was then washed with 100% methanol 7 times, and again with TBST 5 times to ensure any excess DNPH was removed. The membrane was blocked in TBST supplemented with 5% skimmed milk powder, or 5% BSA for 2 hours. The membrane was then incubated with monoclonal rabbit anti-dinitrophenylhydrazone (anti-dnp) (D9656) in blocking buffer at the working dilution of 1:1000, overnight at 4^{o}C. The membrane was then washed extensively for 30 minutes (3x 10 minutes) with TBST, and incubated with HRP-linked goat anti-mouse (6154) antibodies at a working dilution of 1:1000, for 2 hours at room temperature. The membrane was washed again as described above, and the HRP-linked anti-mouse was detected by reacting with enhanced chemiluminescence (ECL kit - 34078, Thermo Fisher Scientific, Hemel Hempstead, UK) for 4 minutes, according to the manufacturer's instructions. The membrane was then captured using a G:BOX system with GeneSys software. The results were analysed with densitometry analysis software, ImageJ, Version 1.48.

2.10 Western Blot For 3-Nitrotyrosine Formation on Fibrinogen

In order to identify nitration of fibrinogen, a more specific 3-nitrotyrosine Western blot was performed. Proteins were firstly resolved by SDS-PAGE. The loaded protein concentration for each sample was 15 µg/well. The gel was then made into a Western sandwich and transferred onto a PVDF membrane (0.45 µm) (Immobilon-P, Millipore Ltd, Feltham UK) in Western transfer buffer, by applying 30 V overnight at 4^{o}C. The membrane was washed for 5 minutes in tris-buffered saline, 0.1% Tween 20 (TBST) with 5% BSA or 5% milk powder. The membrane was blocked in TBST supplemented with 5% skimmed milk powder or 5% BSA for 2 hours. The membrane was then washed with TBST, and incubated in monoclonal rabbit anti-3-nitrotyrosine (Product code: N0409) made into blocking solution at a working dilution of 1:1000, overnight at 4^{o}C. The membrane was then washed extensively for 30 minutes (3 washes of 10 minutes each) with TBST and incubated with a HRP-linked goat anti-rabbit antibody (Product code: 6154), at a working dilution of 1:1000 for 2 hours at room temperature. The membrane was washed again as described above and the HRP-linked anti-mouse antibody was reacted for 4 minutes before detection using enhanced chemiluminescence (ECL kit - 34078, Thermo Fisher Scientific, Hemel Hempstead, UK) according to the manufacturer's instructions. The membrane image was captured using a G: BOX system (Syngene, Cambridge, UK) running the GeneSys software (Syngene, Cambridge, UK). The results were analysed with densitometry analysis software, ImageJ, Version 1.48 (Obtained from: https://imagej.nih.gov/ij/).

2.11 Western Blot Analysis of Nitrated Fibrinogen for STSY- (NO_2)-GTG

Nitrated fibrinogen was blotted for the modifications identified with MS utilizing the produced complementary novel anti-serum. This procedure was similar to the anti-3-nitrotyrosine Western blot, with a modification to the primary antibody used. More specifically, anti-STSY- (NO_2)-GTGC serum was made to half that used in previous ELISAs with the same antibody, 1.5 µg/mL to 0.75 µg/mL, based on multiple manufacturers' recommendations (www.citeab.com) of various other antibodies utilized in Western blotting, previously used at higher concentrations in ELISAs. The remainder of the assay is the same as for the anti-3-nitrotyrosine Western blot.

2.12 Preparation of Protein Samples for MS Analysis

Native, HOCl and SIN-1 treated fibrinogen and HSA protein samples were resolved by SDS-PAGE and stained, as previously mentioned, and as described in Sambrook and Russell (2006). Briefly, the resolving gel (10%) was made up of 3 mL of 40% acrylamide/bis acrylamide, 100 µL of 10% sodium dodecyl sulphate, 90 µL of 10% ammonium persulfate (APS) and polymerized with 12% of 14.4M NNN'-N' Tetramethylethylenediamine (TEMED) (BDH Limited, USA). The stacking gel consisted of 830 µL of 1 M TRIS-HCl pH 6.8, 440 µL of 40% acrylamide/bis-acrylamide, 33 µL of 10% SDS, 20 µL of 10% APS and finally, 5 µL of 14.4 M TEMED (Sambrook and Russell, 2006). A G: BOX system (Syngene) installed with GeneSys© software was then used to capture the images of the gel.

2.13 In-Gel Tryptic Digestion of SDS-PAGE Resolved Proteins

Fibrinogen α, β and γ chains were visibly stained by coomassie as separate bands. These bands were excised with a scalpel and digested with trypsin, essentially, as described by Shevchenko *et al*. (2006). The band fragments were chopped up to aid tryptic digestion. The chopped bands were then washed with 50% acetonitrile/ 100 mM ammonium bicarbonate for 30-60 minutes to remove the stain. The wash supernatant was removed, and discarded. Subsequently, 150 µL of 100 mM ammonium bicarbonate was used to denature the protein, followed by the addition of 10 µL of 45 mM dithiothreitol (DTT) and incubation at 60 ˚C for 30 minutes to allow for the reduction of disulphide bonds. The reduced cysteines were then alkylated, to prevent disulphide bonds re-forming, with the addition of 10 µL of 100 mM iodoacetamide in the dark, to prevent photo-degradation. The gel pieces were washed, as before, and acetonitrile added to expel any liquid, shrinking the gel pieces. The samples were vacuum centrifuged to dryness. Each gel piece (3.3 µg of protein) was tryptically digested with 20 µL of trypsin (2 µg) (Promega, UK) in 20 µL of 25 mM ammonium bicarbonate overnight at 37°C. The gel pieces were pelleted in the centrifuge at 13,000 RPM for 2 minutes. The supernatant was transferred to another 1.5 mL eppendorfs. Gel pieces were further extracted with 20 µL of 5% formic acid for 30 minutes, and then with 40 µL of acetonitrile for a further 20 minutes. The combined extracts were dried using a vacuum centrifuge and stored at -20 °C ready for analysis.

2.14 Mass Spectrometry Analysis of Tryptically Digested Proteins

The samples were analysed on an AB SCIEX TripleTOF® 5600 System (QTOF), coupled with a Dionex Ultimate 3000 High Performance Liquid chromatography (HPLC) system (Thermo Scientific, UK) with an automatic sampler. The mobile phase consisted of eluent A, 98% H_2O, 2% acetonitrile and 0.1% formic acid (solvent A); eluent B consisted of, 98% acetonitrile, 2% H_2O and 0.1% formic acid (solvent B) (Sambrook and Russell *et al.,* 2006). The samples were made to a volume of 30 μl with solvent A, in screw top auto-sampler glass vials (Chromacol, Speck and Burke analytical, UK). Following injection, enrichment and desalting of the peptides was achieved using a C18 pre-column (C18 PepMap™, 5 µm, 5 mm × 0.3 mm i.d. Dionex, Bellefonte, PA, US) washing for 4 minutes with aqueous 2% acetonitrile, 0.1% formic acid at 30 µL/min. A C18: 75 µm x 15 cm reversed phase column with a pore size of 100 Å and a particle size of 3 µm (Dionex) was used to separate the peptides. The flow rate used was 0.2 – 0.3 µL /min, using a gradient elution running from 2% to 45% aqueous acetonitrile (0.1% formic acid) over 45 min followed by a washing gradient from 45 to 90% aqueous acetonitrile (0.1% formic acid) in 1 min. The system was washed with 90% aqueous acetonitrile (0.1% formic acid) for 5 minutes and then re-equilibrated to the starting solvent. The chromatography was controlled by Chromeleon Xpress© software. Ionization of the peptides was achieved with the spray voltage set to 2.4 kV, a source temperature of 150°C, de-clustering potential of 50 V and a curtain gas setting of 15. Survey scans were collected in positive Ion mode in the range of 350 to 1250 Da for 200 ms using the high resolution TOF-MS mode. Information-dependent acquisition (IDA) was used to collect MS/MS data using the following criteria: the 10 most intense ions with 2^+ to 5^+ charge states and a minimum intensity of 500 counts per second (cps) were chosen for analysis, using dynamic exclusion for 30s, 100 ms acquisition and a fixed collision energy setting of 50 ± 15 V.

2.15 Searching the Obtained MS Data Against the Mascot© Database

The MS data was converted into the Mascot© (Matrix-Science, UK) data file format (.mgf) and searched against the Mascot© database within the Homo sapiens taxonomy section of the SwissProt database. The search looked to identify a match to the protein, carbamidomethyl fixed modifications and variable modifications. Variable modifications were not searched for in one run, rather in multiple combinations of the following modifications, nitration of tyrosine (3-nitrotyrosine), oxidation of tyrosine (hydroxytyrosine), oxidation of methionine (methionine sulfoxide), cysteine trioxidation (Sulfonic Acid), chlorination of tyrosine (3-chlorotyrosine), and lysine oxidation (allysine). The protease selected was trypsin, with a maximum number of missed cleavages of one. The search was set to identify peptides by their monoisotopic masses, with 2^+, 3^+ and 4^+ charge states. The peptide and MS/MS tolerance was set to ± 0.5 Da. The Mascot© data was validated using PeakView© analysis software, version 1.2 (ABSciex, UK), by de-novo sequencing of the peptides and any modifications (IonSource, 2016).

2.16 High Performance Liquid Chromatography for Peptide Purification

The nature of solid phase peptide synthesis means that peptide step-by-step yield can be poor. In order to purify out any incomplete sequences of the peptide, a Dionex Ultimate 3000 high performance liquid chromatography (HPLC) machine in reverse phase with ultra violet (UV) detection at 230 nm for peptide bonds, and automated fraction collection was used. The peptide was dissolved in 1mL of 50% acetonitrile and 50% water, and then 6mL of 95% water and 5% acetonitrile with 0.1% TFA. The HPLC machine was run at a flow rate of 4mL/min, with a solvent flow of 95% buffer A (Water and 0.1% TFA) and 5% buffer B (acetonitrile and 0.1% TFA), changing over time with a pre-programmed gradient, with a total run time of 12 minutes. The most abundant peaks were chosen by peak area milli absorbance units (mAU) at 230 nm, and collected by the auto-sampler based on their retention time on the column. Collected fractions were checked with MS, to confirm peptide identity.

2.17 Mass Spectrometry Analysis to Confirm Synthetic Peptide Identity

To check the sequence of the synthesised peptide, firstly, the peptide was cleaved from the resin. In order to do this, 5 mg of the sample was placed into a 35-mL fritted column (Fisher Scientific, UK), a solution of 95% TFA, 2.5% distilled water and 2.5% trisopropylsilone (TIPS) (Sigma-Aldrich, UK) was added to the column and incubated for 2 hours. This procedure cleaves the peptide from the resin support, and removes the protection side groups. The sample was then rinsed with 100% TFA, poured into a round-bottom flask and dried on a rotary evaporator. Once solvents are fully removed, 20 mL of ice-cold diethyl ether was used to precipitate out the peptides. The diethyl ether was carefully decanted, and any remaining diethyl ether was left to evaporate away for 20 minutes. The dry peptide used for MS analysis was then suspended in 50% acetonitrile: distilled water and 0.1% formic acid. The sample identity was confirmed by analysis with mass spectrometry (Micromass, ZMD) in positive ion mode. Each sample was directly infused in volumes of 100 µL, at a flow rate of 30 µL/min, with a source temperature of 100 °C. Acquisition involved 1 minute scans within the mass range of 200 – 2000 Da. Any unused peptide was frozen on dry ice, and freeze-dried for storage at -20°C.

2.18 Keyhole Limpet Haemocyanin Conjugation of Peptides

The peptides were conjugated to keyhole limpet haemocyanin (KLH) to encourage an immune response, according to the protocol recommended by the manufacturer (Thermo-Scientific). The carrier protein, KLH, was activated with maleimide and reconstituted to 10 mg/mL in distilled water. It was then incubated with an equal volume of 10 mM sulfosuccinimidyl-4 -[N-maleimidomethyl] cyclohexane-1-carboxylate (sulfo-SMCC) at room temperature for 1 hour, with gentle periodic mixing. After equilibrating the PD-10 column (Thermo Scientific, UK) with conjugation buffer (100 mM ethylenediaminetetraacetic acid, 83 mM sodium phosphate, 100 mM sorbitol and 900 mM NaCl, pH 7.2), the excess cross-linker was removed by desalting. To ensure efficient conjugation, each peptide was prepared in molar excess to KLH, by preparing molecular weight equivalents of the peptides and protein. This provided a 32-fold excess of peptides (hapten) to carrier protein (KLH). The peptides were reconstituted to 1mg/mL in conjugation buffer, and incubated for 2 hours with the collected column eluate. Again, PD-10 columns were equilibrated (Thermo Scientific, UK) with conjugation buffer, and conjugated peptide-KLH mixture was passed through the column to remove any excess unconjugated peptide. The flow through was collected. The KLH conjugated peptides were injected into sheep (Orygen Antibodies Ltd, UK), and the anti-serum obtained. Each peptide was injected into its own sheep. The serum was collected, pre-immune and once a month for 4 months after the immunization step.

2.19 Injection/immunization of Peptide Conjugates into Sheep

The immunization process was outsourced to specialized companies. KLH conjugates were sent to either Orygen (Pentlands Science Park, Bush Loan, Penicuik, EH26 0PZ) or the National Services Scotland (Castlelaw Building, Pentlands Science Park, Penicuik, EH26 0PZ) at 1 mg/mL of 1mL aliquots, on dry ice. Immunization procedures of DYEDQQKQLC peptide series were carried out by the National Services Scotland, and Orygen carried out all other peptide immunization, including those for the STSYGTGC peptide series. A pre-immune (before injection/immunization) bleed for each sheep was collected and sent to Aston University for testing. Sheep were then injected with 1mL of peptide-KLH conjugate preparations every 28 days, a different peptide for each individual sheep. Each bleed collection was performed 7 days after an additional injection of the 1mL of peptide-KLH conjugate preparation. These bleeds were then collected and sent to Aston University on dry ice for testing. On delivery of sera to Aston University, a portion of the stock sera (300 mL) were aliquoted into 30 µL and 1 mL volumes for storage at -80°C.

2.20 Sheep Anti-Sera Affinity Purification/Enrichment for Antigen

The peptides were coupled to iodoacetyl gel beads (Product code: 53155, Thermo Scientific, UK) in PD-10 columns (Thermo Scientific, UK), by adding 0.75 mg/mL of peptide in coupling buffer (50 mM tris and 5 mM ethylenediaminetetraacetic acid pH 8.5). The coupling solution was gently mixed at 4^{o}C for 20 minutes, and incubated at room temperature for 30 minutes. The protein concentration was checked with the Bicinchoninic acid assay. The peptide mixture was washed with coupling buffer three times. Unbound binding sites were blocked with 50 mM cysteine in coupling buffer for 30 minutes at room temperature. The mixture was then washed with 1 M NaCl followed by phosphate buffered saline, before storage in phosphate buffered saline at 4^{o}C. Anti-sera were purified against bead conjugated peptides with an AKTA Purifier (GE Healthcare, Amersham). The serums were first cleaned up with 0.2 µm syringe filters before purification. A flow rate of 1 mL/ min was used throughout. The AKTA columns were first washed with 1 M NaCl (pH 7) to remove any non-specific bound material from the column, followed by a PBS (pH 7.4) wash. After injecting serum samples onto the column, 0.1 M glycine (pH 2.7) was used to elute antibodies bound to the bead conjugated peptides. In order to remove glycine from the collected fractions, samples were dialysed with 3.5 kDa snakeskin tubing (Product no. 8842, Thermo Scientific, UK) at 4^{o}C in PBS overnight.

2.21 Immunoassay Detection of Various Peptides and Proteins

This in-direct immunoassay was used to test a variety of native, modified and treated peptides and proteins against various anti-sera and antibodies. Nunc immuno maxi sorp plates were coated with 2.5 µM (100 µL of 2 µg/mL) of synthesised peptide (Mologic, UK and Isca Chemicals, UK) or molar equivalents of proteins, overnight at room temperature. Plates were then washed three times with TBST and blocked with 200 µL 1% BSA TBST, pH 7.5, for 2 hours at room temperature. Again, the plates are washed with TBST three times, and then 100 µL of sheep anti-sera dilutions (Ranging from 1:100 – 1:128,000), prepared in 1% BSA TBST, were incubated on the plate for one hour at room temperature. The plates were washed with TBST three times, incubated with 100 µL of 1:25,000 donkey anti-sheep alkaline phosphatase antibody (Product code: A5187) in 1% BSA TBST. The plates were incubated at room temperature for one hour, and the substrate para-nitrophenylphosphate (PNPP) was made to 2.7 mM (1mg/ mL) in 0.1 M glycine buffer containing 1 mM $MgCl_2$, 1 mM $ZnCl_2$, pH 10.4 (PNPP buffer). The PNPP substrate solution was added to each well (100 µL) and allowed to react at room temperature for 15 minutes. The absorbance was measured spectrophotometrically at 405 nm with a plate reader (ELx800 plate reader, Bio-Tek, USA).

2.22 Testing Translation into Clinical Samples by Immunoassay

Anti-sera produced and tested in chapter 4 was further tested against clinical inflammatory samples. The procedure was similar, utilizing an in-direct ELISA type-immunoassay. Modifications to the assay include coating the ELISA plates with dilutions of plasma, with the constituents as antigens and the use of different antibodies. In order to determine appropriate dilution factors, a preliminary experiment of healthy volunteers' plasma was performed. Dilutions of plasma ranged from 1:10 – 1:10,000 in 1% BSA TBST. Each plate also had a positive control for each anti-serum's antigen, a positive control where no plasma was added and a negative control where plasma was added with to a well with no antigen. The plates were incubated overnight at room temperature. Based on the preliminary study, 10 healthy patient plasma samples and 10 type II diabetic plasma samples were coated to ELISA plates at dilutions of 1:100 in 1% BSA TBST. Primary antibodies included the produced anti-sera (Anti- STSYGTGC, Anti- STSY-(Cl)-GTGC, Anti- STSY-(NO_2)-GTGC and Anti- DYEDQQKQLC), which were then detected by 1:25,000 donkey anti-sheep alkaline phosphatase antibody (Product code: A5187) in 1% BSA TBST, and measured spectrophotometrically at 405 nm with a plate reader (ELx800 plate reader, Bio-Tek, USA).

Chapter 3

Detecting Oxidative Modifications to Fibrinogen

3.1 Introduction

3.1.1 Biological Oxidants are Produced During Inflammation

Organisms are constantly exposed to a number of systems that produce biological oxidants, involved in a number of processes that span all biology, from cell signaling to immunity. Biological oxidants are not limited to oxygen; other classes include, reactive nitrogen species (RNS) and reactive halogen species e.g. reactive chlorine and bromine species (RCS and RBS). These are capable of modifying proteins, lipids and nucleic acids that make up our biology (Nathan and Cunningham-Bussel, 2013, and Stadtman, 2006). Neutrophils are among the most abundant immune cells responding to an inflammatory site, and as such are thought to cause most of the tissue damage occurring during inflammation. More specifically, phagocytes, such as neutrophils, produce the biological oxidants hypochlorous acid, superoxide and peroxynitrite to destroy pathogens during inflammation (Pacher, 2007).

3.1.2 Oxidative Modifications to Fibrinogen in Disease

Oxidative modifications to fibrinogen have been implicated in the pathology of a number of diseases, often involving impaired clot formation and the subsequent effects. A study performed by Martinez *et al.* (2013) highlighted fibrinogen as the most oxidized protein in the plasma of smokers, relevant because smokers are the sub-population at the greatest risk of lung cancer and thrombosis. Treatment of fibrinogen with the inflammatory oxidant hypochlorous acid has been shown to modify protein methionine and histidine residues, forming the oxidized products of the residues, methionine sulfoxide and oxidized histidine. As a result of these

modifications, the rate of clot formation was reduced. Conversely, nitrated fibrinogen samples, having formed 3-nitrotyrosine modifications, were shown to have increased clot formation (Martinez *et al.,* 2013). Nitrated fibrinogen has been specifically identified in a number of diseases, such as, acute respiratory distress syndrome (ARD) (Gole *et al*., 2000), lung cancer (Pignatelli *et al*., 2001), end-stage renal disease (Piroddi *et al*., 2011), coronary artery disease (Vadseth *et al*., 2004) and patients with venous thromboembolisms (Martinez *et al*., 2012). More specifically, 3-nitrotyrosine modifications to fibrinogen's β-chain have been detected by Western blotting in the plasma of samples taken from patients with ARD (Gole *et al*., 2000). Elevated levels of fibrinogen, and fibrinogen tyrosine nitration have been implicated in various arterial and venous thrombotic diseases. More specifically, a study performed by Parastatidis *et al*., 2008 showed by MS that there were specific 3-nitrotyrosine modifications to fibrinogen peptides, ^{284}NYCGLPGEY-(NO_2)-WLGNDK^{298} and ^{416}YYWGGQY-(NO_2)-TWDMAK^{428}, in the plasma of smokers (Martinez *et al*., 2013 and Parastatidis *et al*., 2008).

3.1.3 Chapter 3 Focus, Aims and Hypothesis

This chapter focuses on the identification and quantification of *in-vitro* modification sites to human fibrinogen after treatment with similar biological oxidants to those produced during inflammatory conditions. The aim was to identify stable modifications to the fibrinogen protein that might make good potential markers of inflammation, to raise antibodies against. With the hypothesis: a number of concentration dependent oxidative modifications, similar to those that might be expected during inflammation (Section 3.1.2), to human fibrinogen can be consistently identified after treatment with SIN-1 and HOCl.

3.2 Production of Carbonyl Assay Standards

In order to measure the level of oxidation to fibrinogen before mass spectrometry analysis, the carbonyl assay was performed as described by Carty *et al.* (2000). To enable a comparison of oxidation, standards were produced (Figure 3.1A and 3.1B). Bovine serum albumin (BSA) was oxidised with various concentrations of ferrous sulphate, and the negative controls were reduced with sodium borohydride to remove any basal oxidation. Dinitrophenylhydrazine (DNPH) was used to derivatize carbonyl groups, forming dinitrophenylhydrazone adducts, which were quantified by spectrophotometry. Standards were treated with sodium borohydride to remove basal oxidation and then oxidized with ferrous sulphate. Samples were derivatised with 10 mM DNPH in 2 M HCl for 1 hour at room temperature, and read spectrophotometrically at 360 nm. The protein concentration of each sample was measured using the bicinchoninc acid (BCA) assay, in order to normalise for protein content, subsequently, the carbonyl content was calculated as a ratio of each samples protein content (Smith *et al*., 1985). With regard to the standards, a concentration dependent increase in carbonyl group formation can be seen per milligram of protein present with the increase in ferrous sulphate treatment concentration. The standards in figure 3.1A and 3.1B show a small amount of variability throughout, more specifically, the 0.5 mM $FeSO_4$ treated sample showed the greatest deviation from the concentration dependant increasing carbonyl formation trend. In order to check for oxidation of the protein samples that might occur during storage at -20^{o}C, freshly prepared reduced BSA and reduced BSA that had been stored for several months was compared using the the carbonyl assay. No significant differences were seen in the level of carbonyl group formation, hence oxidation, between the freshly prepared and stored reduced BSA (Figure 3.1C).

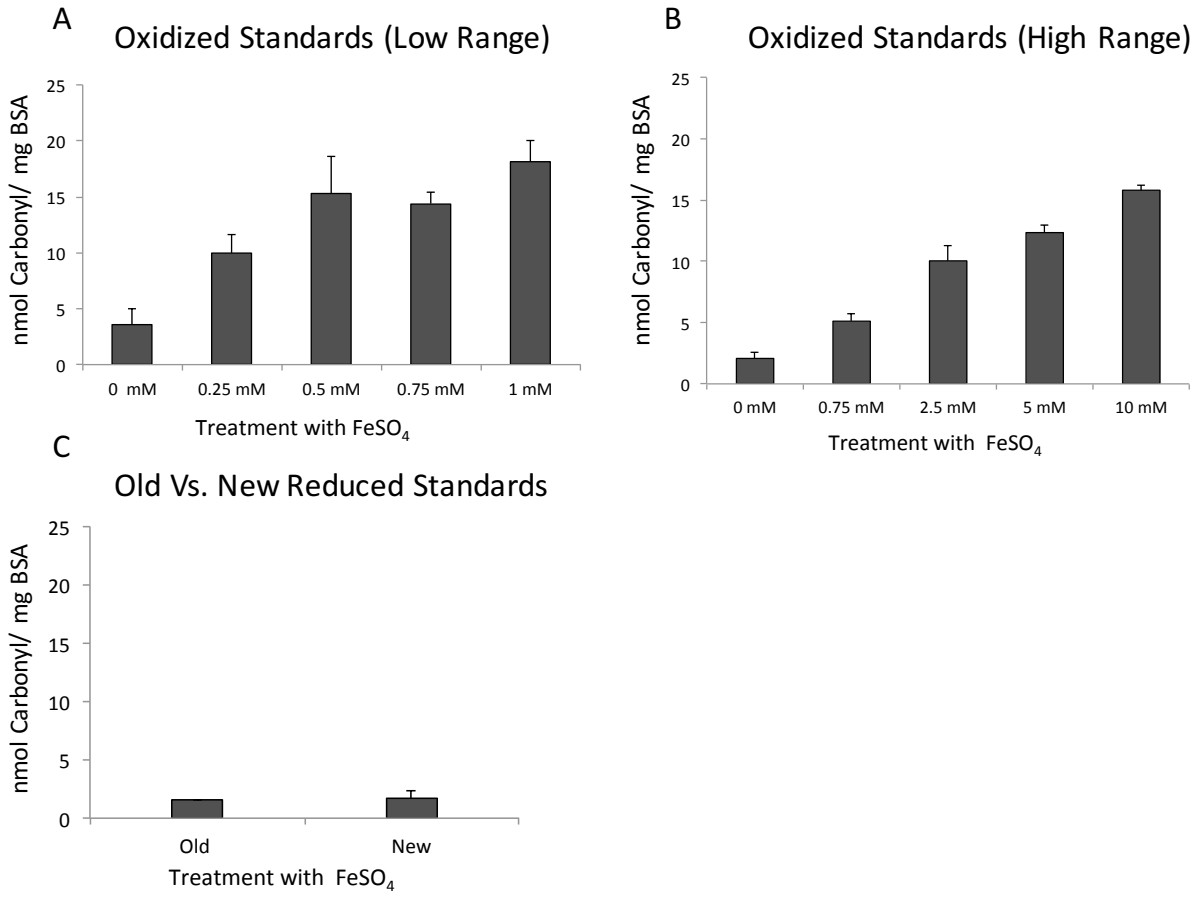

Figure 3.1: Spectrophotometric Oxidized BSA Protein Standards. $n = 3$, error bars are standard error of technical replicates. (A) low ferrous sulphate treatment concentration range (B) high ferrous sulphate treatment concentration range (C) Comparison of freshly prepared vs. stored, reduced standards.

3.3 Using the Carbonyl Assay to Confirm Oxidation of Fibrinogen

The carbonyl assay was utilized to quantify carbonyl group formation, hence oxidation, of fibrinogen treated with the chlorinating and oxidizing agent NaOCl which produces hypochlorous acid (HOCl). The carbonyl assay results of HOCl treated fibrinogen, shown in figure 3.2A, show an increase in the level of oxidation in the treated samples when compared to the untreated controls. More specifically, a concentration dependent exponential increase in carbonyl group formation can be seen. However, a considerable amount of variability between replicates can be seen with large standard error values. Fibrinogen treated with the peroxynitrite generator SIN-1, shown in figure 3.2B, displays a similarly large amount of variability between replicates, with very large standard deviation values. The results for SIN-1 treated fibrinogen do not follow the expected trend of a concentration dependent increase in carbonyl formation. The reactive, sulfur containing, residue methionine was also added to quench any excess unreacted oxidant in both the SIN-1 and HOCl treated samples, with clear meaningful difference in trend.

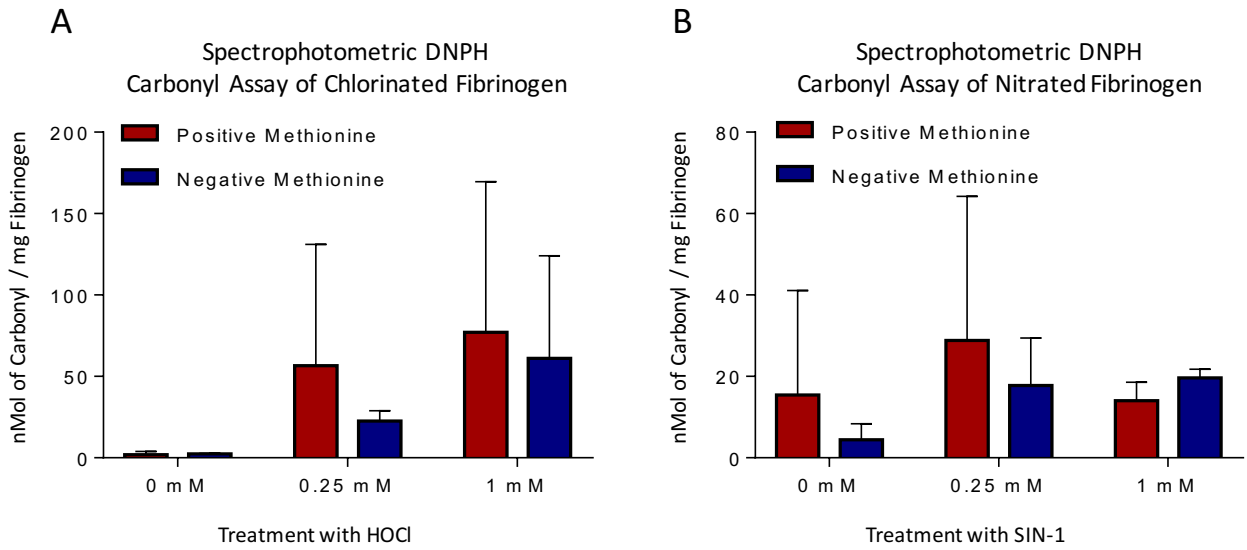

Figure 3.2: Spectrophotometric Measurement of Treated Fibrinogen Carbonyl Content. *n* = 4, error bars are standard deviation based on technical replicates. (A) HOCl Treated Fibrinogen Carbonyl content (B) SIN-1 Treated Fibrinogen Carbonyl content. Samples were derivatised with 10 mM DNPH in 2 M HCl for 1 hour at room temperature, and read spectrophotometrically at 360 nm. The protein content was measured using the BCA assay, and the carbonyl formation calculated based on each samples protein content.

3.4 Western Blot Analysis of Nitrated Fibrinogen

The results from the carbonyl assay confirmed the oxidation of fibrinogen, although the effect did not appear to be very linear, and there was substantial variability in the assay. The lack of consistency seen with large standard error values suggested the need for further testing. Western blot analysis was utilized as another means to measure oxidation of fibrinogen before MS analysis. Fibrinogen was nitrated with the peroxynitrite generator SIN-1 and run on a reducing SDS-PAGE. Of the two gels produced, one was stained with coomassie blue and used to investigate whether the oxidative treatments had caused any major structural changes to fibrinogen, such as degradation or aggregation. The bands at approximately 45, 55 and 65 kDa (Figure 3.3A) represent the α, β and γ chains of fibrinogen. A number of fainter bands are visible, which are probably due to the contaminants in the human fibrinogen, which was only 50- 70% pure. The lanes containing the untreated fibrinogen appeared more prominent, suggesting a higher concentration of protein, despite the fact that aggregation or fragmentation was not apparent. Densitometry analysis with ImageJ software (figure 3.3B) further confirmed these differences between each treatment condition, showing a decrease in protein concentration with the increase of SIN-1 treatment concentration. In parallel to the SDS-PAGE, another gel of the samples was run (figure 3.3C), and treated with DNPH and then anti-DNP antibodies were used to detect the carbonyl bound DNP adducts representative of oxidation. The Western blot results shown in figure 3.3C show a basal level of binding between anti-DNP and fibrinogen's α, β and γ chains, with prominent binding at approximately 45, 55 and 65 kDa. A significant increase in carbonyl formation in the 1 mM SIN-1 treated sample relative to the negative control was visually apparent, whereas little increase between the negative control and the 0.25 mM SIN-1 treated was seen. Densitometry was performed with ImageJ software in order to further understand the Western blot results. Densitometry confirmed differences between

each treatment condition. The 0.25 mM SIN-1 treated fibrinogen showed a very similar amount of carbonyl level to the negative control. The 1 mM SIN-1 treated fibrinogen showed a 2-fold increase in carbonyl formation relative to the control, suggesting that it was oxidized. In addition, it is worth noting that fibrinogen's α-chain showed the greatest level of antibody binding across all sample treatments.

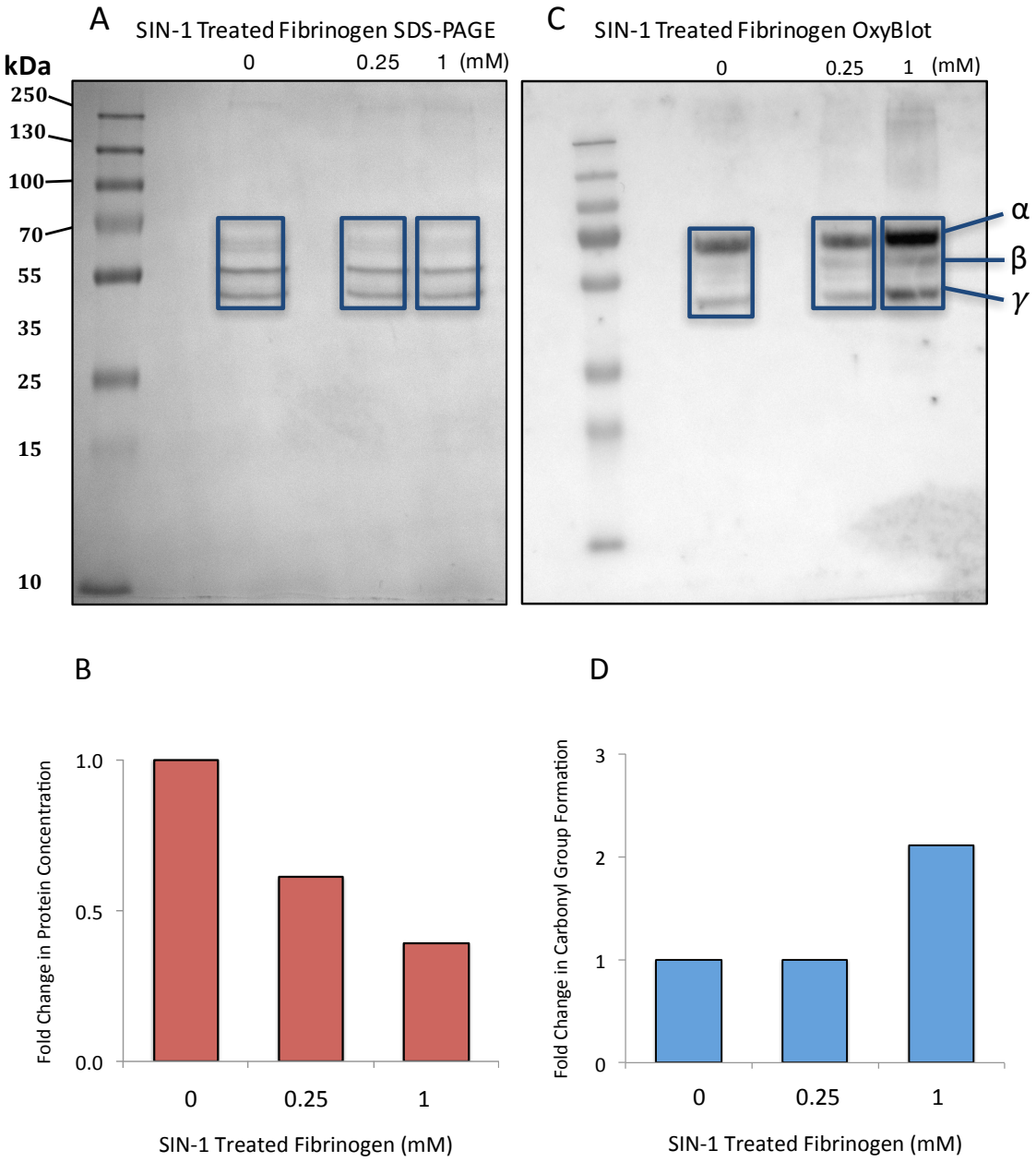

Figure 3.3: Carbonyl Formation Western Blot to Determine Oxidation. (A) Reducing SDS-PAGE of SIN-1 treated fibrinogen (B) Densitometry data (Rectangles show quantified areas) of SDS-PAGE (*n* =1) (C) Reducing Carbonyl Western blot (OxyBlot) of SIN-1 treated fibrinogen (D) Densitometry data (Rectangles show quantified areas) of SIN-1 treated fibrinogen OxyBlot (*n* =1). A 10% SDS-PAGE was loaded with 10 µg/ well of protein for coomassie staining and 15 µg/ well for Oxyblots. Oxyblots were treated with 10 mM DNPH and monoclonal rabbit anti-dnp (D9656) overnight (1:1000), followed by HRP-linked goat anti-mouse (6154) (1:1000), for 2 hours. Densitometry was performed with Image J, 1.6.0 (https://imagej.nih.gov/ij/), with a rectangular selection encompassing all three bands for each individual lane.

3.5 Western Blot for 3-nitrotyrosine in SIN-1 Treated Fibrinogen

Identifying carbonyl group formation allowed the confirmation of general oxidation. In order to look for modifications more relevant to nitration, a Western blot for 3-nitrotyrosine was performed. The gels were prepared with a similar procedure to before (Section 3.4), in this assay the Western blot membranes were not treated with DNPH, rather incubated with anti-3-nitrotyrosine antibody. The coomassie stained SDS-PAGE, shown in figure 3.4A appears to show a similar trend to that seen in the previous coomassie stained SDS-PAGE, shown in figure 3.4A. The densitometry results of each lane confirm these similarities, with a decrease in protein concentration after treatment with SIN-1. However, little difference in protein concentration was seen between the different SIN-1 treated samples. It is also worth noting that protein bands at the bottom of the gel were apparent, potentially indicating protein fragmentation. Various other bands can be seen, indicating contaminants in the fibrinogen, which was only 70% purity (figure 3.4B). In parallel to the coomassie stained SDS-PAGE, a Western blot utilizing 3-nitrotyrosine antibodies was performed (figure 3.4C). Bands for 3-nitrotyrosine, corresponding to the chains of fibrinogen, were apparent. Densitometry was performed on each individual lane, suggesting an increase in anti-3-nitrotyrosine antibody binding with the increase in SIN-1 treatment concentration, and therefore, an increase in 3-nitrotyrosine formation (figure 3.4D).

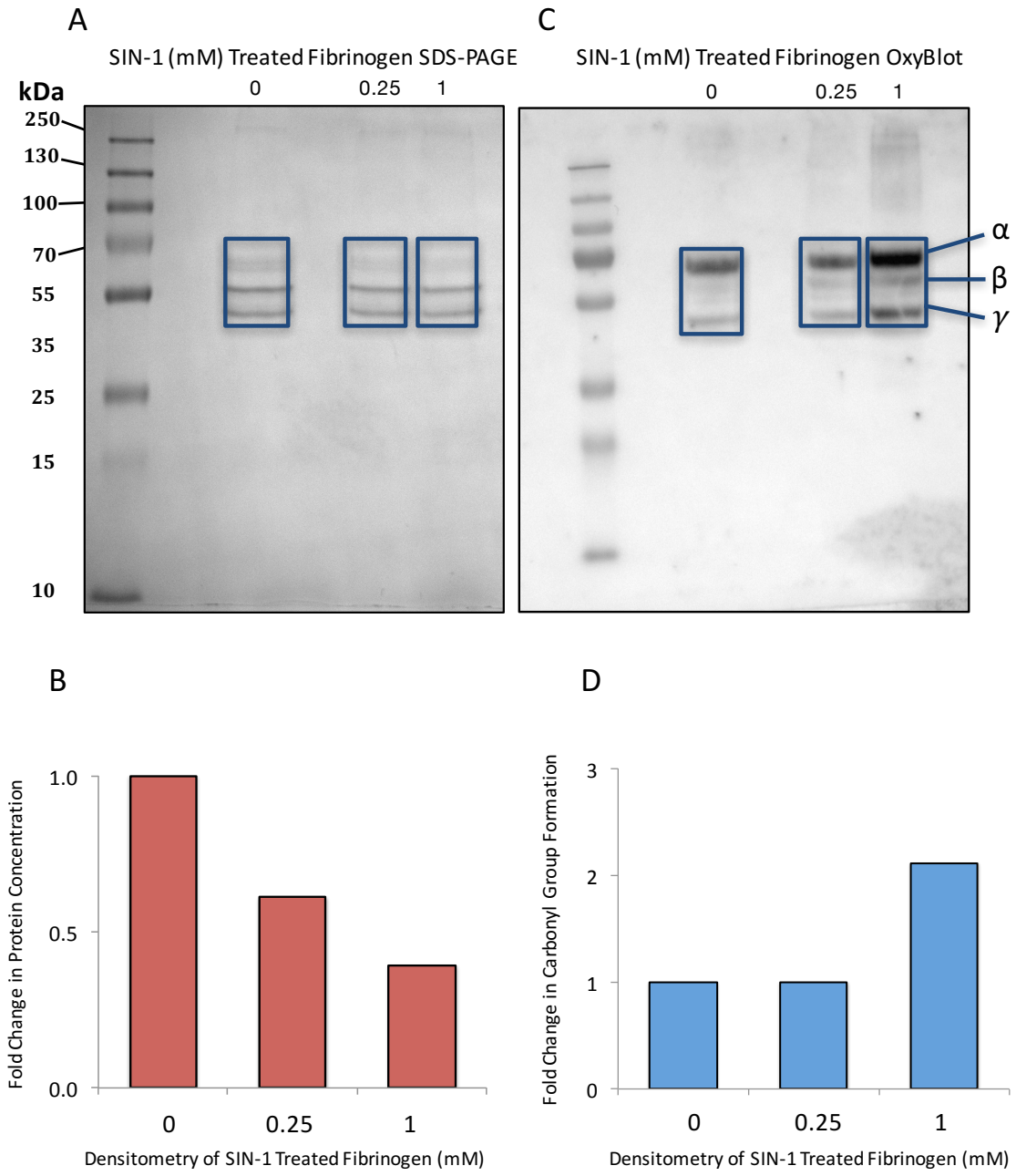

Figure 3.4: 3-nitrotyrosine (3-NT) Western Blot to Determine Nitration. (A) SDS-PAGE of SIN-1 treated fibrinogen (B) Densitometry data of SDS-PAGE, rectangle shows quantified area (*n* =1) (C) 3-NT Western blot of SIN-1 treated fibrinogen (D) Densitometry data of SIN-1 treated fibrinogen 3-NT Western blot, rectangle shows quantified area (*n* =1). A 10% SDS-PAGE was loaded with 10 µg/ well of protein for coomassie staining and 15 µg/ well for Western blots. Western blots were treated with mouse anti-3-NT (Upstate, clone 1A6) overnight (1:4000), followed by HRP-linked goat anti-mouse (6154) (1:1000), for 2 hours. Densitometry was performed with Image J, 1.6.0 (https://imagej.nih.gov/ij/), with a rectangular selection encompassing each individual lane.

3.6 Western Blot Analysis of HOCl Chlorinated Fibrinogen

Sodium hypochlorite (NaOCl) stock solution concentration was checked spectrophotometrically, and diluted as required into phosphate buffer at pH 6.6. This solution was used to generate hypochlorous acid (HOCl), for chlorination of fibrinogen. The SDS-PAGE produced on analysis of the HOCl treated fibrinogen (figure 3.5A) shows bands at approximately 45, 55 and 65 kDa, representing the α, β and γ chains of fibrinogen. A number of fainter bands are visible, which are probably due to contaminants in the fibrinogen, which was only ~ 70 % purity. The higher HOCl treatments of fibrinogen show aggregation in the stacking gel. This effect appears to be concentration dependent, with protein aggregation increasing in parallel to the increase in HOCl treatment concentration. In addition to visual observation, the change in protein concentration was investigated with densitometry (figure 3.5B). Although protein aggregation was apparent, the results showed little difference in absolute lane staining protein concentration between treatments, according to the densitometry analysis. The Western blot analysis (Figure 3.5C) of HOCl treated fibrinogen supports the effect seen in figure 3.5A, with the largest part of anti-DNP binding in the stacking gel, indicating potential protein aggregation at the higher treatment concentrations. In addition, an increase in oxidation at the lower treatment concentrations was seen in the fibrinogen samples treated with 1 mM and 2 mM HOCl.

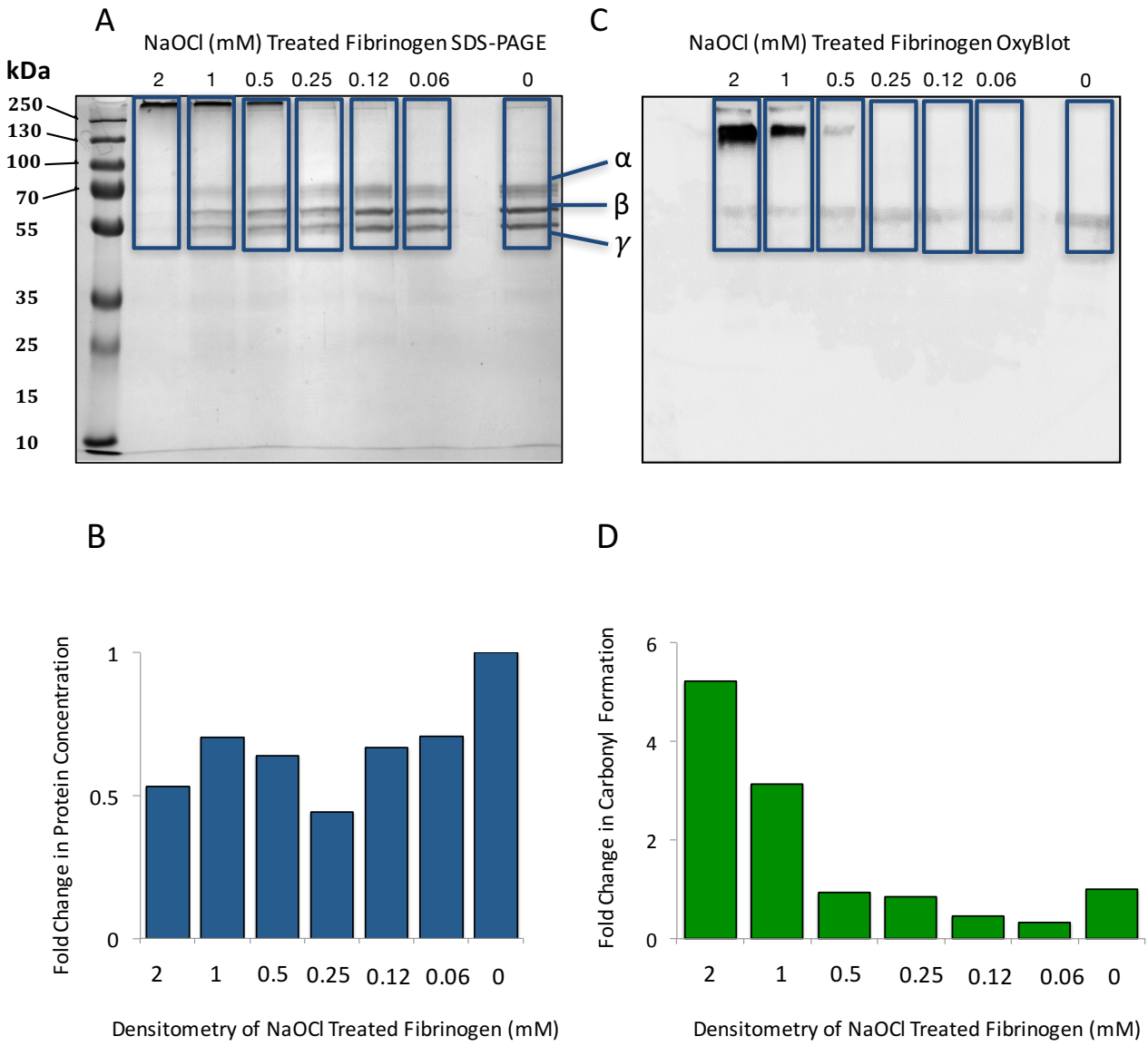

Figure 3.5: Carbonyl Formation Western Blot to Determine Oxidation of NaOCl (HOCl). (A) SDS-PAGE of NaOCl (HOCl) treated fibrinogen (B) Densitometry data of SDS-PAGE (*n* =1) (C) Carbonyl Western blot (OxyBlot) of NaOCl (HOCl) treated fibrinogen (D) Densitometry data of NaOCl (HOCl) treated fibrinogen OxyBlot (*n* =1). A 10% SDS-PAGE was loaded with 10 µg/ well of protein for coomassie staining and 15 µg/ well for Oxyblots. Oxyblots were treated with 10 mM DNPH and monoclonal rabbit anti-dnp (D9656) overnight (1:1000), followed by HRP-linked goat anti-mouse (6154) (1:1000), for 2 hours. Densitometry was performed with Image J, 1.6.0 (https://imagej.nih.gov/ij/), with a rectangular selection encompassing all three bands for each individual lane.

3.7 Identifying Modification Sites of Nitrated Fibrinogen With MS

The coomassie stained counterparts of fibrinogen were identified as modified with Western blotting techniques, and in order to further characterize these modifications, the bands were excised and tryptically digested ready for MS analysis. Several ESI-QTOF MS experimental analyses were carried out in an attempt to confirm the identity of the bands excised from the SDS-PAGE shown in Figure 3.4A, moreover, to investigate the occurrence of oxPTMs to fibrinogen. All MS experiments described throughout were bottom-up MS approaches involving protein tryptic digestions (Summarized in table 3.1). With all experiments, the first step utilised Mascot© to identify the protein chains of fibrinogen, and potential modifications, in all samples. Mascot© searches against the UniProtKB/Swiss-Prot database and allocates an ion score to each peptide ion; this is the probability of a match between the experimental data and the database *in-silico* data. The higher the ion score value, the lower the probability of the match between the experimental and *in-silico* peptides being a random event. On initial inspection of the Mascot© results; peptide ions with ion scores above 30 were selected for manual validation. This was seen to be the value at which the sequence coverage was mostly complete and the peptide ions could be identified and sequenced in the raw spectra. Collectively, the Mascot© results showed an average ion score of 60 to 75, providing good confidence in the peptide identification. Mascot was also used to search for a number of variable modifications, including: methionine sulfoxide; cysteine tri-oxidation (sulfonic acid); 3-nitrotyrosine; 3-chlorotyrosine; 3-hydroxytyrosine, 5-hydroxytryptophan and lysine oxidation (carbonylation). Due to the alkylation of cysteine residues during tryptic digestion the fixed modification for carbamidomethyl was always selected. For the control samples, containing untreated fibrinogen, no modifications were identified by the Mascot© search. In contrast, Mascot© identified

a number of 3-nitrotyrosine modifications by the addition of 45 Da for NO_2 substitution of a hydrogen (1 Da) on tyrosine, to samples treated with SIN-1. More specifically, various 3-nitrotyrosine modified peptides were identified, summarized in table 3.1.

These results were manually validated by de-novo sequencing in PeakView© to further support the Mascot© results. From the list of peptides identified in Mascot©, validated in PeakView©, the peptides containing Y^{277}, Y^{135} and Y^{475} occurred most frequently. The 3-nitrotyrosine containing peptide ^{273}GGSTSY^{+45} GTGSETESPR^{287} was the most frequently occurring peptide ion identified with MS, showing good sequence coverage for both the 0.25 mM and 1 mM SIN-1 treated samples in Mascot©. Comparison of the Mascot© spectra (Figure 3.6A) corresponds to the PeakView© spectrum (Figure 3.6B), identifying most of the peptide ions that allowed the confirmation of the respective sequence. The corresponding amino acid additions (peptide ion) for each peak in figure 3.6A are shown in figure 3.6C. The majority of the peptide ions are Y ions with the charge residing on the N-terminus. As mentioned, the modified peptide was also manually validated in PeakVIew© showing a 45 Da mass increase for the addition of NO_2 to tyrosine (Y- NO_2). The increase from 163.05 Da to 208.05 Da supports the presence of a 3-nitrotyrosine modification at Y^{277}. The extracted ion chromatogram (XIC) results allowed the percentage of modified total peptide ion to be quantified for all peptides. The XIC results for ^{273}GGSTSY^{+45} GTGSETESPR^{287} (figure 3.6D) showed the modified peptide to account for 26%.

The second most occurring peptide, ^{135}Y^{+45} LQEIYNSNNQK^{146}, much like Y^{277} showed good sequence coverage for both the 0.25 mM and 1 mM SIN-1 treated samples in Mascot©. By comparing figures 3.7A and 3.7B it is clear that the Mascot© spectrum (Figure 3.7A), is very similar to the PeakView© spectra (figure 3.7B).

Although the peptide ion generally showed good sequence coverage, there was no coverage of the actual modification site at Y^{135}. Again, most of the peptide ions were Y ions (Figure 3.7C). This was true for both the native and modified versions of the peptide. The presence of 3-nitrotyrosine was therefore deduced from the mass of the parent peptide and the sequencing of the remainder of the peptide. The XIC results for $^{135}Y^{+45}$ LQEIYNSNNQK^{146} (Figure 3.7D) showed the modified peptide to account for 2.19%. The peptide ^{472}GSWY^{+45} SMR^{478}, ranking as the third most commonly occurring peptide ion, showed good sequence coverage in the Mascot© and PeakView©, despite generally having low ion scores (figure 3.9A and 3.9B). The XIC results for ^{472}GSWY^{+45} SMR^{478} (figure 3.9D) showed the modified peptide to account for 3.08% of the total peptide observed.

Table 3.1: Ranked List of the Most Re-Occurring Modified Peptide Ions. (n = 7, error bars represent standard deviation of experimental replicates) The sequence confirmed by manual validation was shown as highlighted in red. The most abundant ion for each peptide was the 2^+ charge state. In some samples the 3^+ charge state version of the peptide was identified. The 3^+ peptide was lower in abundance and frequency than the respective 2^+ peptide ions. The chromatograms for each specific peptide have the same retention times, with a small amount of variability between experiments, and a couple of outliers. The native peptides were eluted from the chromatography column before the modified versions in all chromatograms.

Protein ID in Mascot ©	Mascot© Sequence	Nitration Site	Retention Time Range	Sequencable Instances	Ion Score Range	Sequence Coverage in PeakView©
Fibrinogen α chain	^{273}GGSTSY^{+45}GTGSETESPR^{287}	Y^{277}	18-19 mins	22	68-99	^{272}GGSTSY^{+45}GTGSETESPR^{287}
Fibrinogen γ chain	^{135}Y^{+45}LQEIYNSNNQK^{146}	Y^{135}	28-30 mins	12	15-65	^{135}Y^{+45}LQEIYNSNNQK^{146}
Fibrinogen β chain	^{472}GSWY^{+45}SMR^{478}	Y^{475}	27-28 mins	6	23-33	^{472}GSWY^{+45}SMR^{478}
Fibrinogen β chain	^{54}EEAPSLRPAPPPISGGGY^{+45}R^{72}	Y^{71}	32-47 mins	4	57-76	^{54}EEAPSLRPAPPPISGGGY^{+45}R^{72}
Fibrinogen α chain	^{582}QFTSSTSY^{+45}NR^{591}	Y^{589}	18-21 mins	3	19-39	^{582}QFTSSTSY^{+45}NR^{591}

A

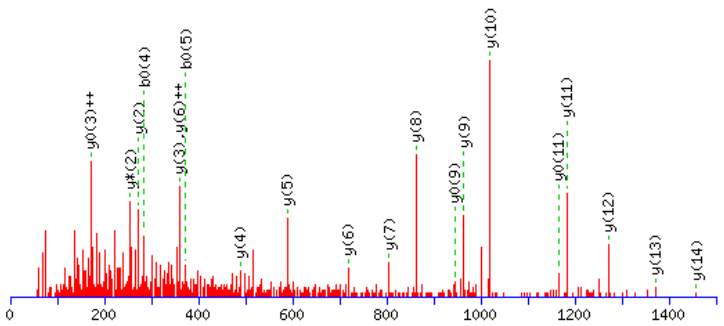

B

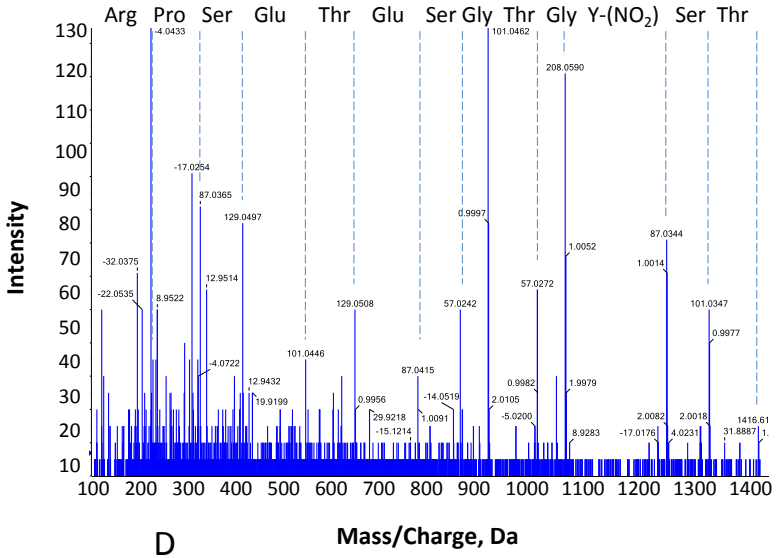

C

#	b	b^{++}	b^{0}	b^{0++}	Seq.	y	y^{++}	y*	y^{*++}	y^{0}	y^{0++}	#
1	58.0287	29.5180			G							16
2	115.0502	58.0287			G	1515.6558	758.3315	1498.6292	749.8182	1497.6452	749.3262	15
3	202.0822	101.5448	184.0717	92.5395	S	*1458.6343*	729.8208	1441.6078	721.3075	1440.6237	720.8155	14
4	303.1299	152.0686	285.1193	143.0633	T	*1371.6023*	686.3048	1354.5757	677.7915	1353.5917	677.2995	13
5	390.1619	195.5846	372.1514	186.5793	S	*1270.5546*	635.7809	1253.5281	627.2677	1252.5440	626.7757	12
6	553.2253	277.1163	535.2147	268.1110	Y	*1183.5226*	592.2649	1166.4960	583.7517	1165.5120	583.2596	11
7	610.2467	305.6270	592.2362	296.6217	G	*1020.4592*	510.7333	1003.4327	502.2200	1002.4487	501.7280	10
8	711.2944	356.1508	693.2838	347.1456	T	*963.4378*	482.2225	946.4112	473.7093	945.4272	473.2172	9
9	768.3159	384.6616	750.3053	375.6563	G	*862.3901*	431.6987	845.3636	423.1854	844.3795	422.6934	8
10	855.3479	428.1776	837.3373	419.1723	S	*805.3686*	403.1880	788.3421	394.6747	787.3581	394.1827	7
11	984.3905	492.6989	966.3799	483.6936	E	*718.3366*	359.6719	701.3101	351.1587	700.3260	350.6667	6
12	1085.4382	543.2227	1067.4276	534.2174	T	*589.2940*	295.1506	572.2675	286.6374	571.2835	286.1454	5
13	1214.4808	607.7440	1196.4702	598.7387	E	*488.2463*	244.6268	471.2198	236.1135	470.2358	235.6215	4
14	1301.5128	651.2600	1283.5022	642.2548	S	*359.2037*	180.1055	342.1772	171.5922	341.1932	171.1002	3
15	1398.5656	699.7864	1380.5550	690.7811	P	*272.1717*	136.5895	255.1452	128.0762			2
16					R	175.1190	88.0631	158.0924	79.5498			1

D

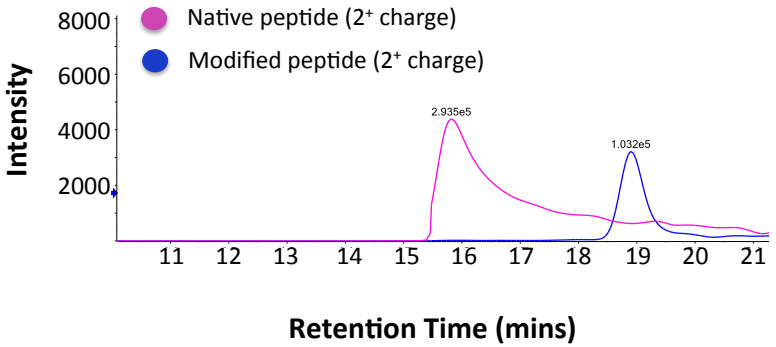

Figure 3.6: Mascot© and PeakView© Spectra for ^{273}GGSTSY^{+45}GTGSETESPR^{287}. (*n* = 7, based on experimental replicates). (A) Mascot© spectrum (B) PeakView© spectrum (C) Mascot ion distribution table (D) Extracted ion chromatogram of modified and native peptide ions. See figure 3.9 for experimental parameters.

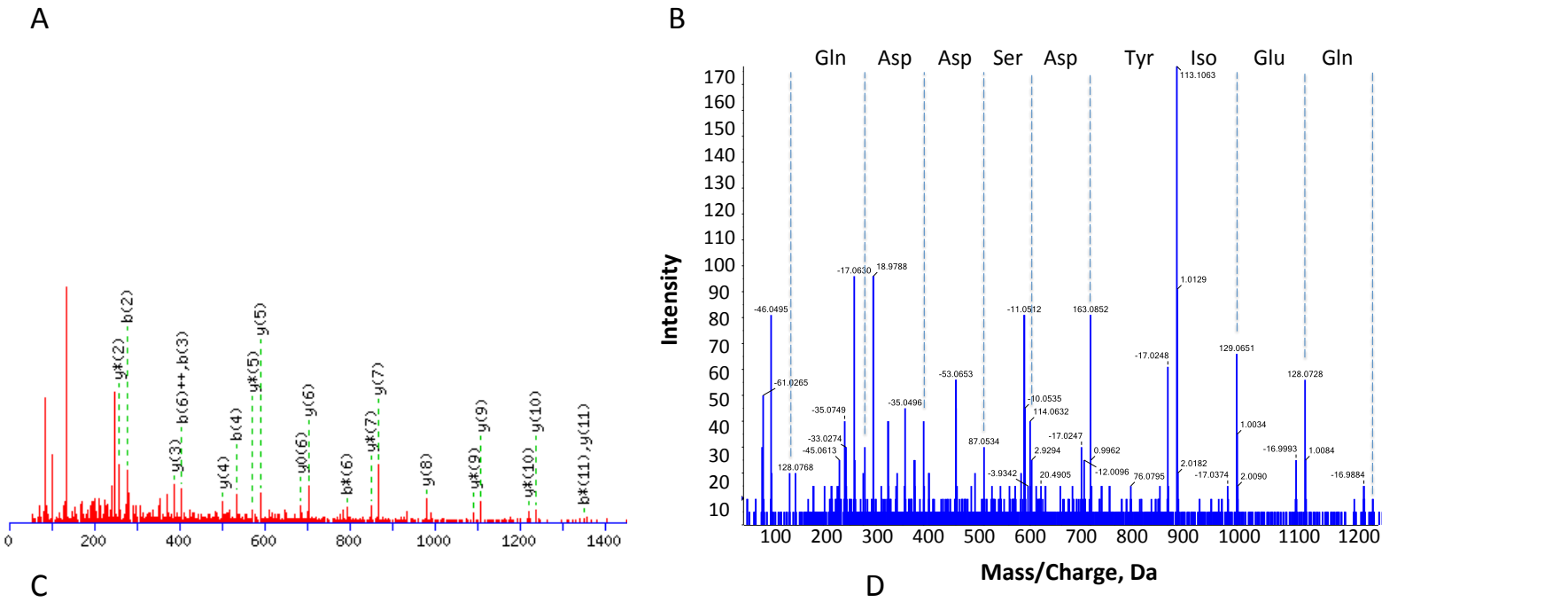

#	b	b^{++}	b*	b*$^{++}$	b^{0}	b^{0++}	Seq.	y	y^{++}	y*	y*$^{++}$	y^{0}	y^{0++}	#
1	164.0706	82.5389					Y							12
2	277.1547	139.0810					L	*1350.6648*	675.8360	1333.6383	667.3228	1332.6543	666.8308	11
3	405.2132	203.1103	388.1867	194.5970			Q	*1237.5808*	619.2940	1220.5542	610.7807	1219.5702	610.2887	10
4	534.2558	267.6316	517.2293	259.1183	516.2453	258.6263	E	*1109.5222*	555.2647	1092.4956	546.7515	1091.5116	546.2594	9
5	647.3399	324.1736	630.3134	315.6603	629.3293	315.1683	I	*980.4796*	490.7434	963.4530	482.2302	962.4690	481.7381	8
6	810.4032	405.7053	793.3767	397.1920	792.3927	396.7000	Y	*867.3955*	434.2014	850.3690	425.6881	849.3850	425.1961	7
7	924.4462	462.7267	907.4196	454.2134	906.4356	453.7214	N	*704.3322*	352.6697	687.3056	344.1565	686.3216	343.6645	6
8	1011.4782	506.2427	994.4516	497.7295	993.4676	497.2374	S	*590.2893*	295.6483	573.2627	287.1350	572.2787	286.6430	5
9	1125.5211	563.2642	1108.4946	554.7509	1107.5105	554.2589	N	*503.2572*	252.1323	486.2307	243.6190			4
10	1239.5640	620.2857	1222.5375	611.7724	1221.5535	611.2804	N	*389.2143*	195.1108	372.1878	186.5975			3
11	1367.6226	684.3149	1350.5961	675.8017	1349.6121	675.3097	Q	275.1714	138.0893	258.1448	129.5761			2
12							K	147.1128	74.0600	130.0863	65.5468			1

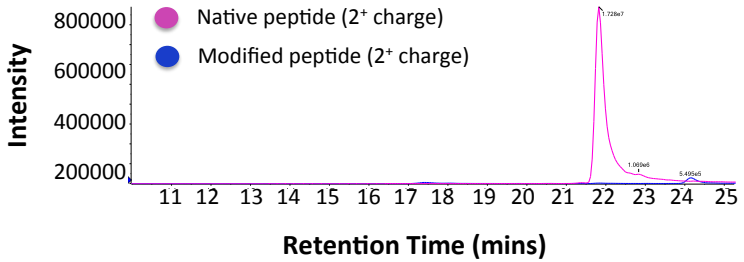

Figure 3.7: Mascot© and PeakView© Spectra for ^{135}Y^{+45}LQEIYNSNNQK^{146}. *n* = 7, based on experimental replicates).(A) Mascot© spectrum (B) PeakView© spectrum (C) Mascot ion distribution table (D) Extracted ion chromatogram of modified and native peptide ions. See figure 3.9 for experimental parameters.

A

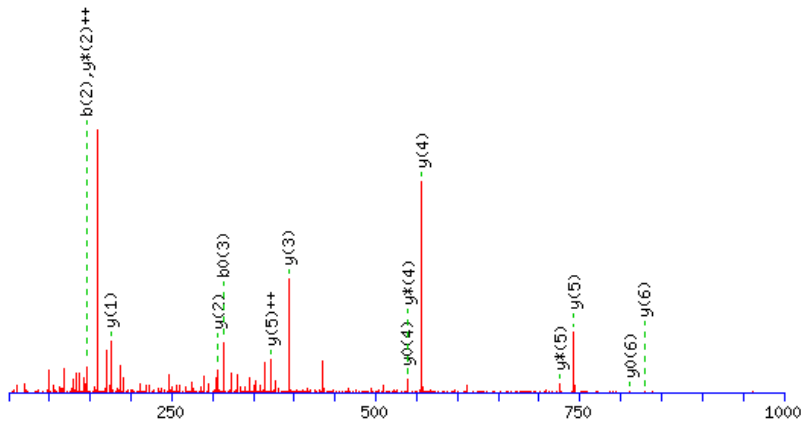

B

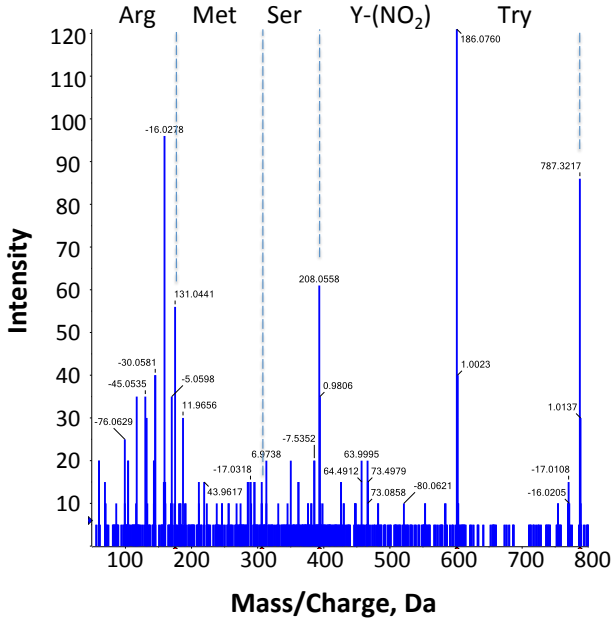

C

b	b^{++}	b^{0}	b^{0++}	Seq.	y	y^{++}	y^{*}	y^{*++}	y^{0}	y^{0++}	#
58.0287	29.5180			G							7
145.0608	73.0340	127.0502	64.0287	S	*829.3661*	415.1867	812.3396	406.6734	811.3556	406.1814	6
331.1401	166.0737	313.1295	157.0684	W	*742.3341*	371.6707	725.3076	363.1574	724.3235	362.6654	5
494.2034	247.6053	476.1928	238.6001	Y	*556.2548*	278.6310	539.2282	270.1178	538.2442	269.6258	4
581.2354	291.1214	563.2249	282.1161	S	*393.1915*	197.0994	376.1649	188.5861	375.1809	188.0941	3
712.2759	356.6416	694.2654	347.6363	M	*306.1594*	153.5834	289.1329	145.0701			2
				R	*175.1190*	88.0631	158.0924	79.5498			1

D

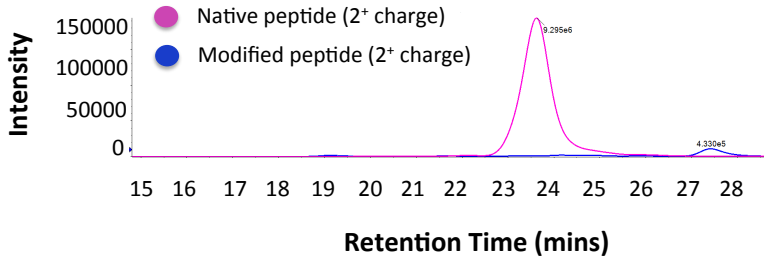

Figure 3.8: Mascot© and PeakView© Spectra for ^{472}GSWY^{+45}SMR^{478}. (*n* = 7, based on experimental replicates). (A) Mascot© spectrum (B) PeakView© spectrum (C) Mascot ion distribution table (D) Extracted ion chromatogram of modified and native peptide ions. See figure 3.9 for experimental parameters.

Comparing the data of several experimental replicates (*n* = 7) showed a large amount of variability between biological replicates. The average percentage that each peptide was modified showed considerable variation, indicated by large standard deviations. This suggests that the percentage of the native peptide that was modified did not fall within a narrow range, or, when comparing both treatment concentrations (Figures 3.9A and 3.9B), show a clear or expected concentration dependent relationship. Modified peptides Y^{475} and Y^{589} were shown to make up less of the total peptide, with a lower level of modification for each in the 0.25 mM SIN-1 treated fibrinogen (Figure 3.9A), when compared to the 1 mM SIN-1 (Figure 3.9Bb). It is also worth noting that the results for Y^{475} and Y^{589} were identified less often, and the average and range values, shown in figure 3.9A and 3.9B, are based on a smaller *n* value. The trend shown could as a result be less informative.

The instances of each modified peptide, and the percentage of which it was shown to be modified varied in distribution between each modified peptide ion (Figure 3.9C), Y^{277} showed an almost even spread with 1% to 90% shown as modified. The higher fibrinogen treatment concentration showed a greater number of instances of Y^{277} modifications, appearing as heavily modified. Whereas the other peptide ions with a tyrosine modification appeared to show a large proportion of the modifications, both from the 0.25 and 1 mM SIN-1 treatment conditions, in the 1-10% modified range (Figure 3.9C). With regard to the overall number of modifications (Figure 3.9D), the 1mM SIN-1 treated fibrinogen accounted for nearly 70% (67.4%) of the total modifications, suggesting that the higher treatment concentrations produced more modifications. The XIC data for the control samples showed intense peaks for the most occurring native peptide ions (Y^{277}, Y^{135} and Y^{475}), with no XIC peaks for the modified versions throughout.

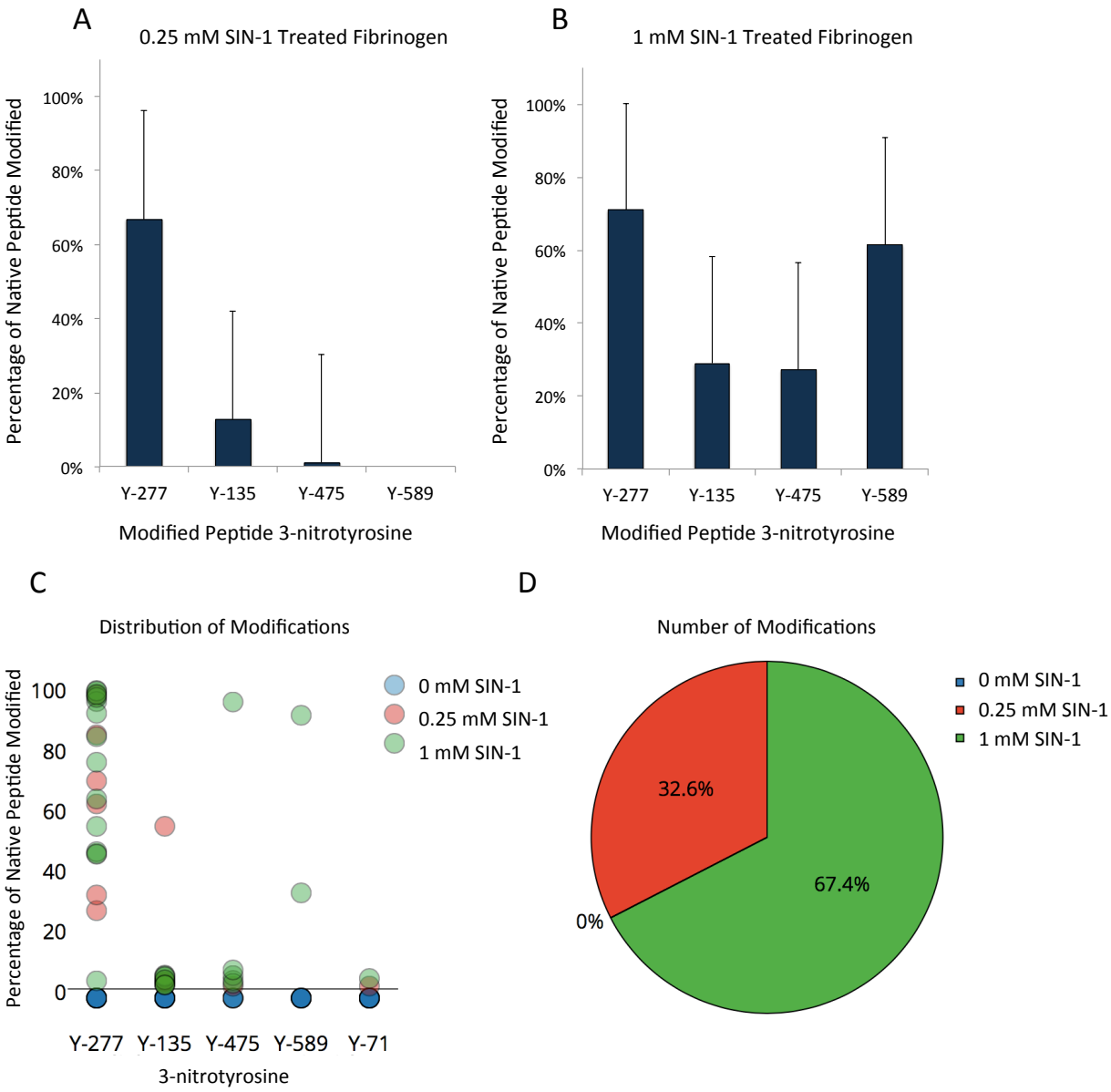

Figure 3.9: Analysis of MS XIC Data. (*n* = 7, error bars represent standard deviation of experimental replicates). Average total percentage of native peptide modified at (A) 0.25 mM and (B) 1 mM SIN-1 treatment (C) Distribution of specific modified peptides based on treatment (0.25 mM or 1 mM SIN-1) and non-treatment (0 mM SIN-1, native fibrinogen) (D) Distribution of total modified peptides based on treatment conditions. The following Mascot© database search settings were used to search the SwissProt database: homo sapien taxonomy, carbamidomethyl fixed modification and three, during any one search, of several variable modifications (described in text) were selected. The digesting protease trypsin was selected, with a maximum number of 1 miss-cleavages, and 2^+, 3^+ and 4^+ charged peptides were allowed based on their monoisotopic masses, with a MS/MS tolerance of ± 0.5 Da. *De-novo* data analysis was performed with PeakView© software (ABSciex, UK). The XIC mass window was set to 0.05 Da for all experiments, and peaks were Gaussian smoothed for clarity to 3. Plotly graphing, version 1 (https://plot.ly) was used to produce the bubble plot (C) and pie chart (D).

3.8 Identifying OxPTMs to HOCl Treated Fibrinogen with MS

Several attempts at identifying modifications to HOCl treated fibrinogen were made, without success. Multiple in-gel digests, similar to that described in section 3.7, were performed. Fibrinogen was treated with HOCl, analysed by a 10% SDS-PAGE gel (Figure 3.10), the bands excised and tryptically digested before being run on the MS. Because HOCl treated fibrinogen can sometimes aggregate, as seen in the SDS-PAGE in figure 3.5, the stacking gel sections were also excised for analysis. Data analysis of the subsequent results provided very good protein sequence coverage in Mascot©, for all of fibrinogen's chains, but no modifications other than methionine oxidation were seen. In an attempt to avoid any protein aggregation limitations of the in-gel digestion procedure, multiple in-solution digests were also performed (Table 3.1). All instances of in-solution digestion, including the use of Waters Rapigest, much like the in-gel digestion results, provided good sequence coverage for the chains of fibrinogen with no modifications other than methionine oxidation.

Table 3.1: Mascot Database Protein Sequence Coverage Results of NaOH Treated Fibrinogen In-Solution Digests.

Tryptic Digestion Exp.	Alpha Chain Sequence Coverage (%)			Beta Chain Sequence Coverage (%)			Gamma Chain Sequence Coverage (%)		
NaOH Treatment	0 mM	0.25 mM	1 mM	0 mM	0.25 mM	1 mM	0 mM	0.25 mM	1 mM
Solution (Exp. 1)	44	41	37	77	76	73	68	66	72
Solution (Exp. 2)	9	24	28	14	43	63	11	42	52
Solution (Exp. 3)	49	49	37	77	77	73	63	62	62
Solution (Rapigest)	29	32	28	51	42	45	41	41	41

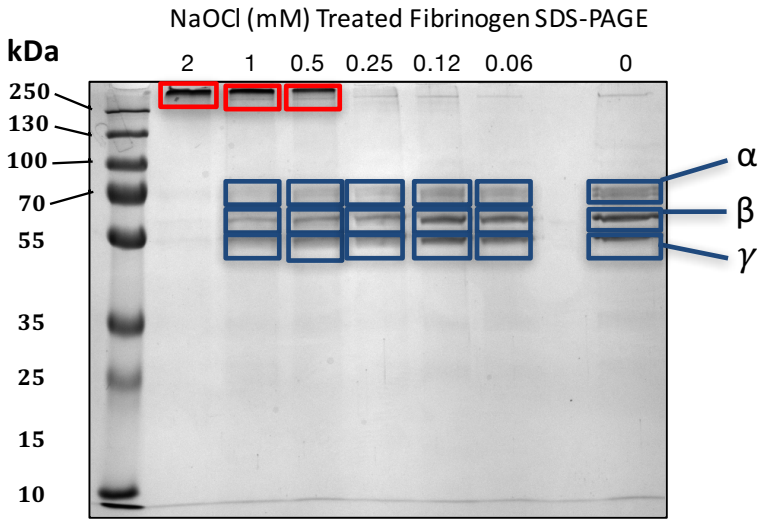

Figure 3.10: Location of Protein Bands Excised from SDS-Gel. Rectangular boxes represent excision area that was digested and run on the MS for analysis, with the red boxes highlighting the bands excised from the stacking gel. The alpha (α), beta (β) and gamma (χ) chains of fibrinogen are also labelled based on their location within the gel.

3.9 Literature Peptide ^{196}DYEDQQKQL^{204} was not found with MS

The fibrinogen α-chain peptide sequence ^{196}DYEDQQKQL^{204} was chosen from a study performed by Bergt *et al*. (2004), on the basis that lysine-containing peptides juxtaposed to tyrosine residues are more readily chlorinated after exposure to activated phagocytes (Bergt *et al*., 2004). This peptide was selected in order to perform an antibody-based proof-of-principle study, discussed further in chapter 4. For the purpose of this chapter, MS analysis was performed in an attempt to identify whether ^{196}DYEDQQKQL^{204} was modified after independent *in-vitro* treatments with HOCl and SIN-1. No modifications were identified. However, the native version of the peptide was identified (Figure 3.11).

Mascot© Search Results for
DYEDQQKQL

Ion Score	Expect	Rank		Peptide
36	0.055	1	U	K.RLEVDIDIK.I
56	0.00061	1	U	R.LEVDIDIK.I
37	0.01	1	U	R.LEVDIDIK.I
26	0.015	1	U	R.EVDLKDYEDQQK.Q
64	3.1e-05	1	U	R.EVDLKDYEDQQK.Q
47	0.00052	1	U	R.EVDLKDYEDQQK.Q
57	0.0004	1	U	K.QLEQVIAK.D

Figure 3.11: Identification of Native ^{196}DYEDQQKQL^{204} in the Mascot© Results. The Mascot© database Homo sapiens taxonomy was selected in the SwissProt database. Carbamidomethyl fixed modifications and three of several variable modifications were selected at any one time. Trypsin, with a maximum number 1 miss-cleaves, 2^+, 3^+ and 4^+ charged peptides were allowed based on their monoisotopic masses, with a MS/MS tolerance of ± 0.5 Da.

3.10 Checking Fibrinogen Peptide Sequence Exclusiveness

In order to determine potential proteins with which the MS identified peptide sequences could share similarities with, a Pubmed BLAST search was performed against the UniProtKB/Swiss-Prot database, with the taxonomy parameter set to *Homo sapiens*. The Blast search result categories include the identity match, the query cover match and the E value (Expect value). The identity match is the similarity between the query and the subject sequences, the query cover is the percentage of the sequences that overlap, and most importantly the E value is the number of positive result returns one can expect to see by chance from the database. The lower the E value, the more significant the match is. The Blast search results (Tables 3.2 - 3.4) for all peptides, including ^{273}GGSTSY^{+45}GTGSETESPR^{287}, ^{135}Y^{+45}LQEIYNSNNQK^{146} and ^{472}GSWY^{+45}SMR^{478}, are not matched to any other proteins or peptides other than to those from fibrinogen. The matches to fibrinogen show low E values, providing significance to the results. With regard to the unmatched returned results, none have both a match to the sequence, and full query coverage.

Table 3.2: Pubmed Blast search results for the peptide ^{273}GGSTSYGTGSETESPR^{287} (Y-277).

Record Name	Max Score	Total Score	Query Cover	E Value	Identity Match
Fibrinogen alpha chain	23.5	39	100%	0.43	100%
Zinc finger FYVE domain	18.5	33.9	85%	30	100%
Contactin associated protein	18.5	28	85%	30	100%
Glutamate receptor protein	18.5	18.5	91%	30	100%

Table 3.3: Pubmed Blast search results for the peptide ^{135}YLQEIYNSNNQK^{146} (Y-135)

Record Name	Max Score	Total Score	Query Cover	E Value	Identity Match
Fibrinogen gamma chain	43.9	43.9	100%	7e-8	100%
Ubiquitin protein ligase MGRN1	27.4	27.4	83%	0.054	100%
Protein POF1B	26.9	26.9	75%	0.077	100%
1-acyl-sn-glycerol 3-phosphate	25.2	25.2	71%	30	100%

Table 3.4: Pubmed Blast search results for the peptide ^{472}GSWYSMR^{478} (Y-472).

Record Name	Max Score	Total Score	Query Cover	E Value	Identity Match
Fibrinogen beta chain	28.6	28.6	100%	0.07	100%
Immunoglobulin superfamily, 3	22.7	42.0	100%	0.87	83%
Gram domain-containing protein 1A	22.7	22.7	71%	0.87	100%
Chromodomain protein (CHD1)	21.0	21.0	71%	3.5	80%

3.11 Determining Predisposition of Fibrinogen Peptides to Modification

Fibrinogen's protein crystal structure was mapped using the software Chimera© (Pettersen *et al*., 2004), allowing the illustration of the MS identified modified peptide sequences. The crystal structure provided an understanding of fibrinogen's peptide surface exposure, and subsequent susceptibility to modification. Crystal structure data was available for the peptides containing Y^{475}, Y^{71}, Y^{135} and Y^{197}. However, Chimera© shows Y^{277} as residing within a region of the protein without crystal structure coverage. The peptide sequences are shown in green, and the tyrosine residues in yellow. The crystal structure (figure 3.12) shows the hydrophobic interactions of fibrinogen, and the surface exposure of Y^{475}, Y^{71} and Y^{135}, further supporting the modifications identified in the MS results. The crystal structure for Y^{197} shows this sequence to be buried, and not surface exposed, due to the hydrophobic interactions of the tertiary and quaternary structure of fibrinogen, further supporting the MS results, in that, Y^{197} only appears as unmodified in Mascot©.

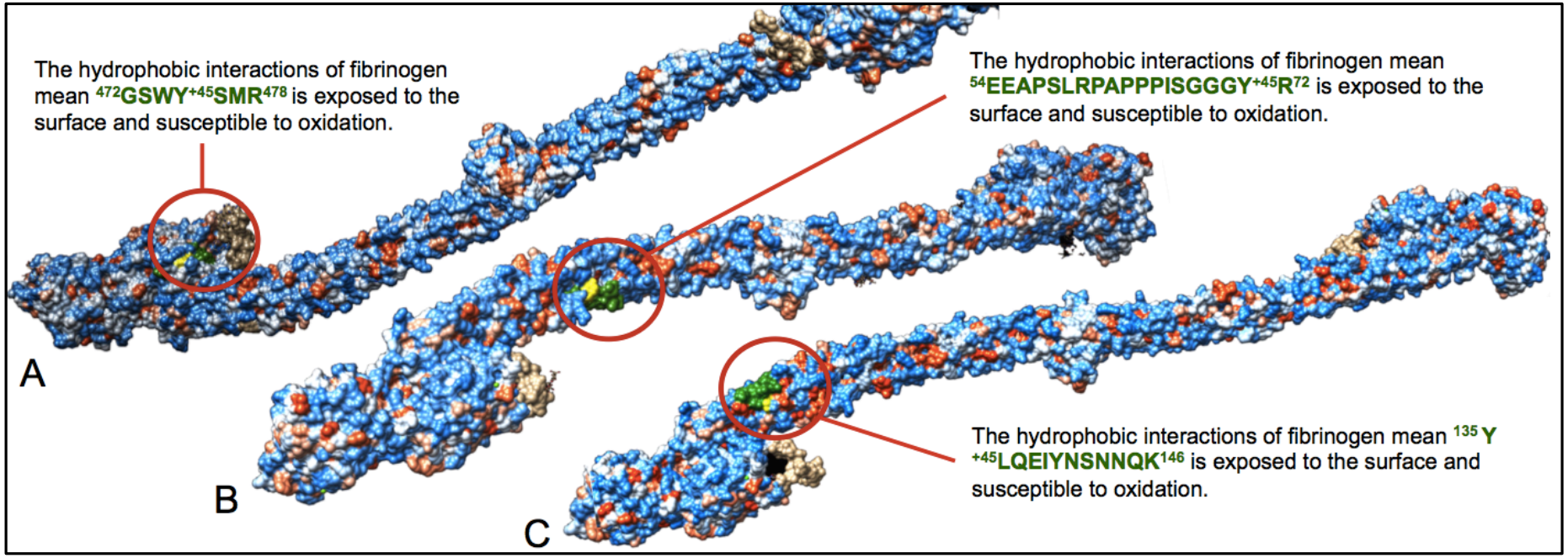

Figure 3.12: Crystal Structure of Fibrinogen Showing MS Identified Peptides' Tertiary Structure Placement. (A) The position of ^{472}GSWYSMR^{478} with the sequence highlighted in green and the tyrosine residue in yellow (B) The position of ^{54}EEAPSLRPAPPPISGGGYR^{72} with the sequence highlighted in green and the tyrosine residue in yellow (C) The position of ^{135}YLQEIYNSNNQK^{146} with the sequence highlighted in green and the tyrosine residue in yellow. The crystal structure data was obtained with Chimera©, version 1.9 (https://www.cgl.ucsf.edu/chimera/).

3.12 Chapter 3 Discussion

The focus of this chapter was on the identification, and quantification of *in-vitro* modification sites to human fibrinogen after treatment with the oxidants SIN-1 and HOCl. The aim was to identify stable modifications to fibrinogen peptides that might make good potential markers of inflammation. The hypothesis was that a number of sequence-specific and concentration dependent oxidative modifications, similar to those that might be expected during inflammation, to human fibrinogen can be consistently identified after treatment with SIN-1 and HOCl.

Carbonyl standards were produced in an attempt to measure the level of oxidation to fibrinogen before mass spectrometry analysis. The carbonyl content of the standards showed a concentration dependent increase up to 20 nmol/ mg of protein, and then no further increase. Fibrinogen has a finite number of residues that are able to form carbonyl groups, and once all of these have reacted to form carbonyl groups, the reaction will have reached its limit. Increasing the oxidant concentration beyond this point will have no further effect. A study performed by Adams *et al*. (2001) supports this, showing a similar effect with HOCl-treated BSA. Carbonyl formation on fibrinogen, after treatment with HOCl and SIN-1, was determined with the Carty *et al*., 2000 method. The fibrinogen used was 70% pure, obtained from human serum, and as a result contained various other plasma proteins. The previously mentioned study performed by Adams *et al*. (2001) showed how various plasma haem-containing proteins, such as haemoglobin, sharing the same absorbance wavelength as DNP, increased absorbance values, representative of carbonyl content. In addition, a decrease in the level of carbonyl formation, due to transition-metal-catalyzed oxidation was shown, concluding substantial variability in protein samples containing haem-proteins.

Western blotting was successfully used to show protein oxidation and nitration. However, HOCl-treated fibrinogen appeared to show a large amount of aggregation. This was apparent in the strong protein signal in the stacking gel area of the SDS-PAGE, and binding of anti-DNP antibodies in the Western blot. A study performed by Hazell *et al.* (1994) showed the mechanism of HOCl-induced protein aggregation to relate to modification of the protein lysine residues. Lysine is one of the cleavage sites of the protease trypsin used in all MS experiments. A study by Zee *et al.* (2012) describes how modifications to protein lysine residues can cause trypsin miscleaveages, and as a result compromise the MS analysis of such proteins. One potential possibility, is that, HOCl induced modifications to protein lysine residues, which can cause aggregation, also hinder MS analysis. However, this is brought into question, as fibrinogen was still successfully identified in several experiments with good sequence coverage in Mascot©.

The peptide ion, ^{273}GGSTSY-(NO_2)-GTGSETESPR^{287}, was shown with MS to be the most frequently modified fibrinogen peptide. However, no crystal structure data was available for this sequence. A study performed by Rasmussen *et al*. 2007 showed how the poor crystal structure of human b2 adrenergic G-protein-coupled receptor could be attributed to its inherent structural flexibility, and as such, one potential explanation for the lack of crystal structure data for ^{273}GGSTSYGTGSETESPR^{287}, is that it displays conformational flexibility. This flexibility may provide some insight into the mentioned sequence's high susceptibility to modification. Comparing the crystal structures of the other MS-identified modified peptides, shows a potential correlation between how well exposed the peptide sequence is to the surface, and the frequency that it occurs as modified in the MS results. More specifically, the ^{35}YLQEIYNSNNQK^{146} sequence, shown to be well exposed, is one of the two modified peptides that are frequently identified with MS.

The literature describes 3-nitrotyrosine residues to account for < 0.1% of total protein tyrosine residues (Nuriel *et al.*, 2008). The percentage of the total modified peptide in this chapter was determined with XIC, and the modified peptide was shown to account for varying amounts of the total peptide, which for the most part was well in excess of 0.1%.

A MS-based study by Parastatidis *et al.* (2008), of the plasma taken from smokers, identified two 3-nitrotyrosine containing peptides of fibrinogen, ^{284} NYCGLPGEY-(NO_2)-WLGNDK^{298} and ^{416}YYWGGQY-(NO_2)-TWDMAK^{428}. These modified peptides were not identified in the discussed study. There are two obvious potential explanations: firstly, the oxidative reactions that occur *in-vivo* differ to those *in-vitro,* and as such, provide different modifications to fibrinogen. In chapter 3 of this study the peroxynitrite generator SIN-1 is used as the source of nitration, and 3-nitrotyosine formation, however, *in-vivo* peroxynitrite is not the only nitrating agent present. Other nitrating agents capable of producing 3-nitrotyrosine include, nitric oxide; nitric dioxide; nitrous acid and nitryl chloride, and these are produced via various physiological processes. The specific type of nitrating agent could influence the selectivity of nitration, and the concentrations of nitrating agents *in-vivo* may differ from those used *in-vitro* (Abello *et al.*, 2009). A study by Jiao *et al.* (2001) describes that with different ratios of peroxynitrite to human serum albumin, the profiles of peptides with 3-nitrotyosine modifications changed. More specifically, the chromatography peaks for 3-nitrotyosine on further analysis with MS showed several 3-nitrotyosine containing peptides. Whereas, at the lower treatment levels the formation of 3-nitrotyrosine was pronounced in two particular peptides. Suggesting concentration-specific modifications. In addition, there are a number of other factors to consider when comparing *in-vivo* and *in-vitro* nitration selectivity, for example, conformational changes to proteins and alternative reaction kinetics based on the different biological conditions seen *in-vivo*.

Another consideration, should be the software used to perform data analysis. The previously mentioned study by Parastatidis *et al.* (2008) utilized SEQUEST© searching algorithm software to identify modified peptides, and this study utilized Mascot©, there is potentially a gap in the overlap between search engine peptide ion identifications. A comparative study of Mascot© and SEQUEST© search engine algorithms by Dorfer *et al.* (2014) supports this possibility, showing how the two search engines have an approximate 20% gap in their overlap (Figure 3.13). A review article by McHugh and Arthur (2008) suggests that, because each protein search engine software package uses its own search algorithm, that they each have their strengths, and weaknesses, and the most accurate approach would be to distill the results from various packages.

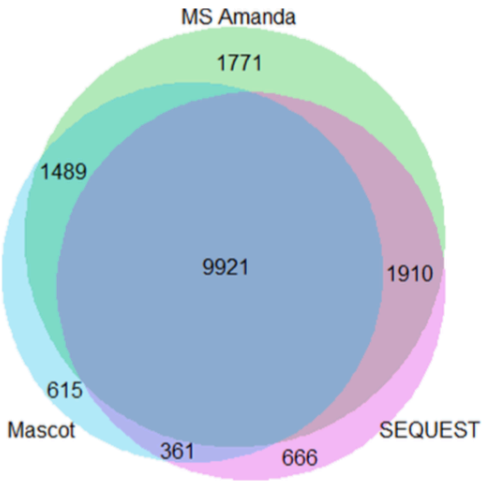

Figure 3.13: Venn Diagram Showing the Overlap in Sequence Identification Between Different Search Engine Software. Based on four protein data sets, 80% of the peptide ions identified by SEQUEST© are also identified by Mascot©, and 83% of the peptide ions identified by Mascot©, are also identified by SEQUEST (Dorfer *et al.,* 2014).

Ionization efficiency determines how accurately protein peptides are identified with MS. Some peptides ionize better than others, and PTM of peptides have been shown to alter ionization efficiency (Gao and Wang, 2007). This highlights some possible factors affecting the interpretation of the results in this chapter relating to poor or altered ionization efficiency, that some of the fibrinogen peptides that were shown as modified after treatment with SIN-1 or HOCl, are not detected with MS, the frequency of occurring modifications is inaccurate, and the XIC results for the amounts of modified peptides are hindered by the ionization efficiency due to PTM.

3.13 Chapter 3 Conclusions

Several modifications to fibrinogen were identified with MS after treatment with SIN-1 and HOCl. Based on the treatment conditions used throughout, no modifications were identified as exclusive to the lower or higher oxidative conditions. The main limitations of this study are, how well the nitrated fibrinogen modifications identified *in-vitro* correspond to those seen in clinical samples (*in-vivo*), potential Mascot© false negatives leading to un-identified peptide ions; poor or altered ionization efficiency of modified peptides with MS, potentially providing an inaccurate representation of the quantitative results. Some aspects of the hypothesis were proved, identifying nitrative modifications to fibrinogen. The the study was not able to identify modifications to fibrinogen after treatment with HOCl, or determine concentration specific modifications. Further work with inflammatory clinical samples is required to determine how well the *in-vitro* modified fibrinogen peptides correspond to an *in-vivo* situation.

3.14 Chapter 3 Future Work and Considerations

In order to identify modifications to HOCl treated fibrinogen, a larger and lower treatment concentration range should be used in an attempt to achieve protein modifications without aggregation. In order to determine whether the identified modified fibrinogen peptides are present in *in-vivo*, and therefore translate. Analysis with MS of various inflammatory clinical samples should be performed. Ideally one low level inflammatory condition, such as diabetes, and one highly inflammatory condition, such as periodontitis to determine if different modifications and or proportions are observed between conditions. More specifically, MS with a MRM program selective for STSY-(NO_2)-GTG and STSY-(Cl)-GTG peptide ions. A study by Tveen-Jensen *et al.* (2013) describes a MS method utilizing XICs generated from high-resolution MS^2 data. The use of narrow mass windows allowed for accurate quantification of 3-nitrotyrosine and 3-chlorotyrosine. The use of narrow window XIC should be considered as supporting alternative method to MRM program quantification of modified peptides.

Chapter 4

Developing Antibodies to Specific Peptide Sequences of Modified Fibrinogen

4.1 Introduction

4.1.1 Modifications to Proteins and Their Implications in Disease

As previously discussed in chapter 3, oxidative modifications to proteins have been detected in various diseases involving inflammation and the subsequent oxidative pathology. Modifications of tyrosine are generally considered stable, and therefore there has been a lot of interest in them as potential biomarkers. The protein fibrinogen is highly abundant in the plasma, and as described in chapter 3, was shown by Western blotting to be most susceptible to oxidative carbonyl group formation (Shacter *et al*., 1994). A study by Vadseth *et al*., in 2003 also showed the ability of fibrinogen to readily form 3-nitrotyosine modifications. Throughout chapter 3, several modifications post *in vitro* oxidative treatment were identified in fibrinogen residues. These modified residues appeared to be the most susceptible to oxidative damage, and as such, have potential for translation into an *in-vivo* system. Interestingly, the modifications identified in chapter 3 do not correlate with the modifications that have been reported previously by Parastatidis *et al*. (2008).

This study identified nitrated fibrinogen peptides *in-vivo* using MS. The observed modified peptides were chosen for further investigation, synthesized, conjugated to carrier proteins, immunized into sheep, and the anti-sera tested.

4.1.2 Immunoassay methods for Detecting Modified Proteins

Antibody-based methods are amongst the most common techniques for identifying and quantifying oxidative post-translational modifications (oxPTMs) to amino acid residues. The most common techniques include ELISA, Western blotting (WB) and immunostaining techniques, such as immunohistochemistry (IHC) and immunocytochemistry (ICC). The accuracy of these respective techniques rely on the specificity of the available antibodies, but not all antibodies are validated for all procedures (Houée-Lévin *et al.,* 2015). Issues with the reproducibility of immunoassays have been shown to be one of the most critical limitations of such techniques.

A study performed by Ray *et al.* 2007, identified a series of potential biomarkers of Alzheimer's disease. The antibody produced showed cross reactivity dependent variability during detection, and as such, a lack of reproducibility (Ray *et al.,* 2007). As stated, not all antibodies are validated for all technical procedures. From examining the antibody databases, CiteAb (www.citeab.com) and Biocompare (www.biocompare.com), antibody application trends were identified. The majority of antibodies for oxPTMs are primarily validated for Western blotting (~75%), with smaller numbers suitable for the other techniques such as IHC (~40%) and ELISA (~35%), and the use of these antibodies are not necessarily interchangeable.

As mentioned, the specificity of the available antibodies determines the selectivity and sensitivity of immunoassay techniques, and the degree of cross-reactivity depends primarily on the antigen that the antibodies are raised against. As the antigen becomes smaller, the number of epitope determinants decrease, and the probability of cross-reactivity increases (Hennion and Barcelo, 1998). This is important when considering small peptides, and modified amino acid residues, as they fall into this category. A comprehensive database search of the sites CiteAb

and Biocompare suggest there are more than 500 commercially available antibodies to modified residues, but on average less than 15% of these have been specifically cited in scientific publications. Multiple searches were performed for each amino acid oxidative modification type, accounting for differences in nomenclature of the same modified amino acid. Some antibodies are more extensively cited than others, and each are used in a different variety of techniques, highlighting the critical importance of selecting the appropriate one. The degree of accuracy obtained in an immunoassay is largely dependent on the specificity of the antibody used, and this can vary according to the immunogen used to generate them, including the carrier.

Cross comparison of the commercially available antibodies on CiteAb and Biocompare, shows the most commonly used approach to be conjugation of the modified residue to either keyhole limpet hemocyanin (KLH) or bovine serum albumin (BSA), but other common methods include immunizing directly with proteins treated with oxidants or nitrating agents. An understanding of how antibodies react to multiple epitopes of a given antigen highlights limitations in such approaches.
More specifically, using modified BSA or other proteins will generate antibodies to a variety of epitopes on the antigen, which may lead to cross reactivity upon translation, especially when considering that most nitrating and chlorinating agents are also oxidizing, so a wide range of oxPTMs may result. Even using synthetic modified residues conjugated to a carrier protein, there are likely to be several antibodies to epitopes that do not include the modification site, so purification is required.

Thus, the resulting polyclonal sera are semi-specific at best; while monoclonal products are better, some cross-reactivity is still possible. For example, limitations of antibodies and antibody-dependent assays for methionine sulfoxide have been reported (Wehr and Levine, 2012, and Ghesquière and Gevaert, 2014).

This indicates the importance of understanding the nature of the antibody being used in order to interpret results correctly, but unfortunately often little information is available from the supplier. It also suggests the benefit of producing better-characterized antibodies, possibly with known sequence specificity in addition to modification specificity.

4.1.3 Chapter 4 Focus, Aims and Hypothesis

This chapter focuses on synthesis and purification of fibrinogen peptides identified in the literature and by MS, and for the most part, the production and testing of the corresponding modified peptide anti-sera. The specific aim of this part of the study was to produce anti-sera with antibodies that bind specifically the modified peptides identified in the literature and by MS in chapter 3, exclusively. Chapter 4 is based on the hypothesis that antibodies can be produced which differentiate between modified and unmodified fibrinogen peptides with sequence context, binding exclusively to the specific modified peptide they were produced against.

4.2 Synthesis of Preliminary DYEDQQKQLC Peptide Series

In parallel to MS identification of sites of fibrinogen modifications, a proof-of-principle study was undertaken, to show that antibodies could be produced with sequence and modification site specificity. The α-chain fibrinogen peptide sequence ^{196}DYEDQQKQL^{204} was chosen, as discussed in chapter 3, based on increased potential tyrosine chlorination by phagocytes when juxtaposed to lysine residues (Bergt *et al*., 2004). The peptide was also a convenient size with the tyrosine (Y^{197}) residue within tryptic cleavage points. A cysteine was added at the C-terminus of the peptide to allow subsequent conjugation to KLH for immunization and purification. In order to develop specific antibodies to the respective peptide, it was first synthesized with purchased FMOC protected/blocked amino acid residues, according to well-established methods (Wade, 2007).

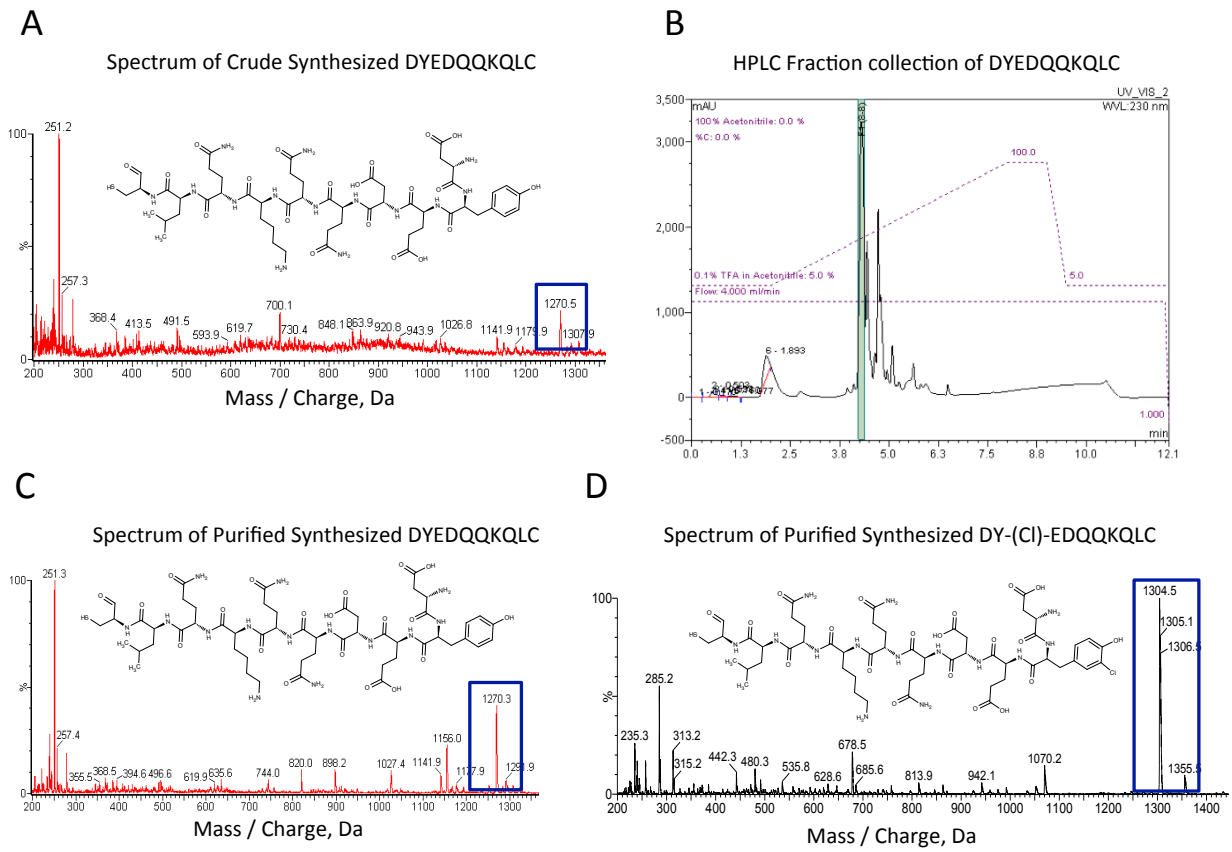

Figure 4.1: Analysis and Purification of Synthetic Peptides. Synthesized peptides, (A) Crude DYEDQQKQLC, (C) Purified DYEDQQKQLC and (D) Purified DY-(Cl)-EDQQKQLC were made up into 1mL 50% Acetonitrile, 50% water and then 6ml 95% water, 5% Acetonitrile and 0.1% trifluoroacetic acid (TFA). The spectra for the synthesized peptides were obtained on a Waters Micromass ZMD mass spectrometer by direct infusion, with a flow rate of 30μl/ min at 100°C (A, C and D). Fractionation and purification of all of the peptides, (B) Purification of DYEDQQKQLC, were performed on a Dionex ultimate 3000 HPLC machine with UV detection and automated fraction collection. The HPLC flow rate was 4mL/ min, 95% buffer A (100% water and 0.1% TFA) and 5% Buffer B (100% Acetonitrile and 0.1% TFA which changed over time with the pre-programmed gradient.

On completion of the step-wise procedure for synthesis of the peptides, MS was utilized to confirm the correct masses for each of the peptides. The initial MS analysis of DYEDQQKQLC shows a larger amount of background peaks (Figure 4.1A). In order to remove impurities, the peptide was purified using HPLC fractionation with peptide elution monitored by the absorbance at 230 nm, corresponding to the peptide bonds (Figure 4.1B). The peptide DYEDQQKQLC eluted at a retention time of 4 minutes, which was demonstrated by mass spectrometry analysis of the eluted fractions. The mass spectrum of the peak at 4 minutes was shown in Figure 4.1C, and confirms the presence of DYEDQQKQLC. Upon successful confirmation, further fractionation of the remaining respective peptide solution was performed, providing a purified solution of DYEDQQKQLC which was freeze dried in preparation for later use. Crude and purified products were analysed for all synthesized peptides to confirm the syntheses. The chlorinated version of the peptide DY-(Cl)-EDQQKQLC was successfully synthesized and purified in a similar fashion to the DYEDQQKQLC peptide. The addition of chlorine (34 Da) was confirmed in the MS spectrum (Figure 4.1D, with a mass increase from 1270 Da (Figure 4.1C) to 1304 Da.

4.3 Immunoassay Screening of DYEDQQKQLC Anti-Sera Series

DYEDQQKQLC and DY-(Cl)-EDQQKQLC peptides were conjugated to keyhole limpet haemocyanin (KLH), in order to improve their immunogenicity, and injected into separate sheep to generate anti-sera containing antibodies to the respective peptide antigens. Four sheep in total were immunized with synthetic peptides, 2 sheep for each peptide, sheep numbers 1 and 2 were immunized with DYEDQQKQLC synthetic peptide, and sheep 3 and 4 with DY-(Cl)-EDQQKQLC synthetic peptide. Aliquots of plasma were collected from the sheep on a monthly basis, and tested for their ability to recognize the peptides. In order to determine an appropriate working dilution, one of the sheep immunized with native peptide (sheep 2) and one with the chlorinated peptide (sheep 4) were selected for preliminary testing. The testing of anti- DYEDQQKQLC (sheep 3) and anti- DY-(Cl)-EDQQKQLC (sheep 3) to their antigens showed increased binding, to their respective antigens, over time after immunization (Figures 4.2A and 4.2B), with no binding of the pre-immune serum to either of the respective antigens. The sera obtained for DYEDQQKQLC (Figure 4.2A) in the later months displayed a reduction in absorbance at higher concentrations/lower dilutions. This was thought to be as a result of the well-established principle known as the “Hook Effect”, whereby agglutination of concentrated anti-sera prevents antibody binding, and as a result a drop off in signal is seen. Subsequently, a dilution of 1:2000 was selected to allow clear definition between sera bleed months with minimal signal loss.

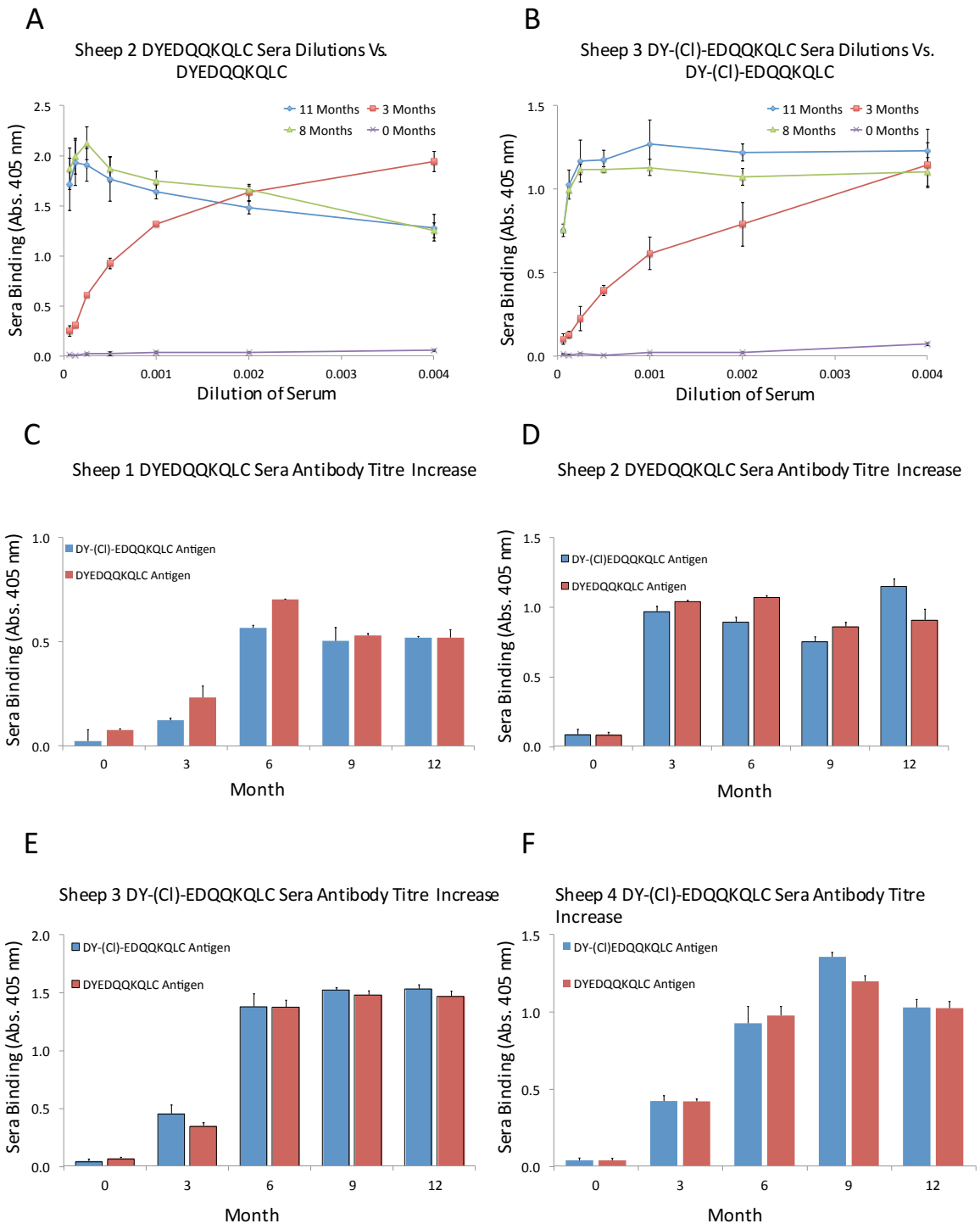

Figure 4.2: Determining Anti-Sera Optimal Dilution and Anti-Sera Monthly Antibody Titre Profile. (*n* = 3, standard deviation of technical replicates). Nunc maxi-sorp plates (Product code: 10098860, Fisher Scientific, UK) were coated with 2 µg/mL of peptide antigens. The sera used in A and B was taken from sheep numbers 2 and 3 and used serial dilution. The sera used in C – F were diluted to 1:2000 in 1% BSA TBST. The tested anti-sera were detected with 1:25,000 donkey anti-sheep antibody conjugated to alkaline phosphatase (Product code: A5187), and 1 mg/mL phosphate substrate in para-nitrophenylphosphate (pNPP) buffer, pH 10.4, with an incubation time of 15 minutes at room temperature before being read on a plate reader at 405 nm.

In order to identify any trends between all of the anti-sera bleed months, each of the sheep bleed months were tested against both the native and chlorinated peptides (DYEDQQKQLC and DY-(Cl)-EDQQKQLC) for comparison (Figures 4.2C to 4.2F). The sera from all sheep collected prior to immunization with synthetic peptides showed no significant binding to either antigen (Figures 4.2C - 4.2F). Post-immunization with the synthetic peptides, an increase in binding of anti-sera to both DYEDQQKQLC and DY-(Cl)-EDQQKQLC, corresponding to the months after immunization was seen. Cross reactivity between the native and chlorinated versions of the peptides were seen for all anti-sera (Figures 4.2C - 4.2F). This cross reactivity is most likely due to the polyclonal nature of the anti-sera, made up of antibodies for various epitopes of the respective antigens, both including and not including the modification site.

4.4 Comparing the DYEDQQKQL Antigen Minus the Cysteine Residue

During peptide synthesis a cysteine residue was included to enable the necessary immunization and purification steps. The produced sheep sera were tested against two similar peptides, identical except for the presence or absence of a cysteine residue (Figure 4.3). This was performed in order to determine if the inclusion of a cysteine in the peptide sequence affected the antibody specificity. As figure 4.3 shows, all sheep sera show binding to both peptides, albeit lower overall binding to the peptide without the cysteine residue. This is most likely relating to the polyclonal nature of the sera.

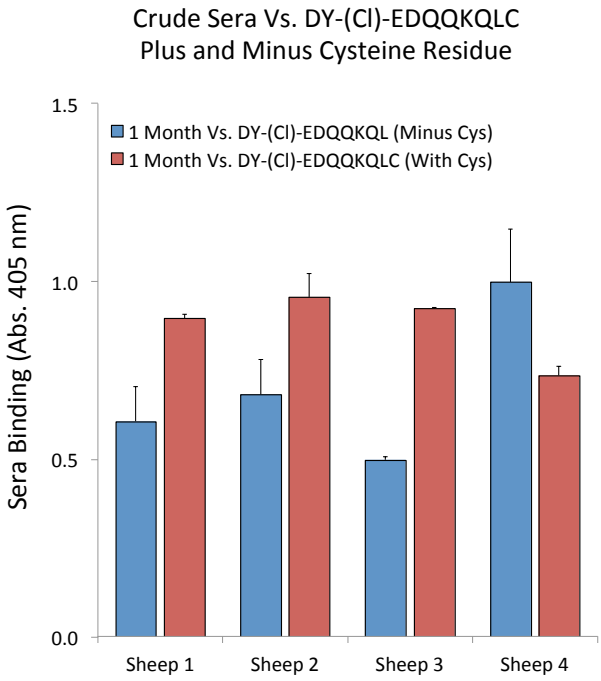

Figure 4.3: Binding Differences of Sera 1 Month After Immunization Vs. Peptides Synthesized Either with or without a Cysteine Residue. (*n* = 3, standard deviation of technical replicates). Nunc maxi-sorp plates (Product code: 10098860, Fisher Scientific, UK) were coated with 2 µg/mL of peptide antigens. The tested anti-sera (1:2000 dilution) were detected with 1:25,000 donkey anti-sheep antibody conjugated to alkaline phosphatase (Product code: A5187), and 1 mg/mL phosphate substrate in pNPP buffer, pH 10.4, with an incubation time of 15 minutes at room temperature before being read on a plate reader at 405 nm.

4.5 Reducing DYEDQQKQLC Anti-Sera Series Cross-Reactivity

In order to obtain more sequence and modification specific anti-sera, affinity enrichment described throughout as affinity purification, was performed on sera in an attempt to remove some of the cross reactivity. The anti-sera from sheep numbers 3 and 4, having been immunized with DY-(Cl)-EDQQKQLC, were initially selected for purification. Affinity purification of sera obtained from both sheep was carried out, but for illustrative purposes the results for sheep number 3's serum purification are shown (Figures 4.4A and 4.4B). To obtain DY-(Cl)-EDQQKQLC specific antibodies, the purification process involved binding DY-(Cl)-EDQQKQLC synthetic peptide to silica beads via the cysteine residue. The anti-serum was then passed through the column to exclude non-specific antibodies (Fraction eluted with PBS, pH 7.4), and collected, figure 4.4A). To elute the bound antibodies, glycine buffer at pH 2.7 was used (Shown in Figure 4.4A). This eluent was then passed through another column containing beads conjugated with DYEDQQKQLC peptide (Figure 4.4b). This time the PBS eluted fraction (Shown in figure 4.4B) contains the antibodies specific for DY-(Cl)-EDQQKQLC. Both the PBS and glycine eluted fractions were collected for testing.

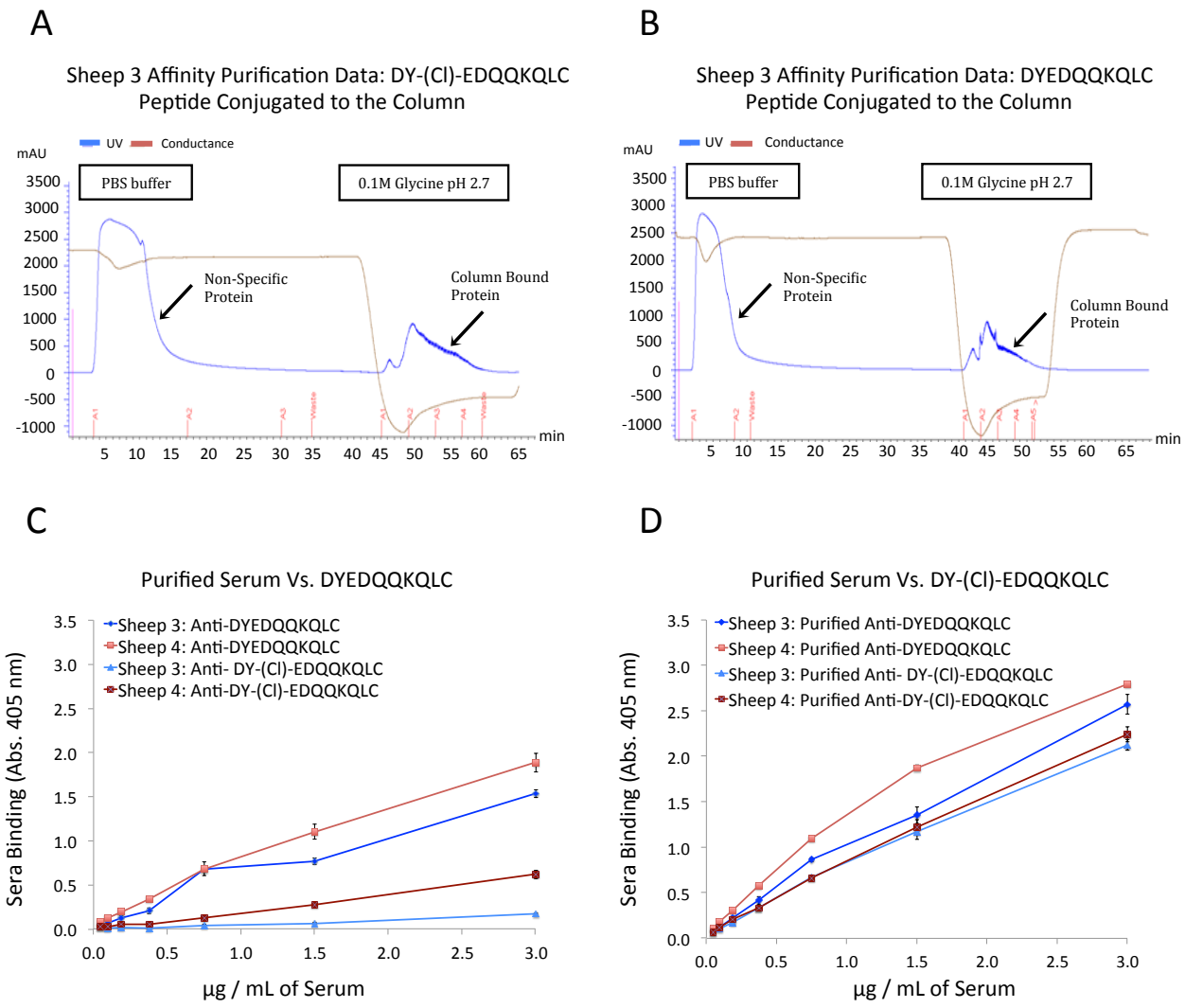

Figure 4.4: Purification and Subsequent Testing of Purified Sera. For affinity purification (A and B) (UV λ = 280 nm) the peptides were bound to iodoacetyl gel beads via cysteine residues (53155, Thermo Scientific, UK) and unbound binding sites were blocked with 50 mM cysteine. Utilizing an AKTA Purifier (GE Healthcare) columns were washed with 1 M NaCl to remove any non-specific bound material, PBS and 0.1 M glycine (pH 2.7) was used to elute antibodies at a flow rate not exceeding 1 mL/ min. The ELISA plates (C and D) (n = 3, standard deviation of technical replicates) were coated to 2 µg/mL in distilled water, with proteins in molar equivalents of peptides antigens, anti -sera concentrations of 1.5 µg / mL. Sera was detected with 1:25,000 donkey anti-sheep antibody conjugated to alkaline phosphatase (Product code: A5187), and 1 mg/mL phosphate substrate in pNPP buffer, pH 10.4, with an incubation time of 15 minutes at room temperature before being read on a plate reader at 405 nm.

Having undergone purification to exclude DYEDQQKQLC antibodies, sheep number 3's anti- DY-(Cl)-EDQQKQLC eluate shows no significant binding to the native DYEDQQKQLC peptide (figure 4.4C). However, from looking at figure 4.4D, the same serum shows a significant amount of binding to its antigen, DY-(Cl)-EDQQKQLC peptide. Sheep number 4 anti- DY-(Cl)-EDQQKQLC eluate shows a similar trend, but with a higher amount of binding/cross-reactivity to the native peptide. The purification process also provided anti-sera for the native DYEDQQKQLC peptide. The respective sera showed some cross reactivity to DY-(Cl)-EDQQKQLC (figure 4.4D), which is to be expected between such similar antigens, as the sera is made up of antibodies that are potentially specific to multiple epitopes of the DYEDQQKQLC peptide. Another factor to consider is that these sera will also contain plasma proteins, and a large number of other antibodies for various other antigens. The serum collected from sheep number 3 showed strong binding to both the native and 3-chlorotyrosine versions of the DYEDQQKQLC peptides, and as such, each individual purification fraction was collected for use. Sheep number 3, anti- DY-(Cl)-EDQQKQLC eluate, is used throughout and as such will now be referred to as affinity purified (AP) anti- DY-(Cl)-EDQQKQLC. In addition to testing against DY-(Cl)-EDQQKQLC and DYEDQQKQLC peptides, the specificity of AP anti- DY-(Cl)-EDQQKQLC was tested against various other antigens. AP anti-DY-(Cl)-EDQQKQLC showed no significant binding to the native, chlorinated or nitrated versions of the MS identified peptide STSYGTGC, and neither did it bind to whole native fibrinogen (figure 4.5A). A nitrated version of DY-(Cl)-EDQQKQLC peptide was synthesized (DY-NO_2-EDQKQQLC) and tested against AP anti- DY-(Cl)-EDQQKQLC to determine the modification site specificity of the anti-serum. AP anti- DY-(Cl)-EDQQKQLC displayed strong cross reactivity to DY-(NO_2)-EDQQKQLC (Figure 4.5B).

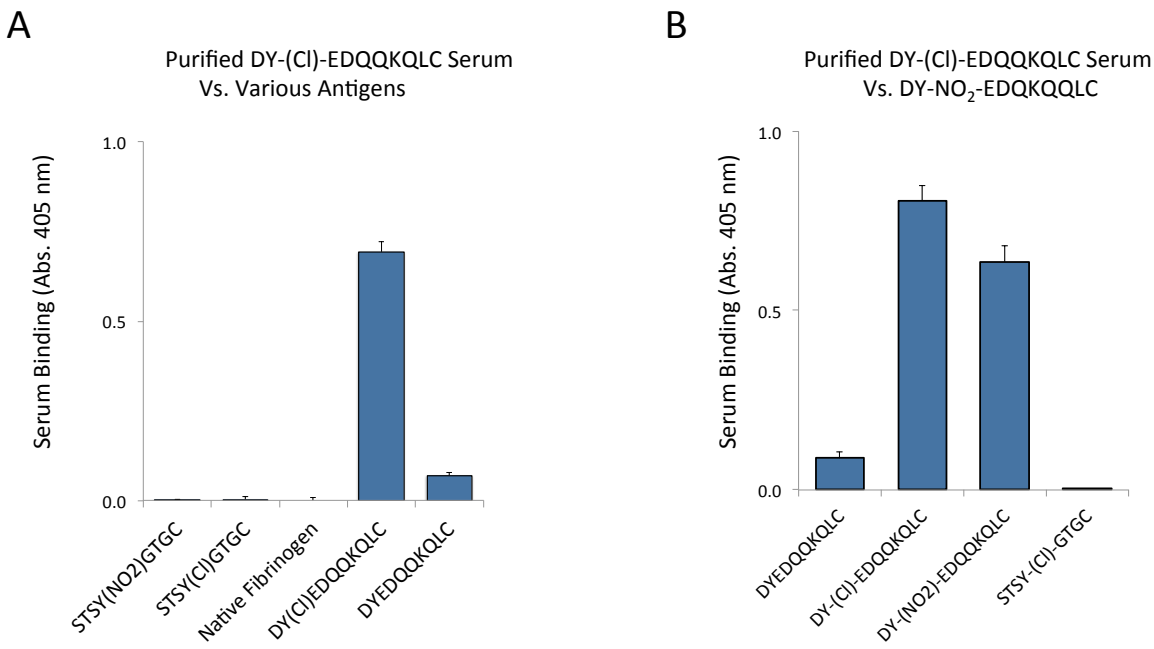

Figure 4.5: Purification and Subsequent Testing of Purified Sera. (*n* = 3, standard deviation of technical replicates) The ELISA (A and B) plates were coated to 2 µg/mL, with proteins in molar equivalents to peptide antigens. The sera concentration was 1.5 µg/mL, detected with 1: 25,000 donkey anti-sheep antibody conjugated to alkaline phosphatase (Product code: A5187), and 1 mg/mL phosphate substrate in pNPP buffer, pH 10.4, with an incubation time of 15 minutes at room temperature before being read on a plate reader at 405 nm.

4.6 Experimental Variability of AP anti- DY-(Cl)-EDQQKQLC

It was noted that there was substantial inter plate variability, with regard to the anti-sera binding values, as can be seen when comparing figures 4.2 and 4.4. In order to make comparisons between the responses to different antigens, and investigate inter-plate variability, three independent ELISA plates with all antigens on the same plate were performed (Figure 4.6). These experimental replicates were performed on different days with new reagents and between two different operators to allow experimental variability to be determined. The variability was determined by calculating the coefficient of variation (CV) of each antigen, based on the results from three independent but identical experiments. Expressing the CV of values close to zero provides unreliable results, and for this reason only antigens that gave absorbance (anti-serum binding) values greater than 0.100 were utilized (Gulhar *et al*., 2012). The CV values based on the three anti- DYEDQQKQLC serum experiments (Figure 4.6) had an average CV of 11%. Cross-comparison of the absorbance values for AP anti- DY-(Cl)-EDQQKQLC serum ELISAs further supports this. Between all experimental work (Figures 4.3 - 4.6) there appears to be large anti-serum binding variability, but the overall specificity trend of serum to antigen binding is however the same. Specifically, there is very little binding to any non-DYEDQQKQLC motif series antigens, and a significantly higher amount of binding to both the chlorinated and nitrated versions of the DYEDQQKQLC peptide. The reduction in signal seen between anti-DYEDQQKQLC sera series ELISA experiments may correspond to the age of the sera. This reduction in signal may be due to protein degradation and aggregation following storage at 2-4°C for a prolonged period of time, and potentially the presence of plasma proteases. Some of the ELISA results were performed 2-3 years after the initial sera were obtained, resulting in decreased anti-sera binding over time, and as such inter-assay variability.

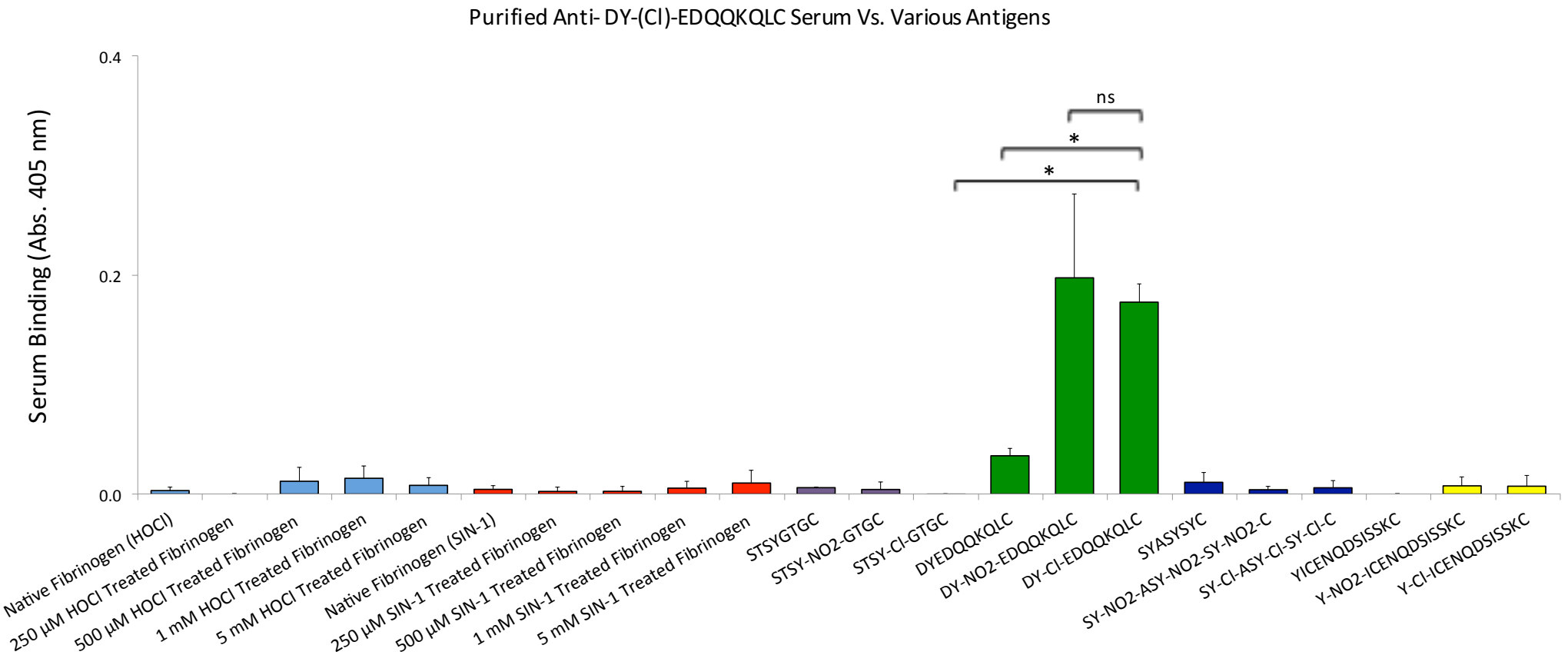

Figure 4.6: Identifying Inter-Experimental Variability and Binding Trends. (*n* = 3, error bars represent standard deviation of experimental replicates). (ns = P > 0.05 and * = P ≤ 0.05). Synthesised peptide antigens were coated onto Nunc maxi-sorp plates (Product code: 10098860, Fisher Scientific, UK) at 2 µg/mL. The proteins were treated with either SIN-1 or HOCl for 1 hour at 37°C before being coated onto Nunc maxi-sorp plates in molar equivalent amounts to the peptide antigens. The primary anti-serum was made to 1.5 µg/mL. The tested anti-sera were detected with 1:25,000 donkey anti-sheep antibody conjugated to alkaline phosphatase (Product code: A5187), and 1 mg/mL phosphate substrate in pNPP buffer, pH 10.4, with an incubation time of 15 minutes at room temperature before being read on a plate reader at 405 nm.

4.7 Testing DY-(Cl)-EDQQKQLC Serum Vs. Abundant Plasma Proteins

Extending the approach taken in the previous section (whereby the ability of anti-serum to recognize native and modified peptides within a protein, was investigated), the binding of AP anti- DY-(Cl)-EDQQKQLC to the most abundant plasma proteins, (Anderson and Anderson, 2002) was studied. More specifically, in order of abundance, native and chlorinated, haemoglobin (Figure 4.7A), human serum albumin (HSA) (Figure 4.7B), fibrinogen (Figure 4.7C) and transferrin (Figure 4.7D) were tested. The AP anti- DY-(Cl)-EDQQKQLC serum showed no significant binding to the chlorinated or native plasma proteins, including fibrinogen (Figures 4.7A-4.7D). An extensive Blast® search of the SwissProt database within the human taxonomy revealed no proteins, other than fibrinogen, with any similar amino acid sequences to DYEDQQKQL, further supporting the lack of binding.

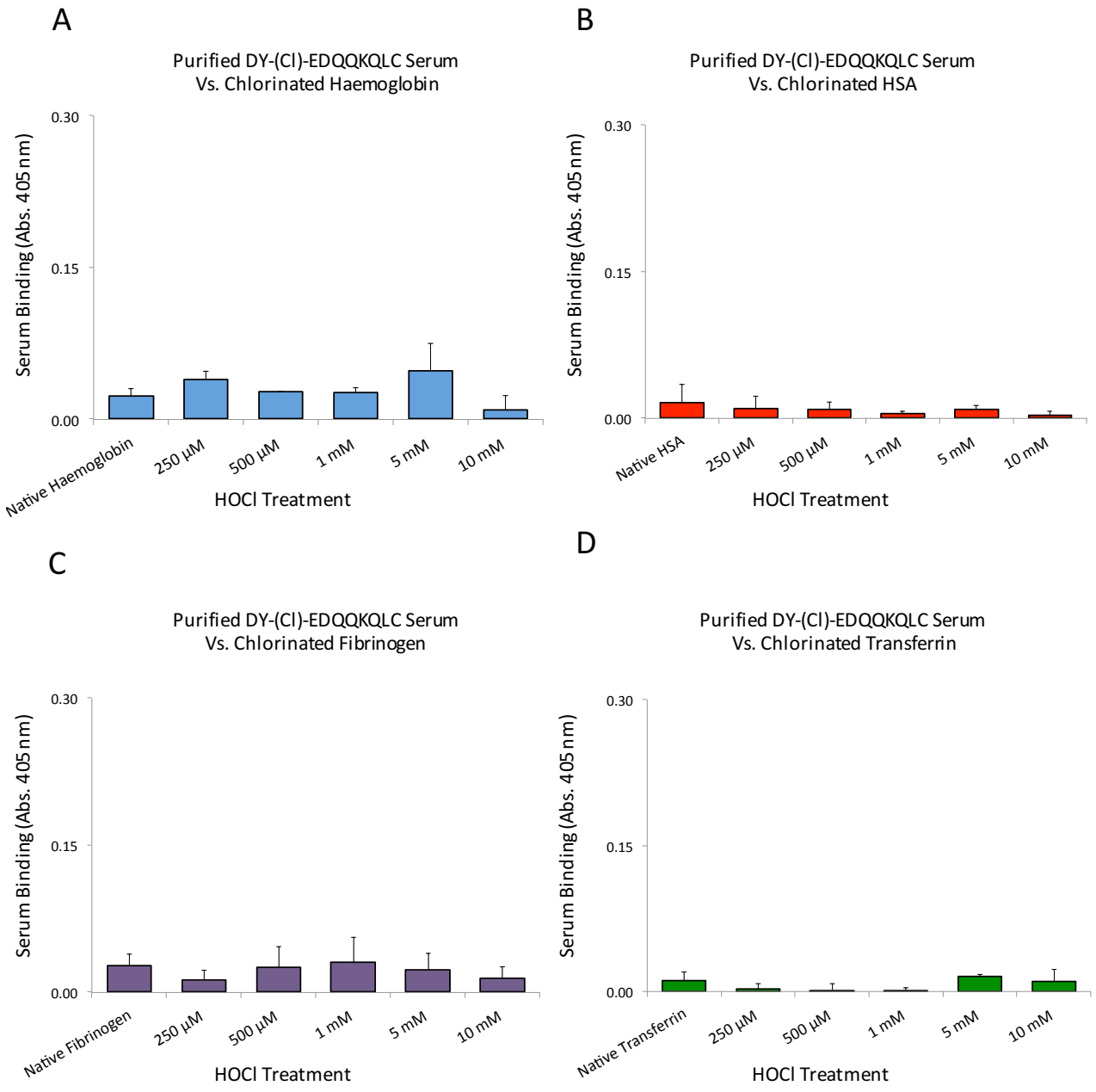

Figure 4.7: Binding of AP Anti- DY-(Cl)-EDQQKQLC serum to Most Abundant Plasma Proteome Proteins. (*n* = 3, standard deviation of technical replicates). The proteins described in A to D were treated with hypochlorous acid (HOCl) for 1 hour at 37°C before being coated to Nunc maxi-sorp plates (Product code: 10098860, Fisher Scientific, UK) in molar equivalent amounts to DYEDQQKQLC peptides. The tested anti-sera were detected with 1:25,000 donkey anti-sheep antibody conjugated to alkaline phosphatase (Product code: A5187), and 1 mg/mL phosphate substrate in pNPP buffer, pH 10.4, with an incubation time of 15 minutes at room temperature before being read on a plate reader at 405 nm.

4.9 Design of Novel 3-nitrotyrosine Peptide for Testing Sera

In order to test the binding specificity of produced anti-sera, a novel 3-nitrotyrosine-containing peptide, along with the native and chlorinated versions, were produced. Two main factors were considered during the design process, firstly, the solubility of the peptide; with tyrosine being a non-polar residue, the addition of polar serine residues was selected to encourage better solubility. Finally, the folding of the peptide into an α-helix, and how well-distributed the tyrosine residues are for antibody binding. The large number of tyrosine resides in the peptide meant that it was very non-polar (hydrophobic), and in an attempt to counteract this serine residues were added to the sequence. The results returned from the Innovagen calculator (Figure 4.8A) showed the SYASYSYC peptide to have poor water solubility. However, upon production and use of the peptide, it readily dissolved in water. The α-helix projections of the peptide with helical wheel projection software showed the tyrosine residues to be evenly distributed (Figure 4.8B). This made the peptide ideal for testing antibodies for 3-nitrotyrosine and 3-chlorotyrosine, and potentially for generating such specific antibodies. This peptide series was produced and used throughout to test antibody specificity.

A

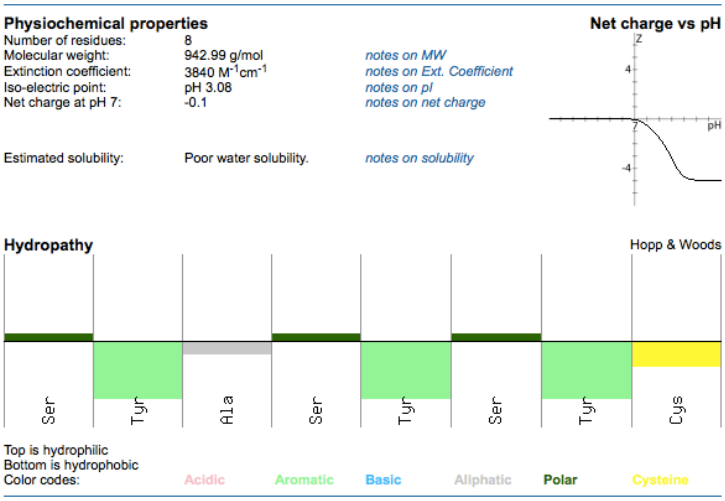

B

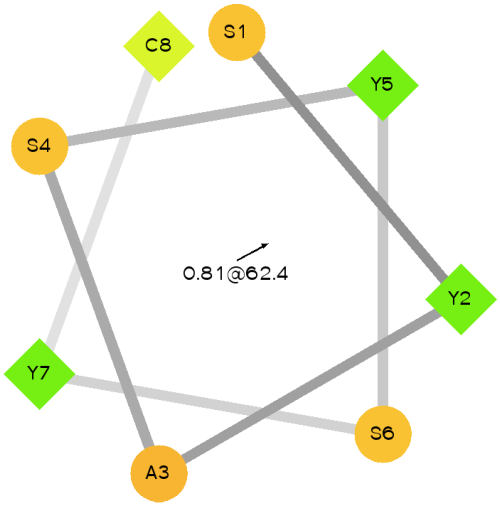

Figure 4.8: Analysis of SYASYSYC Peptide Antigen Properties. (A) The peptide's solubility and charge was determined using Innovagen peptide solubility calculator (http://pepcalc.com). (B) Antigenic properties of the peptide were determined by mapping the positions of the tyrosine residues within the α-helix with Wheel (version 0.10), helical wheel projection software (http://rzlab.ucr.edu/scripts/wheel/wheel.cgi). Each letter represents an amino acid, followed by a number representing where it resides in the peptide sequence. The connecting lines show the peptides spatial arrangement, in that, the lighter coloured lines are further away than the darker lines.

4.10 Details of Synthesis for Designed and Identified Peptides

As described in chapter 3, the modified fibrinogen peptide ^{273}GSTSY-(NO_2)-GTGSETESPR^{287} was the most commonly observed modified peptide with a high ion score, indicating a strong correlation between the *in-silico* and experimental data, making this peptide a good choice against which to produce antibodies. The peptide was shortened in order to improve yield during peptide synthesis, but retaining the tyrosine and surrounding amino acid residues. A cysteine residue was added at the C-terminus of the peptide to later allow conjugation to KLH for immunization, and purification purposes. Native, nitrated and chlorinated versions of the peptide were synthesized, STSYGTGC, STSY-(NO_2)-GTGC and STSY-(Cl)-GTGC. In addition to the MS identified peptides, a modified human serum albumin (HSA) peptide ^{287}Y-(Cl)-ICENQDSISSK^{298} identified in a study performed by Tveen-Jensen *et al*. (2013), and both a native and nitrated version were synthesized. In addition to MS identified peptides, a novel peptide series was designed, discussed above. The custom peptides were synthesized and purified, by a commercial supplier (Isca Biochemicals, UK), according to the methods described previously. The HPLC purification and MS analysis results for the respective peptides can be found in the appendix 1- 27.

4.11 Immunoassay Screening of STSYGTGC Anti-Sera Series

None of the pre-immune anti-sera, STSYGTGC, STSY-(NO_2)-GTGC or STSY-(Cl)-GTGC, showed significant binding to any of the STSYGTGC peptides, or DY-(Cl)-EDQQKQLC (Figures 4.9A – 4.9C). One month after immunization the STSYGTGC anti-serum showed strong binding to its corresponding peptide antigen. The serum also showed a low level of binding to the nitrated and chlorinated versions of the peptide, and no binding to a peptide with a different sequence (DY-(Cl)-EDQKQQLC) (Figure 4.10A). The anti-STSY-(Cl)-GTGC serum from one month after immunization (Figure 4.10B) showed strong binding to STSY-(Cl)-GTGC, and some binding to the other STSYGTGC peptides. However, no significant binding to the peptide DY-(Cl)-EDQKQQLC, which similarly contains a chlorinated tyrosine residue, was apparent. Thus, the anti-STSY-(Cl)-GTGC serum displayed potential modification site specificity. Finally, the serum raised against the modified peptide identified in SIN-1-treated fibrinogen by MS, anti-STSY-(NO_2)-GTGC, displayed specificity to both nitrated and chlorinated versions of STSYGTGC, with greater binding to STSY-(NO_2)-GTGC. No binding to the DY-(Cl)-EDQQKQLC peptide was apparent (Figure 4.10C). Similarly, to the DYEDQQKQLC anti-sera, the STSY-(Cl)-GTGC and STSY-(NO2)-GTGC anti-sera displayed a prominent “Hook Effect” at higher concentrations/lower dilution, presumably due to antibody agglutination (Figures 4.10A - 4.10C). For this reason, a dilution of 1:2000 was selected to allow clear definition between sera bleed months with minimal agglutination dependent signal loss for further ELISA based testing.

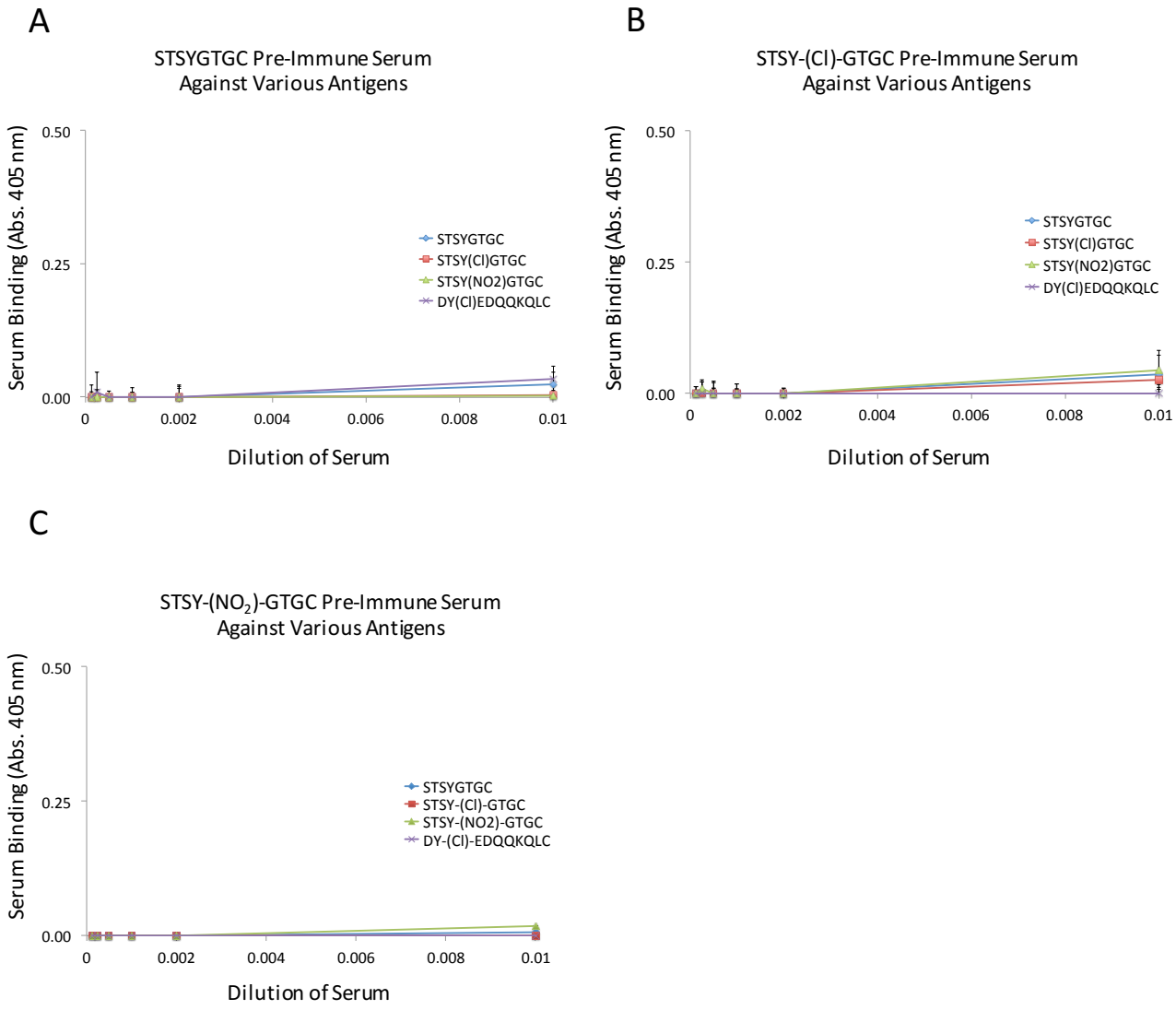

Figure 4.9: Testing Anti-STSYGTGC Series Sheep Pre-Immune Sera. (n = 3, standard deviation of technical replicates). (A to C) Pre-immume ELISA results. Nunc maxi-sorp plates (Product code: 10098860, Fisher Scientific, UK) were coated with 2 µg/mL of peptide antigens. The tested anti-sera were serial diluted and detected with 1:25,000 donkey anti-sheep antibody conjugated to alkaline phosphatase (Product code: A5187), and 1 mg/mL phosphate substrate in pNPP buffer, pH 10.4, with an incubation time of 15 minutes at room temperature before being read on a plate reader at 405 nm.

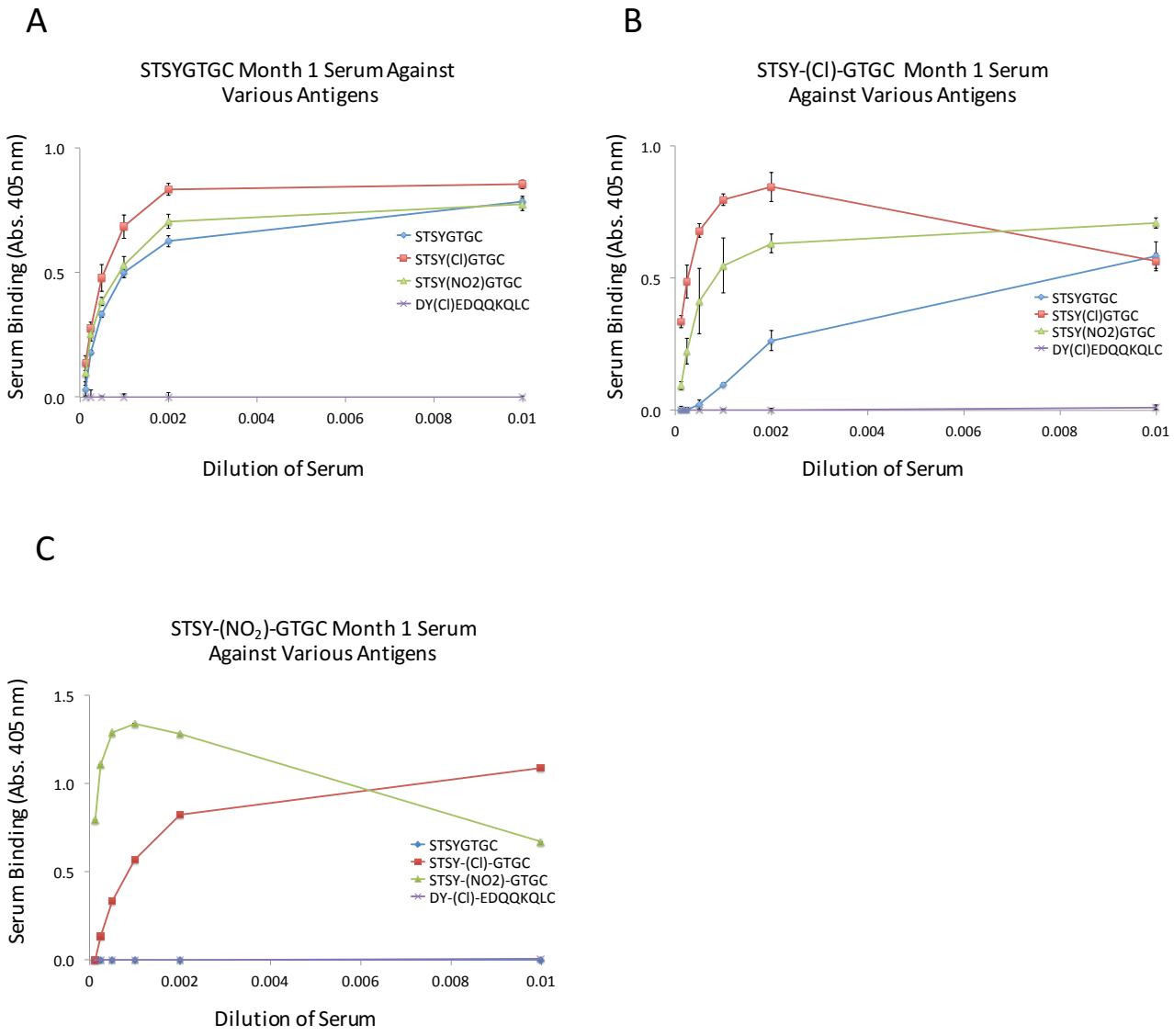

Figure 4.10: Determining Anti-STSYGTGC Anti-Sera Series Optimal Dilution. (*n* = 3, standard deviation of technical replicates). (A to C) 1 month ELISA results. Nunc maxi-sorp plates (Product code: 10098860, Fisher Scientific, UK) were coated with 2 µg/mL of peptide antigens. The tested anti-sera were serial diluted and detected with 1:25,000 donkey anti-sheep antibody conjugated to alkaline phosphatase (Product code: A5187), and 1 mg/mL phosphate substrate in pNPP buffer, pH 10.4, with an incubation time of 15 minutes at room temperature before being read on a plate reader at 405 nm.

4.11 Monthly Antibody Titre Profile of Anti-STSYGTGC Sera Series

With the success of the previous anti-sera production, one sheep for each peptide antigen was utilized during immunization. An ELISA of all respective months for each sheep, STSYGTGC, STSY-(NO_2)-GTGC or STSY-(Cl)-GTGC immunized against all STSYGTGC peptide antigens was carried out (Figures 4.11A – 4.11C). The anti-STSYGTGC (Figure 4.11A) sera increased in antibody titre for the STSYGTGC peptide after immunization, and then plateaued (Figures 4.11A). The anti-STSYGTGC sera also showed cross reactivity for the other STSYGTGC peptides, which was not surprising as the polyclonal sera is expected to contain antibodies for multiple epitopes of the peptide, both including and excluding the modification site. A similar result was seen for anti- STSY - (NO2)-GTGC sera (Figure 4.9B), with an increase in binding to the corresponding peptide antigen after immunization, but with greater binding to the STSY-(Cl)-GTGC peptide, and little binding to the native STSYGTGC peptide. The anti-STSY-(Cl)-GTGC sera (Figure 4.11C) showed an increase in binding to the corresponding peptide antigen and again with cross reactivity to other peptides, with slightly more binding to the modified peptide antigens.

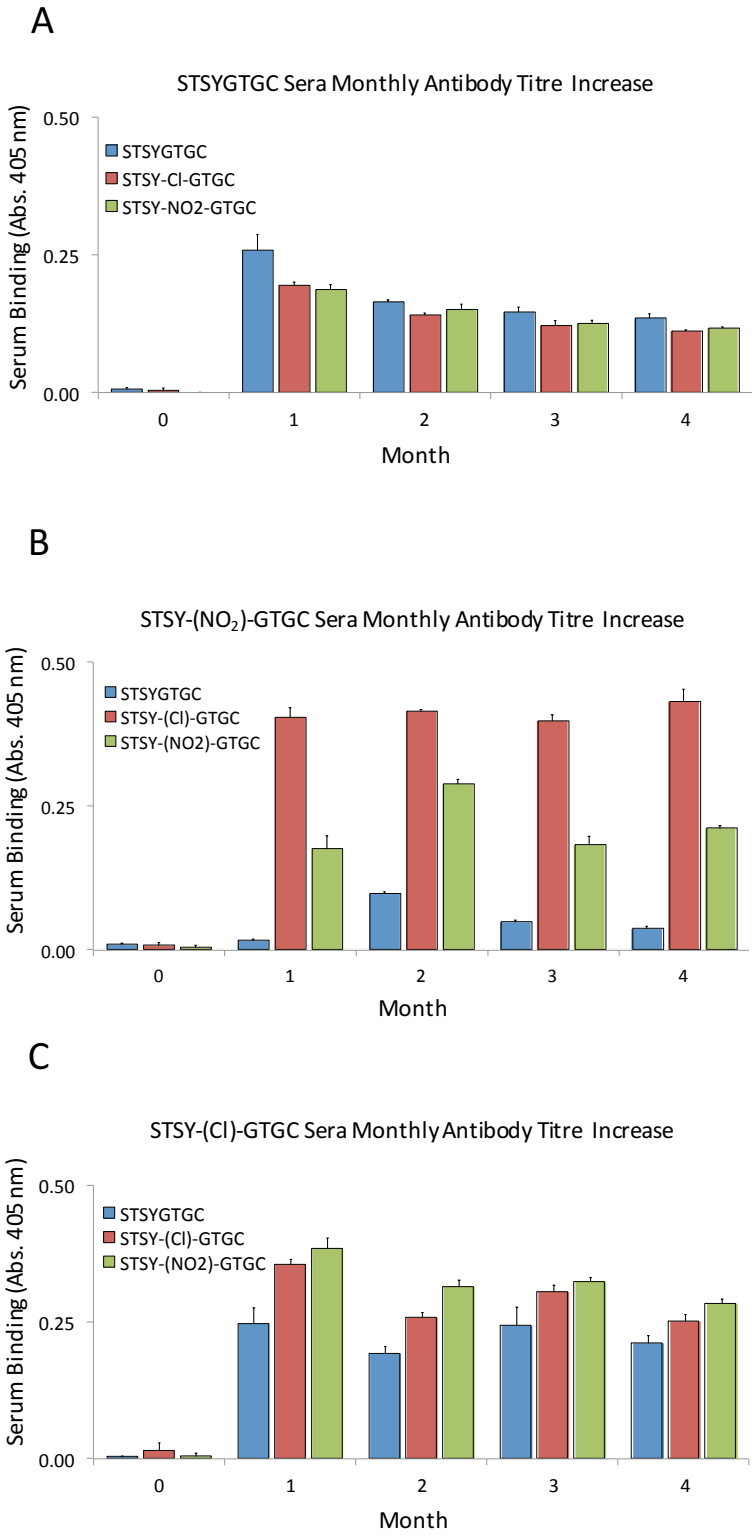

Figure 4.11: Changes in Anti-Sera Antibody Titre Over Time. (n = 3, standard deviation of technical replicates). Nunc maxi-sorp plates (Product code: 10098860, Fisher Scientific, UK) were coated with 2 µg/mL of peptide antigens. The primary anti-sera were diluted to 1:2000. The tested anti-sera were detected with 1:25,000 donkey anti-sheep antibody conjugated to alkaline phosphatase (Product code: A5187), and 1 mg/mL phosphate substrate in pNPP buffer, pH 10.4, with an incubation time of 15 minutes at room temperature before being read on a plate reader at 405 nm.

4.12 Reducing Anti-STSYGTGC Sera Series Cross-Reactivity

The anti- STSYGTGC sera series showed some degree of cross reactivity to similar antigens, and in order to attempt to reduce the cross reactivity, affinity purification was performed, as described previously for DYEDQQKQLC series of sera (Section 4.5). Affinity purification results for all STSYGTGC sera were produced (Appendix 29 and 30), for illustrative purposes the results for sheep STSY-(NO_2)-GTGC serum purification are shown (Figures 4.12A and 4.12B). Enrichment, described as purification, for STSY-(NO_2)-GTGC specific antibodies, involved binding the STSY-(NO_2)-GTGC synthetic peptide to silica beads via the cysteine residue. The anti-serum was then passed through the STSY-(NO_2)-GTGC column with PBS to exclude non-specific antibodies (Figure 4.12A), and the fraction collected. Sodium chloride was then used to remove non-specific binding fractions. The pH was lowered with glycine (pH 2.7) (shown in Figure 4.12A) and the column bound antibody fraction eluted for collection. The described PBS eluted fraction, now enriched for STSY-(NO_2)-GTGC antibodies, was then passed through another column containing beads conjugated with the STSY-(Cl)-GTGC peptide with PBS (Figure 4.12B). This PBS eluted fraction (Shown in figure 4.12B) is now excluded of STSY-(Cl)-GTGC binding fractions, both the PBS and glycine eluted fractions were collected for testing. The results in Figure 4.13 shows the difference in binding specificity of the STSY-(NO_2)-GTGC anti-serum before (Pre-Cl-Y column pass serum) and after (Post-Cl-Y column pass serum) exclusion of STSY-(Cl)-GTGC peptide binding fraction. Figure 4.13 result shows how the original serum cross-reacts, and binds STSY-(Cl)-GTGC, and that after passing the serum through the column bound with the STSY-(Cl)-GTGC peptide, although binding to STS-(NO_2)-GTGC is slightly reduced, cross reactivity is abolished. The affinity purified (AP) collected STSY-(NO_2)-GTGC fraction is now referred to as AP STS -(NO_2)-GTGC.

A

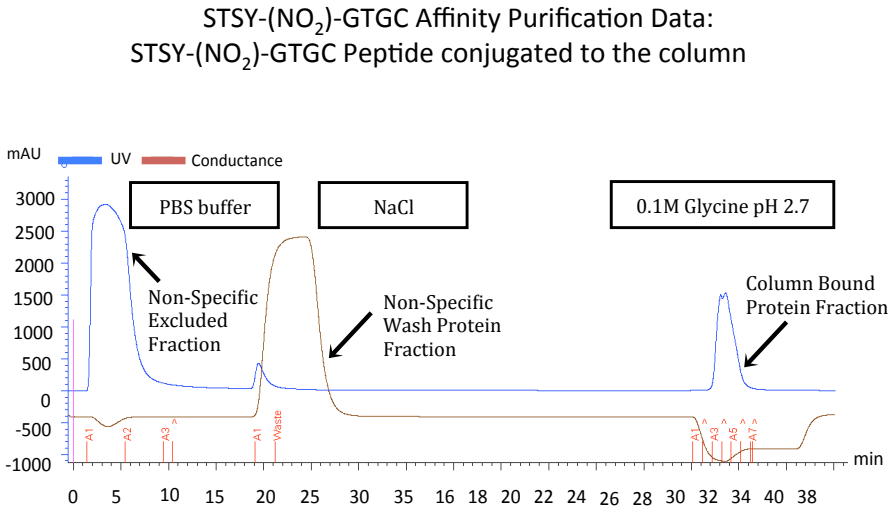

B

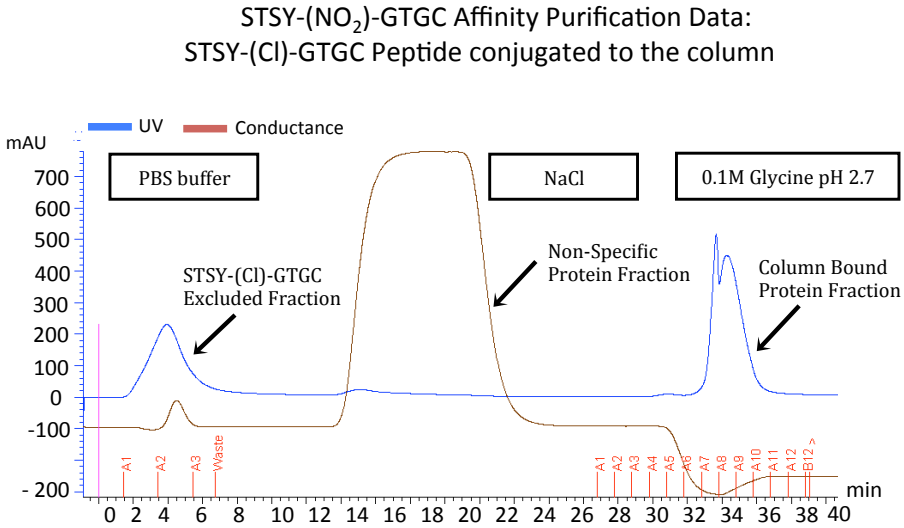

Figure 4.12: Affinity Purification Results For STSY - (NO_2)- GTGC. (UV λ = 280 nm). STSY-(NO_2)-GTGC peptide (A) and STSY-(Cl)-GTGC (B) was bound to iodoacetyl gel beads via the cysteine residues (Product no. 53155, Thermo Scientific, UK), and unbound binding sites were blocked with 50 mM cysteine. Utilizing an AKTA Purifier (GE Healthcare) sera was passed through columns at a flow rate not exceeding 1 mL/ min at room temperature with PBS (pH 7.4), and fractions collected. Columns were washed with 1 M NaCl (pH 7) to remove any non-specific bound material, the fraction collected. Finally, 0.1 M glycine (pH 2.7) was used to elute column bound fractions (A and B). The protein concentration was measured at UV wavelength 280 nm, and the NaCl concentration via conductance.

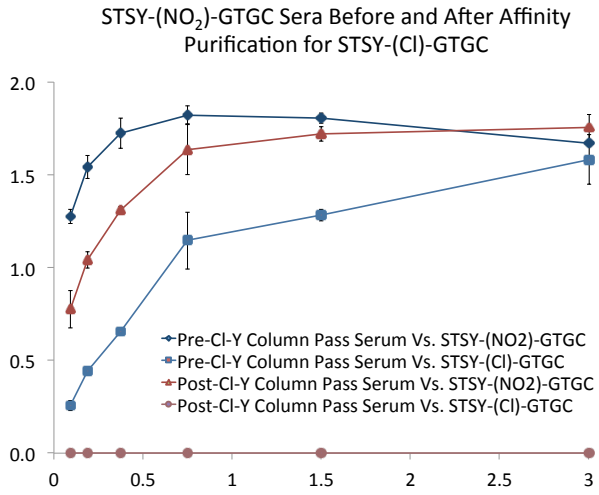

Figure 4.13: Binding Comparison of Serum Fractions Before and After Purification. (*n* = 3, standard deviation of technical replicates) Nunc maxi-sorp plates (Product code: 10098860, Fisher Scientific, UK) were coated with 2 µg/mL of peptide antigens. The primary anti-sera were diluted to 1:2000. The tested anti-sera were detected with 1:25,000 donkey anti-sheep antibody conjugated to alkaline phosphatase (Product code: A5187), and 1 mg/mL phosphate substrate in pNPP buffer, pH 10.4, with an incubation time of 15 minutes at room temperature before being read on a plate reader at 405 nm.

From looking at figure 4.14A, AP STSY-(NO_2)-GTGC shows reduced cross-reactivity, no longer binding to STSY-(Cl)-GTGC or the native STSYGTGC peptide. The serum does however show strong cross reactivity to the DY-(NO_2)-EDQKQQLC peptide. In order to determine whether cross reactivity was specific to the DY-(NO_2)-EDQKQQLC, 3-nitrotyrosine containing peptide, or to the 3-nitrotyrosine modified residue in general, another ELISA of multiple 3-nitrotyrosine containing peptides with different amino acid sequences was performed. It can be seen that binding to the DY-(NO_2)-EDQKQQLC peptide and a model 3-nitrotyrsosine-containing peptide (SY-(NO_2)-ASY-(NO_2)-SYC) occurred with similar affinity (4.14B). The AP antiserum was further tested against whole fibrinogen treated with a range of SIN-1 concentrations, and it can be seen that there was a concentration-dependent increase in binding, with no significant binding to the native protein (Figure 4.14C). The binding to fibrinogen treated with different HOCl concentrations appeared to be

weak, and there was no evidence of a concentration-dependent effect for this modification (Figure 4.14D).

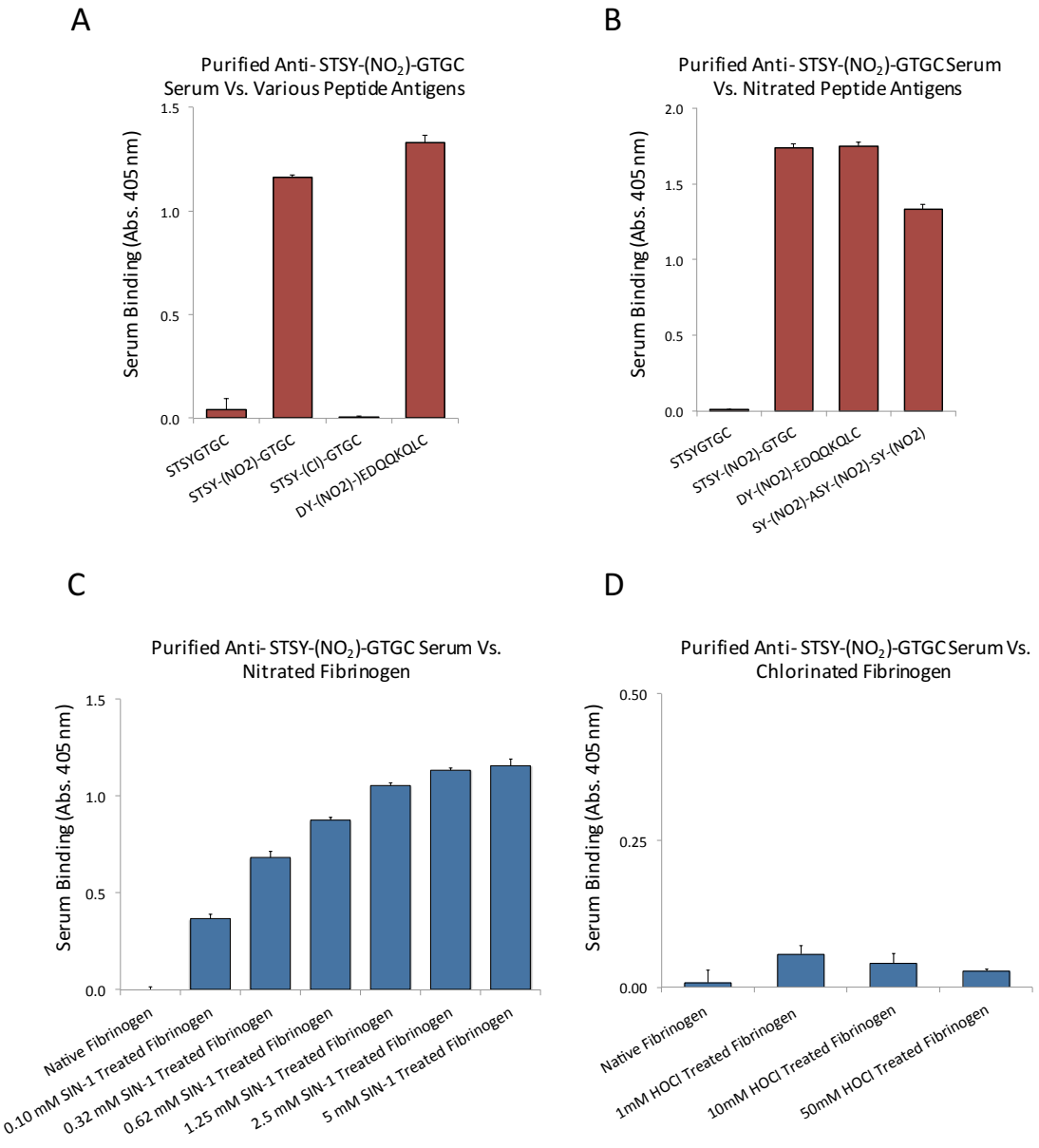

Figure 4.14: Comparing the Binding of AP Anti- STSY - (NO2)- GTGC Serum to Peptide and Protein Antigens. (*n* = 3, standard deviation of technical replicates). Peptide antigens (A and B) were coated onto Nunc maxi-sorp plates (Product code: 10098860, Fisher Scientific, UK) at 2 µg/mL. The proteins described in C and D were treated with either (C) SIN-1 or (D) HOCl for 1 hour at 37°C before being coated onto Nunc maxi-sorp plates in molar equivalent amounts to the peptide antigens. The primary anti-serum was made to 1.5 µg/mL. The tested anti-sera were detected with 1:25,000 donkey anti-sheep antibody conjugated to alkaline phosphatase (Product code: A5187), and 1 mg/mL phosphate substrate in pNPP buffer, pH 10.4, with an incubation time of 15 minutes at room temperature before being read on a plate reader at 405 nm.

4.13 AP Anti- STSY-(NO_2)-GTGC Serum Vs. Other Plasma Proteins

The most abundant plasma proteins are haemoglobin, human serum albumin (HSA), fibrinogen and transferrin (Anderson and Anderson, 2002). Human serum albumin contains 585 amino acid residues, 18 of which are tyrosine (3%) (Meloun *et al.,*1975). Transferrin is made up of 678 amino acids, of which 24 are tyrosine (3.5%) (MacGillivray *et al.,* 1982). Haemoglobin is made up of 574 amino acids and a varying number of tyrosine residues, the average being 2.8 residues (Hill *et al.*, 1962). The UniProt database amino acid sequences for human haemoglobin (Entry code: P68871, P69905 and P69892), human serum albumin (HSA) (Entry code: P02768) and human transferrin (Entry code: P02787) were manually selected and a Blast search comparison made. None of the mentioned proteins shared similar amino acid sequences, or any sequence similar to STSYGTGC.

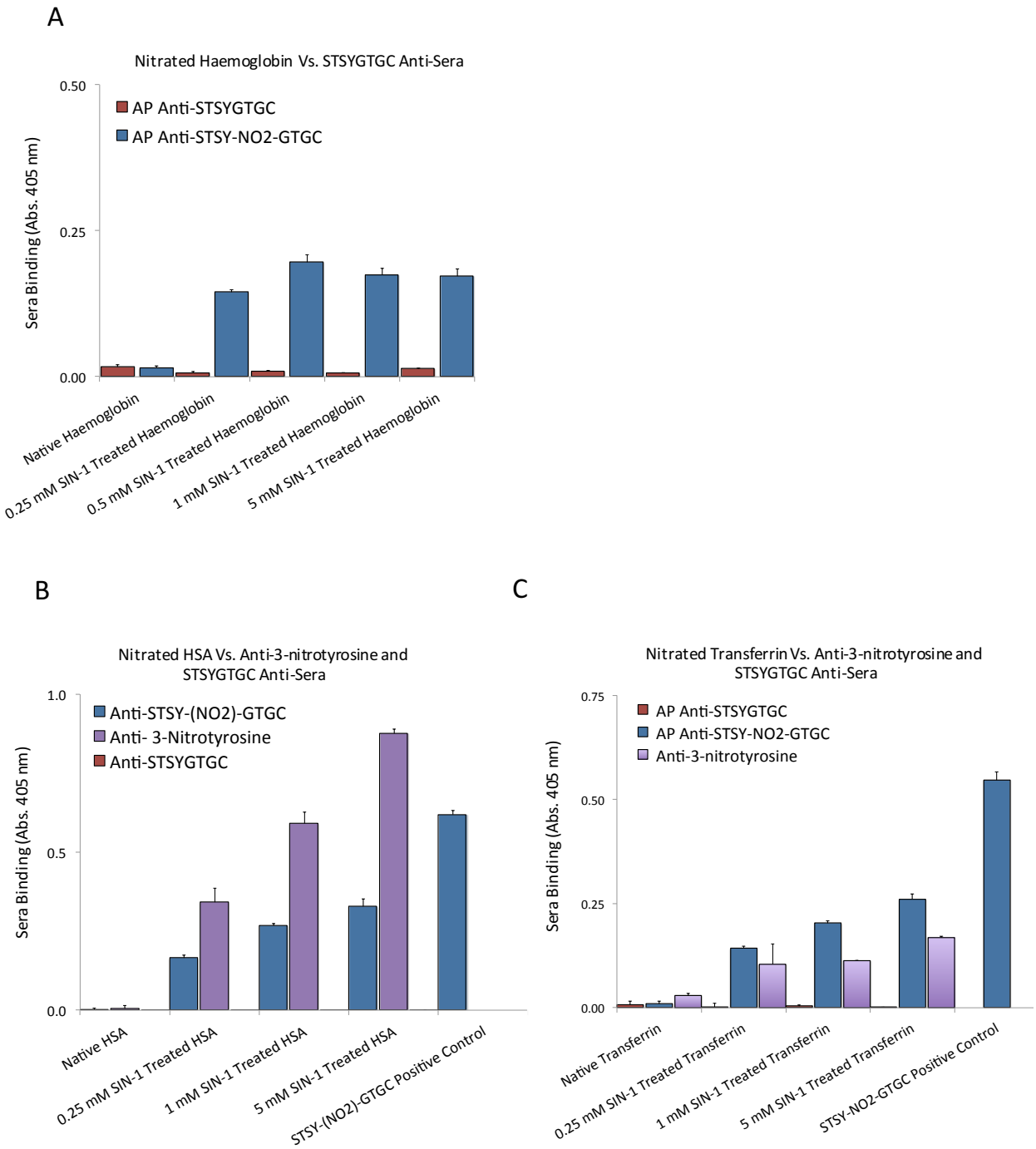

Figure 4.15: Comparing the Binding of AP STSYGTGC Sera and Anti - 3-nitrotyrosine to Plasma Proteins. (*n* = 3, standard deviation of technical replicates). The proteins described in A to D were treated with SIN-1 for 1 hour at 37°C before being coated onto Nunc maxi-sorp plates (Product code: 10098860, Fisher Scientific, UK) in molar equivalent amounts to STSY-(NO_2)-GTGC 2 µg/mL of peptide antigens. The purified primary serum was made to 1.5 µg / mL. Anti-3-nitrotyrosine antibody (N0409) was used at a working dilution of 1:1000. The tested anti-sera were detected with 1:25,000 donkey anti-sheep antibody conjugated to alkaline phosphatase (Product code: A5187), and 1 mg/mL phosphate substrate (S0942) in pNPP buffer, pH 10.4, with an incubation time of 15 minutes at room temperature before being read on a plate reader at 405 nm.

The AP STSY-(NO_2)-GTGC anti-serum does not show binding to native forms of haemoglobin, HSA and transferrin. However, it does show binding to nitrated versions of all three of the proteins (Figures 4.15A - 4.15C) to varying degrees. This could be explained by the polyclonal nature of the anti-serum showing antibodies binding to 3-nitrotyrosine. Although affinity purification removed some of the cross reactivity, previous figures support the idea that the serum contains antibodies directed to 3-nitrotyrosine- containing antigens. The native serum (STSYGTGC) shows no binding to any of the haemoglobin preparations (Figure 4.15A), whereas the STSY-(NO_2)-GTGC serum shows a concentration dependent increase in binding to nitrated haemoglobin (Figure 4.15A). A similar trend is seen for HSA (Figure 4.15B), with no binding of the native anti-STSYGTGC serum to any of the antigens, and a concentration dependent increase in binding to nitrated HSA. A commercial anti-3-nitrotyrosine (N0409) showed greater binding than AP anti- STSY-(NO_2)-GTGC serum, which may suggest that the anti-serum contained antibodies selective for both 3-nitrotyrosine and STSY-(NO_2)-GTGC. A similar level of binding of AP STSY-(NO_2)-GTGC and 3-nitrotyrosine to nitrated transferrin was seen as for haemoglobin, and again no binding of the native anti-serum to any of the antigens (Figure 4.15C).

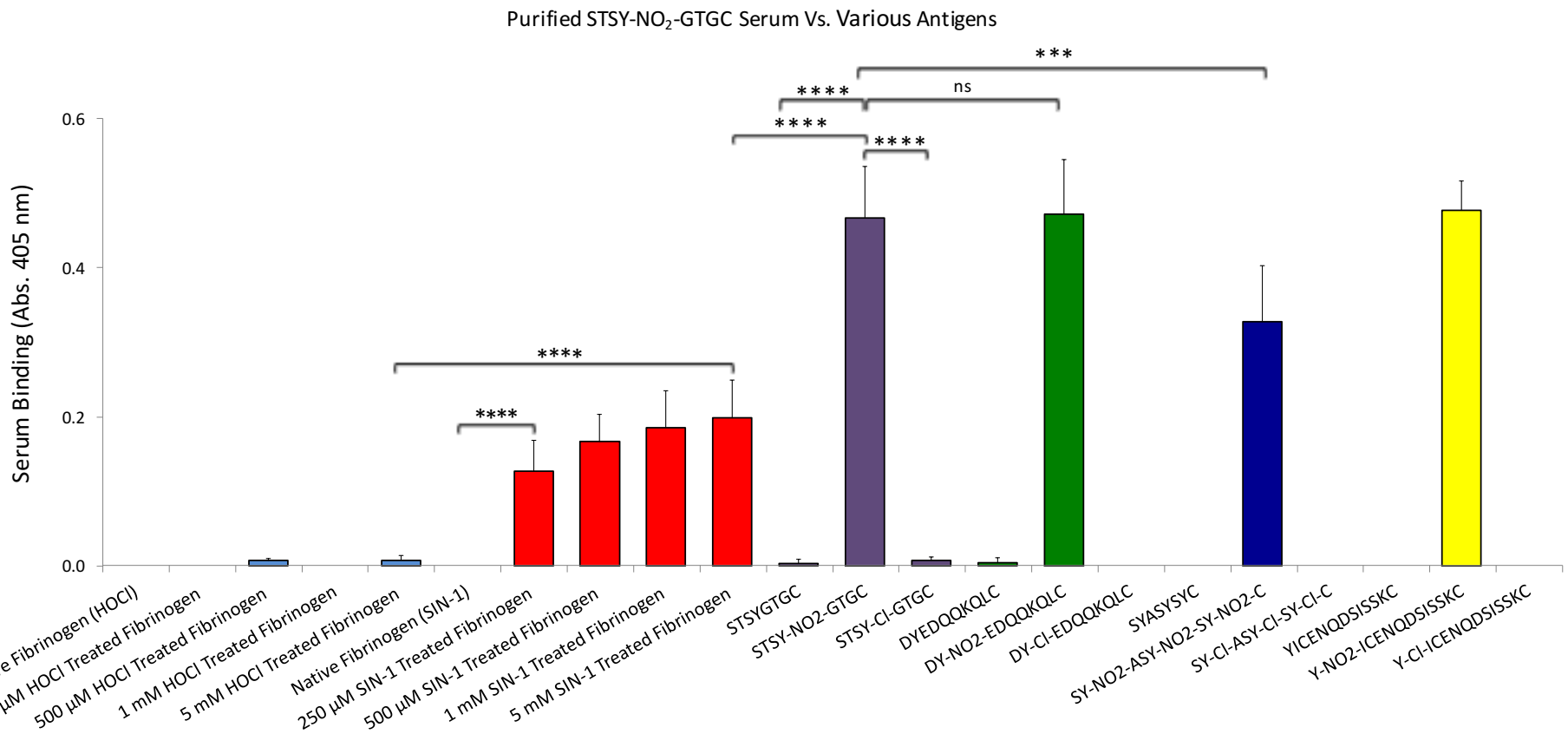

Figure 4.16: Identifying Experimental Variability and Binding Trends of AP STSY-(NO_2)–GTGC Serum. (*n* = 3, error bars represent standard deviation of experimental replicates). (ns = P > 0.05, *** = P ≤ 0.001 and **** = P ≤ 0.0001). Synthesised peptide antigens were coated onto Nunc maxi-sorp plates (Product code: 10098860, Fisher Scientific, UK) at 2 µg/ mL. The proteins treated with either SIN-1 or HOCl for 1 hour at 37°C before being coated onto Nunc maxi-sorp plates in molar equivalent amounts to the peptide antigens. The primary anti-serum was made to 1.5 µg/mL. The tested anti-sera were detected with 1:25,000 donkey anti-sheep antibody conjugated to alkaline phosphatase (Product code: A5187), and 1 mg/mL phosphate substrate in pNPP buffer, pH 10.4, with an incubation time of 15 minutes at room temperature before being read on a plate reader at 405 nm.

4.14 Experimental Variability of AP STSY-(NO_2) –GTGC Serum

A lot of variability can be seen in the values for anti-sera binding between ELISA plates when comparing figures 4.11 to 4.14. In order to make true comparisons between antigens under exactly identical conditions, three independent ELISA plates with all antigens on the same plate were set up (Figure 4.16). These experimental replicates were performed on different days with new reagents, between two different operators to allow experimental variability to be determined. The variability was determined by expressing the coefficient of variation (CV) of each antigen. Expressing the CV of values close to zero provides unreliable results, and for this reason only antigens with an absorbance of greater than 0.100 are considered (Gulhar *et al*., 2012). The CV values for the nitrated peptide antigens (Figure 4.16) had an average CV of 15%, and the nitrated fibrinogen 25%, suggesting a moderate amount of variability between experiments. It is worth noting that as the signal reduces and approaches zero, the values for CV will increase. The reduction in signal seen between anti-STSYGTGC sera series ELISA experiments corresponds to the age of the sera. This is most likely due to protein degradation due to storage at 2-4 °C, and potentially the presence of plasma proteases. In summary, the STSY-NO2 –GTGC anti- serum showed exclusive binding to antigens containing 3-nitrotyrosine, with a concentration dependent increase in binding to nitrated whole fibrinogen, and no binding exceeding basal to other antigens (Figure 4.16).

4.15 Testing the Specificity of AP STSY-(Cl)- GTGC Serum

Although STSY-(Cl)-GTGC was not identified in HOCl-treated fibrinogen by MS, as this peptide has been shown to be susceptible to nitration it is possible the same site may be susceptible to chlorination also, and for this reason anti-serum was produced against this peptide. The affinity purified anti- STSY-(Cl)-GTGC serum, as described previously, was produced and affinity purified (enriched) in the same way as the AP anti- STSY-(NO_2)-GTGC serum. The serum was tested against various peptide antigens, and showed cross reactivity for all versions of the STSYGTGC peptide (Figure 4.17A). The AP-STSY-(Cl)-GTGC serum was tested against various 3-chlorotyrosine containing peptides, and showed no more than basal cross reactivity to any of the other 3-chlorotyrosine-containing samples/preparations (Figure 4.17B). When tested against nitrated fibrinogen, substantial cross reactivity was seen (Figure 4.17C). The lack of binding to the native protein, and binding to SIN-1 treated fibrinogen might suggest that nitration caused conformational changes to the protein, exposing the STSYGTGC peptide for binding. Similarly, the anti-serum for STSY-(Cl)-GTGC showed no specificity to native fibrinogen, but instead bound to the HOCl-treated protein, with a concentration-dependent trend (Figure 4.17D). Reduced binding was seen at the higher HOCl concentrations (Figure 4.17D), which could be due to aggregation induced by the HOCl treatment. AP STSY-(Cl)-GTGC serum was also tested against other abundant plasma proteins, haemoglobin, HSA and transferrin, and subsequently showed no binding to any of the respective chlorinated or nitrated plasma proteins (See appendix 28).

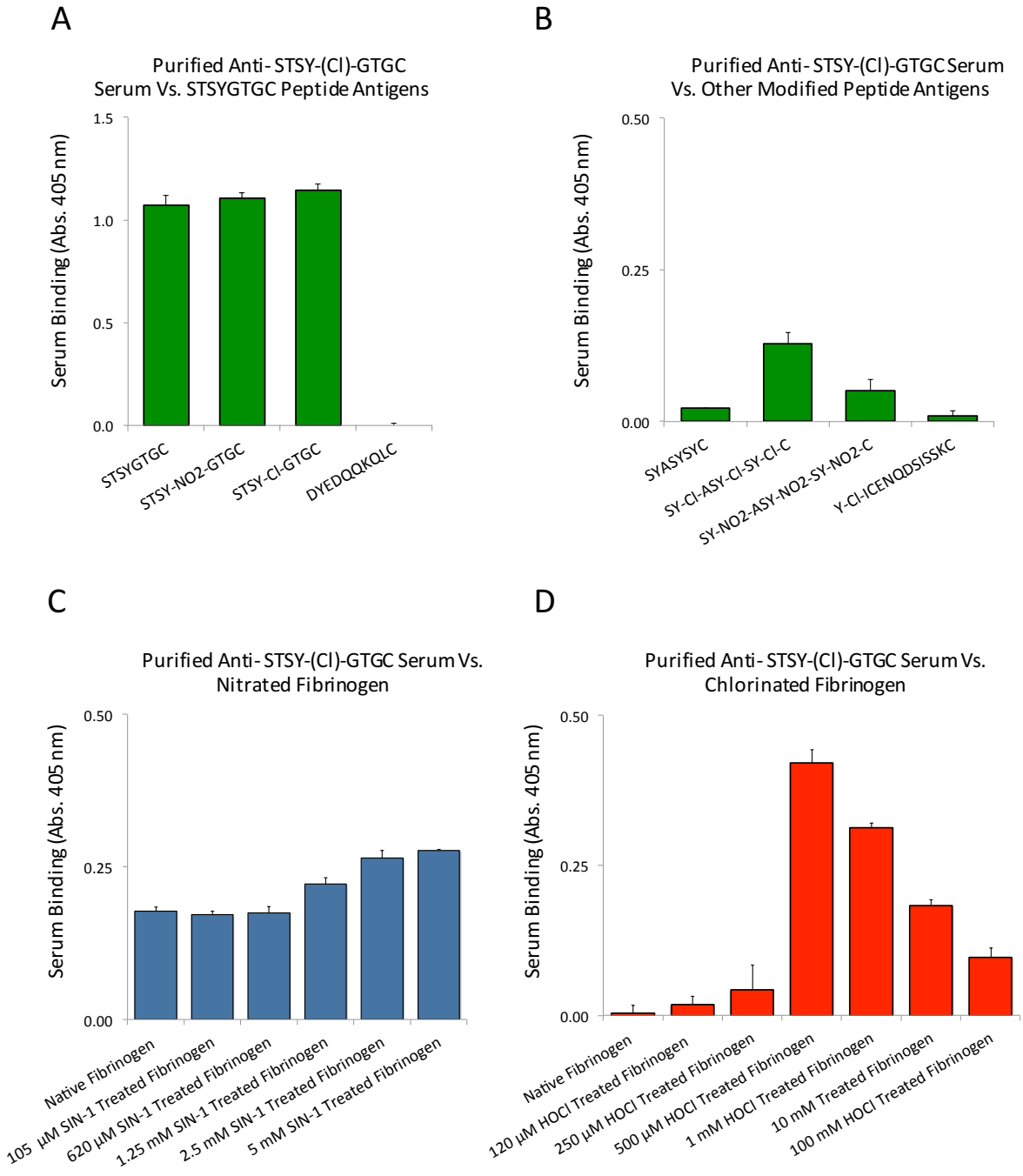

Figure 4.17: Binding of AP STSY-(Cl)-GTGC Serum to Peptide and Protein Antigens. (*n* = 3, standard deviation of technical replicates). Peptide antigens (A and B) were coated onto Nunc maxi-sorp plates (Product code: 10098860, Fisher Scientific, UK) at 2 µg/mL. The proteins described in C and D were treated with either (C) SIN-1 or (D) HOCl for 1 hour at 37°C before being coated onto Nunc maxi-sorp plates in molar equivalent amounts to the peptide antigens. The primary anti-serum was made to 1.5 µg/mL. The tested anti-sera were detected with 1:25,000 donkey anti-sheep antibody conjugated to alkaline phosphatase (Product code: A5187), and 1 mg/mL phosphate substrate in pNPP buffer, pH 10.4, with an incubation time of 15 minutes at room temperature before being read on a plate reader at 405 nm.

4.16 Experimental Variability of AP STSY-Cl –GTGC Anti-Serum

Similar experiments to those carried out for anti- STSY AP STSY-(NO_2)-GTGC serum in Section 4.14. These experimental replicates were performed on different days, with new reagents, and between two different operators. The variability was determined by expressing the coefficient of variation (CV) of each antigen (n = 3). Expressing the CV of values close to zero provides unreliable results, and for this reason only antigens with an absorbance of greater than 0.100 were considered (Gulhar *et al*., 2012). The average CV for the peptide antigens showing above basal binding was 4.6%, and for treated whole fibrinogen 3.4%, suggesting a small amount of variability between experiments. Experimental work comparing variability also showed that AP STSY-(Cl)-GTGC serum displayed some cross reactivity for the 3-chlorotyrosine containing peptide, SY-(Cl)-ASY-(Cl)-SY-(Cl)-C (Figure 4.18). It also showed a small amount of binding to nitrated fibrinogen, a concentration dependent increase in binding to chlorinated fibrinogen, and a lot of cross reactivity to the STSYGTGC series peptides. As previously mentioned with AP anti- STSY-(NO_2)-GTGC serum (Section 4.14), a reduction in signal was seen across experiments, which could possibly be attributed to protease dependent antibody degradation throughout prolonged storage at 2-4°C.

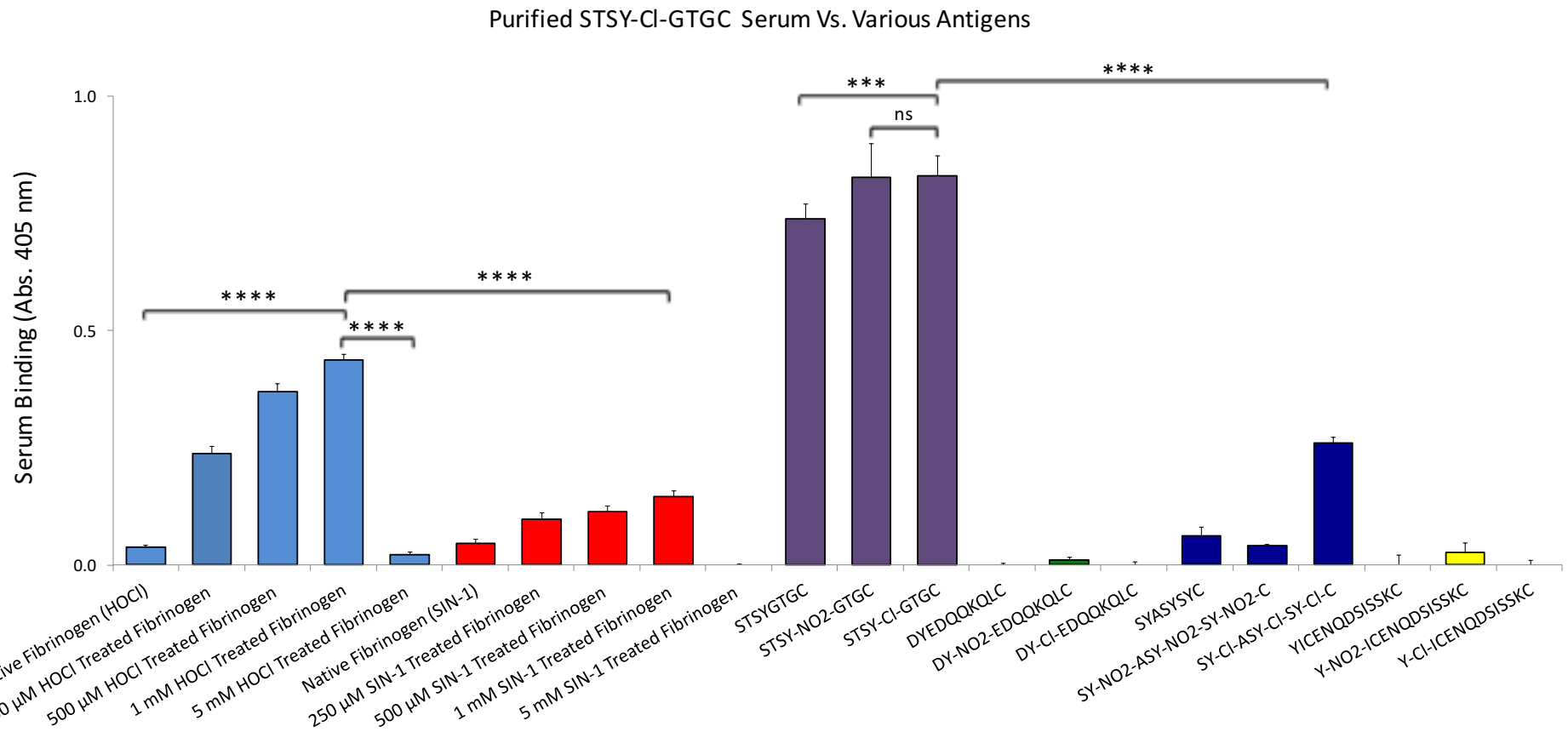

Figure 4.18: Identifying Experimental Variability and Binding Trends of AP STSY-Cl–GTGC Serum. (*n* = 3, error bars represent standard deviation of experimental replicates). (ns = P > 0.05, *** = P ≤ 0.001 and **** = P ≤ 0.0001).Synthesised peptide antigens were coated onto Nunc maxi-sorp plates (Product code: 10098860, Fisher Scientific, UK) at 2 µg/mL. The proteins treated with either SIN-1 or HOCl for 1 hour at 37°C before being coated onto Nunc maxi-sorp plates in molar equivalent amounts to the peptide antigens. The primary anti-serum was made to 1.5 µg/mL. The tested anti-sera were detected with 1:25,000 donkey anti-sheep antibody conjugated to alkaline phosphatase (Product code: A5187), and 1 mg/mL phosphate substrate in pNPP buffer, pH 10.4, with an incubation time of 15 minutes at room temperature before being read on a plate reader at 405 nm.

4.17 Testing the Specificity of AP STSYGTGC Serum

AP anti- STSYGTGC Serum was tested against native, chlorinated and nitrated STSYGTGC peptides, and another peptide with a different amino acid sequence (Figure 4.19A). The serum showed binding specificity for all of the STSYGTGC peptides, and no binding exceeding basal level for the DYEDQQKQLC peptide series (Figure 4.19A). Because the serum showed affinity for both the nitrated and chlorinated versions of the STSYGTGC peptide, and no binding to native DYEDQQKQLC, further testing against other modified peptides was performed (Figure 4.19B). The serum showed no specificity towards peptides with different sequences, both native and modified. The purified serum showed a low level of binding to both nitrated and chlorinated fibrinogen protein (Figures 4.19C – 4.19D). This binding increased with chlorination and nitration treatment, which may relate to conformational changes in the protein encouraged by chlorination/nitration making the peptide more readily accessible (Figures 4.19C – 4.19D). At the higher HOCl treatment concentrations (Figure 4.19D) there was an abrupt decrease in binding, which may be due to protein aggregation blocking antibody binding. The binding of this anti-serum the other abundant plasma proteins, haemoglobin, HSA and transferrin was tested, and no binding was shown (Appendix 27).

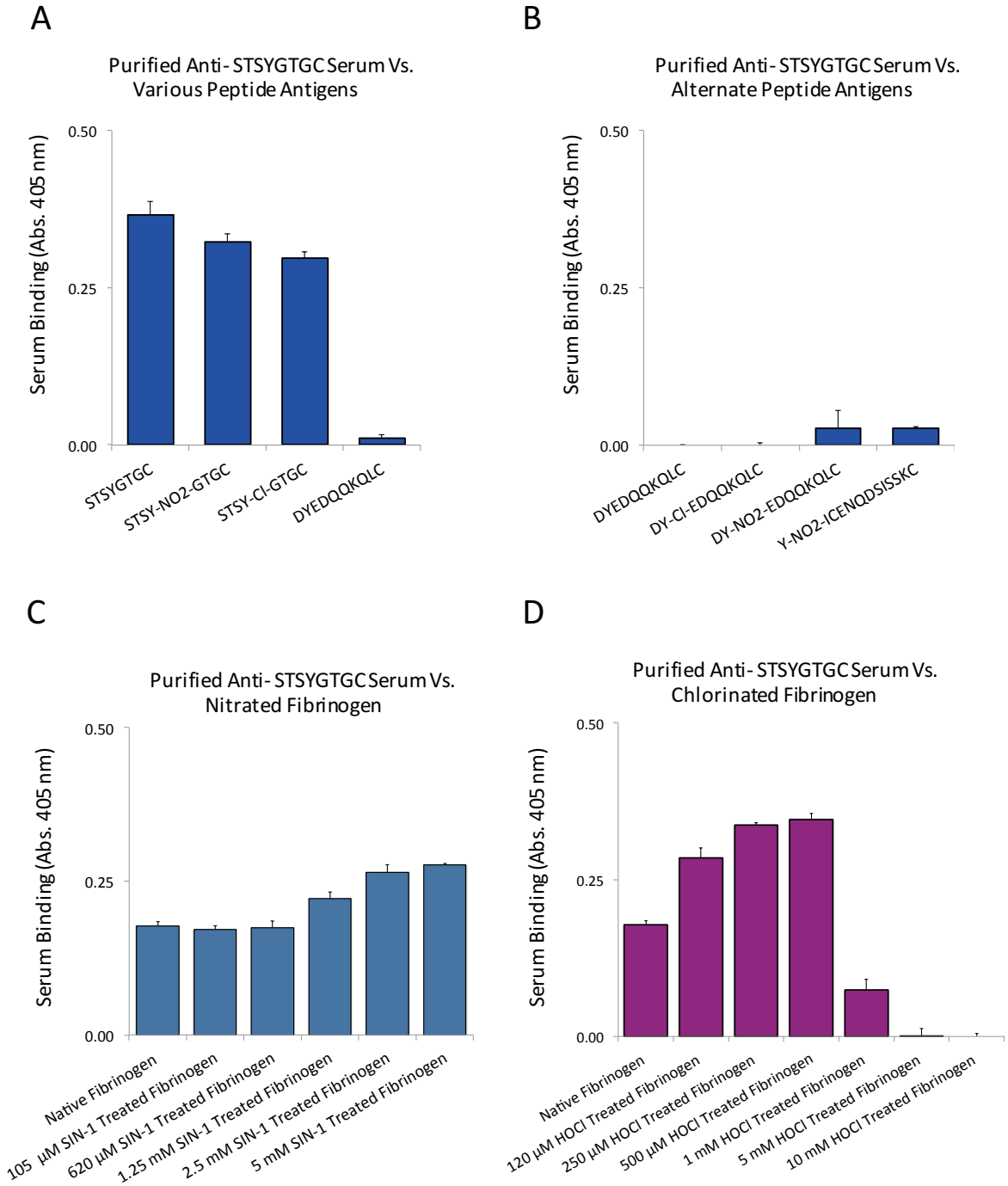

Figure 4.19: Binding of AP STSYGTGC Serum to Peptide and Protein Antigens. (*n* = 3, standard deviation of technical replicates). Peptide antigens (A and B) were coated onto Nunc maxi-sorp plates (Product code: 10098860, Fisher Scientific, UK) at 2 µg/mL. The proteins described in C and D were treated with either (C) SIN-1 ($ONOO^-$) or (D) NaOCl (HOCl) for 1 hour at 37°C before being coated onto Nunc maxi-sorp plates in molar equivalent amounts to the peptide antigens. The primary anti-serum was made to 1.5 µg/mL. The tested anti-sera were detected with 1:25,000 donkey anti-sheep antibody conjugated to alkaline phosphatase (Product code: A5187), and 1 mg/mL phosphate substrate in pNPP buffer, pH 10.4, with an incubation time of 15 minutes at room temperature before being read on a plate reader at 405 nm.

4.18 Experimental Variability of AP STSYGTGC Serum

Similar to the previously discussed sections looking at inter-experimental variability (Sections 4.14 and 4.16), this section looks at the experimental variability seen between the day-to-day experiments, users and reagents. In an attempt to make trend cross comparisons, three independent ELISA plates with all antigens on the same plate were set up (Figure 4.20). As before, experimental replicates were performed on different days with new reagents, between two different operators. Cross reactivity was shown between native and modified versions of STSYGTGC peptides. And, once again, a small amount of binding to nitrated and chlorinated fibrinogen was seen, which could have implications in relation to the conformational changes seen to fibrinogen after such oxidative treatments, and the accessibility of antibodies for binding. The variability was determined by expressing the coefficient of variation (CV) of each antigen (n = 3). Expressing the CV of values close to zero provides unreliable results, and for this reason only antigens with an absorbance of greater than 0.100 were considered (Gulhar *et al.*, 2012). The average CV for the STSYGTGC peptide antigens showing above basal binding is 17.8 %, and for treated whole fibrinogen it was 33.2%. The general trend between the three anti-sera for chlorinated and nitrated fibrinogen is high variability. This could potentially be explained by inaccurate CV values, based on low absorbance values.

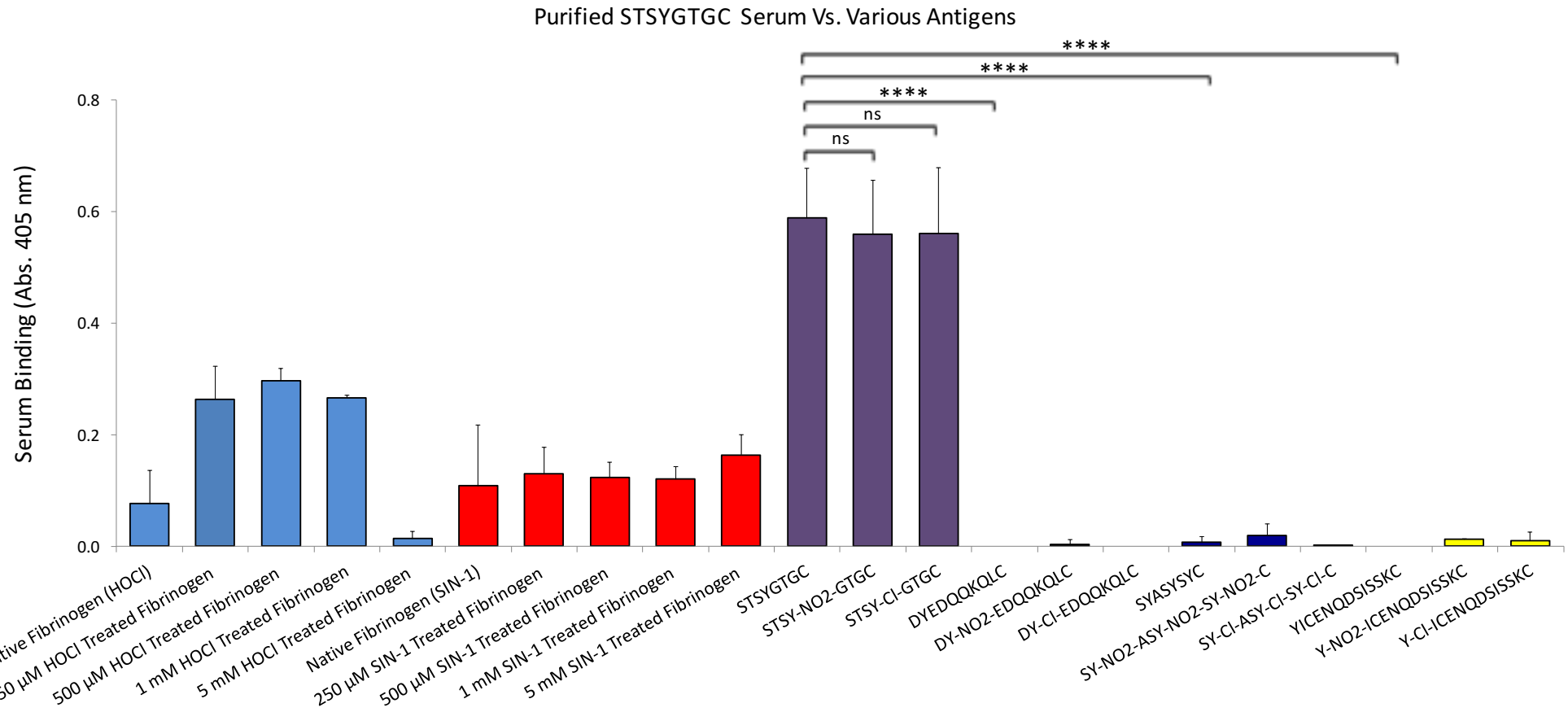

Figure 4.20: Identifying Experimental Variability and Binding Trends of AP STSYGTGC Serum. (For all $n = 3$). Synthesised peptide antigens were coated onto Nunc maxi-sorp plates (Product code: 10098860, Fisher Scientific, UK) at 2 µg/mL. The proteins treated with either SIN-1 or HOCl for 1 hour at 37°C before being coated onto Nunc maxi-sorp plates in molar equivalent amounts to the peptide antigens. The primary anti-serum was made to 1.5 µg/mL. The tested anti-sera were detected with 1:25,000 donkey anti-sheep antibody conjugated to alkaline phosphatase (Product code: A5187), and 1 mg/mL phosphate substrate in pNPP buffer, pH 10.4, with an incubation time of 15 minutes at room temperature before being read on a plate reader at 405 nm.

4.19 Discussion of Chapter 4 Results

The aim of this part of the study was to produce anti-sera containing antibodies which bind exclusively the modified peptides identified in the literature and by MS in chapter 3. The hypothesis was that antibodies can be produced to differentiate between modified and unmodified fibrinogen peptides with sequence context, binding exclusively to the specific modified peptide against which they were produced.

4.19.1 DYEDQQKQLC Series of Anti-Sera

The study described in this chapter attempted to identify if specific antibodies to modified protein antigens could be produced, with both modification site and amino acid sequence specificity. As a preliminary study the literature identified fibrinogen peptide, ^{196}DYEDQQKQL^{204}, and a chlorinated version DY-(Cl)-EDQQKQL was synthesized with the addition of a cysteine residue at the c-terminus preceding lysine, and immunized into sheep. The anti-sera against DYEDQQKQLC and DY-(Cl)-EDQQKQLC showed a month-by-month, time-dependent, increase in antibodies for their respective antigens, with a decrease in binding at the much lower dilutions of the sera. This is most likely explained by the prozone phenomenon/hook effect, whereby the antibody titre is so high that it interferes with the antibody-antigen binding capability, due to agglutination (Sidana *et al.,* 2011). The crude anti-sera showed cross reactivity for the native and chlorinated versions of the peptides. Which is most likely due to the polyclonal nature of the anti-sera, made up of antibodies for various epitopes of the respective antigens, both including and not including the modification site. A cysteine residue was included in the sequence of synthesized peptides in order to allow immunization and purification steps. The overall increase in binding of anti-sera to cysteine-containing sequences might relate to the inclusion of cysteine within some of the respective

complementary antibodies paratope to epitope complexes, meaning absence of this residue might preclude some antibodies in the anti-serum from binding to the peptide. During affinity purification (affinity enrichment) to remove cross-reactivity, a moderate peak for protein content was shown after the pH was changed to elute anti- DY-(Cl)-EDQQKQLC antibodies from the DY-(Cl)-EDQQKQLC peptide bound column, suggesting successful collection of the fraction. The second purification of anti- DYEDQQKQLC serum, provided similar results, suggesting that the anti-DYEDQQKQLC antibodies were removed from the fraction. After this purification step, the anti-serum from sheep 4 no longer showed binding to the native peptide, suggesting the purification steps were successful. The serum from sheep 3 did show a substantial reduction in cross reactivity, with some remaining cross-reactivity for the native peptide. However, there was some remaining cross-reactivity between chlorinated and nitrated versions of anti- DYEDQQKQLC serum. The specificity of the produced antibodies depends on a number of factors, including amino acid sequence, conformation and electrostatic charges. The binding of an antibody paratope to antigen epitope can be by a combination of ionic, hydrogen and van der Waals bonding forces. This bonding involves just few amino acids on the paratope. The overall binding strength and specificity is dependent on the conformational fit and van der Waals forces (Reverberi and Reverberi, 2007). Peptide antigens are known to, for the most part, bind in the cleft between the V regions of the heavy and light chains of an antibody, where they make specific contact with some, but not necessarily all, of the hypervariable loops that make up the paratope (Charles *et al.,* 2001). In order to compare the conformational differences between each version of the DYEDQQKQLC peptides Marvin sketch version 6.1.7 (http://www.chemaxon.com) was used to determine the peptides shape, and the position of each of the potentially influencing atoms.

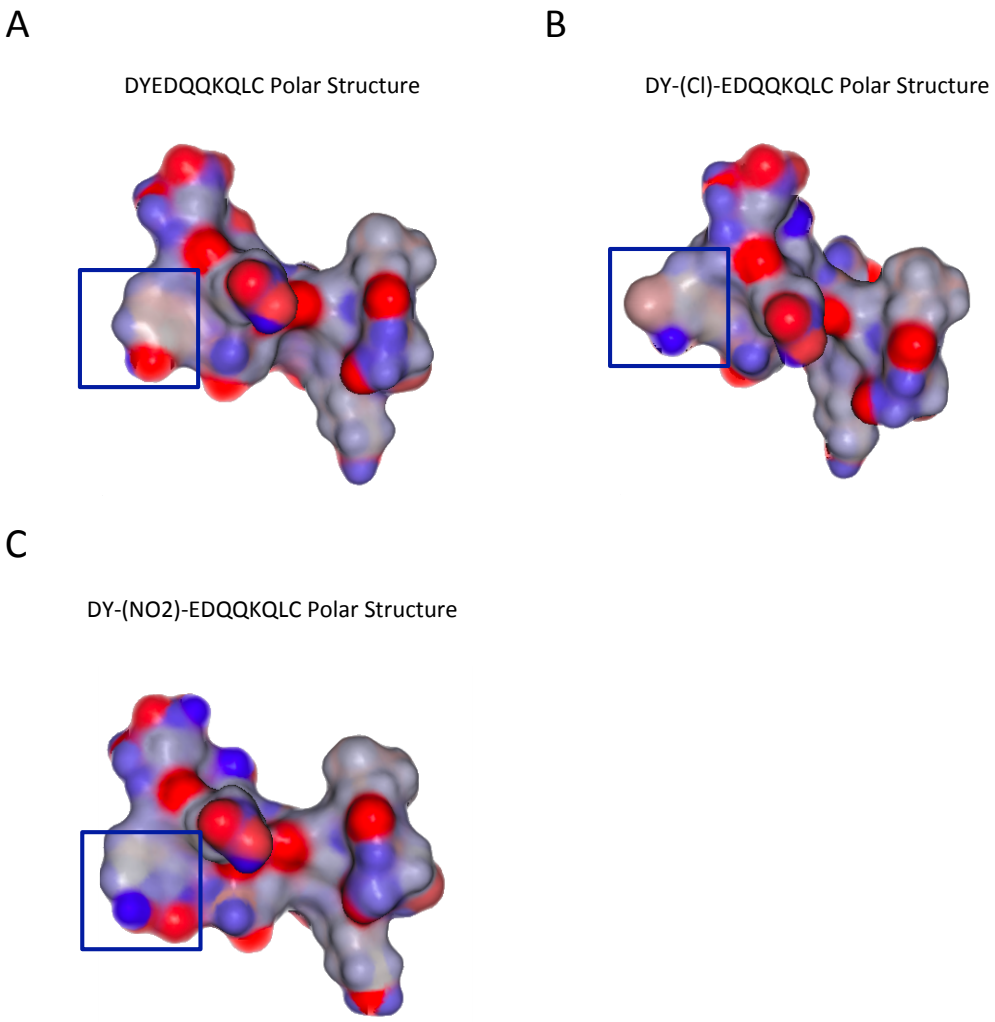

Figure 4.21: Comparing Conformational Changes Between Modified and Unmodified Versions of DYEDQQKQLC. (A) Polar structure of DYEDQQKQLC, (B) Polar structure of DY-(Cl)-EDQQKQLC and (C) Polar structure of DY-(NO_2)-EDQQKQLC. Chemical structure drawing software Marvin Sketch was used to show the hydrophobic interactions and conformation of the different versions of the DYEDQQKQLC peptide. The grey balls represent carbon atoms, the blue nitrogen, the red hydrogen and the orange chlorine. Marvin Sketch 6.1.7, 2014, ChemAxon, (http://www.chemaxon.com).

Figures 4.21A - 4.21C show similarities in conformation, but also the highlighted areas show some differences in both conformation and the available hydrogen bonding atoms around the epitope between the native peptide (A), the chlorinated (B) and nitrated (C) tyrosine residues. Although peptides are linear epitopes, whereby the specificity is determined by the sequence of amino acids, maybe it is possible that the peptide conformation plays a role in specificity, whereby discontinuous amino acid sections make up the antigen. The 3-chlorotyrosine containing peptide (Figure 4.21B) shows a protruding tyrosine residue with a chlorine atom, which could make the peptide more accessible for antibody binding. The 3-nitrotyrosine containing peptide (Figure 4.21B) also shows more polar atoms in the epitope region, but with a similar less protruding conformation to the native peptide (Figure 4.21A). It is worth noting that transferrin and HSA are negative acute phase proteins, decreasing in plasma concentration during inflammation, whereas, fibrinogen is a positive acute phase protein, shown to increase in concentration during inflammation (Ritchie *et al.,* 1999 and, Page and Schroeder, 1976). None of the anti- DYEDQQKQLC series sera showed substantial binding to haemoglobin, transferrin, HSA or fibrinogen plasma proteins.

The peptide ^{196}DYEDQQKQL^{204} is a fibrinogen-derived peptide, identified by MS chapter 3 as unmodified. The produced AP anti-DY-(Cl)-EDQQKQLC serum showed no binding to chlorinated fibrinogen or native fibrinogen. In order to better understand why, the crystal structure was examined (Figure 4.22). The tertiary structure and hydrophobic interactions of fibrinogen show the DYEDQQKQL tyrosine residue to be buried, and not surface exposed, suggesting it to not be susceptible to oxidative modification. This agrees with the protein analysis results reported in Chapter 3, section 3.9, which demonstrates a lack of susceptibility to modification, as only the native peptide was identified. In conclusion, the anti-serum to DY-(Cl)-EDQQKQLC appears to show sequence specificity, only binding to peptide sequences with the same amino acid motif with a modification. However, the anti-serum to DY-(Cl)-EDQQKQLC shows cross-reactivity with DY-(NO_2)-EDQQKQLC, suggesting an inability to differentiate between the 3-cholorotyrosine and 3-nitrotyrosine modifications. Future work to produce and test for a specifically selective monoclonal antibody might potentially allow this problem to be resolved.

Fibrinogen Crystal Structure with DYEDQQKQL Sequence Highlighted in Green and Tyrosine in Yellow

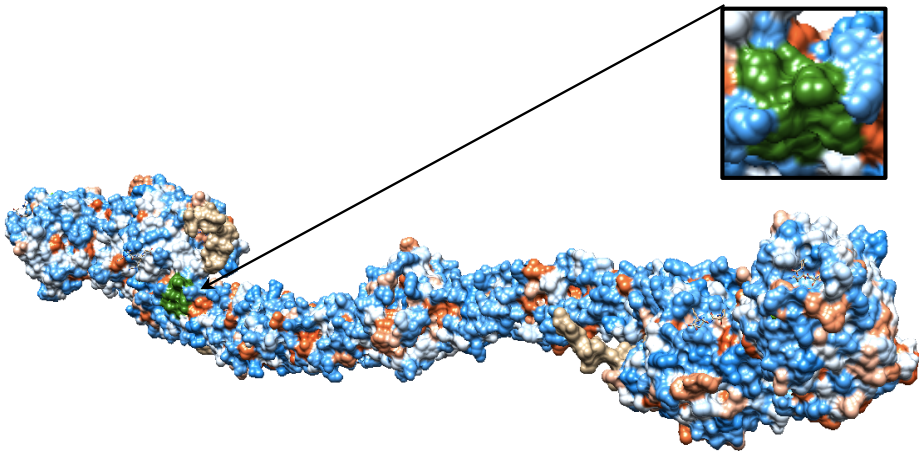

Figure 4.22: Understanding Why AP DY-(Cl)-EDQQKQLC Shows no Binding to Treated or Native Fibrinogen. Chimera software, version 1.9, 2014, with the crystal structure obtained from the Protein Data Bank (http://www.rcsb.org/pdb/home/home.do). The protein hydrophobic interactions are shown (tertiary structure). The DYEDQQKQLC sequence was highlighted in green and the tyrosine in yellow.

4.19.2 STSYGTGC Series of Anti-Sera

Similarly, the MS identified peptide STSYGTG was synthesized, both a native chlorinated and nitrated version, with an added cysteine residue to allow immunization and purification steps. The anti-serum for STSYGTGC, STSY-(NO_2)-GTGC and STSY-(Cl)-GTGC showed no binding in the pre-immune sera, and an abrupt increase in anti-sera binding for their respective antigens after the first month peptides were immunized into sheep. The expected trend of a month-by-month linear increase in antibody-titre is not seen. Instead, some variability in the antibody-titre is apparent, with a general plateau after immunization. This does not correlate to the trend seen with anti- DYEDQQKQLC series sera, with a roughly linear increase in binding month-by-month. This might be explained by the differences sera production, more specifically, the sheep used and or methodology, as the two series of sera were produced by different suppliers. Some cross reactivity between STSYGTGC anti-serum and modified versions of the peptide was seen. The anti-serum complementary to the 3-chlorotyrosine peptide (STSY-(Cl)-GTGC) shows a similar pattern in cross-reactivity for all versions of the peptide as the native serum, suggesting anti-sera are also specific for epitopes that do not include the modification site. In contrast, anti- STSY-(NO_2)-GTGC anti-serum appeared to be specific to modified versions of the peptide, not binding the native, but cross reacting to the chlorinated peptide. The binding complex between the paratope and epitope is dependent on several electrostatic Coulomb forces, previously described, and as such it possible that some antibodies are unable to discriminate between similar 3-chlorotyrosine and 3-nitrotyrsoine containing peptides. Another possibility is that some of the antibodies in the anti-sera are produced against conformational epitopes, rather than linear (sequential) epitopes, and are unable to differentiate between the 3-chlorotyorsine and 3-nitrotyrsoine containing peptides.

In order to further investigate this, the polar structures of the STSYGTGC series peptides were investigated (Figure 4.23). There are clear conformational differences between the (A) native, (B) chlorinated and (C) nitrated versions of the STSYGTGC peptide, more specifically between the modified and native versions. This supports the possibility that some of the differences in specificity of the STSYGTGC series anti-sera are dependent on conformational epitopes, whereas others are peptide motif specific. This is further supported by a study performed by Forsström *et al.* (2015), where the study showed that although most polyclonal sera for peptide antigens are for linear epitopes, a fraction are also complementary to conformational epitopes.

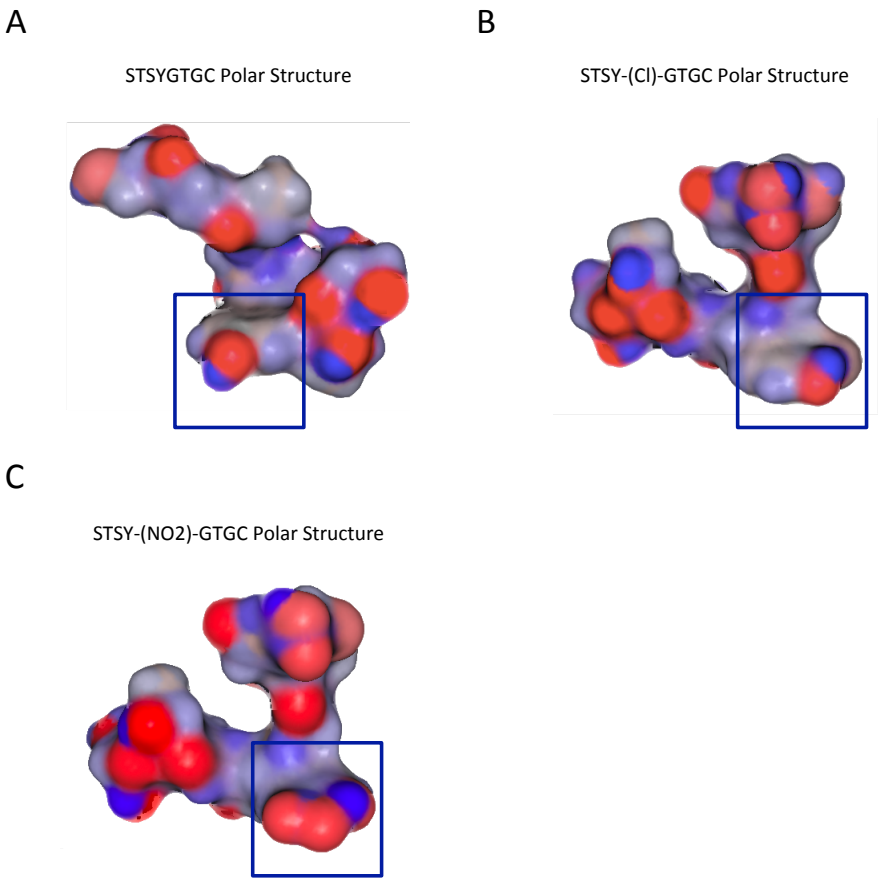

Figure 4.23: Comparing Conformational Changes Between Modified and Unmodified Versions of STSYGTGC. Chemical structure drawing software Marvin Sketch was used to show the hydrophobic interactions and conformation of the different versions of the STSYGTGC peptide. The grey balls represent carbon atoms, the blue nitrogen, the red hydrogen and the orange chlorine., Marvin Sketch 6.1.7, 2014, ChemAxon, (http://www.chemaxon.com).

Affinity purification abolished the cross reactivity for the chlorinated peptide, however, some cross-reactivity to other 3-nitrotyosine containing peptide and protein antigens were seen. This cross-reactivity is most likely explained by the polyclonal nature of the anti-sera, made up of different antibodies for various epitopes of the respective antigens, both including and not including the modification site. More specifically, the anti-serum may include antibodies specific for just 3-nitrotyrosine. The affinity purification process is not able to remove cross-reactivity to 3-nitrotyrosine, as the peptide epitope also contains 3-nitrotyrosine. In order to further check the cross reactivity and determine the involvement of 3-nitrotyorisne specific antibodies, the anti-serum was also tested against the other abundant plasma proteins, haemoglobin, HSA and transferrin. There was no binding of the antiserum to native versions of the proteins, suggesting anti-serum to be somewhat sequence specific. However, binding to nitrated versions of the proteins supports the presence of 3-nitrotyrosine specific antibodies in the polyclonal serum. Noteworthy, is that the number of tyrosine residues in each of the mentioned proteins does not correspond to the level of binding from the 3-nitrotyrosine and STSY-(NO_2)-GTGC antibodies/anti-serums. The higher level of binding of to nitrated HSA compared to the other plasma proteins, haemoglobin and transferrin was further investigated by comparing the crystal structures (Figure 4.24). The tyrosine residues of HSA, haemoglobin and transferrin are shown in figures 4.24A - 4.24C, highlighted in yellow.

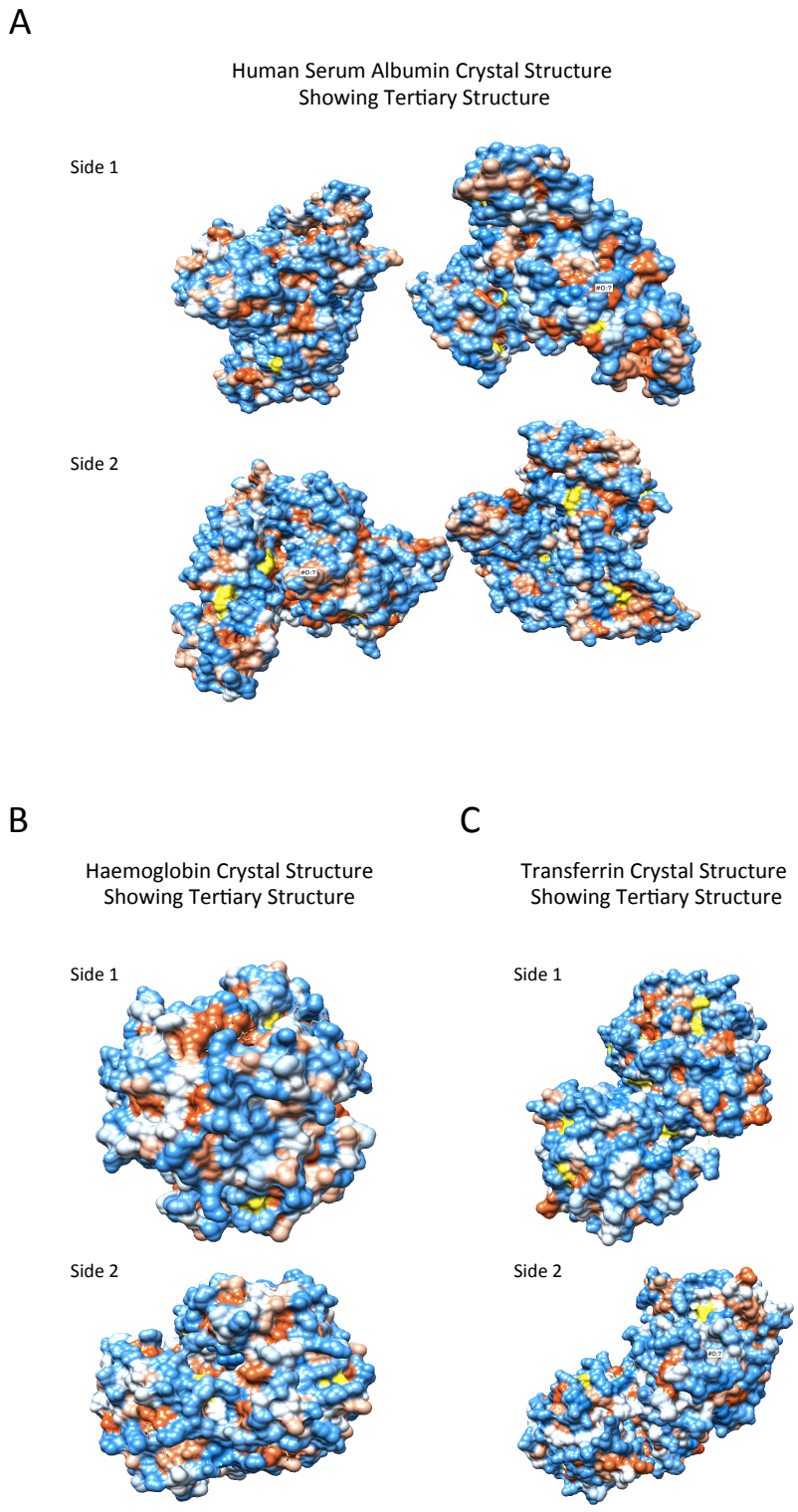

Figure 4.24: Understanding the Level of 3-nitrotyrosine Specific Anti-Sera Binding to Plasma Proteins. The crystal structures of human serum albumin (HSA) (A), haemoglobin (B) and transferrin (C) were determined using Chimera software, version 1.9, 2014, with the crystal structure obtained from the Protein Data Bank (http://www.rcsb.org/pdb/home/home.do). The protein hydrophobic interactions are shown (tertiary structure). The tyrosine residues were highlighted in yellow to show the number of surface exposed and hence susceptible residues.

Figures 4.24A to 4.24C, shows that HSA (A) has more surface exposed, readily accessible, tyrosine residues than haemoglobin (B) and transferrin (B), which, have a similar number of tyrosine residues to one another. Explaining the differences in 3-nitrotyrosine specific anti- STSY-(NO_2)-GTGC binding, and because the antigens are coated onto ELISA plates in molar equivalents, the binding levels are reasonably comparable. The high level of binding of anti-3-nitrotyrosine to nitrated HSA, compared to the modest binding of AP anti-STSY-(NO_2)-GTGC serum suggests, when you consider the high level of binding to the STSY-(NO_2)-GTGC its positive peptide control, may reflect that the serum not only contains 3-nitrotyrosine antibodies, but also STSY-(NO2)-GTGC sequence specific antibodies, and most likely some unrelated antibodies also. The AP STSY-(Cl)-GTGC serum showed a large amount of cross reactivity to the other STSYGTGC series peptides, and a small amount of reactivity to 3-chlorotyrosine and 3-nitrotyrosine containing peptides. The polyclonal nature of the serum means it is likely to contain antibodies complementary to various regions of the peptide antigen, and some of the peptide sequences not only contain 3-chlorotyrosine, but also share some of the same amino acid residues to STSYGTGC. The AP-STSY-(Cl)-GTGC serum also showed some binding to chlorinated and nitrated fibrinogen, but not native fibrinogen. This could potentially be explained by conformational changes induced by oxidation, nitration or chlorination, exposing an STSYGTG sequence epitope of fibrinogen to the surface, enabling anti-serum binding. The binding to chlorinated fibrinogen was shown to decrease at higher HOCl treatment concentrations, which could possibly be explained by HOCl induced protein aggregation (Pattison and Davies, 2001). After testing the binding of the AP STSY-(Cl)-GTGC serum with plasma proteins, haemoglobin, HSA and transferrin, the lack of binding suggests that the serum does not contain high levels of non-specific 3-chlorotyrosine antibodies.

4.20 Chapter 4 Conclusions

A number of different peptides have been produced; including those identified in the literature as susceptible to modifications, by the MS studies described in chapter 3, and designed for testing purposes. These peptides have been used to test the various anti-sera produced (figure 4.25). More specifically, anti-sera has been produced that can discriminate between native and modified peptides, one of the two anti-sera is peptide sequence-specific (DY-(Cl)-EDQQKQLC), whereas, the other is modification-site specific (STSY-(NO_2)-GTGC). Between the two sera there tends to be a lot of cross reactivity between modification sites. The main limitation of this study was firstly, the variability seen inter-experimentally, with regard to experiments being performed on different ELISA plates, providing large variation. And finally, due to the novel nature of this work, no experimental standards were available, and for this reason only the trends intra-experimentally could be considered. Further work is required to better understand and determine specificity of the mentioned anti-sera. This work shows some good potential in proving the hypothesis. However, further work and a more comprehensive statistical analysis are required to show accurate significance/ non- significance, and therefore support or refute the hypothesis.

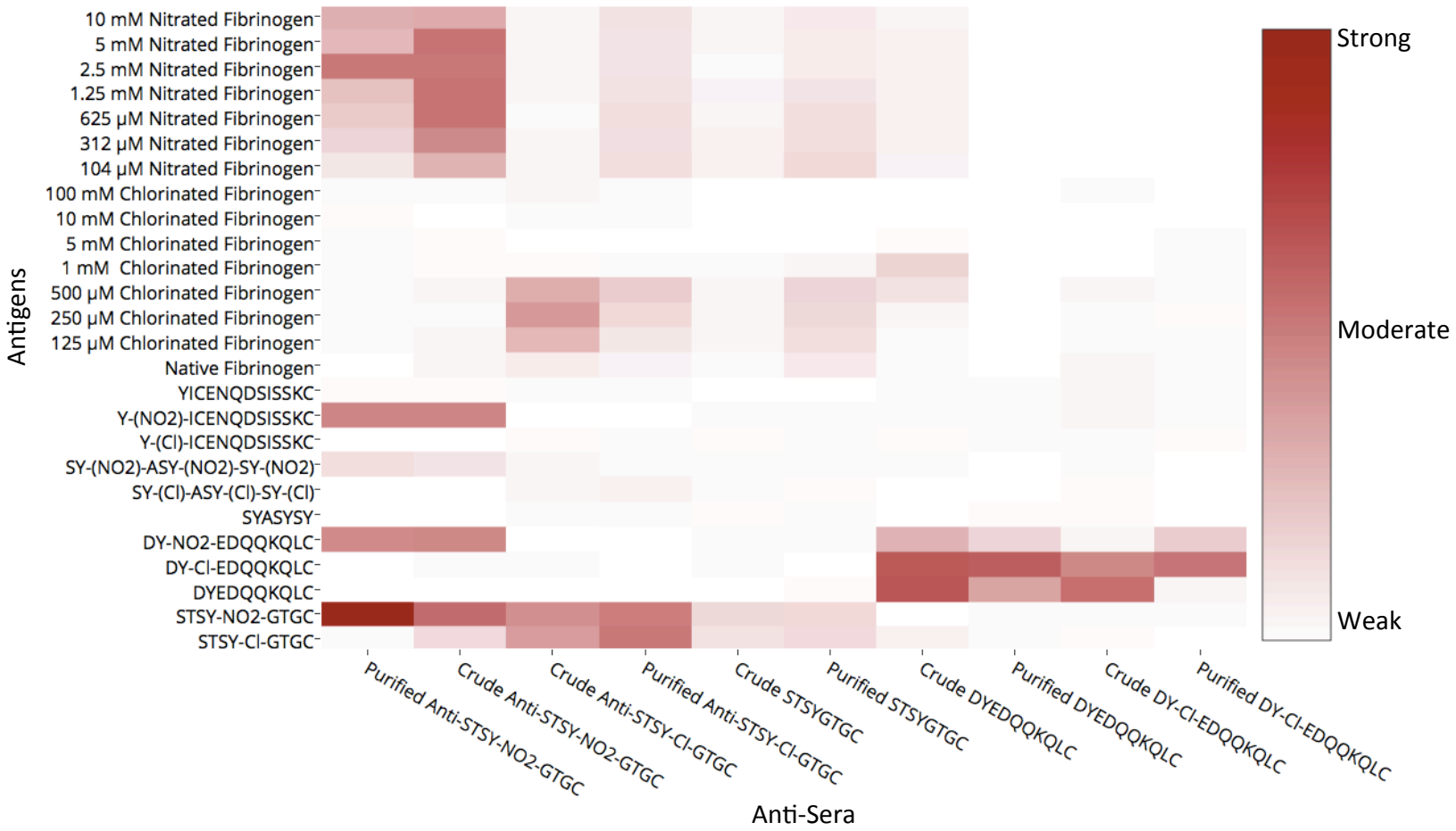

Figure 4.25: Heatmap Overview of Total Anti-Sera Vs. Peptide/Protein Antigens. Results are from multiple ELISA plates performed within a few weeks of one another. Peptides were coated onto Nunc maxi-sorp plates (Product code: 10098860, Fisher Scientific, UK) at 2 µg/mL and proteins in molar equivalents. The purified primary serum was made to 1.5 µg / mL, crude 1:2000, detected with 1: 25,000 donkey anti-sheep antibody conjugated to alkaline phosphatase (Product code: A5187), the substrate was incubated for 15 minutes and read at 405 nm. Plotly graphing, version 1 (https://plot.ly) was used to produce this heatmap.

4.21 Chapter 4 Future Work and Considerations

With regard to future work, for all anti-sera, in order to understand better the binding specificity, monoclonal antibodies should be produced and tested. This will allow testing of the individual constituting antibodies, each with specificity to one particular epitope, with the possibility of identifying an antibody with exclusive specificity for both the modification site and the sequence within which it resides. This might also possibly allow for the exclusion of antibodies specific to just the modification site E.g. 3-nitrotyrosine. Another possible consideration would be epitope mapping, with a peptide microarray, potentially allowing for a clear understanding of the epitope to paratope complex, and hence antibody specificity. Hydrogen-deuterium exchange MS was used in a study by Burkitt *et al.,* 2010 to determine conformational protein changes to immunoglobulin G after methionine residues were oxidized to methionine sulfoxide. This approach has potential to determine oxidation induced conformational changes to the fibrinogen protein, with regard to epitope surface exposure and subsequent availability for binding with respective antibodies. In addition to binding specificity, the strength of the bond formed by intermolecular forces between the epitope and paratope are worth determining. A study performed by Englebienne *et al*., 1998 showed how surface plasmon resonance could be used to measure antibody-binding affinity in real time, under various conditions. This technique might be useful in investigating the binding affinity of the produced antibodies to various peptide and protein antigens (Englebienne *et al*., 1998).

Chapter 5

Testing Translation into Clinical Samples

5.1 Introduction

As mentioned in chapter 1, it is becoming increasingly apparent that a number of inflammatory diseases have an oxidative pathology, whereby the immune cells during respiratory burst produce biological oxidants, such as superoxide, to destroy pathogens (Guzik *et al.*, 2003, Inoguchi *et al.*, 2003 and Shacter, 2000). Exposure to biological oxidants can induce modifications to the amino acid residues that make up proteins, and these modifications can act as markers of inflammation. For example, the formation of 3-nitrotyrosine and 3-chlorotyrosine are considered indicative of oxidative damage during inflammation (Levine, 2002, Mann and Jensen, 2003 and Karve and Cheema et al., 2011). Fibrinogen is one of the most abundant plasma proteins, shown to be susceptible to oxidative modifications (Shacter *et al.,* 1994), and as such, oxidative damage and modifications to fibrinogen offer potential as biomarkers of disease (Weigandt *et al.,* 2012). As mentioned previously, fibrinogen was shown to be nitrated, specifically in various diseases, forming 3-nitrotyrosine modifications (Martinez *et al.,* 2013, Parastatidis *et al.,* 2008, and Gole *et al.,* 2000)

5.1.2 Understanding Protein and Peptide Biomarkers

Protein and peptide biomarkers could be defined as proteins or peptides that are consistently modified or present at abnormal concentrations in specific conditions. A biomarker profile is similar, but made up of a combination of multiple protein or peptide biomarkers. These markers could be used to determine susceptibility and/or progression of disease, as well as the effect of a particular treatment on clinical outcomes (Mischak *et al.,* 2010). Mischak *et al.* (2010) described the validity of a

biomarker as based on its ability to predict future clinical outcome. With this in mind, important factors to consider when working with protein markers in clinical samples include (i) sample size which provide appropriate statistical power, (ii) significant effect, (iii) standardization in the experimental design, (iv) continuity between investigators (Mischak *et al.,* 2010).

5.1.3 Pro-Inflammatory Markers

There are several currently used markers of inflammation, including C-reactive protein (CRP). These markers include adhesion molecules, such as intercellular adhesion molecule-1 and selectins; cytokines, such as interleukin-1 and the tumor necrosis factor; and acute phase reactants, such as fibrinogen, serum amyloid-A protein and C-reactive protein. The pathology of cardiovascular disease (CVD) involves inflammation, and therefore these markers have sometimes been considered as more specific markers of CVD. Translation of which into a clinical setting was met with some limitations. The limitations included, standardization of assay measurement variability; independence of the markers from established risk factors, and as such direct association with CVD. A risk factor is associated with disease by its participation in the pathway that leads to the disease, whereas a risk marker is statistically associated with the disease, and might not be causally linked. The levels of the above-mentioned markers in CVD do not correlate directly with atherosclerosis, and are better considered as risk factors for CVD (markers of general inflammation), rather than as risk markers of the actual disease (Pearson *et al*., 2003).

5.1.4 C-reactive Protein as a Marker of Inflammation

C-reactive protein (CRP) is an acute phase protein produced by hepatocytes and adipocytes and regulated by pro-inflammatory cytokines. CRP is a well-established sensitive marker of systemic inflammation and tissue damage (Koenig *et al*., 1999). Normal blood concentrations of CRP can increase by 10,000-fold after the introduction of an inflammatory stimulus. Generally, the CRP level reflects the level of ongoing inflammation and/or tissue damage in a number of diseases, such as Crohn's disease, rheumatoid arthritis, and systemic vasculitis (Jin *et al.,* 2013, and Black *et al.,* 2004).

5.1.5 The Oxidative Pathology of Type II Diabetes

The main pathophysiological feature of type II diabetes involves impaired insulin resistance (Féry and Paquot, 2010). Type II diabetes is an inflammatory disease, where inflammation is considered to be a primary cause of obesity-linked insulin resistance and hyperglycemia. One of the first indications of a link between obesity and inflammation was the identification of overexpression of the pro-inflammatory cytokine TNF-α in the adipose and muscle tissue of obese humans. In addition to this, obesity has also been characterized as having an accumulation of macrophages in the adipose tissue, which is likely to contribute to the production of pro-inflammatory mediators and the subsequent oxidative stress. In parallel, the increase in glucose delivery to adipose tissue is known to cause an excess production of superoxide in the mitochondria. As a result, this inflicts oxidative damage, and activates pro-inflammatory cytokines (Giacco and Brownlee, 2010, and Wellen and Hotamisligil, 2005).

5.1.6 Clinical Sample Biological Variability

There are a number of variables that must be considered when analyzing clinical sample data for potential biomarkers of inflammatory disease. Firstly, biological variability, with regard to factors that may affect the proteome, such as other existing diseases, gender, age, lifestyle choices (e.g. alcohol consumption and exercise), circadian rhythms and food intake (Mischak *et al.*, 2007).

With regard to oxidative modifications to proteins, it is well established that protein oxidation is part of the pathology of a number of diseases, such as diabetes, atherosclerosis, rheumatoid arthritis, and neurodegenerative diseases such as Alzheimer's (Griffiths, 2000). The free radical hypothesis of aging suggests a senescence-related loss of function due to the increasing and irreversible oxidative damage to biomolecules. Commonly there is a two to threefold age-related increase in the abundance of oxidatively-damaged proteins, which is indicated by a loss of protein thiol groups, protein carbonylation, and a loss of catalytic activity of some enzymes in senescence (Sohal and Weindruch, 1996). A study performed by Knez *et al.* (2006) reported that intermittent bouts of exercise at 40-70% of VO_2 max significantly reduced plasma malondialdehyde (MDA) levels, a marker of oxidative lipid damage, and oxidative stress. On the other hand, as the exercise intensity increased so did the levels of plasma MDA, and after prolonged exhaustive exercise, such as ultra-endurance exercise, the plasma MDA levels were shown to be very high (Knez et al., 2006). Illustrating the importance of understanding patient lifestyle choices when examining changes in biomolecules.

5.1.7 Chapter 5 Focus, Aims and Hypothesis

This chapter focuses on testing the translation of anti-serum produced in chapter 4 to detect the *in-vitro* modified fibrinogen peptide identified in chapter 3, *in-vivo*. The aim was to test whether anti-serum produced in chapter 4 could be used to detect STSY-(NO_2)-GTG peptide in type 2 diabetic samples (Ethical consent shown in appendix 31). The hypothesis was that anti- STSY-(NO_2)-GTGC serum could be used to detect the STSY-(NO_2)-GTG peptide of fibrinogen in type 2 diabetic samples, with increased binding correlating to the increase in CRP level.

5.1.8 Clinical Sample Ethical Consent and Approval Information

The type 2 diabetes samples were provided by the Brown research group at Aston University. Samples were provided blind, and were made up of 10 healthy and 10 type 2 diabetic blood plasma samples prepared by the Brown research group (ethical approval and informed consent form is shown in appendix 31).

5.2 Testing Anti-Sera Vs. Type 2 Diabetic Plasma Samples

To avoid confusion, the sera containing antibodies produced in sheep will be referred to as serum, and the blood samples that might potentially contain modified fibrinogen peptide epitopes, are referred to as plasma. As a preliminary experiment, a healthy volunteer's plasma was tested against various anti-sera (Figure 5.1A), including a commercial polyclonal anti-fibrinogen antibody, anti-STSYGTGC, anti-STSY-(NO_2)-GTGC, and anti-DY-(Cl)-ED anti-sera, all of which produced and tested in chapter 4. The human plasma showed no binding to anti-STSY-(NO_2)-GTGC or any substantial binding to anti-DY-(Cl)-EDQKQQLC sera (figure 5.1A). However, a concentration dependent increase in binding of anti-fibrinogen and anti-STSYGTGC to the human plasma can be seen. The binding (absorbance) values from figure 5.1A were then normalized against their respective fibrinogen concentrations, as the most convenient method of standardization (Figure 5.1B). After normalization, the binding of anti-sera to human plasma showed a more prominent concentration dependent increase in binding of anti-STSYGTGC, and very little binding of the other sera (Figure 5.1B).

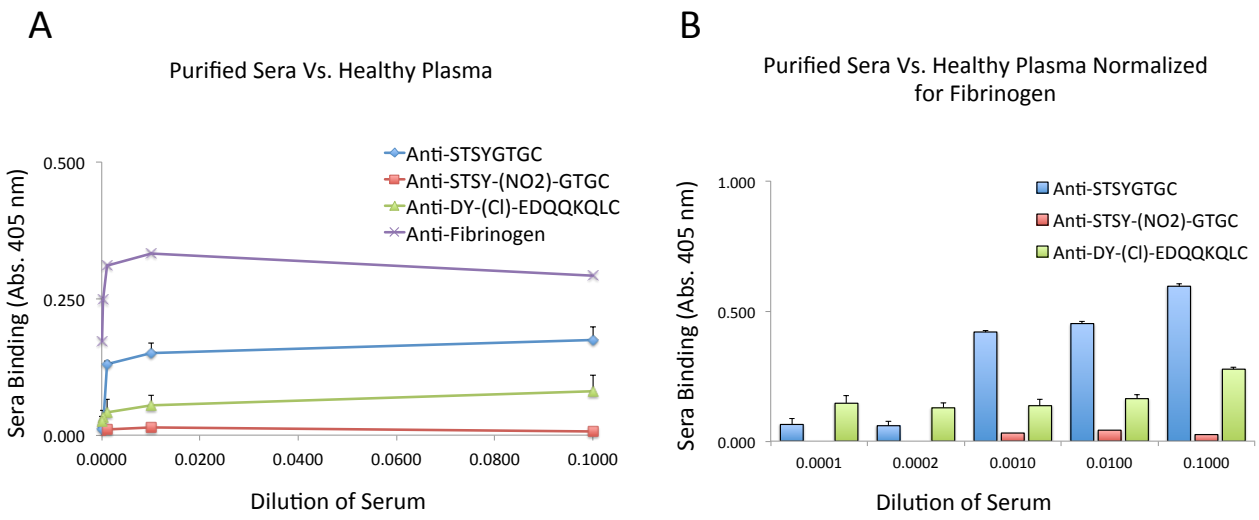

Figure 5.1: Testing Antibody Binding to Human Plasma Samples. (*n* = 3, standard deviation of technical replicates) (A) Serial dilution of human plasma against various anti-sera (B) Serial dilution of human plasma normalized for fibrinogen content against produced anti-sera. Nunc maxi-sorp plates (Product code: 10098860, Fisher Scientific, UK) were coated with serial dilutions of plasma samples. Anti-fibrinogen (Product code: F8512) was used at a working dilution of 1:10,000, anti-sera was made to 1.5 µg/ mL and detected with 1: 25,000 donkey anti-sheep antibody conjugated to alkaline phosphatase (Product code: A5187), and 1 mg/mL phosphate substrate in pNPP buffer, pH 10.4, with an incubation time of 15 minutes at room temperature before being read on a plate reader at 405 nm.

Based on the preliminary results in figures 5.1A and 5.1B, human plasma dilutions of 1:2000 were chosen to investigate samples from type II diabetic patients against the anti-STSYGTGC series sera (Figure 5.2). The boxplot representation of the clinical data (Figure 5.2A) shows there was little difference in the binding of anti-STSY-(NO_2)-GTGC serum between the healthy and diabetic samples. However, it was noted that there were 2 outliers in the diabetic cohort with very high binding levels. The outliers of anti-STSY-(NO_2)-GTGC serum Vs. diabetic samples (Disease) do however suggest some greater binding (figure 5.2A).

The plasma samples used in figure 5.2A were then normalized for their fibrinogen concentrations, based on the binding of the anti-fibrinogen antibody (Figure 5.2B). More specifically, the absorbance values of the produced anti-sera used in figure 5.2A, representative of binding, were divided by those of anti-fibrinogen, which were representative of the plasma sample fibrinogen content. After normalization, the trend of binding remained similar to figure 5.2A, with anti-STSYGTGC and anti-STSY-(Cl)-GTGC binding both healthy and disease samples almost indiscriminately. This is not surprising, as it would be expected for anti-STSYGTGC to bind native fibrinogen, and anti-STSY-(Cl)-GTGC displayed cross-reactivity for STSYGTGC in chapter 4. In addition, Anti-STSY-(NO_2)-GTGC bound poorly to both healthy and disease samples. However, after normalization for fibrinogen content, the outliers for anti-STSY-(NO_2)-GTGC seen in figure 5.2A showed greater binding (figure 5.2B). The values from figure 5.2B were then plotted against the CRP levels for each of the samples (figure 5.3). The healthy plasma samples showed no substantial binding to anti-STSY-(NO_2)-GTGC serum, and similarly, most of the diabetic samples also showed very little binding. With regard to these outliers, two of the diabetic samples did show increased binding, compared to the base-line binding seen for the other samples, but large standard deviation values suggest sample variability between replicates.

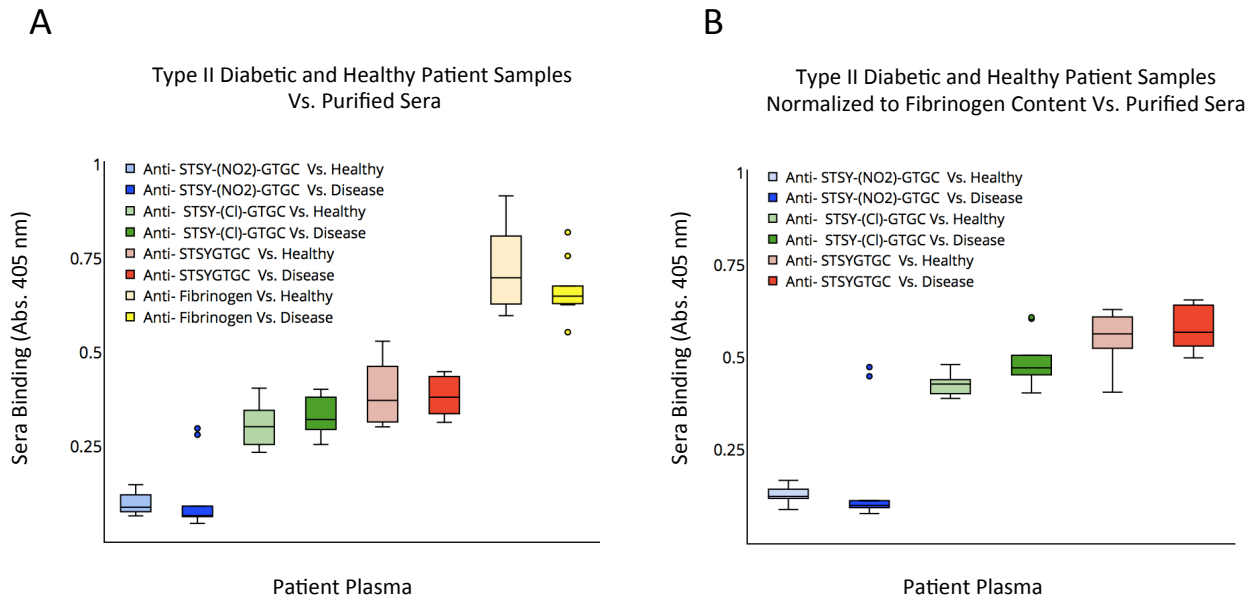

Figure 5.2: Testing Antibody Binding to Human Diabetic (Disease) and Healthy Plasma Samples. (Diabetic, *n* = 10, healthy, *n* = 10) (A) Boxplot showing distribution of various anti-sera and antibodies binding to healthy and type 2 diabetic human plasma samples (B) Anti-sera binding to healthy and type 2 diabetic human plasma samples normalized to fibrinogen content. Nunc maxi-sorp plates (Product code: 10098860, Fisher Scientific, UK) were coated with serial dilutions of plasma samples. Anti-fibrinogen (Product code: F8512) was used at a working dilution of 1:10,000, anti-sera was made to 1.5 µg/ mL and detected with 1:25,000 donkey anti-sheep antibody conjugated to alkaline phosphatase (Product code: A5187), and 1 mg/mL phosphate substrate in pNPP buffer, pH 10.4, with an incubation time of 15 minutes at room temperature before being read on a plate reader at 405 nm. Clinical samples were obtained from the Brown research group at Aston University (Appendix 31). Plotly graphing, version 1 (https://plot.ly) was used to produce boxplots (A and B).

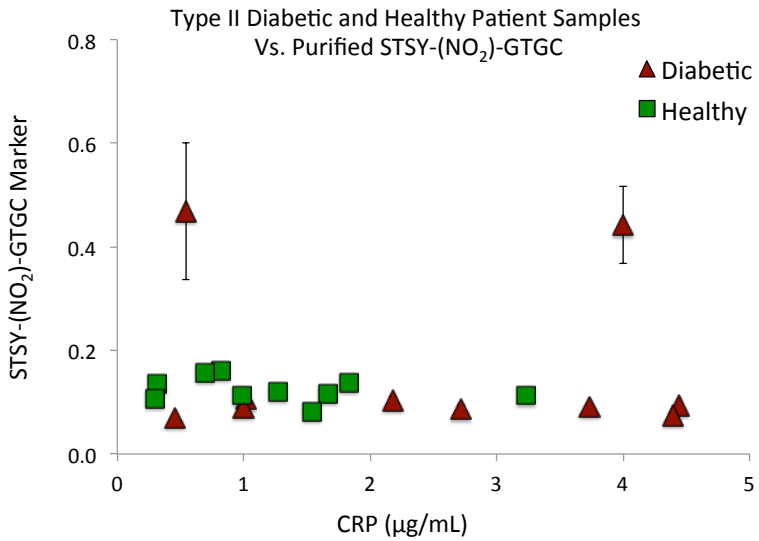

Figure 5.3: STSY-(NO_2)-GTGC Peptide (from figure 5.2) Vs. CRP serum concentration. (*n* = 3, standard deviation of technical replicates). Clinical samples were obtained from the Brown research group at Aston University (Appendix 31). Plotly graphing, version 1 (https://plot.ly) was used to produce this graph.

5.3 Chapter 5 Discussion

The aim of this chapter was to investigate whether anti-serum produced in chapter 4 could be used to detect STSY-(NO_2)-GTG peptide in type 2 diabetic samples, with the hypothesis that anti-STSY-(NO_2)-GTGC serum could be used to detect the STSY-(NO_2)-GTG peptide of fibrinogen in type 2 diabetic samples, with increased binding correlating to the increase in CRP level.

Both healthy and diabetic plasma samples, after testing an ELISA type immunoassay, showed binding to both anti-fibrinogen and anti-STSYGTGC, in line with the fact that fibrinogen is abundant in plasma. The fibrinogen content for each sample was measured using a commercial anti fibrinogen antibody, as a way of standardizing the fibrinogen protein content between each human plasma sample. This is important because fibrinogen is a positive acute phase protein, and increases in concentration during inflammation. And, as previously discussed in the introduction, many lifestyle factors can induce varying levels of inflammation (Mischak et al., 2007). This highlights an important factor worth consideration. We must also consider the different binding affinities between antibodies, and for this reason, comparisons of antibody binding can only be based on trend profiles, rather than absolute values. To understand such values better, future work should include utilizing surface plasmon resonance to determine antibody-antigen binding affinities. As previously described in chapter 4, surface plasmon resonance has been shown to measure antibody binding affinity in real time, under various conditions (Englebienne *et al.*, 1998).

The anti-STSYGTGC series versus type 2 diabetic and healthy clinical plasma samples show little difference between the healthy and diabetic (disease) samples. However, two outliers represented as circles above the boxes, suggest greater binding in two of the diabetic samples. The presence of 3-nitrotyrosine has previously been detected in the plasma of type 2 diabetic patients with ELISA, in a study by Ceriello *et al*., (2001). More specifically, 3-nitrotyrosine was detected in all type 2 diabetic plasma samples but none of the healthy controls (Ceriello *et al*., 2001). The anti-fibrinogen suggests greater amounts of fibrinogen in the healthy samples compared to the disease samples. This contradicts the literature, as fibrinogen is a positive acute phase protein, expected to increase in concentration during inflammation (Vadseth *et al*., 2003). The overlap between the error bars and median values for both healthy and disease fibrinogen samples do suggest sample variability, which suggests better standardization may be required. A comparison of the existing fibrinogen antibody discussed and a different anti-fibrinogen antibody, to determine the accuracy of the sample fibrinogen content obtained should be performed. The binding of anti-STSY-(NO_2)-GTGC serum to the clinical plasma samples was plotted against plasma CRP concentrations, showing no apparent trend in binding profile. The concentration of plasma CRP (indicative of systemic inflammation) can vary as a result of several factors, including, body mass index (BMI), diabetes, hypertension, cigarette smoking, estrogen replacement therapy, cholesterol concentrations, and genetic polymorphisms in the CRP gene (Dhingra *et al.,* 2008). Further work is required to compare the other parameters that affect plasma CRP levels, and in order to standardize CRP levels based on the discussed lifestyle factors. One of the main limitations of this study is the small sample size considered, and future work should involve analysis of a larger sample set, in order to obtain more representative data.

An article by Ioannidis (2005) describes the importance of sample size in studies of clinical samples, stating that the smaller a study is, the less likely the research findings are to be true. The level of CRP was shown to vary depending on the level of inflammation (Henriksen *et al.*, 2008). The level of inflammation is dependent on the disease pathology, which means different diseases involve different levels of inflammation, and as such different plasma CRP concentrations. The level of inflammation seen in type 2 diabetes is considered mild (low-grade), whereas, diseases such as rheumatoid arthritis (RA) are defined by high-grade inflammation, and high plasma CRP concentrations (Duncan, 2003, Sattar *et al.*, 2003, and Gonzalez-Gay *et al.*, 2008). For these reasons we might expect to see a greater inflammatory profile in diseases defined by high-grade inflammation, and as such future work should include testing anti-STSY-(NO_2)-GTGC serum against diseases defined by high-grade inflammation.

5.3.1 Chapter 5 Conclusions and Future Work

In conclusion, no substantial binding of anti-STSY-(NO_2)-GTGC was seen in diabetic samples, and no correlation between the sample CRP concentration and STSY-(NO_2)-GTG could be made. Further work should include analysis of a larger sample set, ideally, of clinical samples with a higher inflammatory profile.

Chapter 6

Summary and Conclusions

6.1 Summary and Discussion of all Chapters

Protein oxidation has been reported in a variety of diseases with an inflammatory pathology, relating to immune cell activation and the subsequent release of reactive oxidants. The oxidative nature of inflammatory pathology also offers potential for diagnostic or prognostic markers of disease. The most commonly used translatable methods are those involving antibody-based assays, such as ELISA and Western blotting; these techniques are popular because of their simplicity, but they are often limited by the availability of antibodies with suitable specificity, especially when considering oxPTMs, where they might be required to identify both the modification site and specific protein.

Fibrinogen is one of the most abundant plasma proteins, and has been implicated in the pathology of various inflammatory diseases. Therefore, the overall aim of the research project was to develop new biomaterials for detecting inflammatory protein oxidative damage to fibrinogen. More specifically, in order to achieve this, the initial goal was to identify stable modifications to fibrinogen as good potential markers of oxidative damage by various oxidizing species, and to produce anti-sera that bind the modified peptides with sequence and modification site-specificity. The hypothesis was that antibodies could be produced for human fibrinogen peptides with both sequence and modification site specificity, to a number of oxidative modifications, similar to those that might be expected during inflammation.

In this work, fibrinogen was treated with SIN-1(peroxynitrite generator) and several peptides containing 3-nitrotyrosine were identified by a non-targetted LC-MS^2 approach. The most frequently occurring modified peptides were ^{273}GGSTSY-(NO_2)-GTGSETESPR^{287}, ^{135}Y-(NO_2)-LQEIYNSNNQK^{146} and ^{472}GSWY-(NO_2)-SMR^{478}. The lack of crystal structure data for ^{273}GGSTSY-(NO_2)-GTGSETESPR^{287} suggested that the sequence displayed conformational flexibility, which may support its susceptibility to modification (Rasmussen *et al.*, 2007). These fibrinogen modifications were different to those identified in the literature (Parastatidis *et al.*, 2008), which might relate to differences between *in-vivo* and *in-vitro* nitration. There was no clear trend in the amount or percentage of the peptides that were modified between treatment concentrations, and the percentage of modified peptides did not correlate to the literature (Nuriel *et al.*, 2008). With regard to chlorinative modifications to fibrinogen, with a similar MS approach, HOCl treated fibrinogen showed good protein sequence coverage, but no modifications other than methionine oxidation were observed. Due to the susceptibility of methionine to oxidation, it acts as an oxidative quenching residue, and therefore such modifications are not distinctly specific to inflammation (Berlett and Stadtman, 1997). The lack of chlorinative modifications might be as a result of HOCl treatment induced lysine modifications, causing protein aggregation and potentially, tryptic miscleaves, hindering the MS analysis, as discussed previously. These results were disappointing as a number of previous studies have reported HOCl-induced modifications of proteins, including 3-chlorotyrosine formation in HSA (Tveen-Jensen *et al.*, 2013). The differences in observed modifications might relate to conformational differences between fibrinogen and HSA, and the subsequent susceptibility to modification, both before and after HOCl induced conformational changes. Two peptides were identified from reports in the literature and

subsequently synthesized, specifically, a 3-chlorotyrosine modified HSA peptide, ^{287}Y-(Cl)-ICENQDSISSK^{298} (Tveen-Jensen *et al.*, 2013), and a fibrinogen peptide, ^{196}DYEDQQKQL^{204}, which was selected from the literature based on its potential to form 3-chlorotyrosine (Bergt *et al.,* 2004). In addition, peptide antigens containing either multiple 3-nitrotyrosines or 3-chlorotyrosines were designed, based on the exposure of the modification sites as epitopes. Sheep were immunized with either the native, chlorinated or nitrated versions of peptide series, STSYGTGC, and, native or chlorinated versions of DYEDQQKQLC series. The anti-sera obtained from these sheep were tested against all of the synthesized peptides, and several treated plasma proteins. Subsequently, the anti-DY-(Cl)-EDQQKQLC serum showed sequence specificity with cross-reactivity between modification sites, whereas, anti-STSY-(NO_2)-GTGC serum showed modification site specificity with cross-reactivity between peptide sequences (Tables 6.1 and 6.2).

Table 6.1: Anti-STSY-(NO_2)-GTGC Serum Specificity

Peptide Sequence	Binding
STSYGTGC	✗
STSY-(Cl)-GTGC	✗
STSY-(NO_2)-GTGC	✓
DY-(NO_2)-EDQQKQLC	✓
SY-(NO_2)-ASY-(NO_2)-SY-(NO_2)	✓
Nitrated Fibrinogen	✓

Table 6.2: Anti-DY-(Cl)-EDQQKQLC Serum Specificity

Peptide Sequence	Binding
DYEDQQKQLC	✗
DY-(Cl)-EDQQKQLC	✓
SY-(Cl)-ASY-(Cl)-SY-(Cl)	✗
DY-(NO_2)-EDQQKQLC	✓
STSY-(Cl)-GTGC	✗
STSY-(Cl)-GTGC	✗
Nitrated Fibrinogen	✗

The cross reactivity was thought to relate to the polyclonal nature of the obtained anti-sera. Translation of the identified peptides and produced anti-sera were tested in 10 type 2 diabetic clinical samples and 10 age-matched controls. The modified peptide identified in chapter 3, STSY-(NO_2)-GTG, was not identified in type 2 diabetic samples with the produced anti-STSY-(NO_2)-GTGC serum, and no correlation between STSY-(NO_2)-GTG and plasma CRP concentration could be made. Future work with clinical samples should include analysis of a larger sample set, and ideally should be, of clinical samples with a higher inflammatory profile, such as RA. The polyclonal nature of the anti-sera produced means there is no certainty which epitopes the antibodies are binding to. Affinity purification was performed to reduce cross reactivity to various other antigens. However, there is no certainty to how successful this procedure was. The production and testing of monoclonal antibodies could potentially allow the specificity of antibodies specific to one individual epitope to be tested, with the possibility of identifying an antibody with exclusive specificity for both the modification site and amino acid sequence.

As previously discussed, even with successful production of specific antibodies for the peptides identified with MS in chapter 3, it is possible that due to differences between *in-vitro* and *in-vivo* environments, these modified peptides do not occur *in-vivo.* In order to test this, future work should involve an MRM programme and narrow window XIC to search for the modified peptides identified in chapter 3 in inflammatory clinical samples such as those discussed in chapter 5. Although an understanding of binding specificity is important, the nature of antibody and epitope interactions also illustrates the importance of understanding binding efficiency. A study by Englebienne *et al*. (1998) utilized surface plasmon resonance (SPR) to determine antibody to epitope binding efficiency, and the use of such techniques in

future work is recommended. Fibrinogen is known to be an abundant plasma protein involved in various inflammatory diseases. However, it is less abundant than HSA.

A study performed by Tveen-Jensen *et al.*, 2013 identified a 3-chlorotyrosine modification to HSA after treatment with HOCl. Chlorination and nitration of other abundant plasma proteins, such as HSA, followed by MS to identify modifications should be considered.

In conclusion, some aspects of the aims were met and the general hypothesis described in section 1.11 was to some extent supported. However, some aspects of the hypothesis were not supported, and some of the aims were not met. More specifically, the modifications identified with MS, although consistent, did not appear to be concentration specific. New biomaterials for detecting protein oxidative damage were developed, capable of differentiating between native and modified peptides of fibrinogen. One of the anti-sera series appeared to show sequence specificity, and the other anti-serum showed modification site specificity, but neither showed both. As discussed, further work is required to understand anti-sera sequence specificity by producing monoclonal antibodies, to determine differences in binding efficiency with SPR, and if the *in-vitro* modifications identified appear *in-vivo* with MS analysis of inflammatory clinical samples.

Chapter 7

References

References

Aalberse R, Akkerdaas JH, and Van Ree R. (2001). Cross-reactivity of IgE antibodies to allergens. *Allergy*, 56 (1), 478–490.

Abello N, Kerstjens H, Postma D and Bischoff R. (2009). Protein tyrosine nitration: selectivity, physicochemical and biological consequences, denitration, and proteomics methods for the identification of tyrosine-nitrated proteins. *Journal of Proteome Research*. 8 (7), 3222-3238.

Adams S, Green P, Claxton R, Simcox S, Williams MV, Walsh K and Leeuwenburgh C. (2001). Reactive carbonyl formation by oxidative and non-oxidative pathways. *Frontiers in Bioscience*. 6 (1), 17-24.

Alvarez B and Radi R. (2003). Peroxynitrite reactivity with amino acids and proteins. *Amino Acids*. 25 (3-4), 295-311.

Anderson L and Hunter C (2005). Quantitative mass spectrometric multiple reaction monitoring assays for major plasma proteins. *Molecular and Cellular Proteomics*. 5 (4), 573-588.

Anderson NL and Anderson NG. (2002). The human plasma proteome: history, character, and diagnostic prospects. *Molecular and Cellular Proteomics*. 1 (11), 845-867.

Ashraf M, Ebner M, Wallner C, Haller M, Khalid S, Schwelberger H, Koziel K, Enthammer M, Hermann M, Sickinger S, Soleiman A, Steger C, Vallant S, Sucher R, Brandacher G, Santer P, Dragun D and Troppmair J . (2014). A p38MAPK/MK2 signaling pathway leading to redox stress, cell death and ischemia/reperfusion injury. *Cell Communication and Signaling*. 14 (6), 1478-1811.

Aulak K, Koeck T, Crabb J and Stuehr D. (2004). Proteomic method for identification of tyrosine-nitrated proteins. *Methods in Molecular Biology*. 279 (1), 151-165.

Beckman KB and Ames BN. (1998). The free radical theory of aging matures. Physiological. Reviews. 78 (2), 547–581.

Bergt C, Fu X, Huq N, Kao J and Heinecke J. (2004). Lysine Residues Direct the Chlorination of Tyrosines in YXXK Motifs of Apolipoprotein A-I When Hypochlorous Acid Oxidizes High Density Lipoprotein. *Journal of Biological Chemistry*, 279 (9), 7856–7866.

Berlett B and Stadtman E. (1997). Protein oxidation in aging, disease, and oxidative stress. *The Journal of Biological Chemistry*. 272 (33), 20313-6.

Berlett BS and Stadtman ER. (1997). Protein oxidation in aging, disease, and oxidative stress. Journal of Biological Chemistry. 272 (1), 20313–20316.

Beutler B, Jiang Z, Georgel P, Crozat K, Croker B, Rutschmann S, Du X and Hoebe K. (2006). Genetic analysis of host resistance: Toll-like receptor signaling and immunity at large. *Annual Review of Immunology*. 24 (1), 353-389.

Black S, Kushner I and Samols D. (2004). C-reactive Protein. *Journal of Biological Chemistry*. 279 (47), 48487-90.

Brunette, N. (1980). “Western Blotting”: electrophoretic transfer of proteins from sodium dodecyl sulfate-polyacrylamide gels to unmodified nitrocellulose and radiographic detection with antibody and radioiodinated protein. *Analytical Biochemistry* . 112 (1), 195-203.

Burkitt W, Domain P and O'Connor G. (2010). Conformational changes in oxidatively stressed monoclonal antibodies studied by hydrogen exchange mass spectrometry. *Protein Science* . 19 (4), 826-835.

Butler A, Megson I and Wright P. (1998). Diffusion of nitric oxide and scavenging by blood in the vasculature. *Biochimica et Biophysica Acta*. 1425 (1), 168-76.

Carp H, Miller F, Hoidal J, and Janoff A. (1982). Potential mechanism of emphysema: alpha 1-proteinase inhibitor recovered from lungs of cigarette smokers contains oxidized methionine and has decreased elastase inhibitory capacity. *Proceedings of the National Academy of Sciences*. 79 (6), 2041–2045.

Carty J, Bevan R, Waller H, Mistry N, Cooke M, Lunec J and Griffiths H. (2000). The effects of vitamin C supplementation on protein oxidation in healthy volunteers. *Biochemical and Biophysical Research Communications*. 273 (2), 729-35.

Carty J, Bevan R, Waller H, Mistry N, Cooke M, Lunec J and Griffiths H. (2000). The effects of vitamin C supplementation on protein oxidation in healthy volunteers. *Biochemical and Biophysical Research Communications*. 273 (2), 729-35.

Castell JV, Gomez-Lechon MJ, David M, Andus T, Geiger T, Trullenque R, Fabra R, Heinrich PC. (1989). Interleukin-6 is the major regulator of acute phase protein synthesis in adult human hepatocytes. *FEBS Letters*. 242 (2), 237–239.

Castell JV, Gomez-Lechon MJ, David M, Andus T, Geiger T, Trullenque R, Fabra R, Heinrich PC. (1989). Interleukin-6 is the major regulator of acute phase protein synthesis in adult human hepatocytes. *FEBS Letters*. 242 (2), 237–239.

Chan W and White P (2000). *Fmoc Solid Phase Peptide Synthesis: A Practical Approach.* New York: Oxford University Press. 14.

Charles A, Janeway, J, Travers, P Walport, M and Shlomchik M J. (2001). The interaction of the antibody molecule with specific antigen. *Immunobiology* . New York: Garland Science.

Clarke RA. (1999). Activation of the neutrophil respiratory burst oxidase. *Journal of Infectious Disease*. 179 (1), S309-317.

Dahl M, Tybjaerg-Hansen A, Vestbo, Lange and Nordestgaard. (2001). Elevated Plasma Fibrinogen Associated with Reduced. *American Journal of Respiratory and Critical Care Medicine*. 164 (6), 2001.

Dalle-Donne I, Rossi R, Giustarini D, Milzani A and Colombo R. (2003). Protein carbonyl groups as biomarkers of oxidative stress. *Clinica Chimica Acta; International Journal of Clinical Chemistry*. 329 (1-2), 23-38.

Devenport A, Reynolds J, Parkash V, Cook J, Weston D and Creaser C. (2011). Determination of free desmosine and isodesmosine as urinary biomarkers of lung disorder using ultra performance liquid chromatography-ion mobility-mass spectrometry. *The Journal of Chromatography*. 879 (32), 3797-3801.

Domon B and Aebersold R. (2006). Mass Spectrometry and Protein Analysis. *Science*. 80 (312), 212–217.

Dorfer V, Pichler P, Stranzl T, Stadlmann J, Taus T, Winkler S and Mechtler K. (2014). MS Amanda, a universal identification algorithm optimized for high accuracy tandem mass spectra. *Journal of Proteome Research*. 13 (8), 3679-3684.

Doyle. (2006). William Hewson (1739–74): the father of haematology. *British Journal of Haematology*. 133 (1), 375–381.

Duncan M. (2002). A review of approaches to the analysis of 3-nitrotyrosine. *Amino Acids*. 25 (3-4), 351-361.

Duvoix A, Dickens J, Haq I, Mannino D, Miller B, Tal-Singer R, Lomas D . (2012). Blood fibrinogen as a biomarker of chronic obstructive pulmonary disease. *Thorax*. 68 (7), 670-676.

Englebienne P. (1998). Use of colloidal gold surface plasmon resonance peak shift to infer affinity constants from the interactions between protein antigens and antibodies specific for single or multiple epitopes. *Analyst*. 123 (7), 1599-1603.

Ermert D, Niemiec MJ, Röhm M, Glenthøj A, Borregaard N and Urban CF. (2013). Candida albicans escapes from mouse neutrophils. *Journal of Leukocyte Biology*. 94 (2), 223-236.

Fenn JB, Mann M, Meng CK, Wong SF and Whitehouse CM. (1989). Electrospray ionization for mass spectrometry of large biomolecules. *Science.* 246 (4926), 64–71.

Forsström B, Axnäs B, Rockberg J, Danielsson H, Bohlin A and Uhlen M. (2015). Dissecting antibodies with regards to linear and conformational epitopes. *PLoS ONE*, 10 (3), 1–11.

Franze T, Weller M, Niessner R and Poschl U. (2004). Comparison of nitrotyrosine antibodies and development of immunoassays for the detection of nitrated proteins. *The Analyst*. 129 (7), 589-596.

Gani R, Griffin J, Kelly S, Rutten-van Mölken M. (2010). Economic analyses comparing tiotropium with ipratropium or salmeterol in UK patients with COPD. *Primary Care Respiratory Journal*. 19 (1), 68-74.

Gao Y and Wang Y. (2007). A Method to Determine the Ionization Efficiency Change of Peptides Caused by Phosphorylation. *Journal of the American Society for Mass Spectrometry*, 18 (11), 1973–1976.

Ghesquière B and Gevaert K. (2014). Proteomics methods to study methionine oxidation. *Mass Spectrometry Reviews*. 33 (2), 147-156.

Ghesquière B, Goethals M, Van Damme J, Staes A, Timmerman E, Vandekerckhove J and Gevaert K. (2006). Improved tandem mass spectrometric characterization of 3-nitrotyrosine sites in peptides. *Rapid Communications in Mass Spectrometry*. 20 (19), 2885-2893.

Gianazza E, Crawford J and Miller I (2007). Detecting oxidative post-translational modifications in proteins. *Amino Acids*. 33 (1), 51-56.

Goldstein R and Starcher B. (1978). Urinary excretion of elastin peptides containing desmosine after intratracheal injection of elastase in hamsters. *The Journal of Clinical Investigation*. 61 (5), 1286-1290.

Graham GJ and Locati M. (2013). Regulation of the immune and inflammatory responses by the 'atypical' chemokine receptor D6. *Journal of Pathology*. 229 (2), 168-175.

Green RJ, Frazier RA, Shakesheff KM, Davies MC, Roberts CJ and Tendler SJ. (2000). Surface plasmon resonance analysis of dynamic biological interactions with biomaterials. *Biomaterials*. 21 (18), 1823-1835.

Griffiths H. (2000). Antioxidants and protein oxidation. *Free Radical Research*. 33 (1), S47-58.

Gulhar M, Kibria G, Albatineh A and Ahmed N. (2012). A comparison of some confidence intervals for estimating the population coefficient of variation: A simulation study. *Sort*, 36 (1), 45–68.

Gutteridge J. (1984). Reactivity of hydroxyl and hydroxyl-like radicals discriminated by release of thiobarbituric acid-reactive material from deoxy sugars, nucleosides and benzoate. *Biochemical Journal*. 224 (3), 761–767.

Guzik T, Korbut R and Adamek-Guzik T. (2003). Nitric oxide and superoxide in inflammation and immune regulation. *Journal of Physiology and Pharmacology: An Official Journal of the Polish Physiological Society*. 54 (4), 469-87.

Hames B, Hooper N and Houghton J (1997). *Instant Notes in Biochemistry*. Oxford: BIOS. 92-95.

Harman, D. (1956). Aging: a theory based on free radical and radiation chemistry. Journal of Gerontology. 11 (3), 298–300.

Harris and Markl. (1999). Keyhole limpet hemocyanin (KLH): a biomedical review. *Micron*. 30 (6), 597–623.

Harris D (2010). *Quantitative Chemical Analysis*. 8th ed. New York: W. H. Freeman and Company. 514-515.

Hayyan M, Hashim MA and AlNashef IM. (2016). Superoxide Ion: Generation and Chemical Implications. *Chemical Reviews*. 116 (5), 3029-3085.

Hazel LJ, Van Den Berg JJ and Stocker R. (1994). Oxidation of low-density lipoprotein by hypochlorite causes aggregation that is mediated by modification of lysine residues rather than lipid oxidation. *Biochemical Journal*. 302 (1), 297–304.

Hazen S and Heinecke J. (1997). 3-Chlorotyrosine, a specific marker of myeloperoxidase-catalyzed oxidation, is markedly elevated in low density lipoprotein isolated from human atherosclerotic intima. *The Journal of Clinical Investigation*. 99 (9), 2075–2081.

Hazen S and Heinecke J. (1997). 3-Chlorotyrosine, a specific marker of myeloperoxidase-catalyzed oxidation, is markedly elevated in low density lipoprotein isolated from human atherosclerotic intima. *The Journal of Clinical Investigation*. 99 (9), 2075–2081.

Hennion M and Barcelo D. (1998). Strengths and limitations of immunoassays for effective and efficient use for pesticide analysis in water samples: A review. *Analytica Chimica Acta*. 362 (1), 3-34.

Hennion, MC and Barcelo, D. (1998). Strengths and limitations of immunoassays for effective and efficient use for pesticide analysis in water samples: A review. *Analytica Chimica Acta*, 362 (1), 3–34.

Hill R J, Konigsberg W, Guidotti G and Craig LC. (1962). The structure of human hemoglobinhaemoglobin. I. The separation of the alpha and beta chains and their amino acid composition. *Journal of Biological Chemistry*. 237 (1), 1549-1554.

Hipkiss A. (2006). Accumulation of altered proteins and ageing: causes and effects. *Experimental gerontology*. 41 (5), 464-473.

Hoffmann E and Stroobant V (2007). *Mass Spectrometry: Principles and Applications*. 3rd ed. Chichester: Wiley-Blackwell. 85-134.

Hoshi T and Heinemann S. (2001). Regulation of cell function by methionine oxidation and reduction. *The Journal of Physiology*. 531 (1), 1–11.

Houée-Lévin C, Bobrowski K, Horakova L, Karademir B, Schöneich C, Davies MJ and Spickett CM. (2015). Exploring oxidative modifications of tyrosine: an update on mechanisms of formation, advances in analysis and biological consequences. *Free Radical Research*. 49 (4), 347-373.

Hwang CS, Shemorry A, Varshavsky A. (2010). *N-terminal acetylation of cellular proteins creates specific degradation signals. Science 327: 973–977.*

Ichinose. (2009). Differences of inflammatory mechanisms in asthma and COPD. *Allergology International*. 58 (3), 307-313.

Inada Y, Hessel B, Blombäck B. (1978). Photooxidation of fibrinogen in the presence of methylene blue and its effect on polymerization. *Biochimica et Biophysica Acta*. 532 (1), 161-170.

Inoguchi T, Sonta T, Tsubouchi H, Etoh T, Kakimoto M, Sonoda N, Sato N, Sekiguchi N, Kobayashi K, Sumimoto H, Utsumi H and Nawata H. (2003). Protein kinase C-dependent increase in reactive oxygen species (ROS) production in vascular tissues of diabetes: role of vascular NAD(P)H oxidase. *Nature*. 8 (3), S227-32.

IonSource. (2016). *De Novo Peptide Sequencing Tutorial.* Available: http://www.ionsource.com/tutorial/DeNovo/b_and_y.htm. Last accessed 29th September 2016.

Jiao K, Mandapati S, Skipper PL, Tannenbaum SR and Wishnok JS. (2001). Site-selective nitration of tyrosine in human serum albumin by peroxynitrite. *Analytical Biochemistry* . 293 (1), 43-52.

Jones (2002). *Amino Acid and Peptide Synthesis*. 2nd ed. Oxford: Oxford University Press.

Karve T and Cheema A. (2011). Small Changes Huge Impact: The Role of Protein Posttranslational Modifications in Cellular Homeostasis and Disease. *Journal of Amino Acids*. 2011 (1), 1-13.

Karve T and Cheema M . (2011). Small changes huge impact: the role of protein posttranslational modifications in cellular homeostasis and disease. *Journal of Amino Acids*. 4061 (10), 1-13.

Kettle A. (1996). Neutrophils convert tyrosyl residues in albumin to chlorotyrosine. *European Journal of Biochemistry Letters*. 379 (1), 103-106.

Kettle AJ. (1996). Neutrophils convert tyrosyl residues in albumin to chlorotyrosine. *FEBS Letters*. 379 (1), 103-106.

Khan J, Brennand D,Bradley N, Gao B, Bruckdorfer R and Jacobs M. (1998). 3-Nitrotyrosine in the proteins of human plasma determined by an ELISA method. *Biochemistry Journal*. 332 (3), 807–808.

Kim H and Gladyshev V. (2007). Methionine sulfoxide reductases: selenoprotein forms and roles. *The Biochemical Journal*. 407 (3), 321-329.

Koenig W, Sund M, Fröhlich M, Fischer HG, Löwel H, Döring A, Hutchinson WL and Pepys MB. (1999). C-Reactive protein, a sensitive marker of inflammation, predicts future risk of coronary heart disease in initially healthy middle-aged men: results from the MONICA (Monitoring Trends and Determinants. *Circulation*. 99 (2), 237-42.

Kumar N, Abbas A, Fausto N and Aster J (2010). *Robbins and Cotran Pathologic Basis of Disease, Volume 1*. 8th ed. Michigan: Elsevier Saunders. 500.

Kumar V, Calamaras T, Haeussler D, Colucci W, Cohen R, McComb M, Pimentel D, Bachschmid MM. (2012). Cardiovascular redox and ox stress proteomics. *Antioxidants and Redox Signalling*. 17 (11), 1528-1559.

Larin. (2013). *Protective Groups for Peptide Synthesis.* Available: http://www.peptideguide.com/protecting-groups-spps.html. Last accessed 24/05/2013.

Levine R. (2002). Carbonyl modified proteins in cellular regulation, aging, and disease. *Free Radical Biology and Medicine*. 32 (9), 790-796.

Levine RL, Wehr N, Williams JA, Stadtman ER and Shacter E. (2000). Determination of carbonyl groups in oxidized proteins. *Methods in Molecular Biology*. 99 (1), 15-24.

Lu N, Xie S, Li J, Tian R and Peng Y. (2015). Myeloperoxidase-mediated oxidation targets serum apolipoprotein A-I in diabetic patients and represents a potential mechanism leading to impaired anti-apoptotic activity of high density lipoprotein. *Clinica Chimica Acta: International Journal of Clinical Chemistry*. 441 (1), 163-170.

Luisetti M, Ma S, Iadarola P, Stone P, Viglio S, Casado B, Lin Y, Snider G and Turino G. (2008). Desmosine as a biomarker of elastin degradation in COPD: current status and future directions. *The European Respiratory Journal*. 32 (5), 1146-1157.

Lupidi G, Angeletti M, Eleuteri AM, Tacconi L, Coletta M and Fioretti E. (1999). Peroxynitrite-mediated oxidation of fibrinogen inhibits clot formation. *European Journal of Biochemistry Letters*. 462 (3), 236-240.

Lushchak, VI. (2014). Classification of oxidative stress based on its intensity. *EXCLI Journal*. 13 (1), 922–937.

MacBeath G. (2002). Protein microarrays and proteomics. *Nature Genetics*. 32 (1), 526-532.

MacGillivray RT, Mendez E, Sinha S, Sutton M, Lineback-Zins J and Brew K. (1982). The complete amino acid sequence of human serum transferrin. *PNAS*. 79 (8), 2504–2508.

MacMillan-Crow L, CrowJ, Kerby J, Beckman J, and Thompson J. (1996). Nitration and inactivation of manganese superoxide dismutase in chronic rejection of human renal allografts. *PNAS*. 93 (21), 11853–11858.

MacNee. (2001). Oxidative stress and lung inflammation in airways disease. *European Journal of Pharmacology*. 429 (1-3), 195-207.

MacNee. (2006). ABC of chronic obstructive pulmonary disease pathology, pathogenesis, and pathophysiology. *British Medical Journal*. 332 (1), 1202-1204.

Mahmood T and Yang P. (2012). Western Blot: Technique, Theory, and Trouble Shooting. *North American Journal of Medical Sciences* . 4 (9), 429–434.

Mann M and Jensen O. (2003). Proteomic analysis of post-translational modifications. *Nature Biotechnology*. 21 (1), 255 - 261.

Martinez M, Cuker A, Mills A, Lightfoot R, Fan Y, Tang WH, Hazen SL and Ischiropoulos H. (2012). Nitrated fibrinogen is a biomarker of oxidative stress in venous thromboembolism. *Free Radical Biology and Medicine*. 53 (2), 230-236.

Martinez M, Weisel, JW, and Ischiropoulos H. (2013). Nitrated fibrinogen is a biomarker of oxidative stress in venous thromboembolism. *Free Radical Biology and Medicine*. 65 (1), 411–418.

Matheson N, Wong P and Travis J. (1979). Enzymatic inactivation of human alpha-1-proteinase inhibitor by neutrophil myeloperoxidase. *Biochemical and Biophysical Research Communications*. 88 (2), 402-409.

Matyas G, Wassef N, Rao M and Alving C. (2002). Induction and detection of antibodies to squalene. *Journal of Immunological Methods*. 267 (1), 119– 129.

McHugh L. and Arthur JW. (2008). Computational methods for protein identification from mass spectrometry data. *PLoS,. Computational Biology*, 4 (2), 1- 12.

Meloun B, Morávek L and Kostka V. (1975). Complete amino acid sequence of human serum albumin. *FEBS Letters*. 58 (1), 134-137.

Mischak H, Allmaier G, Apweiler R, Attwood T, Baumann M, Benigni A, Bennett SE, Bischoff R, Bongcam-Rudloff E, Capasso G, Coon JJ, D'Haese P, Dominiczak AF, Dakna M, Dihazi H, Ehrich JH, Fernandez-Llama P, Fliser D, Frokiaer J, Garin J, Girolami M, Hancock WS, Haubitz M, Hochstrasser D, Holman RR, Ioannidis JP, Jankowski J, Julian BA, Klein JB, Kolch W, Luider T, Massy Z, Mattes WB, Molina F, Monsarrat B, Novak J, Peter K, Rossing P, Sánchez-Carbayo M, Schanstra JP, Semmes OJ, Spasovski G, Theodorescu D, Thongboonkerd V, Vanholder R, Veenstra TD, Weissinger E, Yamamoto T and Vlahou A. (2010). Recommendations for biomarker identification and qualification in clinical proteomics. *Science Translational Medicine*. 25 (2), 46ps42-46ps42.

Mischak H, Apweiler R, Banks RE, Conaway M, Coon J, Dominiczak A, Ehrich JH, Fliser D, Girolami M, Hermjakob H, Hochstrasser D, Jankowski J, Julian BA, Kolch W, Massy ZA, Neususess C, Novak J, Peter K, Rossing K, Schanstra J, Semmes OJ, Theodorescu D, Thongboonkerd V, Weissinger EM, Van Eyk JE and Yamamoto T

(2007). Clinical proteomics: A need to define the field and to begin to set adequate standards. *Proteomics.Clinical Approaches*. 1 (2), 148-56.

Miseki K. (1993). Quadrupole mass spectrometer. *US Patent 5,227,629*. 1 (1), 1-2.

Mitchell Wells J and McLuckey SA. (2005). Collision-induced dissociation (CID) of peptides and proteins. *Methods in Enzymology*. 402 (1), 148–185.

Murphy K, Travers P and Walport M (2008). *Immuno biology*. 4th ed. Oxford: Garland Science. 10-12.

Nagai R, Unno Y, Hayashi MC, Masuda S, Hayase F, Kinae N, Horiuchi S. (2002). Peroxynitrite induces formation of N(epsilon)-(carboxymethyl) lysine by the cleavage of Amadori product and generation of glucosone and glyoxal from glucose: novel pathways for protein modification . *Diabetes*. 51 (9), 2833-2839.

Nathan C, Cunningham-Bussel A. (2013). Beyond oxidative stress: an immunologist's guide to reactive oxygen species. *Nature Reviews. Immunology*. 13 (5), 349-361.

Nishikawa T, Miyahara E, Horiuchi M, Izumo K, Okamoto Y, Kawai Y, Kawano Y, Takeuchi T. (2012). Benzene metabolite 1,2,4-benzenetriol induces halogenated DNA and tyrosines representing halogenative stress in the HL-60 human myeloid cell line. *Environmental Health Perspectives*. 120 (1), 62-67.

Nuriel T, Deeb RS, Hajjar DP and Gross SS. (2008). Protein 3-nitrotyrosine in complex biological samples: quantification by high-pressure liquid chromatography/electrochemical detection and emergence of proteomic approaches for unbiased identification. *Methods in Methodology*. 441 (1), 1-17.

O'Reilly P, Jackson P, Noerager B, Parker S, Dransfield M, Gaggar A and Blalock J. (2009). N-alpha-PGP and PGP, potential biomarkers and therapeutic targets for COPD. *Respiratory Research*. 38 (10), 10-38.

O'Reilly P and Bailey W. (2007). Clinical use of exhaled biomarkers in COPD. *International Journal of Chronic Obstructive Pulmonary Disease*. 4 (2), 403–408.

Onorato J, Thorpe S and Baynes J. (1998). Immunohistochemical and ELISA assays for biomarkers of oxidative stress in aging and disease. *Annals of the New York Academy of Sciences* . 854 (1), 277-290.

Owen J (2012). *Kuby Immunology*. 7th ed. New York: Macmillan. 500.

Owen J and Butterfield D. (2010). Measurement of oxidized/reduced glutathione ratio. *Methods in Molecular Biology*. 648 (1), 269-77.

P.White, Novabiochem peptide synthesis 2012-2013 catalogue*, MerckMillipore,* Germany, 2012 pg. 3.3.

Pacher P, Beckman J and Liaudet L. (2007). Nitric Oxide and Peroxynitrite in Health and Disease. *Physiological Reviews*. 87(1), 315-424.

Page RC and Schroeder HE. (1976).Pathogenesis of inflammatory periodontal disease. A summary of current work. *Laboratory Investigations*. 34 (3), 235-249.

Parastatidis I, Thomson L, Burke A, Chernysh I, Nagaswami C, Visser J, Stamer S, Liebler D, Koliakos G, Heijnen H, Fitzgerald G, Weisel J and Ischiropoulos H. (2008). Fibrinogen beta-chain tyrosine nitration is a prothrombotic risk factor. *The Journal of Biological Chemistry*. 283 (49), 33846-33853.

Pattison DI and Davies MJ. (2001). Absolute rate constants for the reaction of hypochlorous acid with protein side chains and peptide bonds. *Chemical Research in Toxicology*, 14 (10), 1453–1464.

Pearson TA, Mensah GA, Alexander RW, Anderson JL, Cannon RO 3rd, Criqui M, Fadl YY, Fortmann SP, Hong Y, Myers GL, Rifai N, Smith SC Jr, Taubert K, Tracy RP, Vinicor F, and Centers for Disease Control and Prevention; American Heart Association. (2003). Markers of inflammation and cardiovascular disease: application to clinical and public health practice: A statement for healthcare professionals from the Centers for Disease Control and Prevention and. *Circulation*. 107 (3), 499-511.

Peng HP, Lee KH, Jian JW and Yang AS. (2014). Origins of specificity and affinity in antibody–protein interactions. *PNAS*. 111 (26), E2656–E2665.

Pettersen E, Goddard T, Huang C, Couch G, Greenblatt D, Meng E, Ferrin T. (2004). UCSF Chimera—A visualization system for exploratory research and analysis. *Journal of Computational Chemistry* . 13 (1), 1605-1612.

Pierce J, Hocott J and Ebert R. (1961). The Collagen and Elastin Content of the Lung in Emphysema. *Annals of Internal Medicine*. 55 (1), 210-22.

Pitt A and Spickett C. (2008). Mass spectrometric analysis of HOCl- and free-radical-induced damage to lipids and proteins. *Biochemical Society Transactions*. 36 (1), 1077–1082.

Pitt A. (1998). Application of electrospray mass spectrometry in biology. *Natural Products Reports*. 15 (1), 59-72.

Prütz W. (1996). Hypochlorous acid interactions with thiols, nucleotides, DNA, and other biological substrates. *Archives of Biochemistry and Biophysics*. 332 (1), 110-120.

Radi R. (2013). Peroxynitrite, a Stealthy Biological Oxidant. Journal of Biological Chemistry. 288 (37), 26464-26472.

Rasmussen SG, Choi HJ, Rosenbaum DM, Kobilka TS, Thian FS, Edwards PC, Burghammer M, Ratnala VR, Sanishvili R, Fischetti RF, Schertler GF, Weis WI and Kobilka BK. (2007). Crystal structure of the human beta2 adrenergic G-protein-coupled receptor. *Nature Medicine*. 7168 (450), 383-387.

Ray S, Britschgi M, Herbert C, Takeda-Uchimura Y, Boxer A, Blennow K, Friedman LF, Galasko DR, Jutel M, Karydas A, Kaye JA, Leszek J, Miller BL, Minthon L, Quinn JF, Rabinovici GD, Robinson WH, Sabbagh MN, So YT, Sparks DL, Tabaton M, Tinklenberg J, Yesavage JA, Tibshirani R and Wyss-Coray T (2007). Classification and prediction of clinical Alzheimer's diagnosis based on plasma signaling proteins. *Nature Medicine*. 13 (11), 1359-1362.

Raynes R, Pomatto LCD and Davies KJA (2016). Degradation of oxidized proteins by the proteasome: Distinguishing between the 20S, 26S, and immunoproteasome proteolytic pathways. *Molecular Aspects of Medicine* 50 (1), 1–15.

Regalado EL, Schafer W, McClain R, Welch, CJ. (2013). Chromatographic resolution of closely related species: Separation of warfarin and hydroxylated isomers. Journal of Chromatography. A. 1314, 266–275.

Reverberi R and Reverberi L. (2007). Factors affecting the antigen-antibody reaction. *Blood Transfusion*. 5 (4), 227–240.

Ritchie R, Palomaki GE, Neveux LM, Navolotskaia O, Redue TB and Craig WY. (1999). Reference distributions for the negative acute-phase serum proteins, albumin, transferrin and transthyretin: a practical, simple and clinically relevant approach in a large cohort. *Journal of Clinical Laboratory Analysis*. 13 (6), 273-279.

Robaszkiewicz A, Bartosz G, Soszynski M. (2011). Detection of 3-chlorinated tyrosine residues in human cells by flow cytometry. *Journal of Immunological Methods*. 369 (1-2), 141-145.

Rodriguez J, Seals J, Radin A, Lin J, Mandl I and Turino G. (1979). Neutrophil lysosomal elastase activity in normal subjects and in patients with chronic obstructive pulmonary disease. *The American Review of Respiratory Disease*. 119 (3), 409-417.

Rogowska-Wrzesinska A, Wojdyla K, Nedić O, Baron CP, Griffiths HR. (2014). Analysis of protein carbonylation--pitfalls and promise in commonly used methods. *Free Radical Research*. 48 (10), 1145-1162.

Ross PL, Huang YN, Marchese JN, Williamson B, Parker K, Hattan S, Khainovski N, Pillai S, Dey S, Daniels S, Purkayastha S, Juhasz P, Martin S, Bartlet-Jones M, He F, Jacobson A and Pappin DJ. (2004). Multiplexed protein quantitation in Saccharomyces cerevisiae using amine-reactive isobaric tagging reagents. Molecular and Cellular Proteomics. 3 (12), 1154-69.

Ruchi Sidana, H. C. Mangala, S. B. Murugesh, and K. Ravindra. (2011). Prozone phenomenon in secondary syphilis. *Indian Journal of Sexually Transmitted Diseases and AIDS*. 32 (1), 47–49.

Rudolph V, Andrié RP, Rudolph TK, Friedrichs K, Klinke A, Hirsch-Hoffmann B, Schwoerer AP, Lau D, Fu X, Klingel K, Sydow K, Didié M, Seniuk A, von Leitner EC,

Szoecs K, Schrickel JW, Treede H, Wenzel. (2010). Myeloperoxidase acts as a profibrotic mediator of atrial fibrillation. *Nature Medicine*. 16 (4), 470-474.

Safinowski M, Wilhelm B, Reimer T, Weise A, Thomé N, Hänel H, Forst T, Pfützner A. (2009). Determination of nitrotyrosine concentrations in plasma samples of diabetes mellitus patients by four different immunoassays leads to contradictive results and disqualifies the majority of the tests. *Clinical Chemistry and Laboratory Medicine*. 47 (4), 483-488.

Sambrook J and Russell D. (2006). SDS-polyacrylamide gel electrophoresis of proteins. *Cold Spring Harbor Protocols.* 3 (1), 18-47.

Satoh M, Fujimoto S, Arakawa S, Yada T, Namikoshi T, Haruna Y, Horike H, Sasaki T, Kashihara N. (2008). Angiotensin II type 1 receptor blocker ameliorates uncoupled endothelial nitric oxide synthase in rats with experimental diabetic nephropathy. *Nephrology Dialysis Transplantation*. 23 (12), 3806-3813.

Shacter E, Williams J and Levine R. (1995). Oxidative modification of fibrinogen inhibits thrombin-catalyzed clot formation. *Free Radical Biology and Medicine*. 18 (4), 815-821.

Shacter E, Williams J, Lim M and Levine R. (1994). Differential susceptibility of plasma proteins to oxidative modification: examination by Western blot immunoassay. *Free Radical Biology and Medicine*. 17 (5), 429-437.

Shacter E. (2000). Quantification and significance of protein oxidation in biological samples. *Drug Metabolism Reviews*. 32 (3-4), 307-26.

Shevchenko A, Tomas H, Havlis J, Olsen J and Mann M. (2006). In-gel digestion for mass spectrometric characterization of proteins and proteomes . *Nature Protocols*. 6 (1), 2856-60.

Shibata A, Morioka I, Ashi C, Nagasaki S, Tode C, Morikawa S, Miwa A, Enomoto M, Saiki K, Yokoyama N, Takeuchi A and Matsuo M. (2009). Identification of N-acetyl Proline–Glycine–Proline (acPGP) in human serum of adults. *Clinica Chimica Acta*. 402 (1-2), 124-128.

Shishehbor M, Aviles R, Brennan M, Fu X, Goormastic M, Pearce G, Gokce N, Keaney J Jr, Penn M, Sprecher D, Vita J and Hazen S.. (2003). Association of Nitrotyrosine Levels With Cardiovascular Disease and Modulation by Statin Therapy. *JAMA*. 238 (13), 1675-1680.

Shoal R and Weindruch R. (1996). Oxidative stress, caloric restriction, and aging. *Science*. 273 (5271), 59-63.

Sies H. (1993). Strategies of antioxidant defense. *European Journal of biochemistry*. 215 (2), 213-9.

Sies H. (1997). Oxidative stress: oxidants and antioxidants. *Experimental Physiology*. 82 (2), 291-5.

Siwak J, Lewinska A, Wnuk M, Bartosz G. (2013). Protection of flavonoids against hypochlorite-induced protein modifications. *Food Chemistry*. 141 (2), 1227-1241.

Smith P, Krohn R, Hermanson G, Mallia A, Gartner F, Provenzano M, Fujimoto E, Goeke N, Olson B, and Klenk D. (1985). Measurement of protein using bicinchoninic acid. *Analytical Biochemistry*. 150 (1), 76–85.

Smith P, Krohn R, Hermanson G, Mallia A, Gartner F, Provenzano M, Fujimoto E, Goeke N, Olson B, and Klenk D. (1985). Measurement of protein using bicinchoninic acid. *Analytical Biochemistry*. 150 (1), 76–85.

Sohal R and Weindruch R. (1996). Oxidative stress, caloric restriction, and aging.. *Science*. 273 (1), 59-63.

Souza J, Peluffo G and Radi R . (2008). Protein tyrosine nitration—Functional alteration or just a biomarker?. *Free Radical Biology & Medicine*. 45 (1), 357–366.

Stadtman E and Berlett B. (1998). Reactive oxygen-mediated protein oxidation in aging and disease. *Drug metabolism reviews*. 30 (2), 225-43.

Stadtman ER and Levine RL. (2003). Free radical-mediated oxidation of free amino acids and amino acid residues in proteins. *Amino Acids.* 25 (1), 207–218.

Stadtman ER. (2006). Protein oxidation and aging. *Free Radical Research*. 40 (12), 1250-1258.

Stevens, Prokai-Tatrai and Laszlo Prokai. (2008). Factors That Contribute to the Misidentification of Tyrosine Nitration by Shotgun Proteomics. *Molecular and Cellular Proteomics* . 7 (1), 2442-2451.

Teixeira D, Fernandes R, Prudêncio C, Vieira M. (2016). 3-Nitrotyrosine quantification methods: Current concepts and future challenges. *Biochimie*. 125 (1), 1-11.

Tsuneki M, Nakamura Y, Kinjo T, Nakanishi R and Arakawa H. (2015). Mieap suppresses murine intestinal tumor via its mitochondrial quality control. *Scientific Reports*. 12472 (5), 1-12.

Vadseth C, Souza J, Thomson L, Seagraves A, Nagaswami C, Scheiner T, Torbet J, Vilaire G, Bennett J, Murciano J, Muzykantov V, Penn M, Hazen S, Weisel J, Ischiropoulos H (2004). Pro-thrombotic state induced by post-translational

modification of fibrinogen by reactive nitrogen species. *The Journal of Biological Chemistry*. 279 (10), 8820-8826.

Valko M, Leibfritz D, Moncol J, Cronin M, Mazur M and Telser J. (2007). Free radicals and antioxidants in normal physiological functions and human disease. *The International Journal of Biochemistry and Cell Biology*. 39 (1), 44-84.

Wade G (2007). *Organic chemistry*. 7th ed. London: Pearson. 1153-1199.

Walker J and Rapley R (2008). *Molecular Biomethods Handbook.* 2nd ed. UK: Humana press. 516.

Wall S, Oh J, Diers A and Landar A. (2012). Oxidative modification of proteins: an emerging mechanism of cell signaling. *Frontiers of Physiology*. 3 (1), 1-9.

Watt K, Takagi T and Doolittle R. (1979). Amino acid sequence of the beta chain of human fibrinogen: homology with the gamma chain. *Biochemistry*. 18 (1), 68-76.

Wehr N and Levine R. (2012). Wanted and Wanting: Antibody Against Methionine Sulfoxide. *Free Radical Biology and Medicine*. 53 (6), 1222–1225.

Weigandt K, White N, Chung D, Ellingson E, Wang Y, Fu X and Pozzo D. (2012). Fibrin clot structure and mechanics associated with specific oxidation of methionine residues in fibrinogen. *Biophysical Journal*. 103 (11), 2399-2407.

Weisel J. (2005). Fibrinogen and Fibrin. *Advances in Protein Chemistry*. 70 (1), 247–299.

Winter J, Ilbert, Graf, Ozcelik, Jakob. (2008). Bleach Activates A Redox-Regulated Chaperone by Oxidative Protein Unfolding. *Cell*. 135 (4), 691-701.

Winterbourn C. (2002). Biological reactivity and biomarkers of the neutrophil oxidant, hypochlorous acid. *Toxicology*. 181-182 (1), 223-227.

Winterbourn C. (2002). Biological reactivity and biomarkers of the neutrophil oxidant, hypochlorous acid. *Toxicology*. 181-182 (1), 223-227.

Winterbourn C. (2002). Biological reactivity and biomarkers of the neutrophil oxidant, hypochlorous acid. *Toxicology*. 181-182 (1), 223-227.

Winterbourne C and Kettle AJ. (2000). Biomarkers of myeloperoxidase-derived hypochlorous acid. *Free Radical Biology and Medicine*. 29 (5), 403-409.

Wright H, Moots R, Bucknall R, Edwards S. (2010). Neutrophil function in inflammation and inflammatory diseases. *Rheumatology*. 49 (9), 1618-1631.

Zhang X, Fu Y, Xu X, Li M, Du L, Han Y and Ge Y. (2014). PERK pathway are involved in NO-induced apoptosis in endothelial cells cocultured with RPE under high glucose conditions. *Nitric Oxide*. 40 (1), 10–16.

Zhou J, Wang Q, Ding Y, Zou MH. (2015). Hypochlorous acid via peroxynitrite activates protein kinase Cq and insulin resistance in adipocytes. *Journal of Molecular Endocrinology*. 54 (1), 25-37.

Appendices

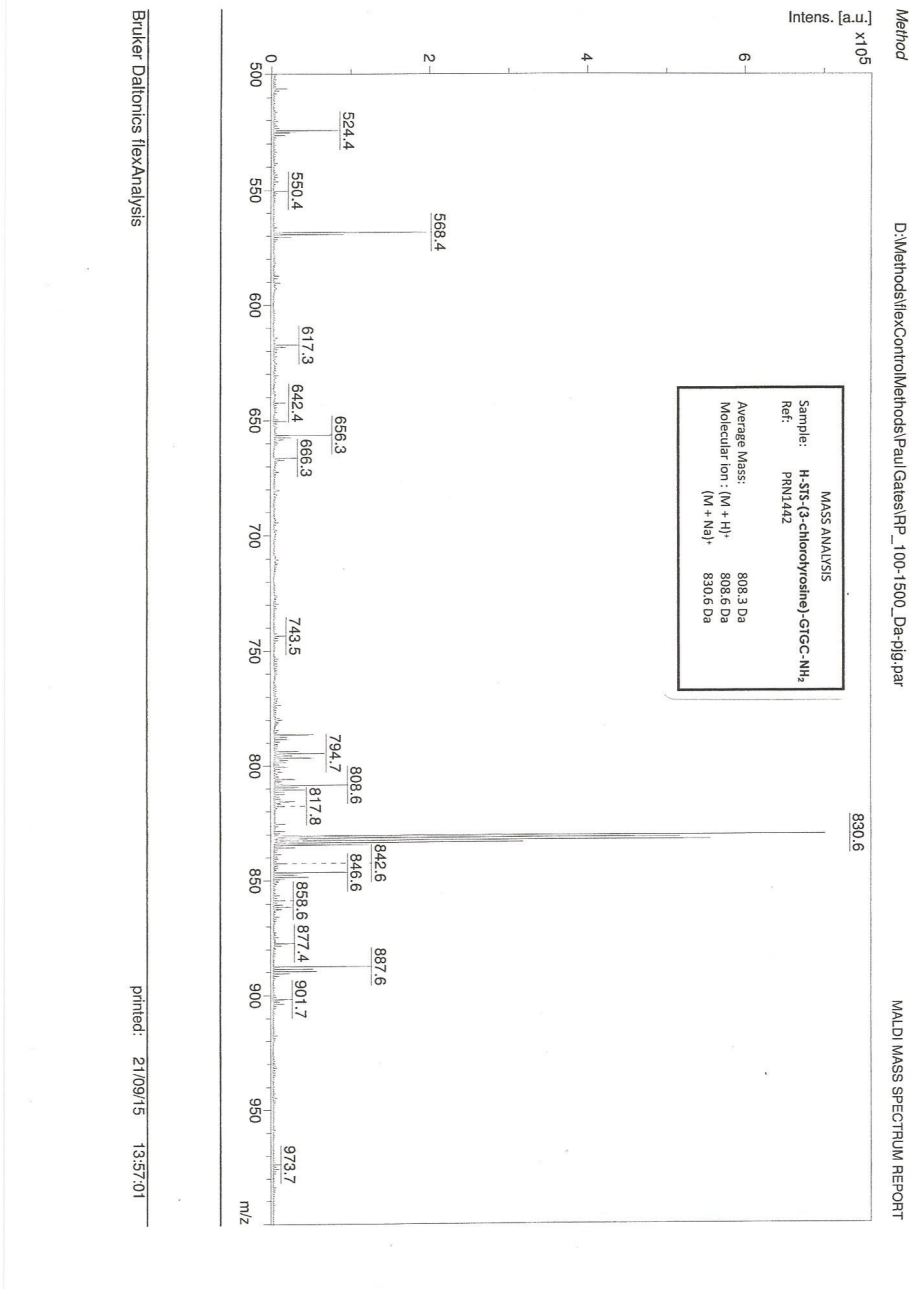

Appendix 1: STSY-(Cl)-GTGC Peptide Synthesis MS Results

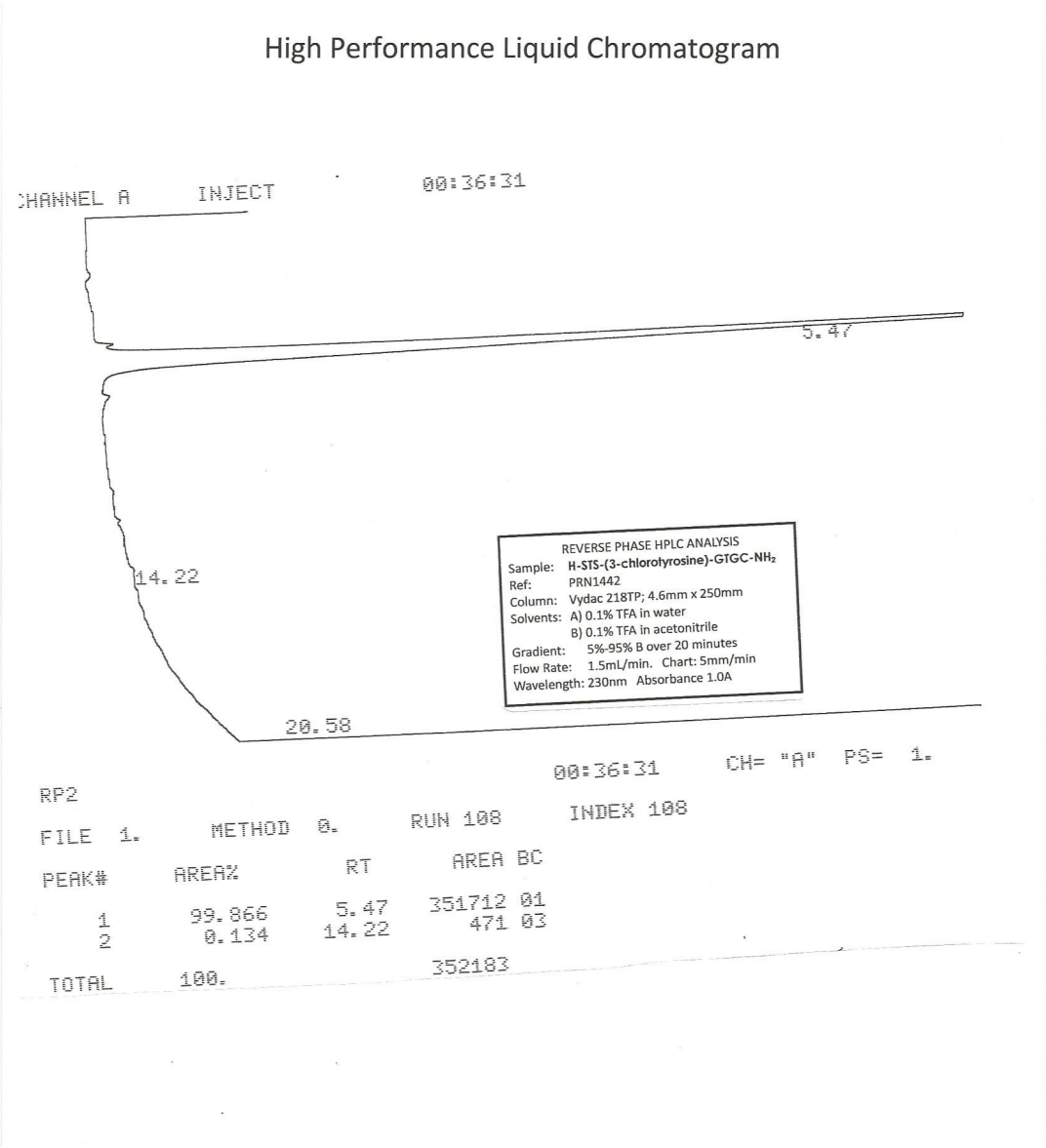

Appendix 2: STSY-(Cl)-GTGC Peptide Purification Results

High Performance Liquid Chromatogram

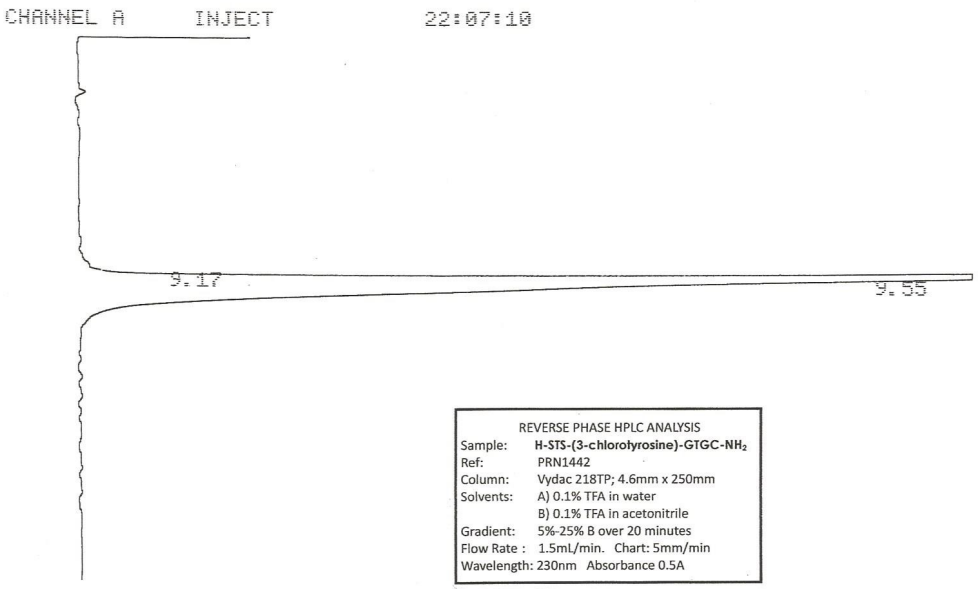

RP2 22:07:10 CH= "A" PS= 1.

FILE 1. METHOD 0. RUN 96 INDEX 96

PEAK#	AREA%	RT	AREA	BC
1	0.276	9.17	1580	02
2	99.724	9.55	571258	03
TOTAL	100.		572838	

Appendix 3: STSY-(Cl)-GTGC Peptide Purification Results

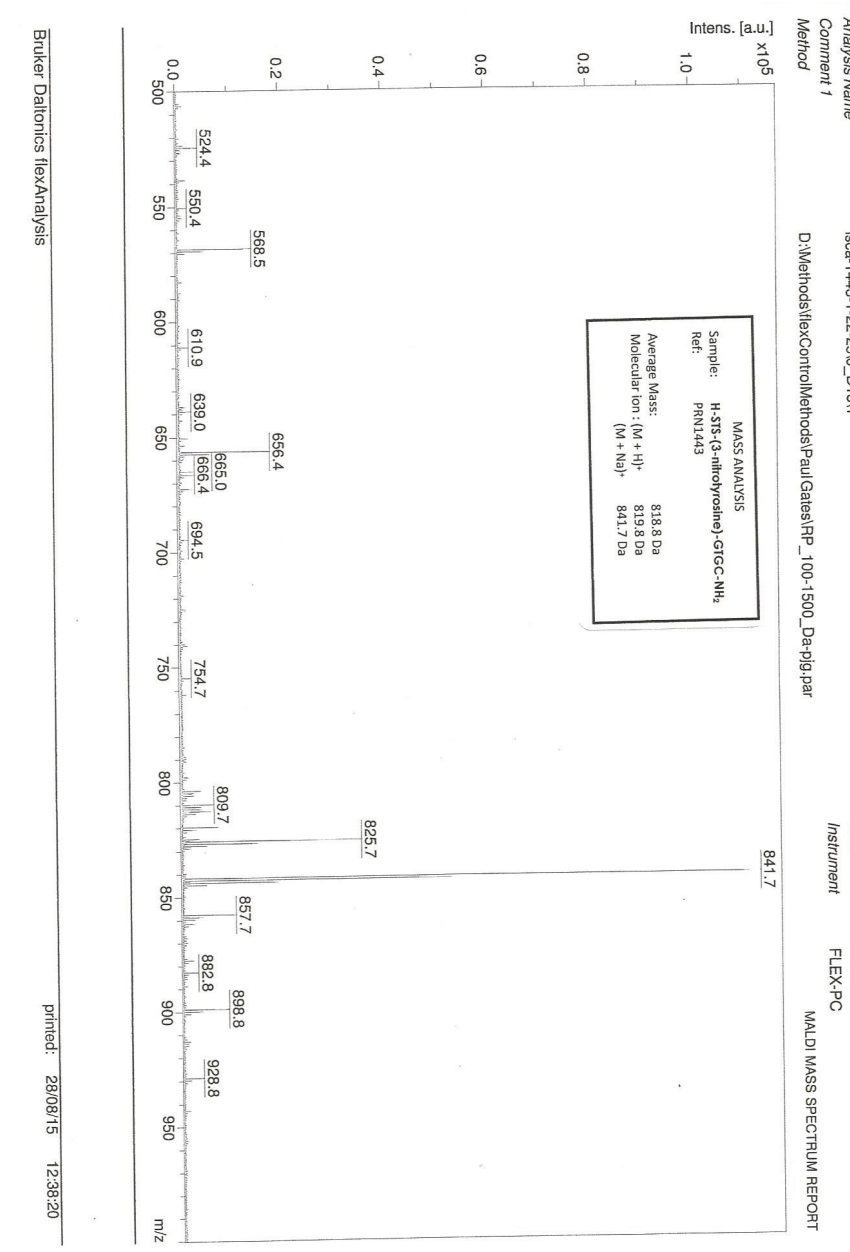

Appendix 4: STSY-(NO_2)-GTGC Peptide Synthesis MS Results

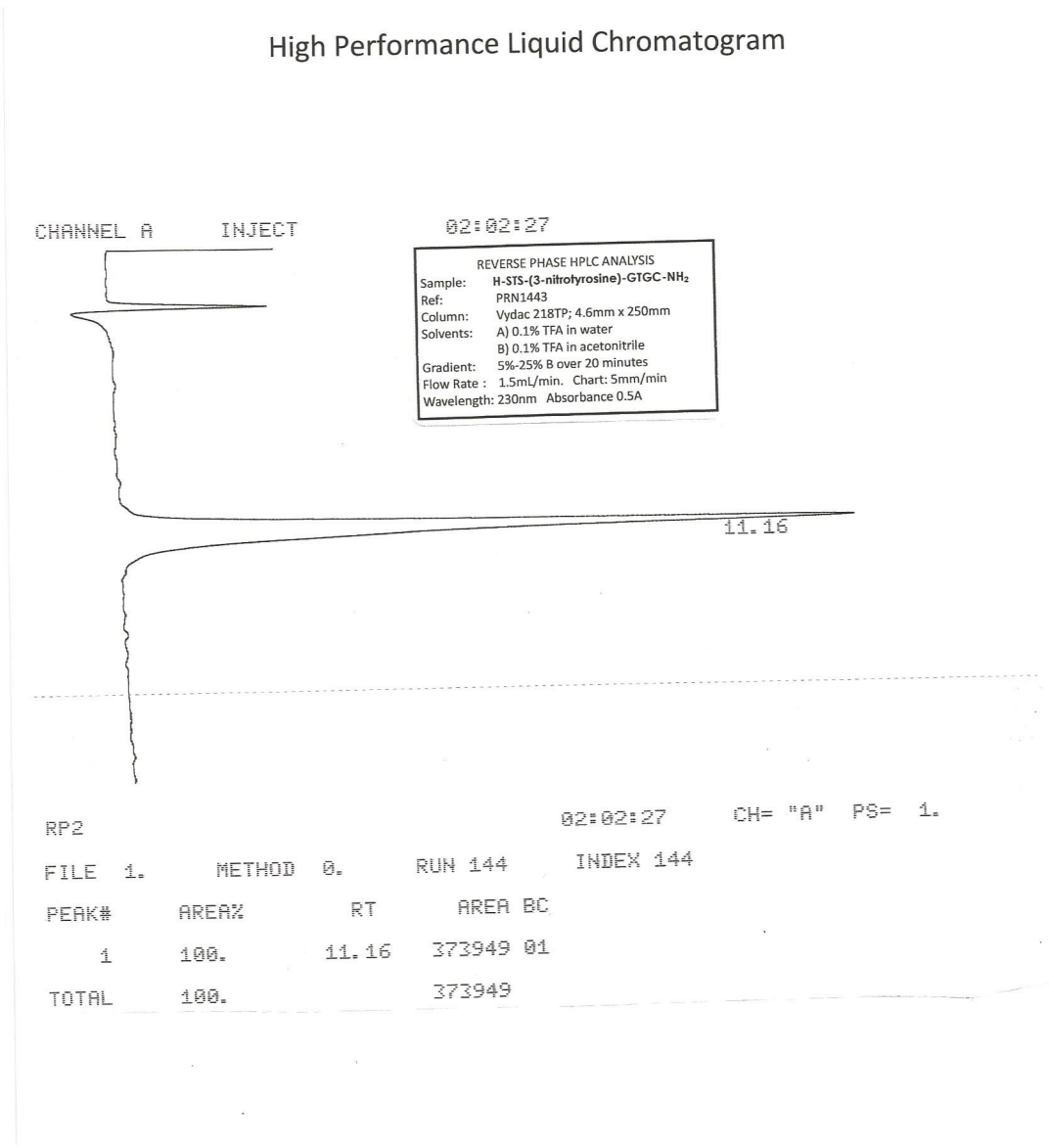

Appendix 5: STSY-(NO_2)-GTGC Peptide Synthesis Purification Results

High Performance Liquid Chromatogram

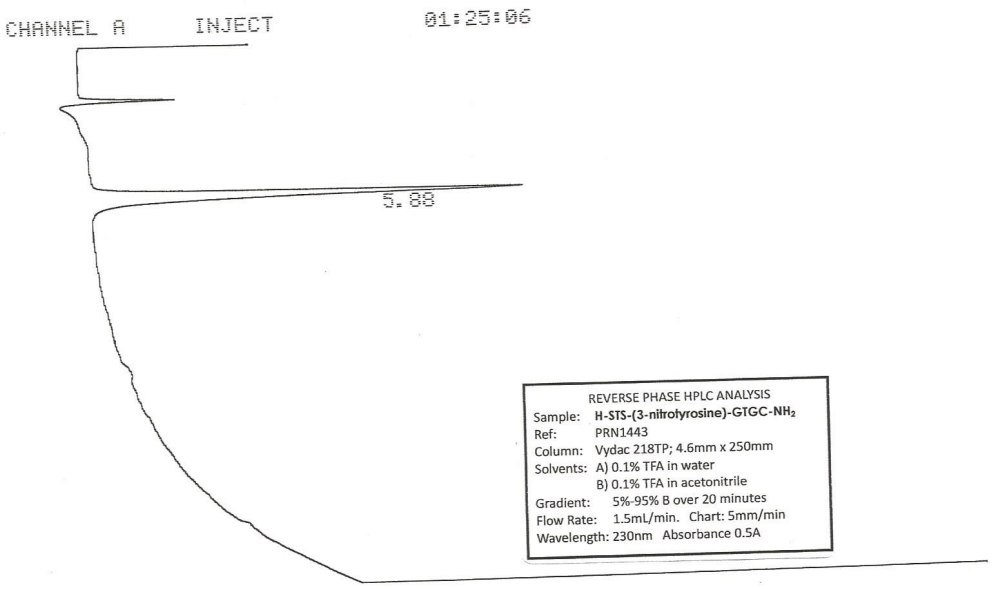

01:25:06 CH= "A" PS= 1.

RP2

FILE 1. METHOD 0. RUN 143 INDEX 143

PEAK#	AREA%	RT	AREA BC
1	100.	5.88	107481 01
TOTAL	100.		107481

Appendix 6: STSY-(NO_2)-GTGC Peptide Synthesis Purification Results

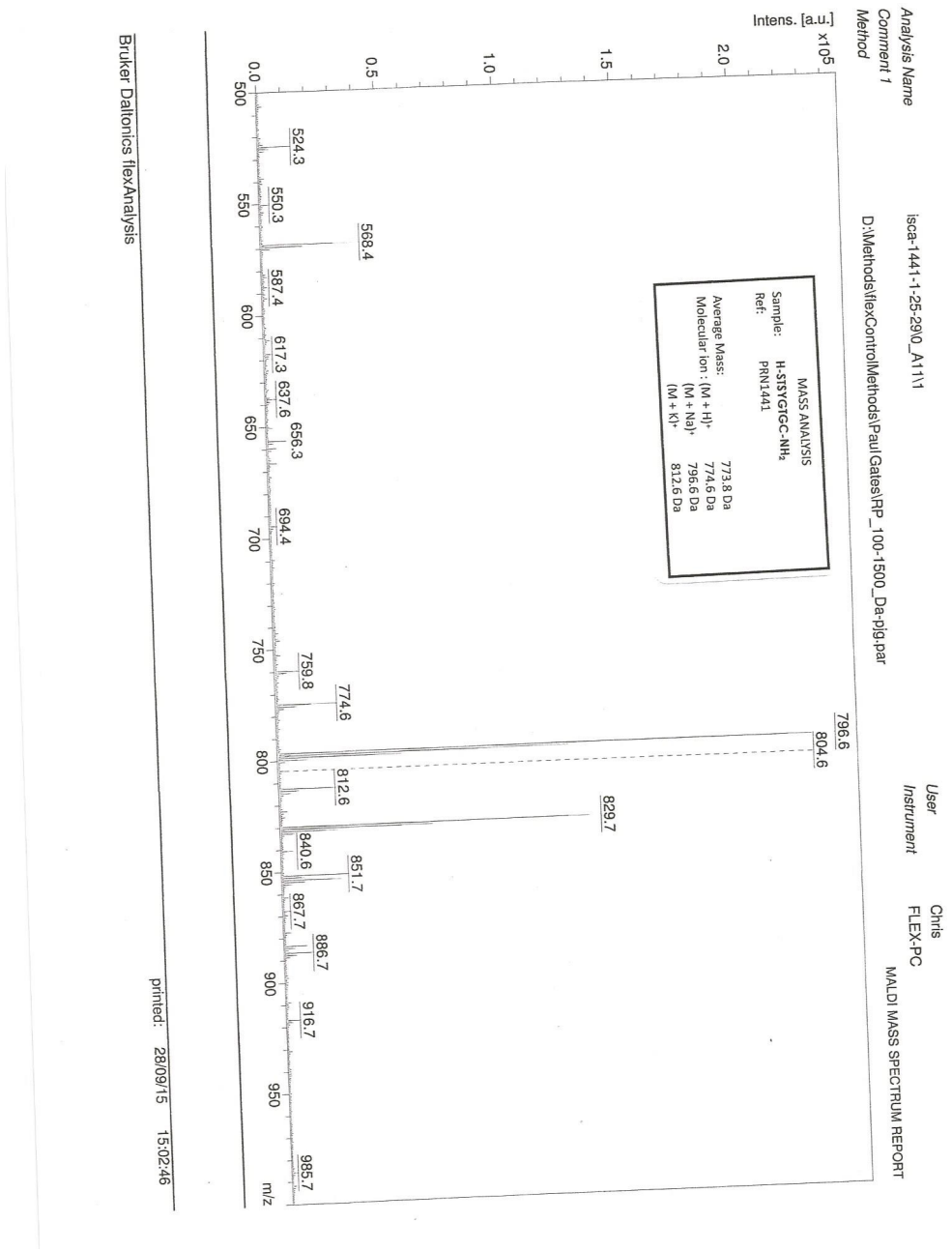

Appendix 7: STSYGTGC Peptide Synthesis MS Results

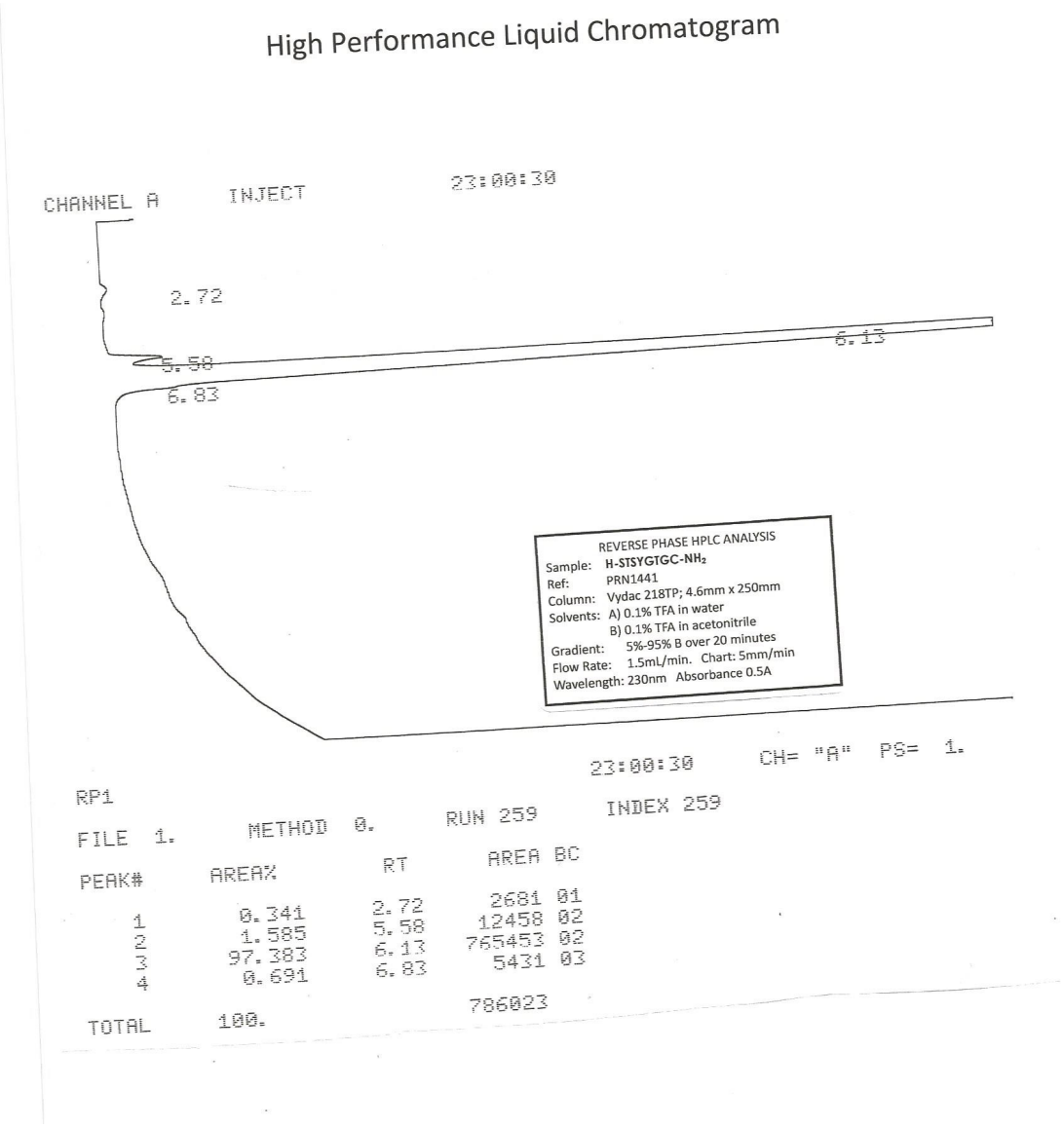

Appendix 8: STSYGTGC Peptide Synthesis Purification Results

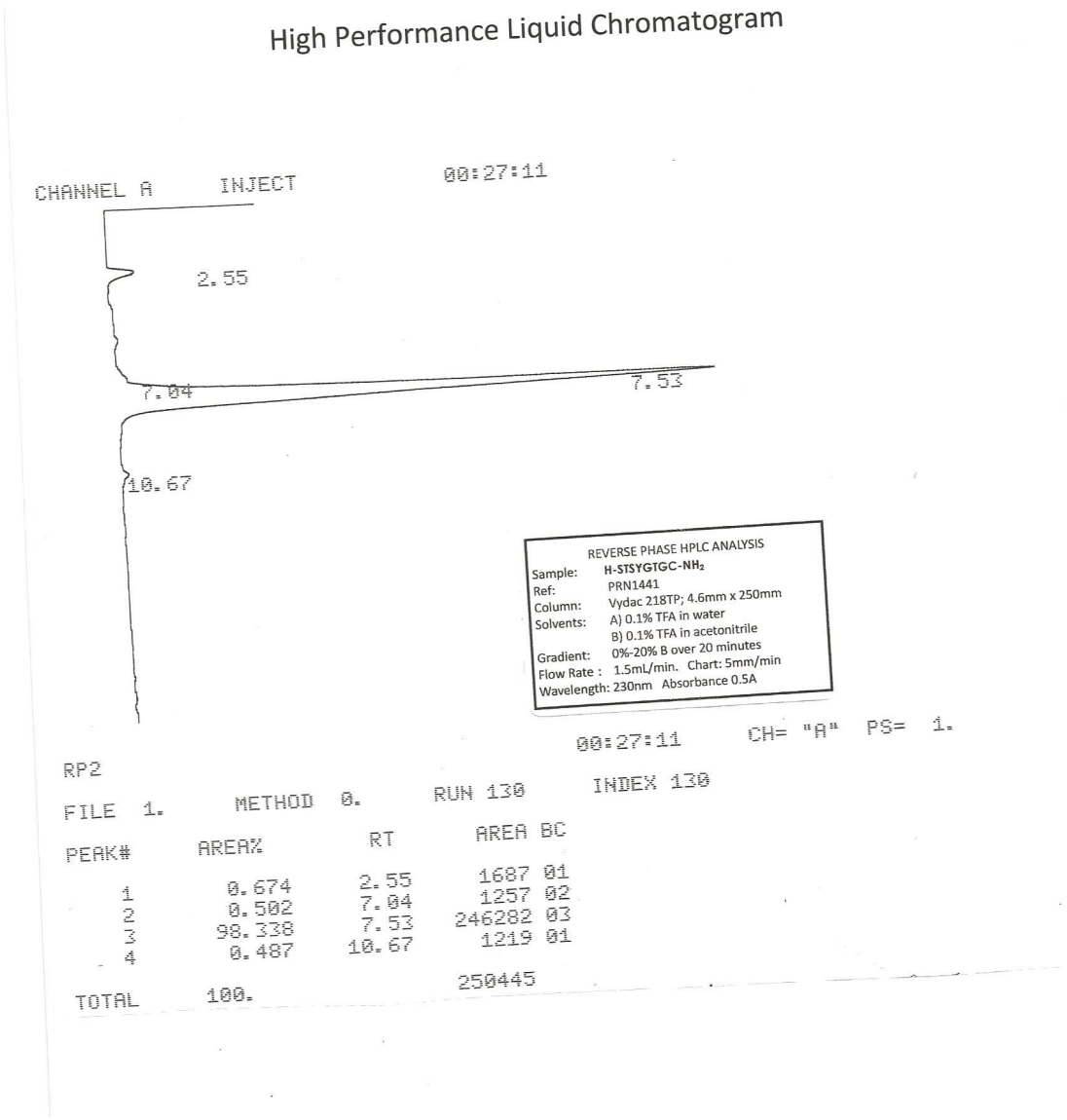

Appendix 9: STSYGTGC Peptide Synthesis Purification Results

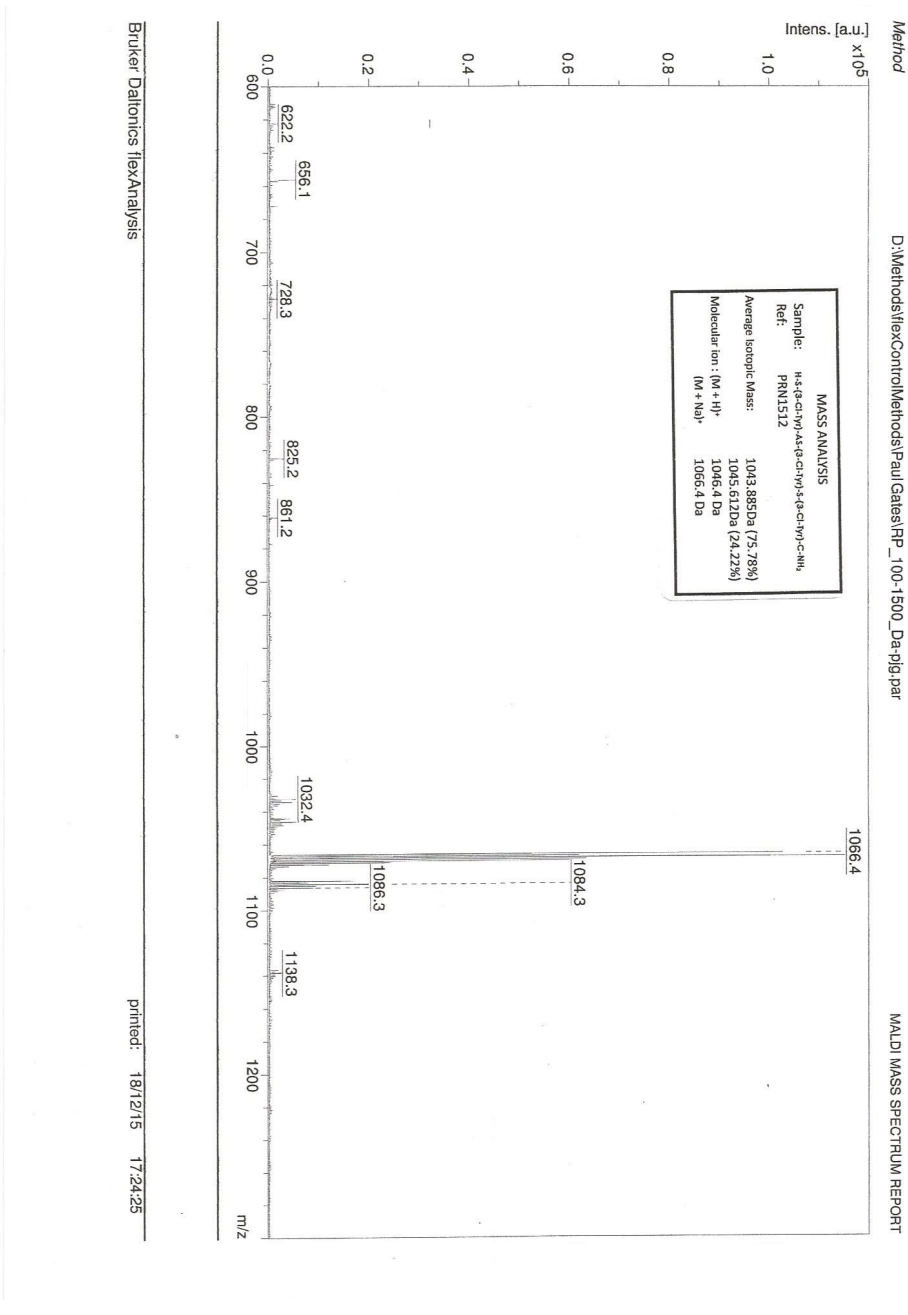

Appendix 10: SY-(Cl)-ASY-(Cl)-SY-(Cl)-C Peptide Synthesis MS Results

High Performance Liquid Chromatogram

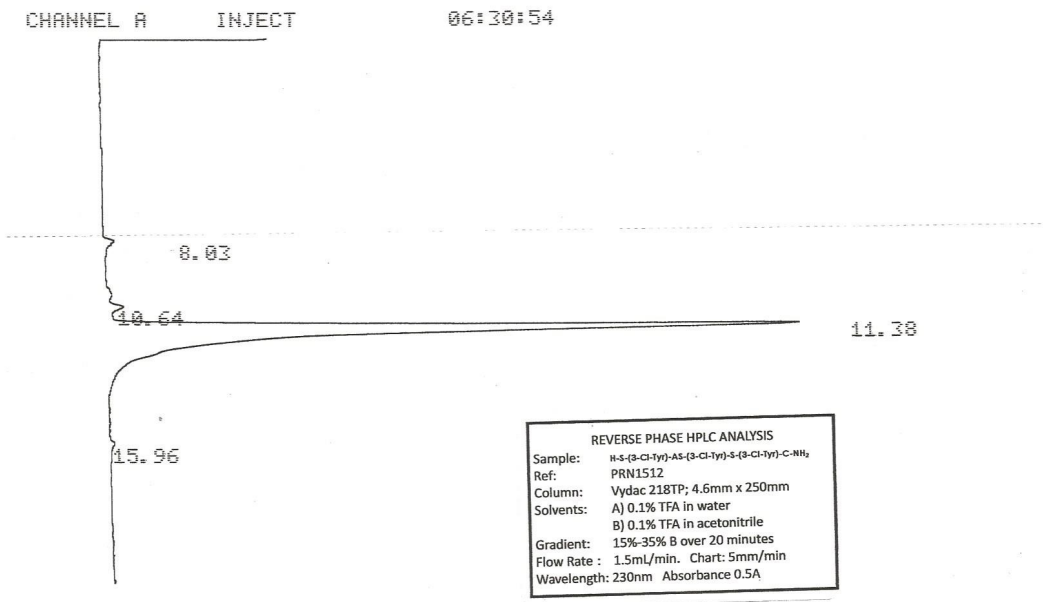

RP2 06:30:54 CH= "A" PS= 1.

FILE 1. METHOD 0. RUN 347 INDEX 347

PEAK#	AREA%	RT	AREA	BC
1	0.866	8.03	2280	01
2	1.039	10.64	2735	01
3	97.755	11.38	257313	01
4	0.34	15.96	894	01
TOTAL	100.		263222	

Appendix 11: SY-(Cl)-ASY-(Cl)-SY-(Cl)-C Peptide Synthesis Purification Results

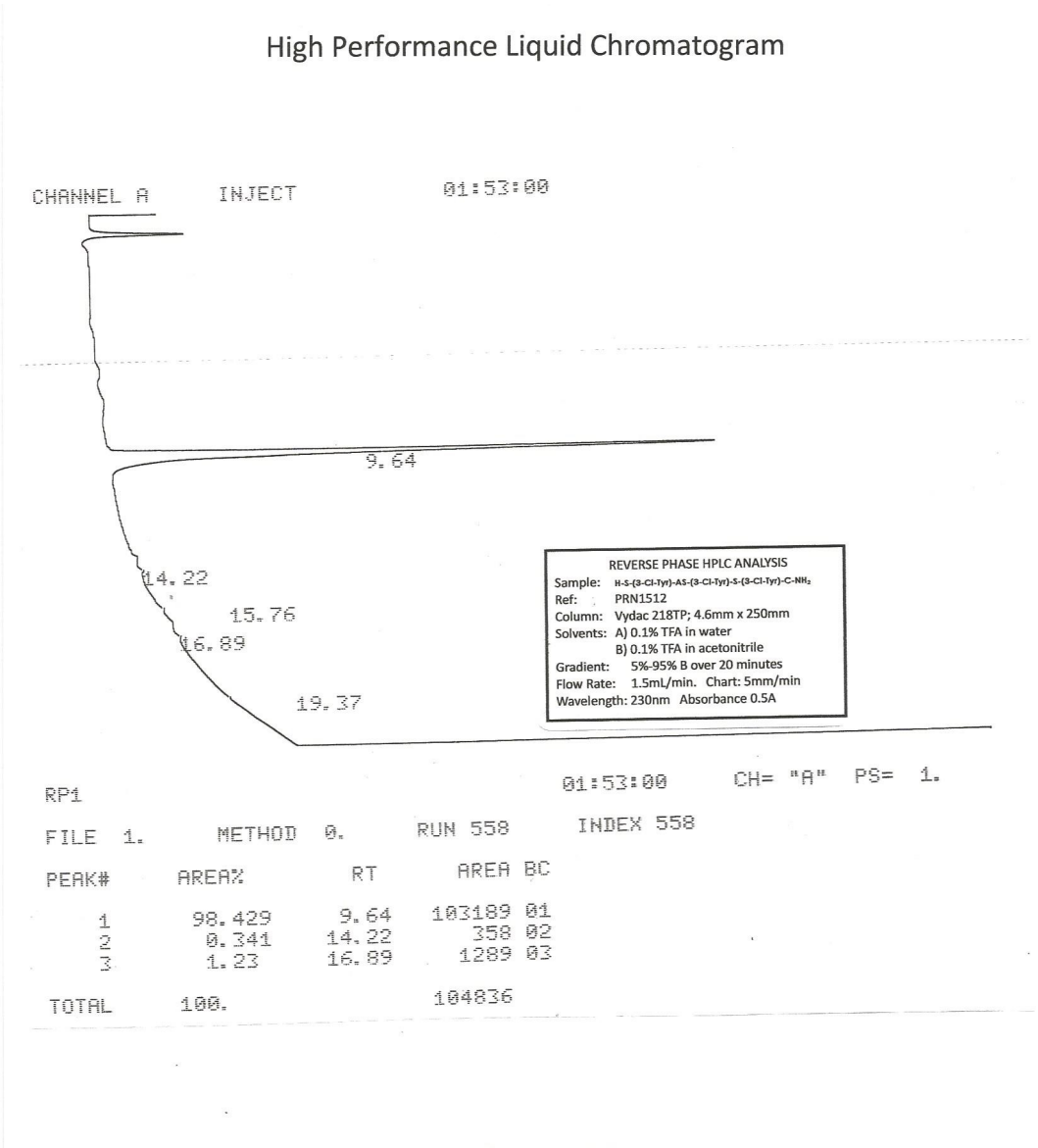

Appendix 12: SY-(Cl)-ASY-(Cl)-SY-(Cl)-C Peptide Synthesis Purification Results

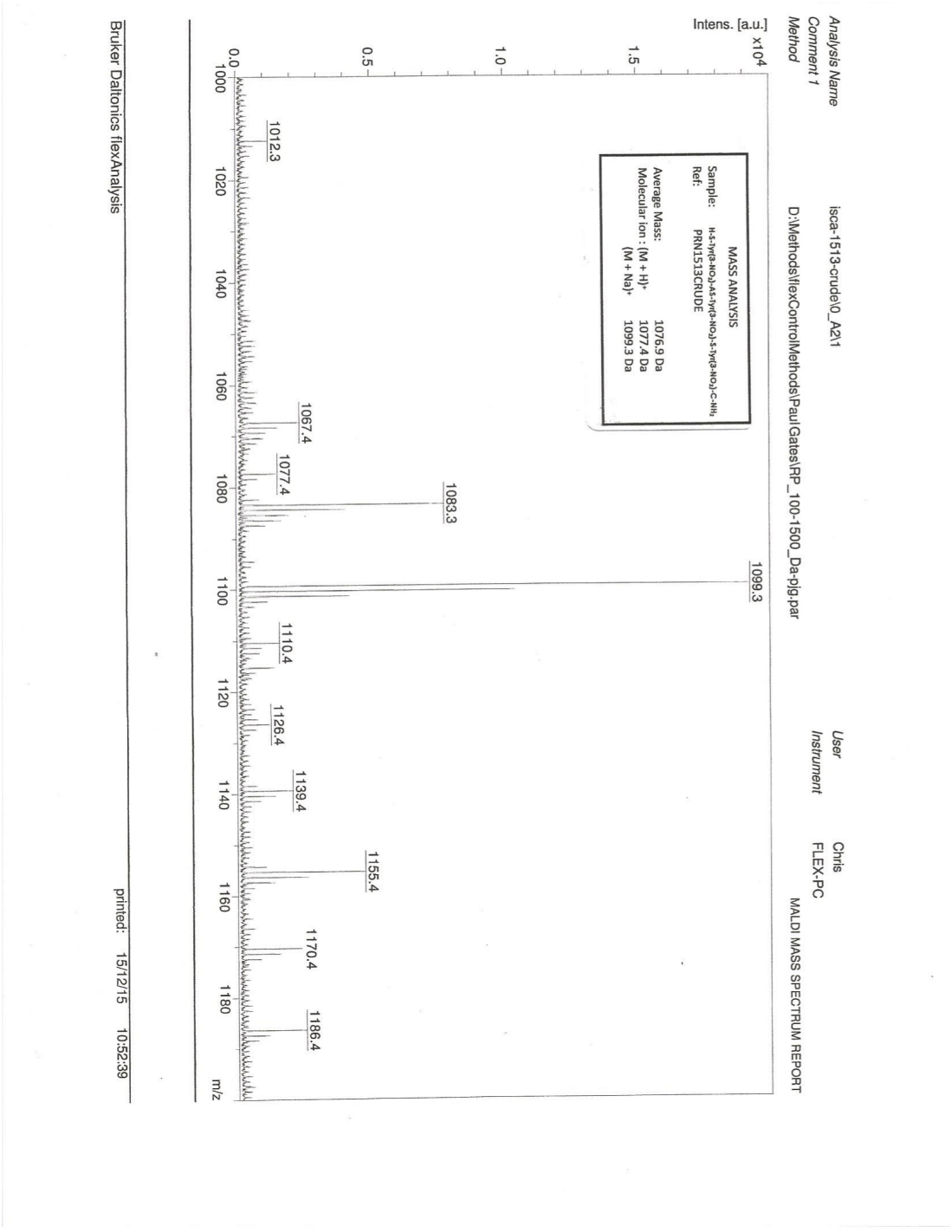

Appendix 13: SY-(Cl)-ASY-(Cl)-SY-(Cl)-C Peptide Synthesis MS Results

High Performance Liquid Chromatogram

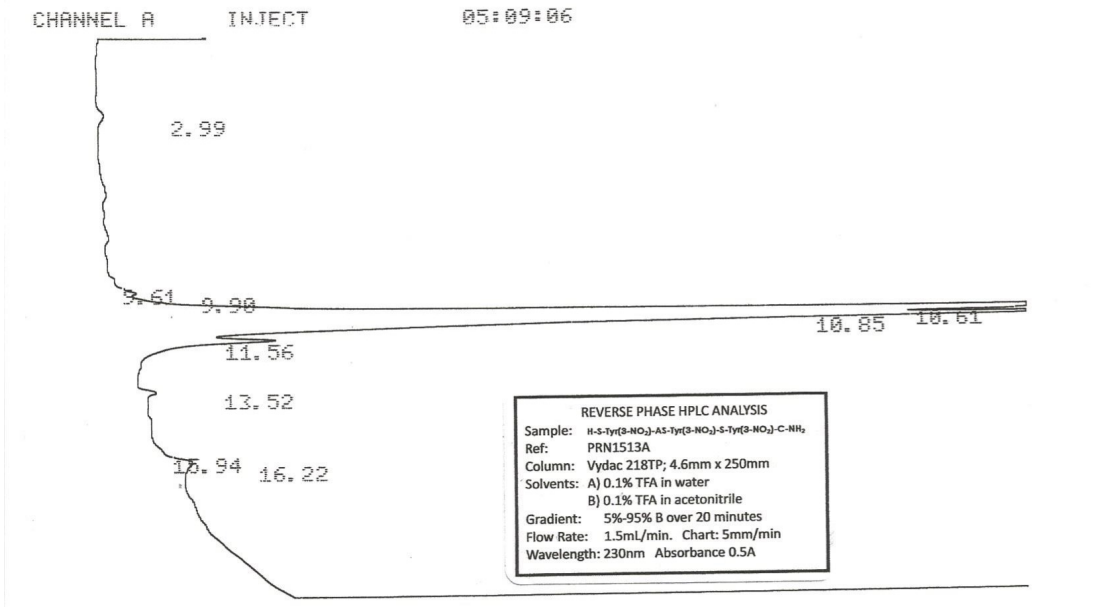

RP1 05:09:06 CH= "A" PS= 1.

FILE 1. METHOD 0. RUN 530 INDEX 530

PEAK#	AREA%	RT	AREA	BC
1	0.247	2.99	1667	01
2	0.159	9.61	1078	02
3	0.747	9.9	5051	02
4	51.24	10.61	346490	02
5	39.779	10.85	268987	02
6	6.648	11.56	44955	03
7	0.443	13.52	2993	01
8	0.016	15.94	107	02
9	0.722	16.22	4879	03
TOTAL	100.		676207	

05:38:13

Appendix 14: SY-(NO_2)-ASY-(NO_2)-SY-(NO_2)-C Peptide Synthesis Purification Results

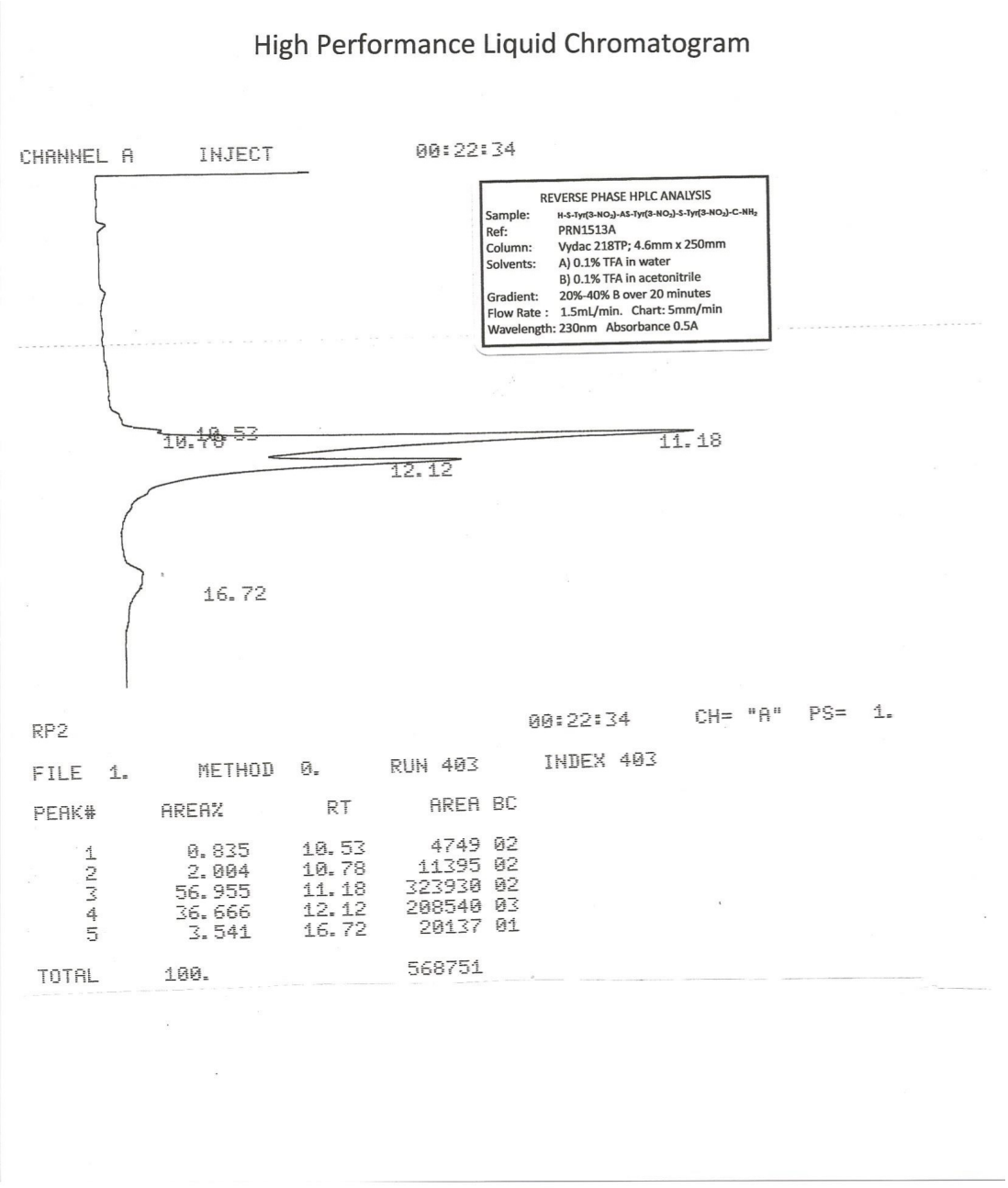

Appendix 15: SY-(NO_2)-ASY-(NO_2)-SY-(NO_2)-C Peptide Synthesis Purification Results

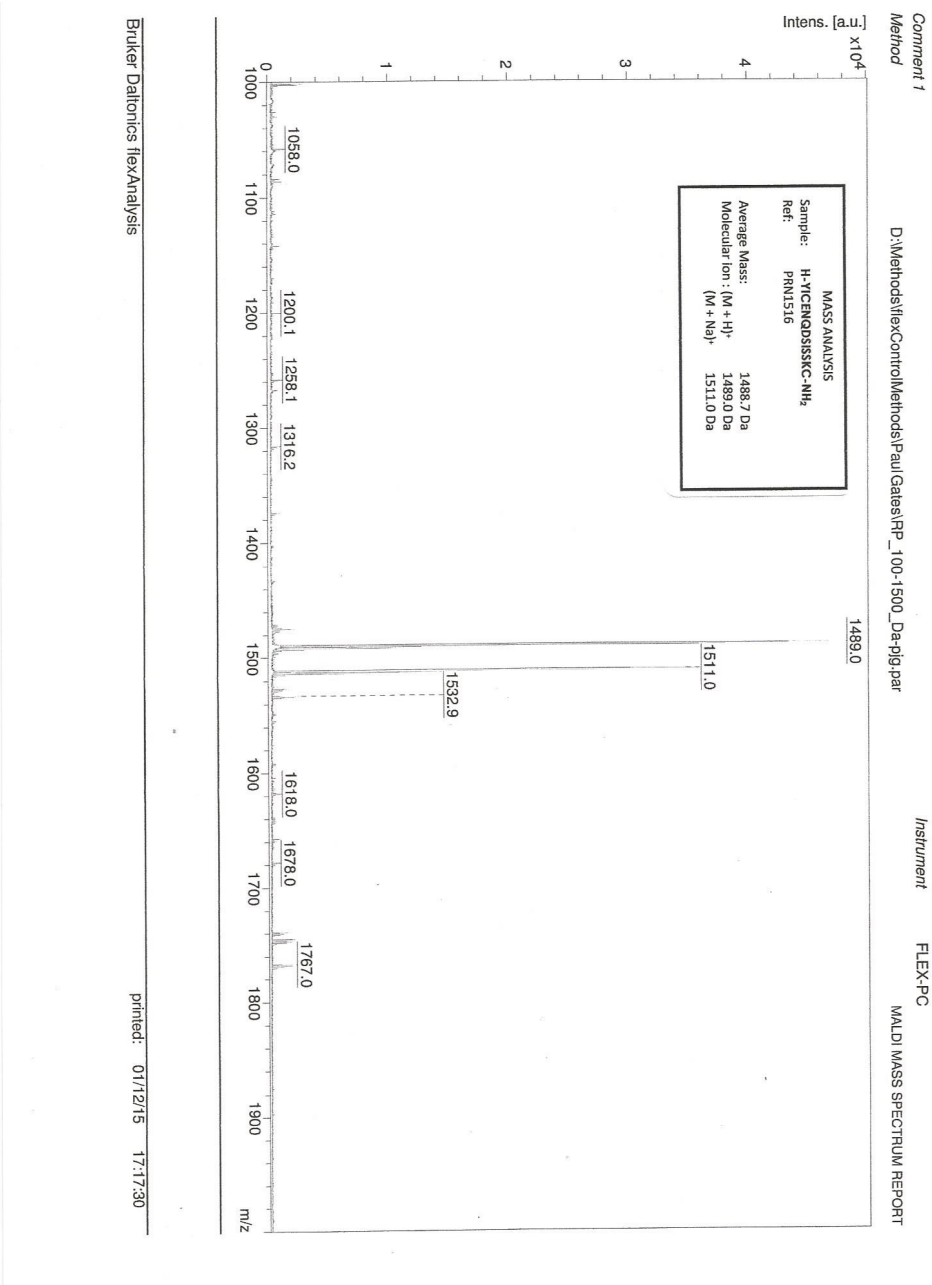

Appendix 16: YICEQDSISSKC Peptide Synthesis MS Results

High Performance Liquid Chromatogram

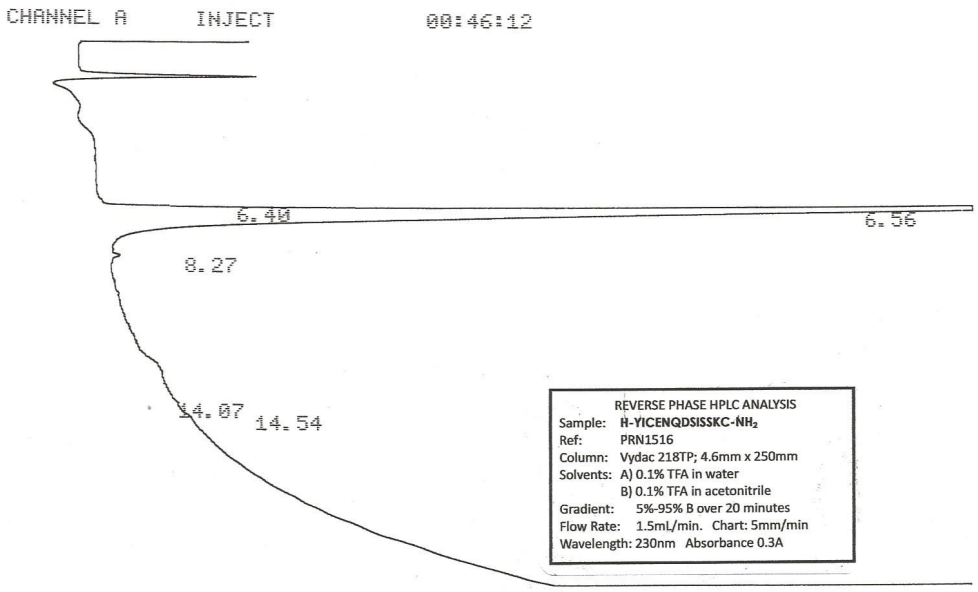

RP2 00:46:12 CH= "A" PS= 1.

FILE 1. METHOD 0. RUN 381 INDEX 381

PEAK#	AREA%	RT	AREA	BC
1	0.09	6.4	351	02
2	99.673	6.56	387185	03
3	0.237	8.27	919	01
TOTAL	100.		388455	

Appendix 17: YICEQDSISSKC Peptide Synthesis Purification Results

High Performance Liquid Chromatogram

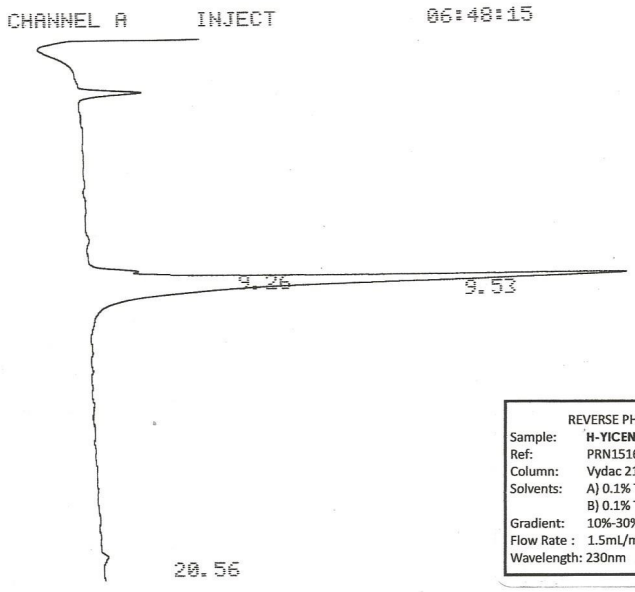

RP2 06:48:15 CH= "A" PS= 1.

FILE 1. METHOD 0. RUN 358 INDEX 358

PEAK#	AREA%	RT	AREA BC
1	3.578	9.26	7690 02
2	95.697	9.53	205670 03
3	0.724	20.56	1557 01
TOTAL	100.		214917

Appendix 18: YICEQDSISSKC Peptide Synthesis Purification Results

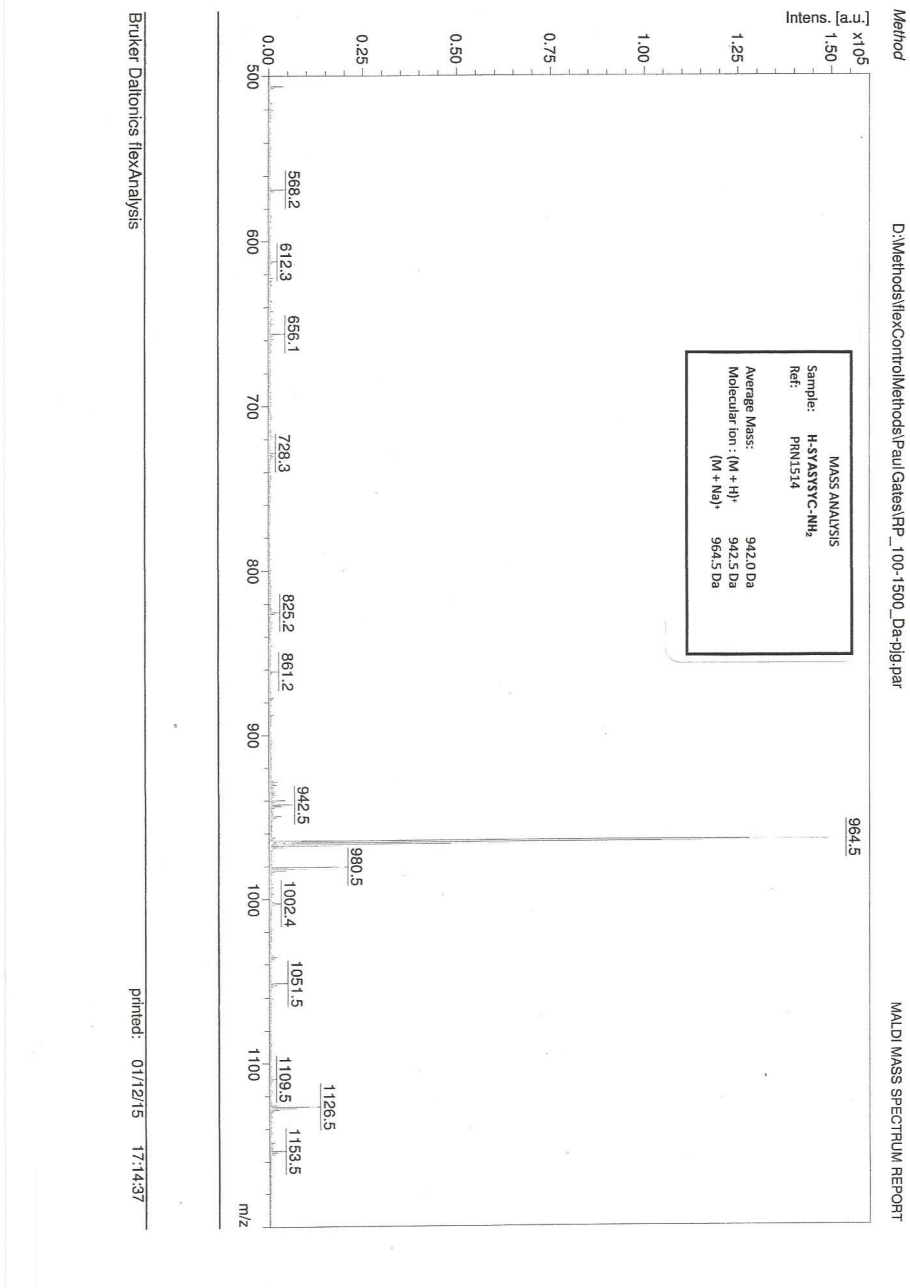

Appendix 19: SYASYSYC Peptide Synthesis MS Results

High Performance Liquid Chromatogram

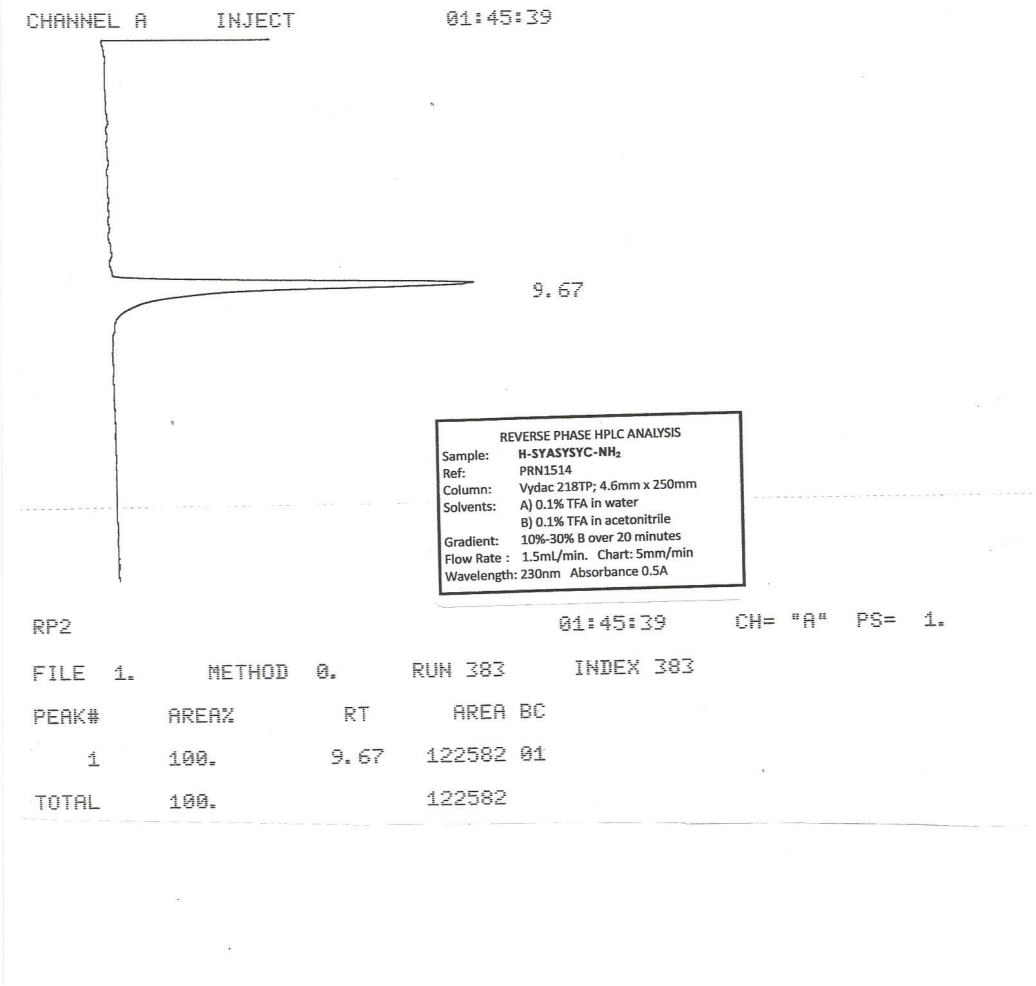

Appendix 20: SYASYSYC Peptide Synthesis Purification Results

High Performance Liquid Chromatogram

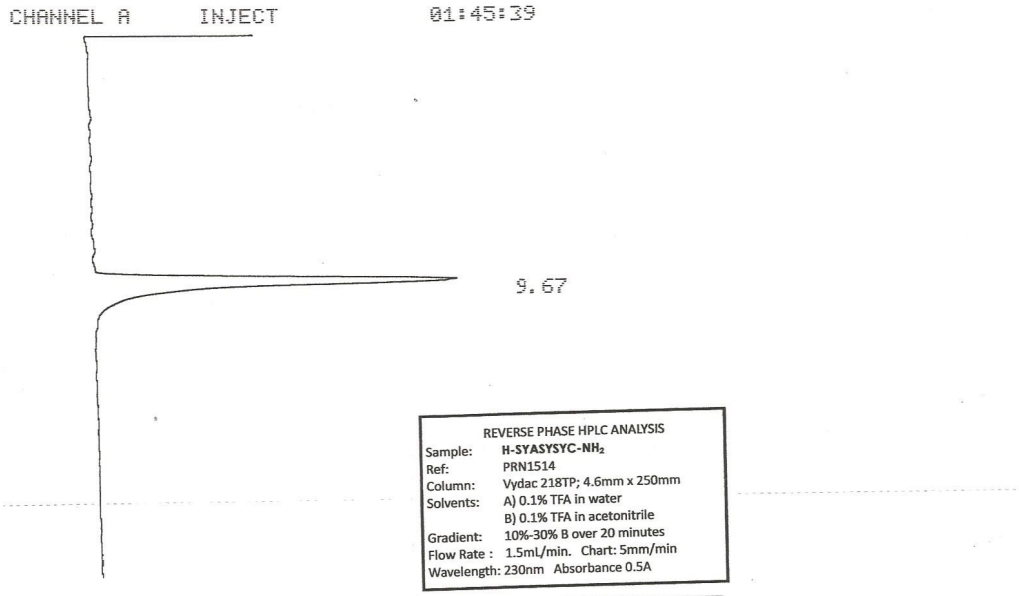

RP2 01:45:39 CH= "A" PS= 1.

FILE 1. METHOD 0. RUN 383 INDEX 383

PEAK#	AREA%	RT	AREA	BC
1	100.	9.67	122582	01
TOTAL	100.		122582	

Appendix 21: SYASYSYC Peptide Synthesis Purification Results

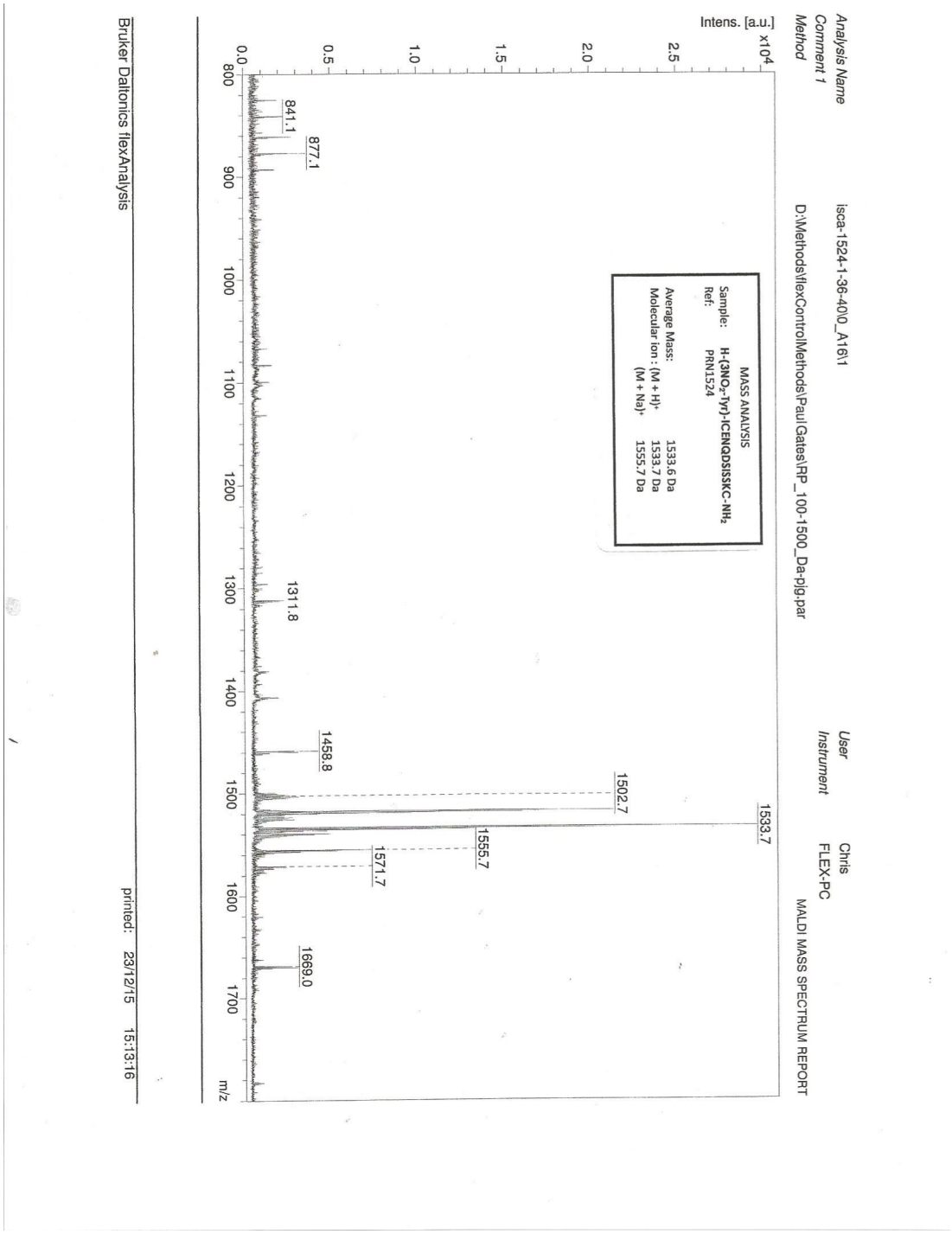

Appendix 22: Y-(NO_2)-ICEQDSISSKC Peptide Synthesis MS Results

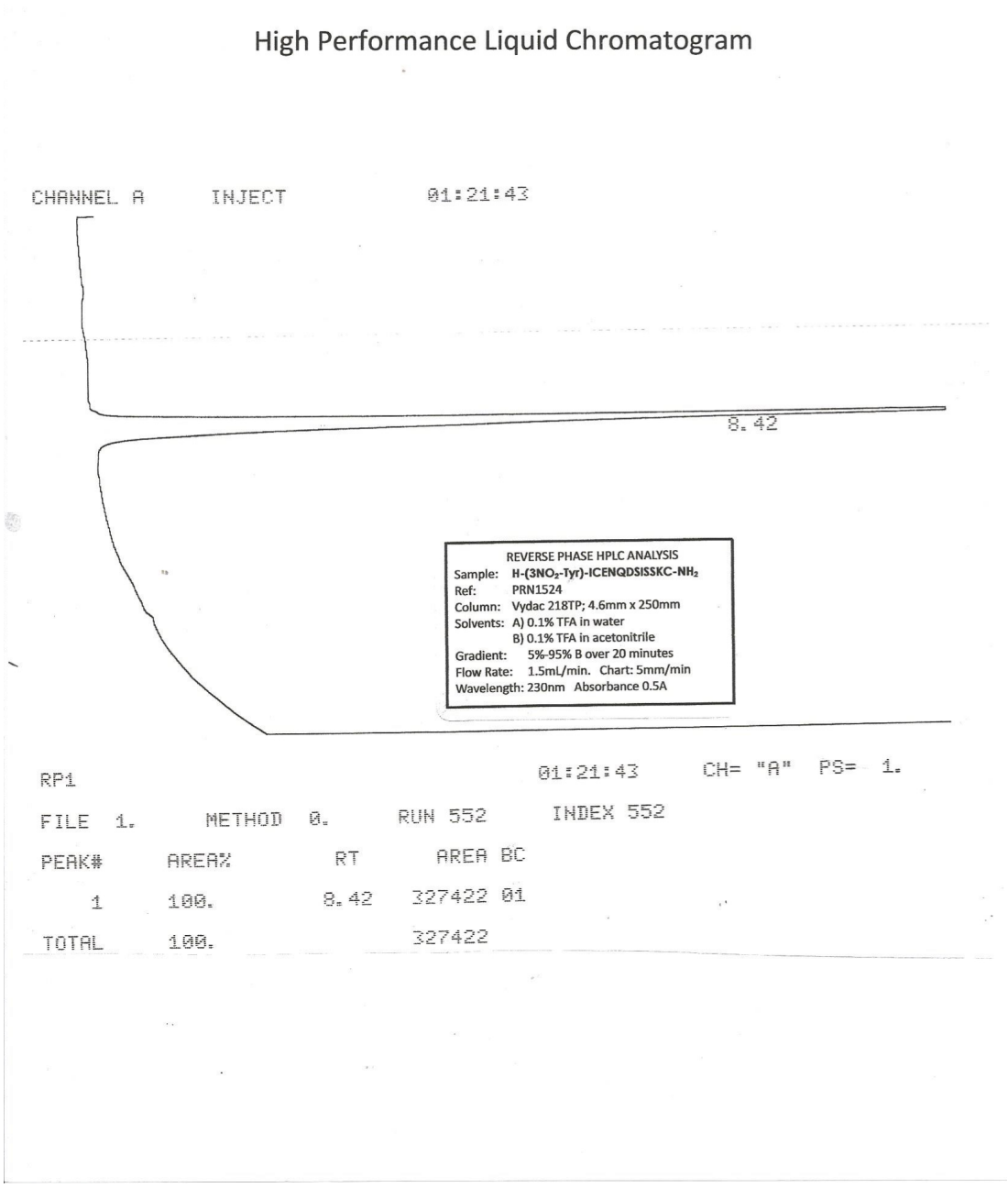

Appendix 23: Y-(NO_2)-ICEQDSISSKC Peptide Synthesis Purification Results

High Performance Liquid Chromatogram

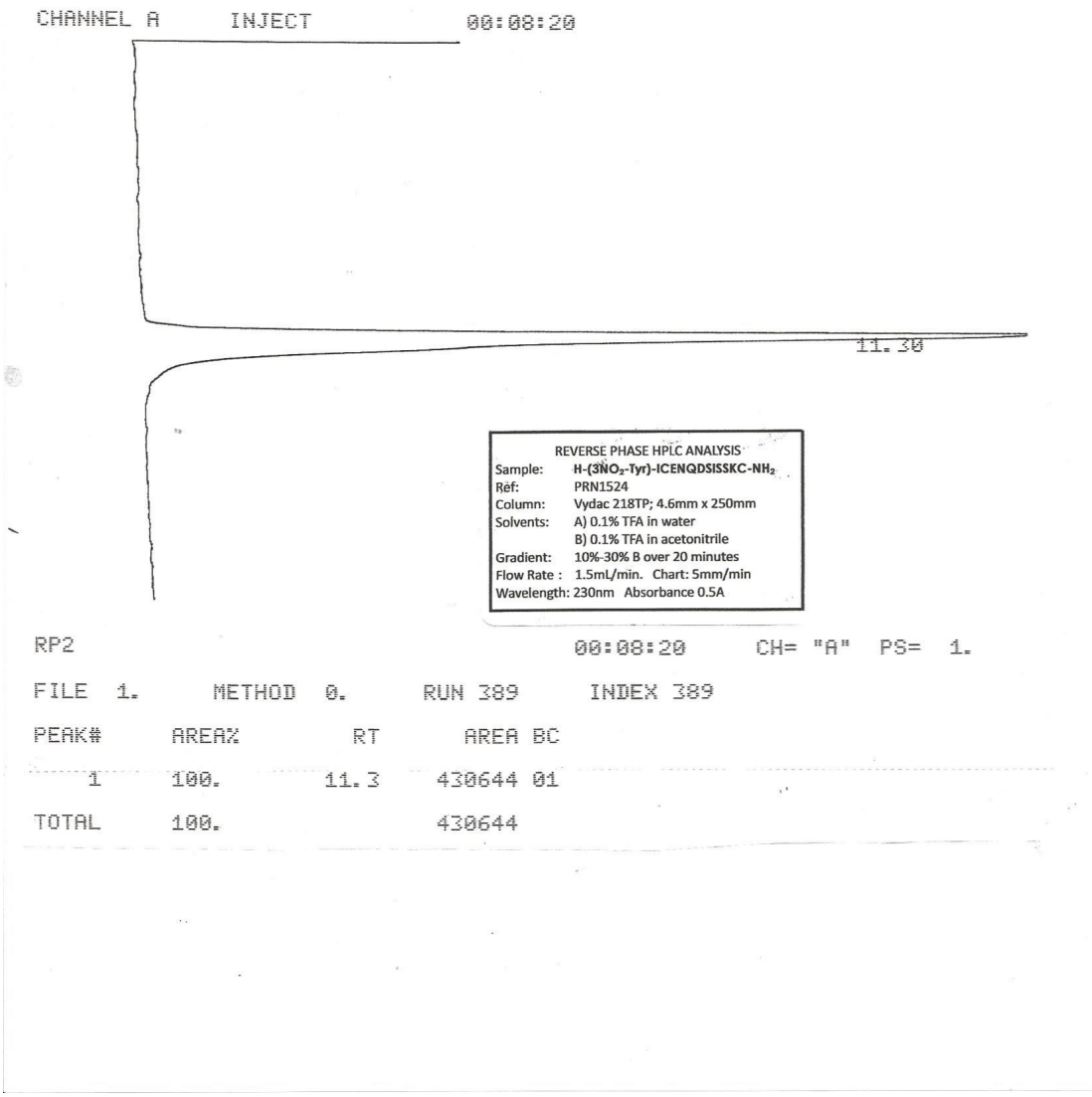

Appendix 24: Y-(NO_2)-ICEQDSISSKC Peptide Synthesis Purification Results

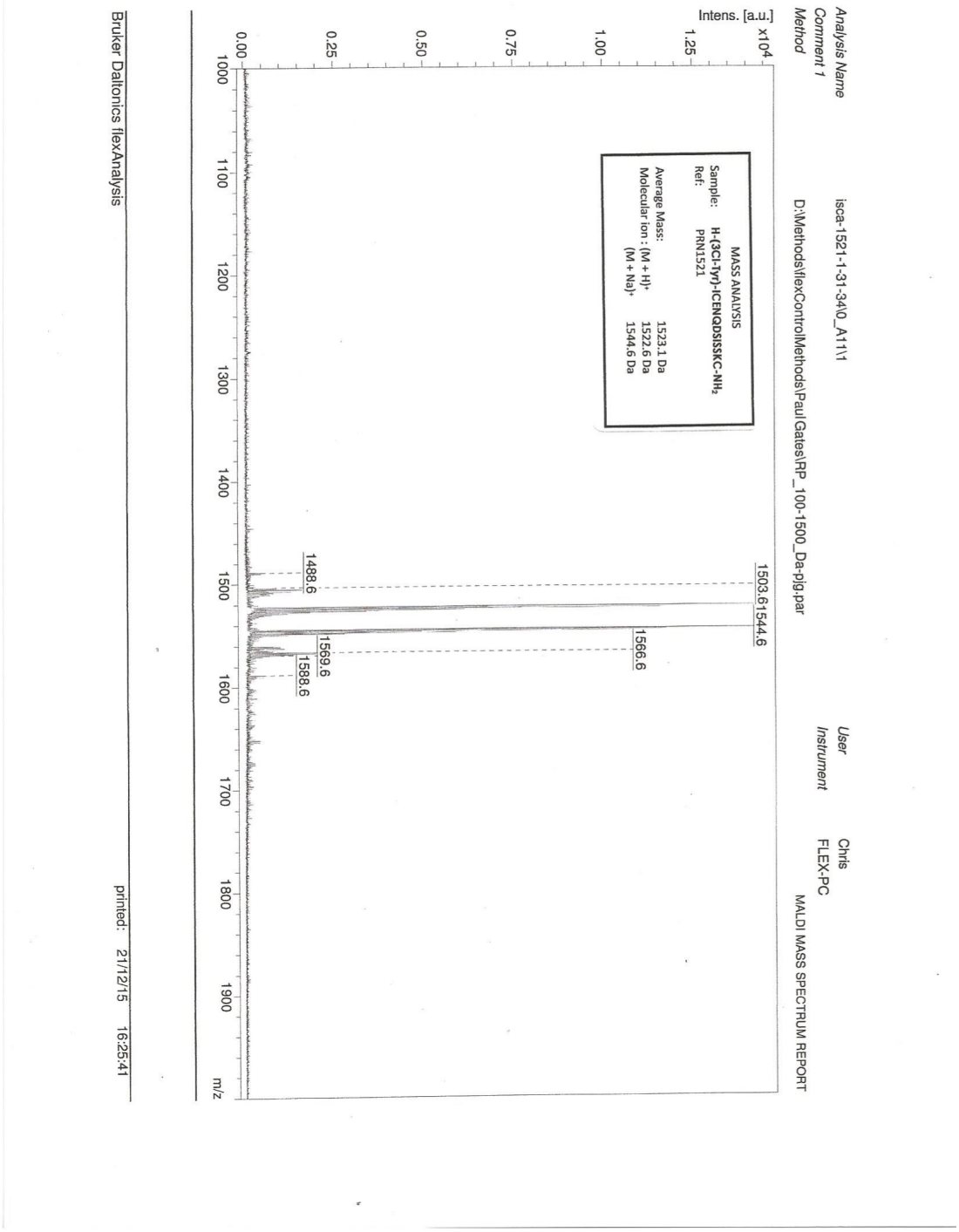

Appendix 25: Y-(Cl)-ICEQDSISSKC Peptide Synthesis MS Results

High Performance Liquid Chromatogram

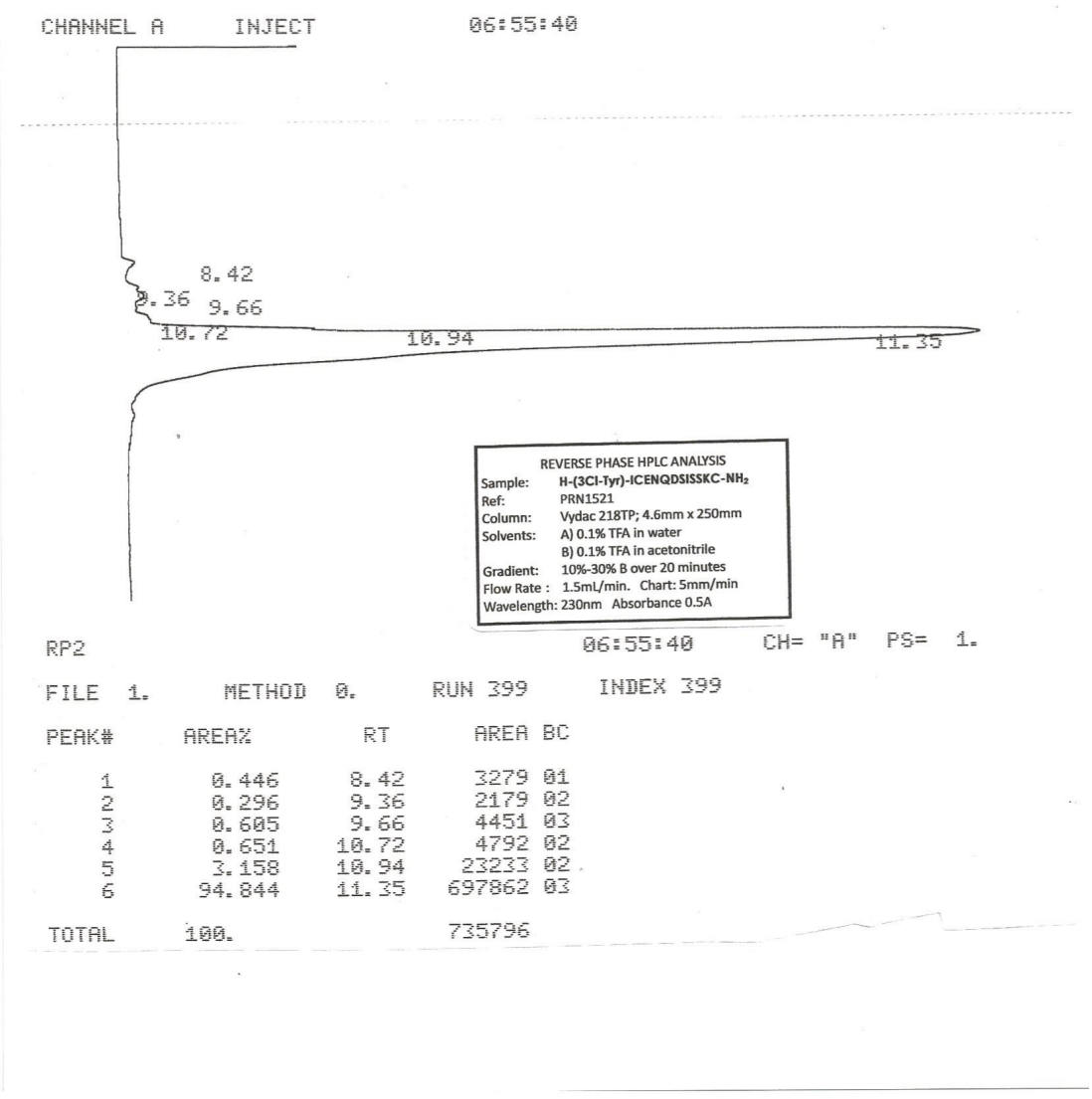

PEAK#	AREA%	RT	AREA	BC
1	0.446	8.42	3279	01
2	0.296	9.36	2179	02
3	0.605	9.66	4451	03
4	0.651	10.72	4792	02
5	3.158	10.94	23233	02
6	94.844	11.35	697862	03
TOTAL	100.		735796	

ppendix 26: Y-(Cl)-ICEQDSISSKC Peptide Synthesis Purification Results

High Performance Liquid Chromatogram

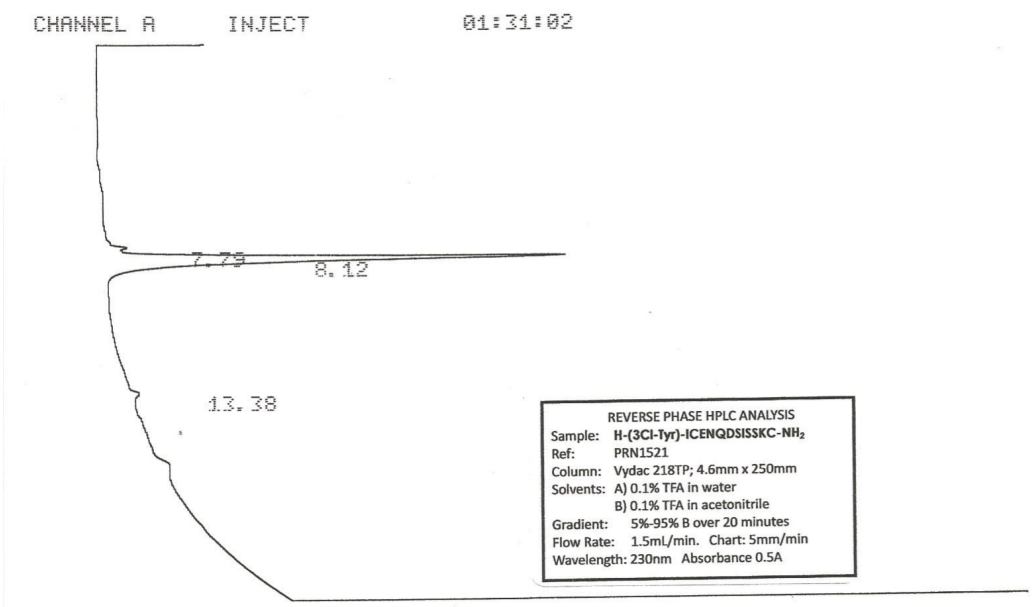

RP1 01:31:02 CH= "A" PS= 1.

FILE 1. METHOD 0. RUN 527 INDEX 527

PEAK#	AREA%	RT	AREA	BC
1	3.255	7.79	3492	02
2	95.531	8.12	102489	03
3	1.214	13.38	1302	01
TOTAL	100.		107283	

Appendix 27: Y-(Cl)-ICEQDSISSKC Peptide Synthesis Purification Results

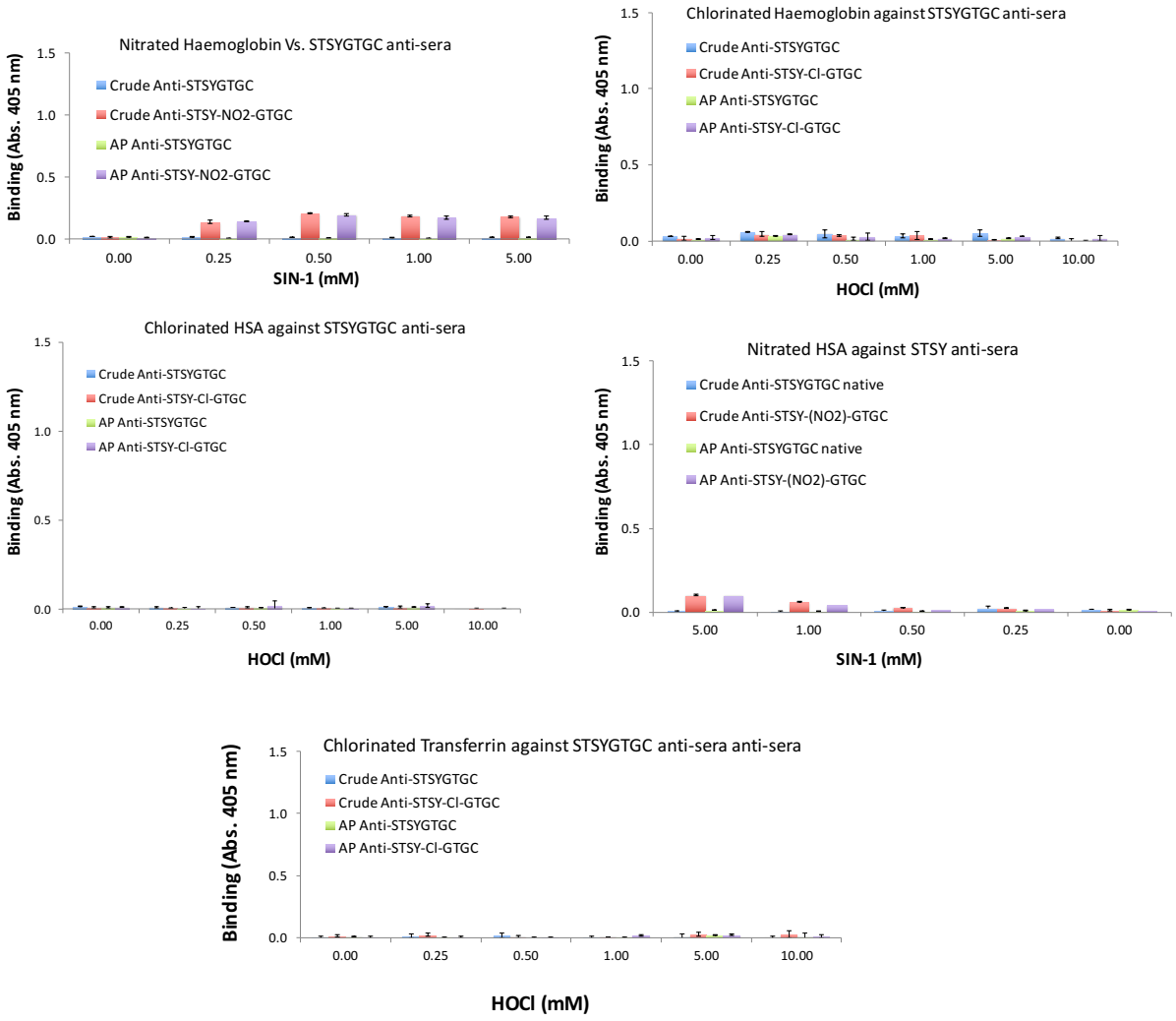

Appendix 28: ELISA of Chlorinated and Nitrated Haemoglobin and HSA

A

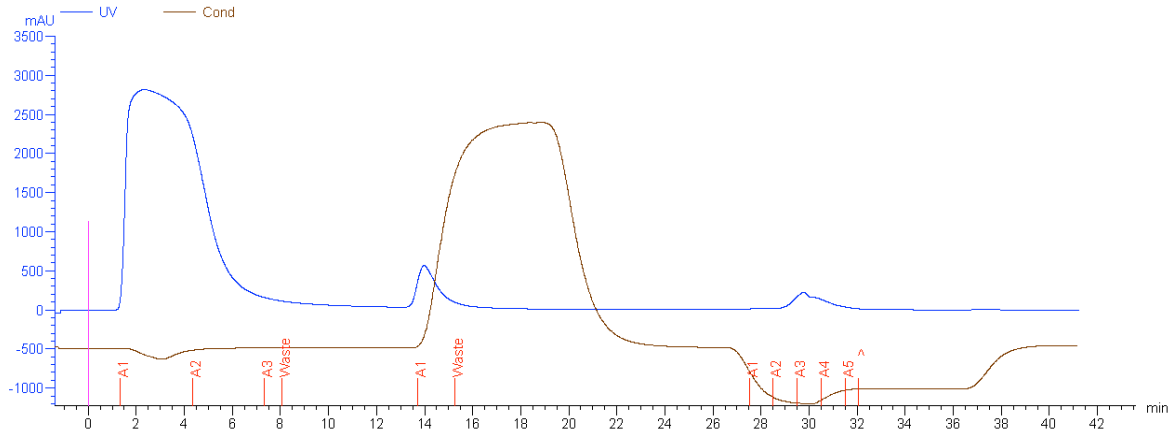

B

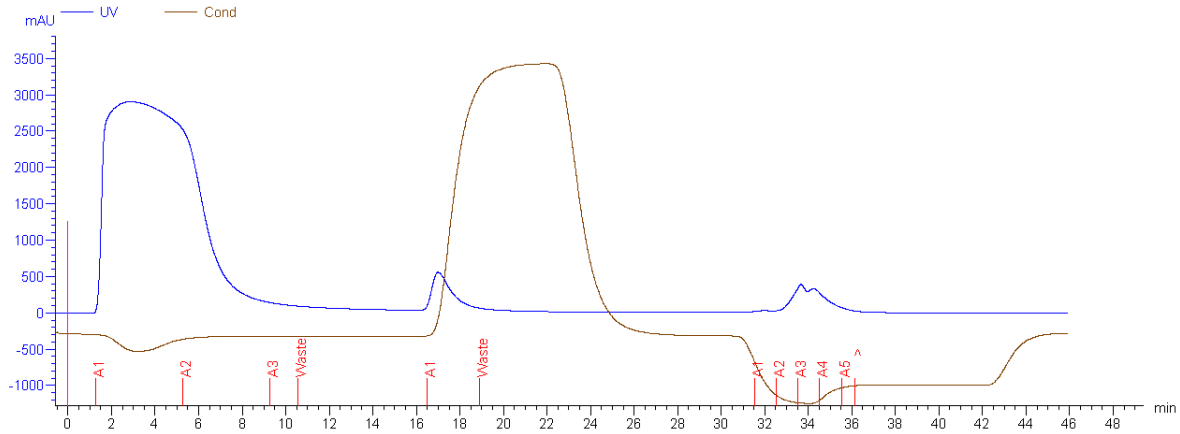

Appendix 29: Anti-STSYGTGC Serum Affinity Purification/enrichment. (A) Column: Native STSTYGTGC peptide bound to Iodoacetyl gel bead. Serum Loaded: Native STSYGTGC (month 3) serum, 1mL was loaded onto the column. (B) Column: Native STSTYGTGC peptide bound to Iodoacetyl gel bead Serum Loaded: Native STSYGTGC (month 3) serum, 2mL was loaded onto the column.

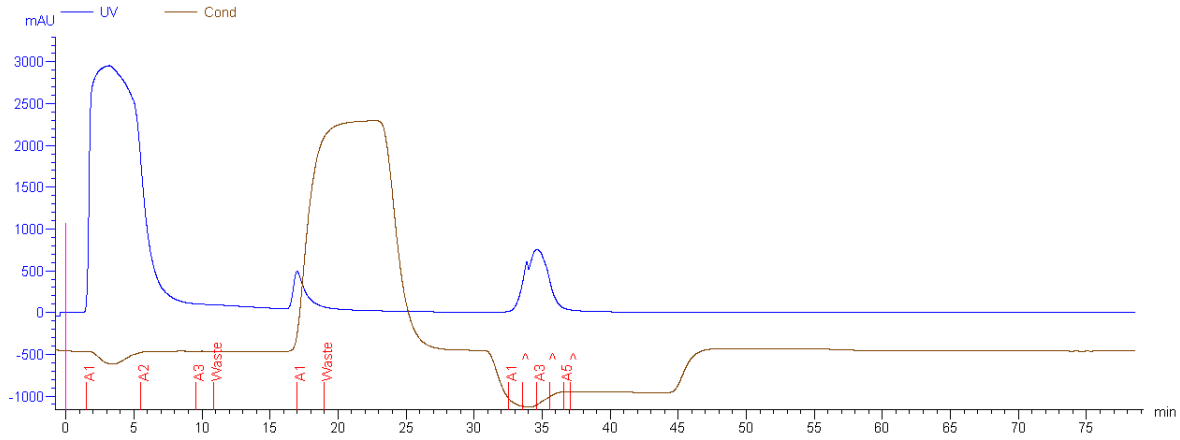

Appendix 30: Anti-STSY-(Cl)-GTGC Serum Affinity Purification/enrichment. Column: Chlorotyrosine STSTYGTGC peptide bound to Iodoacetyl gel bead. Serum Loaded: Chlorotyrosine STSYGTGC (month 3) serum, 2mL was loaded onto the column.

Appendix 31: Ethical approval and consent forms for type 2 diabetic samples

Appendix 31 (Ctd. II): Ethical approval and consent forms for type 2 diabetic samples

Appendix 31 (Ctd. III): Ethical approval and consent forms for type 2 diabetic samples

Appendix 31 (Ctd. IV): Ethical approval and consent forms for type 2 diabetic samples